



Programa de Doctorado en Bioingeniería
Universidad Miguel Hernández de Elche

**Regulación del reciclaje del
ribosoma citoplásmico por el
gen *ABCE2* de *Arabidopsis***

Carla Navarro Quiles

Director de la tesis
José Luis Micol Molina

Elche, 2021

Regulación del reciclaje del ribosoma citoplásmico por el gen *ABCE2* de *Arabidopsis*

Trabajo realizado por la Graduada Carla Navarro Quiles, en la Unidad de Genética del Instituto de Bioingeniería de la Universidad Miguel Hernández de Elche, para optar al grado de Doctora.

Elche, 25 de junio de 2021

La presente Tesis Doctoral, titulada “Regulación del reciclaje del ribosoma citoplásmico por el gen *ABCE2* de *Arabidopsis*”, se presenta bajo la modalidad de **tesis por compendio** de la siguiente **publicación**:

Navarro-Quiles, C., Mateo-Bonmatí, E., y Micol, J.L. (2018). ABCE proteins: from molecules to development. *Frontiers in Plant Science* **9**, 1-10.

JOSÉ LUIS MICOL MOLINA, Catedrático de Genética de la Universidad Miguel Hernández de Elche (UMH)

HAGO CONSTAR:

Que el presente trabajo ha sido realizado bajo mi dirección y recoge fielmente la labor desarrollada por la Graduada Carla Navarro Quiles para optar al grado de Doctora. Las investigaciones reflejadas en esta memoria se han desarrollado íntegramente en la Unidad de Genética del Instituto de Bioingeniería de la UMH, según los términos y condiciones definidos en el Plan de Investigación de la doctoranda, y cumpliendo los objetivos inicialmente previstos de forma satisfactoria y lo establecido en el Código de Buenas Prácticas de la UMH.

José Luis Micol Molina

Elche, 25 de junio de 2021

PIEDAD NIEVES DE AZA MOYA, Coordinadora del Programa de Doctorado en Bioingeniería de la Universidad Miguel Hernández de Elche por Resolución Rectoral 0169/17, de 1 de febrero de 2017

HACE CONSTAR:

Que da su conformidad a la presentación de la Tesis Doctoral de Doña Carla Navarro Quiles, titulada “Regulación del reciclaje del ribosoma citoplásmico por el gen *ABCE2* de *Arabidopsis*”, que se ha desarrollado en el Programa de Doctorado en Bioingeniería bajo la dirección del profesor José Luis Micol Molina.

Lo que firmo en Elche, a instancias de la interesada y a los efectos oportunos, a veinticinco de junio de dos mil veintiuno.

Profesora PIEDAD NIEVES DE AZA MOYA
Coordinadora del Programa de Doctorado en Bioingeniería

A mon pare, ma mare i ma germana.

A David.

ÍNDICE DE MATERIAS

ÍNDICE DE FIGURAS	II
ÍNDICE DE TABLAS	II
I.- PREFACIO	1
II.- RESUMEN	2
III.- SUMMARY	4
IV.- INTRODUCCIÓN	6
IV.1.- Estructura, función y clasificación de las proteínas ABC	6
IV.1.1.- Los transportadores ABC	6
IV.1.2.- Las proteínas ABC solubles	8
IV.2.- Relación entre la formación de la venación foliar, la auxina y la traducción	9
IV.2.1.- Diferenciación del tejido vascular en Arabidopsis	9
IV.2.2.- Papel de la síntesis, el transporte y la señalización de la auxina en la formación del patrón de venación foliar	12
IV.2.3.- Papel regulador de las regiones no traducidas (UTR) de los ARNm eucarióticos	16
IV.2.3.1.- Regulación mediada por las uORF de las 5' UTR	16
IV.2.3.2.- Regulación mediada por las 3' UTR	20
IV.3.- Antecedentes y objetivos	21
IV.3.1.- Un abordaje mutacional al estudio del desarrollo foliar	21
IV.3.2.- Los mutantes <i>apiculata</i>	22
IV.3.3.- Objetivos de esta Tesis	23
V.- MATERIALES Y MÉTODOS	24
VI.- RESULTADOS Y DISCUSIÓN	25
VII.- CONCLUSIONES Y PERSPECTIVAS	28
VII.1.- Las proteínas ABCE de las plantas participan en la traducción	28
VII.2.- La caracterización del mutante <i>api7-1</i> contribuye a la comprensión de la relación entre la traducción y el desarrollo	28
VIII.- BIBLIOGRAFÍA DE LOS APARTADOS IV-VII	30
IX.- PUBLICACIONES	39
X.- AGRADECIMIENTOS	132

ÍNDICE DE FIGURAS

Figura 1.- Representación esquemática de las estructuras y funciones conservadas de varias proteínas ABC.....	7
Figura 2.- Representación esquemática de la formación y disposición final de los elementos de los haces vasculares de la raíz, el tallo y las hojas de Arabidopsis.....	11
Figura 3.- Representación esquemática de la formación del patrón de venación de la hoja del primer nudo de Arabidopsis	13
Figura 4.- Representación esquemática del mecanismo de acción de la termoespermidina sobre la regulación postranscripcional de <i>SAC51</i> y la diferenciación vascular	19
Figura 5.- Fenotipo foliar de los mutantes <i>apiculata</i>	22
Figura 6.- Hipótesis sobre la función de la proteína ABCE2 y los efectos de la mutación <i>api7-1</i>	26

ÍNDICE DE TABLAS

Tabla 1.- Genes que codifican proteínas relacionadas con la traducción, cuyas mutaciones alteran la regulación de la expresión génica mediada por las uORF y la formación del patrón de venación foliar	17
----------------------------------------------------------------------------------------------------------------------------------------------------------------------------------------------------------------------	----

I.- PREFACIO

I.- PREFACIO

Siguiendo la normativa de la Universidad Miguel Hernández de Elche para la “Presentación de Tesis Doctorales por compendio de publicaciones”, este documento se ha dividido en las partes siguientes:

I.- Este *Prefacio*.

II.- Un *Resumen* en español.

III.- Un *Summary* en inglés.

IV.- Una *Introducción*, en la que se presenta el tema de la Tesis y los antecedentes y objetivos del trabajo realizado.

V.- Un resumen de los *Materiales y métodos* de las publicaciones de la Tesis.

VI.- Un resumen de los *Resultados y discusión* de las publicaciones de la Tesis.

VII.- Un resumen de las *Conclusiones y perspectivas* del trabajo realizado.

VIII.- Una *Bibliografía de los apartados IV-VII*; algunas de las referencias que incluye se repiten en las bibliografías de los artículos incluidos en esta memoria.

IX.- Un apartado de *Publicaciones*, que incluye las dos siguientes, en las que se indica el factor de impacto [FI] del año correspondiente.

Navarro-Quiles, C., Mateo-Bonmatí, E., y Micol, J.L. (2018). ABCE proteins: from molecules to development. *Frontiers in Plant Science* 9, 1-10 [FI: 4,106].

Navarro-Quiles, C., Mateo-Bonmatí, E., Candela, H., Robles, P., Martínez-Laborda, A., Ponce, M.R., y Micol, J.L. The Arabidopsis ATP-Binding Cassette E protein ABCE2 is a conserved component of the translation machinery. En preparación.

Los “Supplementary Data Sets” de este último artículo no se han incluido en esta memoria por su gran longitud. Las correspondientes hojas de cálculo se remitirán a los miembros del tribunal en formato electrónico.

X.- Un apartado de *Agradecimientos*.

Durante mi periodo predoctoral en el laboratorio de J.L. Micol también he presentado 16 comunicaciones a congresos que no se incluyen en esta Tesis, de las cuales, 9 son nacionales, y 7 internacionales, y soy primera autora en 9 de ellas.

II.- RESUMEN

II.- RESUMEN

La mayoría de los genes que codifican proteínas implicadas en la traducción en *Arabidopsis thaliana* (en adelante, *Arabidopsis*) tienen parálogos cercanos. Sus alelos nulos son viables y causan un fenotipo morfológico débil pero distinguible del silvestre: generan hojas apuntadas e indentadas, con un patrón de venación aberrante, rasgo que se ha atribuido tradicionalmente a la perturbación de la homeostasis de la auxina.

Las secuencias de las proteínas ATP-Binding Cassette E (ABCE) están conservadas entre las arqueas y los eucariotas. Se ha demostrado en la arquea *Saccharolobus solfataricus*, la levadura *Saccharomyces cerevisiae* y la especie humana que las ABCE son esenciales para el reciclaje de los ribosomas citoplásmicos. En estas tres especies distintas y distantes, una proteína ABCE separa las dos subunidades del ribosoma tras la terminación de la traducción, y acompaña a la subunidad 30S/40S hasta la iniciación de un nuevo ciclo de síntesis de proteínas. No se ha obtenido evidencia experimental alguna de la implicación de una ABCE en la traducción en el reino vegetal.

En casi todos los genomas estudiados el gen *ABCE* es de copia única y solo los de algunos insectos, peces y plantas, como *Arabidopsis*, contienen dos, usualmente denominados *ABCE1* y *ABCE2*. En esta Tesis hemos estudiado el mutante *apiculata7-1* (*api7-1*) de *Arabidopsis*, que fue aislado en el laboratorio de J.L. Micol y es portador de un alelo puntual, hipomorfo, recesivo y viable del gen *ABCE2*. El fenotipo morfológico de *api7-1* es similar al causado por los alelos nulos viables de genes que codifican componentes de la maquinaria de la traducción. También hemos estudiado *api7-2*, un alelo insercional y letal recesivo de *ABCE2*.

Hemos caracterizado los fenotipos morfológico, histológico y molecular de *api7-1*, prestando especial atención al patrón de venación de sus órganos planos, concluyendo que está muy alterado en las hojas del primer nudo de la roseta, pero no tanto en los cotiledones, las hojas del tercer nudo y las caulinares, y que es silvestre en los sépalos y los pétalos. Dado que la biosíntesis, el transporte polar y la señalización de la auxina contribuyen a la formación del patrón de venación foliar, hemos obtenido plantas *api7-1 PIN1_{pro}:PIN1:GFP*, portadoras de una fusión traduccional de los genes que codifican el exportador de la auxina PIN-FORMED 1 (PIN1) y la proteína fluorescente verde (GFP), y *api7-1 DR5_{pro}:3XVENUS:N7*, portadoras de un transgén testigo de la señalización de la auxina. El estudio mediante microscopía confocal de las raíces de estas plantas transgénicas indicó que el transporte de la auxina está disminuido, y su percepción, incrementada. Hemos realizado un análisis global del transcriptoma de *api7-1*, concluyendo que los genes que codifican las enzimas de la ruta

principal de la biosíntesis de la auxina están desreprimidos. Nuestros resultados sugieren que una de las causas de las aberraciones de la venación foliar de *api7-1* es el exceso de auxina.

La ABCE2 de *Arabidopsis* contiene dos grupos hierro-azufre (FeS). Hemos constatado que los genes de respuesta a los déficits de hierro y azufre están desreprimidos en *api7-1*, posiblemente para compensar la insuficiencia de función de la ABCE2 mutante. El aumento de la concentración intracelular de hierro podría conllevar el de las especies reactivas de oxígeno, tal como sugiere la desrepresión de genes de respuesta a estrés oxidativo, que también se constata en nuestro análisis transcriptómico de *api7-1*.

Hemos obtenido un transgén *ABCE2_{pro}:ABCE2:YFP*, que restablece el fenotipo silvestre en el mutante *api7-1*. Hemos demostrado, en un ensayo de coimmunoprecipitación, que la proteína de fusión ABCE2:YFP interacciona con varios componentes de la maquinaria de la traducción. Uno de ellos es EUKARYOTIC TRANSLATION INITIATION FACTOR 3J (eIF3j), cuyo papel como proteína accesoria de las ABCE durante el reciclaje de los ribosomas se ha demostrado en células de *Saccharomyces cerevisiae* y humanas. Esta observación sugiere que la ABCE2 de *Arabidopsis* —y por extensión, sus ortólogas vegetales— participa en el reciclaje del ribosoma citoplásmico.

Las regiones no traducidas 5' (5' UTR, de 5' untranslated region) y 3' UTR de los ARNm eucarióticos contienen secuencias que regulan postranscripcionalmente la expresión génica. La insuficiencia de la función de la ABCE1 de *Saccharomyces cerevisiae* y células humanas dificulta la disociación de los ribosomas, y propicia que se internen en la 3' UTR, desplazando a su paso a los factores reguladores unidos a esta última, prolongando o acortando la vida media del ARNm. El mutante *api7-1* es un buen candidato para establecer si este fenómeno también ocurre en las plantas; de ser así, se obtendría por esta vía una confirmación adicional de que la ABCE2 de *Arabidopsis* participa en el reciclaje del ribosoma.

Hemos constatado que varias brassicáceas presentan dos genes *ABCE*. Nuestro análisis filogenético indica que la duplicación del correspondiente gen ancestral se produjo en las rósidas antes de la diversificación de las brassicáceas y sugiere que los genes *ABCE1* de las brassicáceas están sujetos a una menor presión selectiva que sus parálogos *ABCE2*. El transgén *ABCE2_{pro}:ABCE1* —pero no el *ABCE1_{pro}:ABCE2*— restablece parcialmente el fenotipo silvestre en las plantas *api7-1*. *ABCE1* se expresa muy poco en *Arabidopsis*, siendo el órgano en que se detecta su mayor nivel la flor, cuya morfología es aparentemente silvestre en el mutante *api7-1*. Estas observaciones sugieren que las proteínas codificadas por los genes *ABCE1* y *ABCE2*, pero no sus promotores, son funcionalmente redundantes. *ABCE2* parece conservar su función ancestral, mientras que *ABCE1* está en vías de subfuncionalización o pseudogenización.

III.- SUMMARY

III.- SUMMARY

Most of the genes that encode proteins involved in translation in *Arabidopsis thaliana* (hereafter referred to as *Arabidopsis*) have close paralogs. Their null alleles are viable and cause a morphological phenotype that is mild but distinguishable from the wild type: they produce pointed and dentate leaves, with an aberrant venation pattern usually ascribed to a perturbed auxin homeostasis.

The sequences of ATP-Binding Cassette E (ABCE) proteins are conserved among archaea and eukaryotes. It has been shown in the archaeon *Saccharolobus solfataricus*, the yeast *Saccharomyces cerevisiae* and humans, that ABCEs are essential for cytoplasmic ribosome recycling. In these three distinct and distant species, an ABCE protein dissociates the two ribosomal subunits after translation termination, and escorts the 30S/40S subunit to the initiation of a new cycle of protein synthesis. There is no experimental evidence of the involvement in translation of any ABCE from the plant kingdom.

In almost all studied genomes, *ABCE* is a single-copy gene, and only those from some insects, fishes and plants, like *Arabidopsis*, contain two, usually named *ABCE1* and *ABCE2*. In this Thesis, we studied the *Arabidopsis apiculata7-1 (api7-1)* mutant, which was isolated in the laboratory of J.L. Micol, and carries a viable, recessive and hypomorphic allele of *ABCE2*. The morphological phenotype of *api7-1* is similar to those caused by viable null alleles of genes encoding components of the translation machinery. We also studied *api7-2*, an insertional, recessive lethal allele of *ABCE2*.

We characterized the morphological, histological and molecular phenotypes of *api7-1*, paying special attention to the venation pattern of its flat organs, concluding that it is severely perturbed in first-node rosette leaves, at a lesser extent in cotyledons, and third-node and cauline leaves, and wild-type in sepals and petals. Given that auxin biosynthesis, polar transport and signaling contribute to leaf venation patterning, we obtained *api7-1 PIN1_{pro}:PIN1:GFP* plants, which carry a translational fusion of the genes encoding the auxin efflux carrier PIN-FORMED 1 (PIN1) and the green fluorescent protein (GFP). We also obtained *api7-1 DR5_{pro}:3XVENUS:N7* plants, which carry a reporter transgene of auxin signaling. The study of the roots of these transgenic plants using confocal microscopy indicated that auxin transport and perception are decreased and increased, respectively. We performed an RNA-seq analysis of the *api7-1* transcriptome, concluding that the genes that encode enzymes involved in the main auxin biosynthesis pathway are upregulated. Our results suggest that an overproduction of auxin is partially responsible of the aberrations observed in the venation of *api7-1* leaves.

Arabidopsis ABCE2 contains two iron-sulfur (FeS) clusters. We observed that genes involved in the response to iron and sulfur starvation are upregulated in *api7-1*, possibly to compensate for the loss of function of the mutant ABCE2 protein. The increase in intracellular iron content might induce that of reactive oxygen species, as suggested by the upregulation of genes involved in the response to oxidative stress that we also observed in our RNA-seq of *api7-1*.

We obtained an *ABCE2_{pro}:ABCE2:YFP* transgene that restores the wild-type phenotype in the *api7-1* mutant. In a co-immunoprecipitation assay, we found that the ABCE2:YFP fusion protein interacts with several components of the translation machinery. One of these is EUKARYOTIC TRANSLATION INITIATION FACTOR 3J (eIF3j), whose role in ribosome recycling as an ABCE accessory factor has been described in *Saccharomyces cerevisiae* and human cells. This observation suggests that the Arabidopsis ABCE2 protein and, by extension, all its plant orthologs, participate in ribosome recycling.

The 5' untranslated region (5' UTR) and 3' UTR of eukaryotic mRNAs contain sequences for the post-transcriptional regulation of gene expression. In *Saccharomyces cerevisiae* and human cells, ABCE1 loss of function hinders ribosome dissociation, and allows ribosomes to enter the 3' UTR. In turn, the passage of the ribosomes through the 3' UTR displaces the regulatory elements bound to that region, increasing or decreasing mRNA lifespan. The *api7-1* mutant is a suitable candidate to ascertain whether this process also occurs in plants; in that case, this would corroborate the involvement of Arabidopsis ABCE2 in ribosome recycling.

We found that several Brassicaceae species contain two *ABCE* genes. Our phylogenetic analysis indicates that the duplication of the ancestral gene occurred in Rosidae before the divergence of the Brassicaceae family. In addition, we determined that the *ABCE1* genes are under a lower evolutionary pressure than their *ABCE2* paralogs. The *ABCE2_{pro}:ABCE1* transgene, but not *ABCE1_{pro}:ABCE2*, partially restores the wild-type phenotype in *api7-1* plants. *ABCE1* expression is very low in Arabidopsis, with a maximum at the flower, whose morphological phenotype is indistinguishable from wild type in the *api7-1* mutant. These observations suggest that the proteins encoded by the *ABCE1* and *ABCE2* genes, but not their promoters, are functionally redundant. *ABCE2* seems to conserve its ancestral function, while *ABCE1* is undergoing subfunctionalization or pseudogenization.

IV.- INTRODUCCIÓN

IV.- INTRODUCCIÓN

IV.1.- Estructura, función y clasificación de las proteínas ABC

IV.1.1.- Los transportadores ABC

No se conoce ningún ser vivo que carezca de proteínas ATP-Binding Cassette (ABC). La mayoría de los miembros de la familia ABC son proteínas de membrana y actúan como transportadores primarios de una amplia gama de sustratos, que varían tanto en tamaño como en naturaleza molecular (Theodoulou y Kerr, 2015). Los transportadores ABC contienen dos dominios transmembrana (TMD, de transmembrane domain) y dos de unión a ATP (NBD, de nucleotide-binding domain). Estos dominios corresponden a cuatro polipéptidos diferentes en las bacterias. La mayoría de los transportadores ABC eucarióticos, sin embargo, son una única proteína que contiene los cuatro dominios, o dos proteínas, cada una con un TMD y un NBD, que forman homo o heterodímeros (Higgins, 1992).

El sitio de unión al sustrato de las ABC está ubicado entre sus TMD. El transporte ocurre merced a un cambio de conformación del transportador, que acaba exponiendo su sitio de unión al sustrato hacia el lado de la membrana en el que este último es liberado (Locher, 2016). Este cambio de conformación se origina en los NBD, situados en la parte citoplásmica de la membrana, como consecuencia de su unión a dos moléculas de ATP y la ulterior hidrólisis de estas últimas, con la consiguiente liberación de ADP y fosfato inorgánico (Figura 1A, en la página 7). Los NBD tienen un origen filogenético común en todas las especies estudiadas y contienen varios motivos característicos, como los denominados Walker A y B, que también están presentes en otras proteínas de unión a ATP, y el ABC, que es exclusivo de la familia de proteínas del mismo nombre (Walker *et al.*, 1982; Holland y Blight, 1999).

Cada TMD incluye 6 hélices alfa, que atraviesan la membrana lipídica para facilitar el paso del sustrato. Aunque no están conservados filogenéticamente, los TMD comparten ciertos rasgos estructurales, en base a los cuales se ha clasificado a los transportadores ABC (Thomas *et al.*, 2020): los tipos I, II y III son importadores, y los VI y VII, exportadores y procarióticos. Los de los tipos IV y V están presentes tanto en los procariotas como en los eucariotas; en estos últimos actúan como exportadores, salvo algunas excepciones, como el importador ABCA4 humano y otros descritos en las plantas (Quazi *et al.*, 2012; Voith von Voithenberg *et al.*, 2019; Choi y Ford, 2021).

Las proteínas ABC eucarióticas también se han clasificado en subfamilias en base a sus relaciones filogenéticas y a la organización interna de sus dominios. Aunque esta

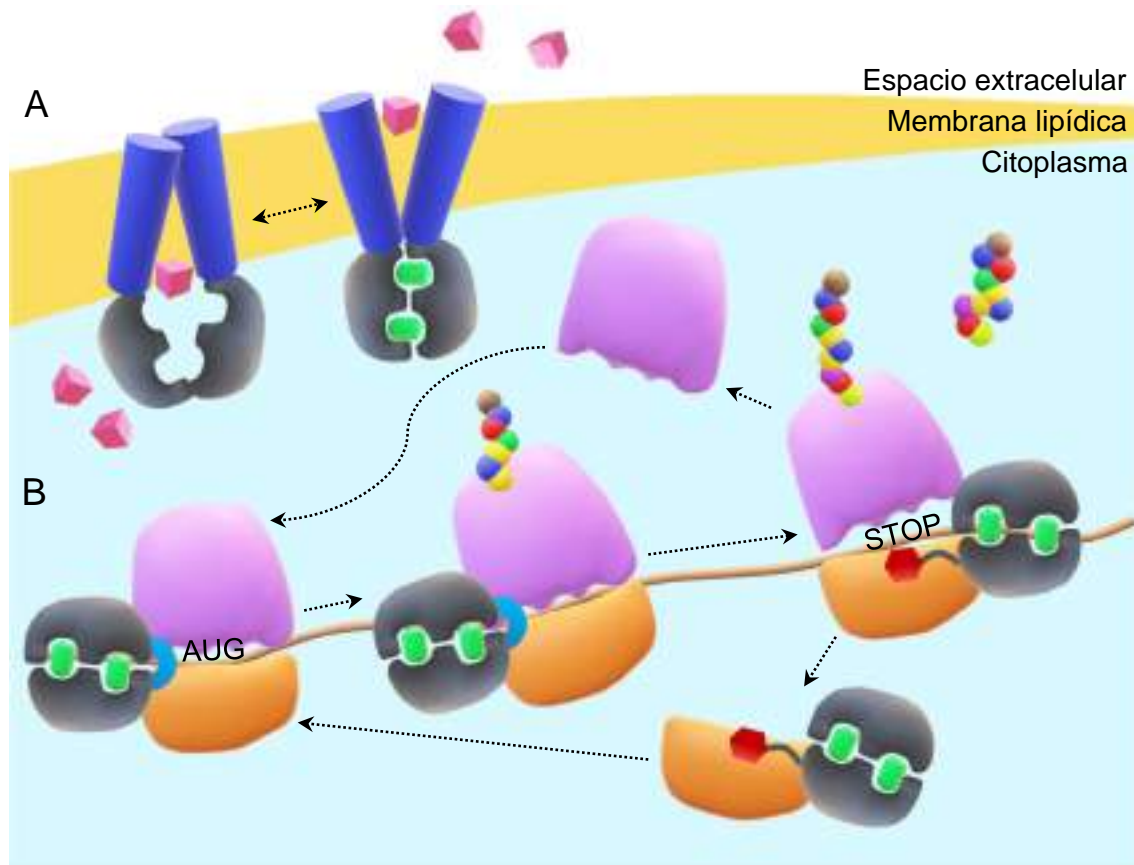


Figura 1.- Representación esquemática de las estructuras y funciones conservadas de varias proteínas ABC. (A) Transporte de un sustrato (cubos de color rosa) por un transportador ABC, cuyos TMD (cilindros azul oscuro) atraviesan la membrana lipídica (en amarillo), y los NBD (en gris) se sitúan en el citoplasma. Los NBD se cierran al unirse a dos moléculas de ATP (en verde), movilizándolo a los TMD, que acaban exponiendo al espacio extracelular su sitio de unión al sustrato, al que finalmente liberan. (B) Las proteínas ABC solubles participan en diferentes etapas de la traducción. Se representan dos proteínas ABCF con sus NBD unidos a dos moléculas de ATP y el motivo PtIM (en azul claro): una de estas dos proteínas (a la izquierda de la figura) facilita el reconocimiento del codón de iniciación de la traducción de un ARNm (AUG) por el ribosoma (la subunidad 60S se representa en rosa, y la 40S, en naranja), y la otra (en el centro de la figura) regula la traducción durante la síntesis de un polipéptido (cadena de esferas de varios colores). También se representan dos proteínas ABCE con sus NBD unidos a ATP y su dominio de unión a FeS (hexágono rojo): una (a la derecha de la figura) disocia un ribosoma tras el reconocimiento del codón de terminación (STOP), y la otra acompaña a una subunidad 40S para iniciar un nuevo ciclo de traducción. Las moléculas representadas no están a escala. Adaptado de (A) ter Beek *et al.* (2014) y (B) Hopfner (2016).

clasificación se propuso inicialmente para la especie humana e incluía 7 subfamilias (de la ABCA a la ABCG; Dean y Allikmets, 2001), su extensión a otras especies ha conllevado la creación de dos subfamilias más: la ABCH, que está representada en los artrópodos y los peces, y la ABCI, en las plantas (Dean y Annilo, 2005; Verrier *et al.*, 2008; Sturm *et al.*, 2009;

Popovic *et al.*, 2010). Se crearon posteriormente dos subfamilias más (ABCJ y ABCK), que incluyen transportadores descritos en las plantas no vasculares (Choi y Ford, 2021). Esta última clasificación, al contrario que la comentada en el párrafo anterior, no solo incluye a las proteínas ABC que son transportadores sino también a las que no lo son.

IV.1.2.- Las proteínas ABC solubles

Se denomina proteínas ABC solubles a las que carecen de TMD y no se asocian a membranas; se agrupan en las subfamilias ABCE y ABCF. Sus dos NBD están unidos por una región flexible, que permite su plegamiento durante la unión a dos moléculas de ATP y su hidrólisis subsiguiente. Las proteínas ABCE presentan un dominio de unión a dos grupos de hierro-azufre (FeS) de tipo $[4\text{Fe-4S}]^{2+}$ en su extremo amino (Barthelme *et al.*, 2007; Karcher *et al.*, 2008) y, las ABCF, un motivo de unión a ARNt (PtIM, de P-site tRNA interaction motif) situado entre sus dos NBD (Boël *et al.*, 2014). La subfamilia ABCE está presente en las arqueas y los eucariotas, y la ABCF, en las bacterias y los eucariotas. Ambas subfamilias suelen estar representadas por pocos genes en cada genoma, sus productos proteicos se localizan en el citoplasma, y sus funciones —conservadas en mayor o menor medida— están relacionadas con la síntesis de proteínas (Figura 1B).

Los genes *ABCE* son de copia única en la mayoría de las especies en las que se han estudiado, y solo algunos insectos, peces y plantas cuentan con dos (Liu *et al.*, 2013; Saha *et al.*, 2015; Lu *et al.*, 2016). Además, son esenciales en todos los organismos estudiados. La estructura y la función molecular de las proteínas ABCE se han estudiado fundamentalmente en la arquea *Saccharolobus solfataricus*, la levadura *Saccharomyces cerevisiae* y en células de mamíferos (Heuer *et al.*, 2017; Mancera-Martínez *et al.*, 2017; Nürenberg-Goloub *et al.*, 2018; Kratzat *et al.*, 2021). Los efectos de su insuficiencia de función sobre el desarrollo se han analizado principalmente en *Drosophila melanogaster* y *Cardamine hirsuta* (Andersen y Leever, 2007; Kougioumoutzi *et al.*, 2013; Kashima *et al.*, 2014).

La función conservada de las ABCE es separar las dos subunidades del ribosoma tras la terminación de la traducción de una molécula de ARNm, y acompañar a la subunidad 30S/40S hasta el inicio de un nuevo ciclo de traducción. Además, las proteínas ABCE disocian los ribosomas en otros contextos, como tras el último paso de la maduración de la subunidad 40S en *Saccharomyces cerevisiae*, que ocurre en un ribosoma formado por una subunidad 60S madura y una pre-40S, en el citoplasma (Strunk *et al.*, 2012). También participan en el rescate de ribosomas inmovilizados en moléculas de ARNm aberrantes. Estos ARNm pueden contener estructuras secundarias que impiden el avance del ribosoma, o carecer de codón de terminación. Esta última circunstancia propicia que el ribosoma no se separe del ARNm y siga

recorriéndolo, internándose en la región 3' no traducida (3' UTR, de untranslated region) e incluso en la cola poli(A), en donde queda finalmente retenido (Inada, 2017). Aunque la relación de las proteínas ABCE con el reciclaje del ribosoma no está descrita en las plantas, se ha establecido que las proteínas ABCE1 humana y ABCE2 de *Arabidopsis* actúan como supresores endógenos del silenciamiento génico postranscripcional (Sarmiento *et al.*, 2006; Kärblane *et al.*, 2015; Möttus *et al.*, 2020).

Mediante su interacción con el centro peptidil transferasa de la subunidad 50S/60S del ribosoma, las proteínas ABCF modulan diferentes etapas de la síntesis de proteínas (Fostier *et al.*, 2021). La subfamilia ABCF suele estar representada por 4 o 5 genes en cada especie estudiada (Murina *et al.*, 2019): por ejemplo, son 2 las proteínas ABCF en *Saccharomyces cerevisiae*, 3 en la especie humana y 5 en *Arabidopsis*. La ABCF humana más estudiada es ABCF1, que facilita el reconocimiento por el ribosoma del codón de iniciación de la traducción (Paytubi *et al.*, 2009; Stewart *et al.*, 2015). Una de las dos ABCF de *Saccharomyces cerevisiae*, ATP-Binding Cassette protein involved in Ribosome Biogenesis (Arb1), actúa durante el rescate de ribosomas que han sintetizado polipéptidos aberrantes, promoviendo la liberación del peptidil-ARNt para su degradación (Su *et al.*, 2019). Además, la expresión heteróloga de la ABCF2 humana complementa el fenotipo de los mutantes *arb1* (Kachroo *et al.*, 2015), lo que demuestra la conservación de la función de Arb1 y ABCF2. La otra ABCF de *Saccharomyces cerevisiae*, ABCF3 (también llamada General Control Nonderepressible 20 [GCN20]), reduce junto con GCN1 la traducción en presencia de ARNt vacíos, causada por un déficit de aminoácidos (Marton *et al.*, 1997; Garcia-Barrio *et al.*, 2000).

Aunque las ABCF se han estudiado poco en *Arabidopsis*, se ha propuesto que ABCF3 (GCN20), ortóloga de la GCN20 de *Saccharomyces cerevisiae*, también participa en la adaptación a diferentes tipos de estrés mediante la regulación de la traducción (Izquierdo *et al.*, 2018). Las plantas portadoras de alelos nulos de los genes *GCN20* y *ABCF4* de *Arabidopsis* son más sensibles a las infecciones debido a que sus estomas no se cierran ante la presencia de patógenos, lo que sugiere una relación directa entre la regulación de la traducción y la respuesta al estrés biótico (Zeng *et al.*, 2011; Kaundal *et al.*, 2017).

IV.2.- Relación entre la formación de la venación foliar, la auxina y la traducción

IV.2.1.- Diferenciación del tejido vascular en *Arabidopsis*

Las venas de las gimnospermas y las angiospermas constituyen un sistema ininterrumpido de haces vasculares que distribuye agua, nutrientes y moléculas señalizadoras entre órganos distantes, y confiere resistencia mecánica a la planta. Estas venas incluyen tres elementos: el xilema, que transporta agua y minerales de las raíces a las hojas; el floema, que

distribuye nutrientes, hormonas y otras moléculas; y el procámbium, durante el crecimiento primario o longitudinal, o el cámbium, durante el secundario o en grosor, formados por células pluripotentes cuya diferenciación genera el xilema y el floema.

En *Arabidopsis*, el cámbium solo se forma en el hipocótilo, las raíces y la zona basal del tallo (Chaffey *et al.*, 2002; Mazur *et al.*, 2014). La disposición de estos tres elementos en el haz vascular varía según el órgano en que se encuentran, el estado de desarrollo, y la especie. Las venas de los órganos con simetría radial de *Arabidopsis*, como las raíces y el tallo, también adoptan esta simetría, con el xilema en la zona interna y el floema en la externa (Figura 2A, B, en la página 11). En los órganos con simetría bilateral, como las hojas, el xilema se sitúa en la región adaxial (o dorsal) y el floema, en la abaxial (o ventral; Figura 2C). En ambos casos, el procámbium se dispone entre el xilema y el floema (McConnell y Barton, 1995; Baum *et al.*, 2002).

Durante la embriogénesis de *Arabidopsis*, el procámbium se forma y da lugar a la venación del hipocótilo y las raíces, y tras la germinación, el meristemo apical del tallo genera las venas de los tejidos aéreos (Mähönen *et al.*, 2000; Scarpella *et al.*, 2004). En ambos casos, un aumento local en la concentración de auxina señala el inicio de la formación del tejido vascular (Mattsson *et al.*, 2003). La auxina activa al factor de transcripción AUXIN RESPONSE FACTOR 5 (ARF5), que a su vez desencadena una cascada de señalización en las células preprocambiales, que son morfológicamente indistinguibles de sus vecinas. En dicha cascada, ARF5 activa directamente la expresión de *ARABIDOPSIS THALIANA HOMEBOX GENE 8* (*ATHB8*), que codifica un factor de transcripción que especifica la identidad procambial (Donner *et al.*, 2009). Durante la adquisición de la identidad procambial, estas células se alargan, adquieren la capacidad de drenar auxina de los tejidos colindantes y de dividirse periclinalmente, y finalmente se diferencian formando xilema o floema, aunque algunas conservan la identidad meristemática.

La diferenciación y la división de las células del procámbium se mantienen en equilibrio merced a la retroalimentación negativa causada por la señalización de la auxina y las citoquininas, que promueven la diferenciación del xilema, y la división celular y la identidad procambial, respectivamente. En el procámbium de la raíz, las citoquininas promueven la exportación de la auxina por el eflujo que llevan a cabo los transportadores PIN-FORMED (PIN) hacia las células que darán lugar al xilema. En estas últimas, la acumulación de la auxina activa simultáneamente la síntesis de las citoquininas y la transcripción de *ARABIDOPSIS HISTIDINE PHOSPHOTRANSFER PROTEIN 6* (*AHP6*), cuyo producto proteico restringe la actividad de las citoquininas a las células del procámbium (Figura 2D; Mähönen *et al.*, 2006; Bischoff *et al.*, 2011; De Rybel *et al.*, 2014).

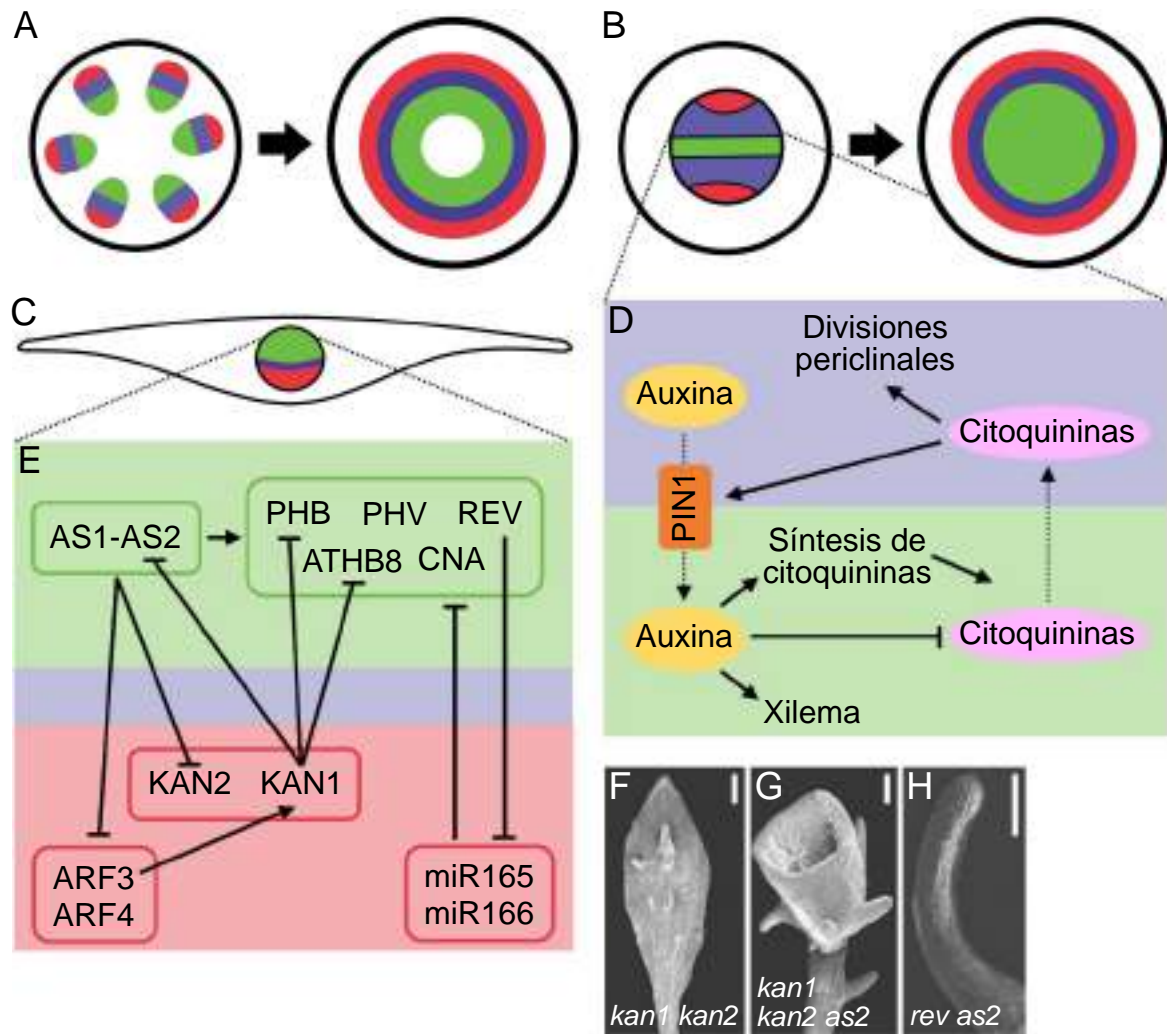


Figura 2.- Representación esquemática de la formación y disposición final de los elementos de los haces vasculares de la raíz, el tallo y las hojas de *Arabidopsis*. (A-C) Disposición del xilema (en verde), el floema (en morado) y el procámbium (en rojo), en cortes transversales de (A) la raíz, (B) el tallo y (C) la hoja. (A, B) Las flechas señalan la transición del crecimiento primario al secundario. (D, E) Interacciones moleculares entre los principales factores que regulan la formación del tejido vascular en (D) la raíz y (E) la hoja, en la que también se establece el eje dorsoventral. Los factores que se indican en este esquema, excepto los miARN, se representan sin cursiva porque pueden corresponder a una proteína, al gen que la codifica o a ambos. Las flechas punteadas indican flujo; las continuas terminadas en punta, activación; y las terminadas con una barra, represión de la expresión génica o, en el caso de los miARN, inhibición de su actividad. La auxina y las citoquininas se representan como elipses amarillas y rosas, respetivamente. (F-H) Pérdida de la dorsoventralidad foliar en los mutantes múltiples (F) *kan1 kan2*, (G) *kan1 kan2 as2*, y (H) *rev as2*. Las barras de escala indican (F, G) 1 mm y (H) 200 μ m. Adaptado de (A-E) Campbell y Turner (2017), y (F-H) Fu *et al.* (2007).

La formación de la venación de las hojas de *Arabidopsis* ocurre a la vez que el desarrollo del primordio foliar, y depende de una compleja red de interacciones entre pequeños ARN, factores de transcripción de diferentes familias y otras proteínas que

contribuyen al establecimiento del eje dorsoventral de la hoja y a la disposición de los elementos vasculares a lo largo de dicho eje (Figura 2E; Iwasaki *et al.*, 2013; Ramachandran *et al.*, 2017). El núcleo de esta red de interacciones está formado por dos grupos de factores de transcripción, uno de los cuales promueve la identidad adaxial: la familia HOMEODOMAIN-LEUCINE ZIPPER III (HD-ZIP III), constituida por las proteínas REVOLUTA (REV), PHABULOSA (PHB o ATHB14), PHAVOLUTA (PHV o ATHB19), ATHB8 y CORONA (CNA o ATHB15; también llamado INCURVATA4 [ICU4]; Ohashi-Ito y Fukuda, 2003; Ochando *et al.*, 2006; Ramachandran *et al.*, 2017). El segundo grupo incluye a KANADI1 (KAN1) y KAN2, que promueven la identidad abaxial (Reinhart *et al.*, 2013).

En la red de interacciones mencionada en el párrafo anterior, ARF3 induce la expresión de *KAN1*, y el complejo formado por los factores de transcripción ASYMMETRYC LEAVES 1 (AS1) y AS2, la de *REV*, *PHB* y *PHV* (Fu *et al.*, 2007; Kelley *et al.*, 2012). A su vez, AS1 y AS2 inhiben a ARF3, ARF4 y KAN2; y KAN1 reprime a AS2 (Iwakawa *et al.*, 2007; Wu *et al.*, 2008; Iwasaki *et al.*, 2013). Los genes de la familia HD-ZIP III son reprimidos postranscripcionalmente por los microARN (miARN) miR165 y miR166 (Zhou *et al.*, 2007), que están a su vez indirectamente reprimidos por REV (Figura 2E; Zhang y Zhang, 2012; Reinhart *et al.*, 2013). El resultado final de estas interacciones es la restricción de la expresión de los factores de identidad adaxial o abaxial a sus respectivos dominios, propiciando que la hoja se desarrolle como un órgano plano. La alteración del equilibrio entre las identidades adaxial y abaxial conduce a la pérdida de la dorsoventralidad de las hojas —y de su venación—, que en los casos más extremos adquieren una simetría radial, como en las hojas severamente abaxializadas del doble mutante *rev as2* (Figura 2H). Por el contrario, las hojas del doble mutante *kan1 kan2* se adaxializan y desarrollan protuberancias ectópicas en la cara abaxial, que se originan como consecuencia de un crecimiento perpendicular al plano mediolateral y proximodistal de la hoja (Figura 2G). El triple mutante *kan1 kan2 as2* presenta algunas hojas peltadas (con forma de copa), en las que la identidad adaxial se ve alterada y cuya cara exterior, de identidad abaxial, también desarrolla protuberancias ectópicas (Figura 2F; Fu *et al.*, 2007; Caggiano *et al.*, 2017).

IV.2.2.- Papel de la síntesis, el transporte y la señalización de la auxina en la formación del patrón de venación foliar

La complejidad del patrón de venación foliar de *Arabidopsis* es superior a la de los órganos con simetría radial. En efecto, además de organizar internamente sus haces vasculares respecto al eje dorsoventral de la hoja, la venación debe extenderse por todo el limbo foliar para asegurar una distribución uniforme de recursos y aportar resistencia

mecánica al órgano (Scarpella, 2017). A pesar de haber sido estudiado durante décadas (Nelson y Dengler, 1997; Berleth *et al.*, 2000; Scarpella *et al.*, 2010; Biedroń y Banasiak, 2018; ten Tusscher, 2021), son muchas las preguntas sin responder sobre la formación del patrón de venación foliar. No obstante, el desarrollo de herramientas moleculares (Baima *et al.*, 1995; Heisler *et al.*, 2005; Liao *et al.*, 2015; Yoshimoto *et al.*, 2016; Herud-Sikimić *et al.*, 2021; Pařízková *et al.*, 2021) y computacionales (Dhondt *et al.*, 2012; Bühler *et al.*, 2015; Xu *et al.*, 2021) ha permitido establecer que algunos de los procesos celulares que lo modulan son la biosíntesis, el transporte polar y la señalización de la auxina (Figura 3).

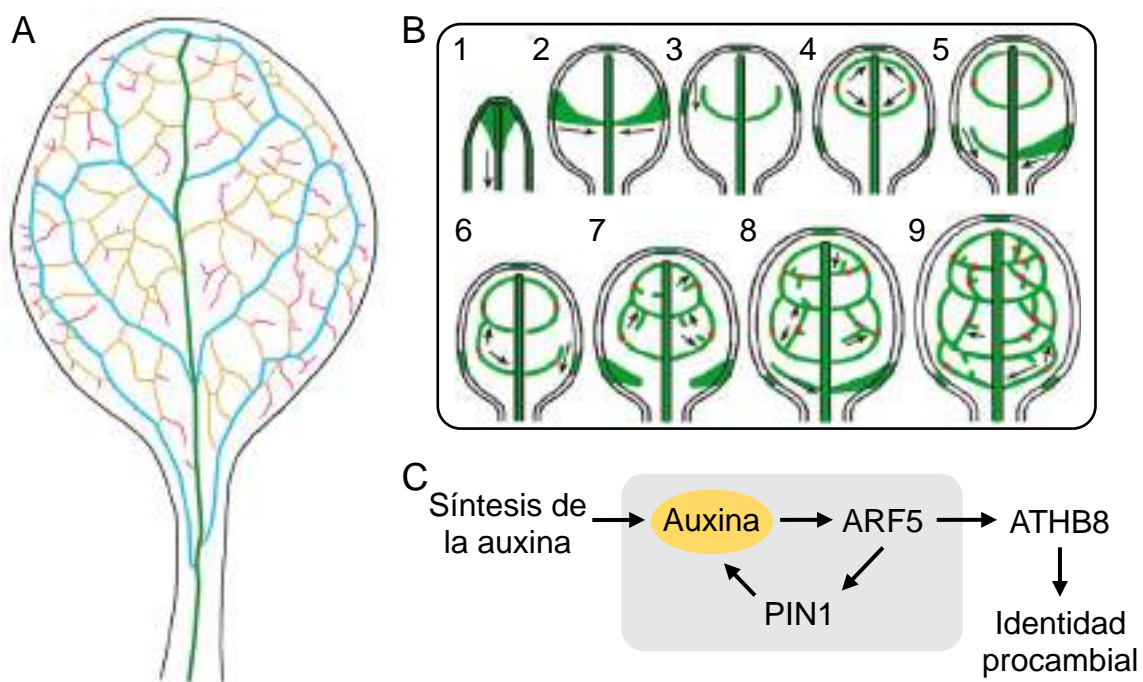


Figura 3.- Representación esquemática de la formación del patrón de venación de la hoja del primer nudo de *Arabidopsis*. (A) Diagrama de una hoja del primer nudo de la estirpe silvestre Landsberg *erecta* (*Ler*). El margen se representa en negro; la vena primaria, en verde; las secundarias, en azul; las de órdenes superiores conectadas por sus dos extremos, en amarillo, y las de terminación libre, en rosa. (B) Dominios de expresión de PIN1 (en verde) durante la formación del patrón de venación foliar. Las flechas indican la polarización de PIN1 en la membrana plasmática de las células, y en consecuencia, la dirección en la que efluye la auxina. Los puntos rojos indican células en las que PIN1 se distribuye de forma bipolar. Los números indican el orden en que se suceden las fases. Adaptado de Biedroń y Banasiak (2018). (C) Modelo molecular que integra la síntesis de la auxina, el bucle de retroalimentación positiva entre la señalización (ARF5) y el transporte polar (PIN1) de la auxina (rectángulo gris), y la inducción de la diferenciación del tejido vascular en el primordio foliar, mediada por ATHB8.

La hoja del primer nudo de *Arabidopsis* ha sido la más usada como modelo para el estudio del desarrollo de la venación foliar. Su patrón de venación (Figura 3A) incluye una

vena primaria situada en el centro de la hoja, que la recorre a lo largo de su eje proximodistal, desde el ápice del limbo hasta el peciolo, en donde se conecta con la venación del tallo. De la vena primaria emergen, lateralmente y por pares, las secundarias, que se vuelven a unir a la primaria formando arcos, y de estas últimas, otras de órdenes superiores. La manifestación de las venas de sucesivos órdenes ocurre de forma gradual durante el desarrollo del primordio foliar (Candela *et al.*, 1999).

El primordio foliar del primer nudo comienza a emerger del meristemo apical del tallo unos dos días después de la germinación. En este momento también se inicia la diferenciación vascular en la zona que ocupará la vena primaria, con la generación de un máximo de auxina en el tejido subepidérmico del ápice del primordio, que se extiende en sentido basípeto, es decir, desde el ápice hacia la base (Mattsson *et al.*, 2003). Aunque se propuso que la auxina acumulada en el tejido interno procedía de la epidermis por el eflujo llevado a cabo por PIN1 (Scarpella *et al.*, 2006), se ha demostrado recientemente que la presencia de este transportador en las células epidérmicas no tiene efecto alguno sobre la formación del patrón de venación (Govindaraju *et al.*, 2020). Alternativamente, se ha propuesto que el máximo de auxina antes mencionado se debe a la síntesis local de la hormona (Kneuper *et al.*, 2021).

El incremento en la concentración de la auxina en el tejido subepidérmico activa la expresión de *ARF5*, que a su vez induce la de *PIN1* (Wenzel *et al.*, 2007; Krogan *et al.*, 2016). *PIN1* se localiza en la membrana basal de estas células, que ya han adquirido identidad preprocambial, y dirige el flujo de la auxina hacia el tejido vascular preexistente del meristemo apical del tallo (fase 1 de la Figura 3B; Scarpella *et al.*, 2006). La hipótesis de la canalización de la auxina (Sachs, 1969; 1981) propone que el transporte polar de esta hormona induce la diferenciación en tejido provascular de las células que la perciben. Esta diferenciación, a su vez, incrementa la capacidad de transportar auxina de estas células y de drenarla de sus vecinas. Como consecuencia, las células preprocambiales con mayor capacidad de transportar auxina se diferencian en tejido vascular, mientras que las restantes vuelven a un estado indiferenciado para formar finalmente parte del mesófilo (Sachs, 1981; Scarpella *et al.*, 2004; Donner *et al.*, 2009). Según la hipótesis de la canalización, las células con mayores concentraciones de *PIN1* transportan más auxina, de modo que el flujo de la hormona se va restringiendo a un número cada vez menor de filas de células. El aumento en la concentración de la auxina en estas últimas incrementa la expresión de *ARF5*, y a su vez, la de *PIN1*, creando un bucle de retroalimentación positiva (Wenzel *et al.*, 2007). Finalmente, tal como se ha descrito en el apartado IV.2.1, en la página 9, *ARF5* induce la expresión de *ATHB8*, que especifica la identidad procambial y, posteriormente, la diferenciación vascular (Figura 3C; Donner *et al.*, 2009).

El proceso descrito en el párrafo anterior se repite en las venas de órdenes superiores (fase 2 y siguientes de la Figura 3B), con una peculiaridad: dado que durante la especificación de la identidad vascular de una célula, PIN1 está polarizado en su membrana hacia la vena preexistente adyacente, las que están conectadas por sus dos extremos se forman en dos etapas consecutivas. En efecto, PIN1 se polariza en sentidos opuestos y siempre hacia la vena preexistente más cercana en cada etapa (Scarpella *et al.*, 2006). Por ejemplo, el primer par de venas secundarias, las más apicales, comienza a manifestarse un día después que la vena primaria. En una primera etapa, la aparición de un máximo de auxina a cada lado del margen foliar induce la expresión de *PIN1*, que se extiende de forma basolateral hasta la vena primaria, iniciando la diferenciación vascular en las células que formarán la parte basal de la secundaria; en estas últimas células, PIN1 está polarizado hacia la vena primaria (fase 2). En una segunda etapa, la expresión de PIN1 en el margen se hace indetectable (fase 3) y comienza a manifestarse gradualmente en sentido acrópeto, en la zona en la que se formará la parte apical de la vena secundaria. En las primeras células en las que se expresa PIN1 en esta segunda etapa, esta proteína está polarizada hacia la vena secundaria en formación; cuando su dominio de expresión se acerca a la vena primaria, PIN1 se polariza hacia esta última. De esta forma, las células provasculares que darán lugar a la vena secundaria se agrupan en dos dominios, en los que PIN1 está polarizado en sentidos opuestos, y que están unidos por una única célula en la que el transportador se localiza de forma bipolar (fase 4 de la Figura 3B; Scarpella *et al.*, 2006).

Aunque son muchas las observaciones que apoyan la hipótesis de la canalización de la auxina, aún quedan preguntas por responder sobre la formación de las venas. Una de ellas es cuál es el mecanismo que dirige a PIN1 hacia un lado concreto de la membrana plasmática de cada célula, que además coordina su polarización entre células vecinas. Se sabe que la auxina induce la transcripción de *PIN1*, y se han descrito procesos que modulan la actividad de PIN1 y su presencia en la membrana plasmática, pero se desconoce cómo la auxina distribuye polarmente a esta proteína (ten Tusscher, 2021).

Paradójicamente, se ha demostrado también que el transporte polar de la auxina mediado por las proteínas PIN es innecesario para la formación de un patrón de venación foliar reproducible (Verna *et al.*, 2019). En ausencia de los transportadores PIN, el patrón de venación es más denso que el silvestre cerca del margen y a lo largo de la vena primaria, cuyos elementos vasculares se disponen correctamente a lo largo del eje proximodistal. Esta observación sugiere que el transporte polar de la auxina no es necesario para que las células vasculares se alineen formando venas (Ravichandran *et al.*, 2020). Tampoco parece necesaria la señalización de la auxina, pues su inhibición parcial solo conlleva una reducción

en el número de venas de órdenes superiores, manteniéndose el patrón de venación silvestre (Verna *et al.*, 2019). Sin embargo, cuando se inhiben simultáneamente la señalización de la auxina de forma parcial y su transporte polar mediado por los transportadores PIN, aparece un tercer patrón de venación, también reproducible, con agrupaciones de células vasculares desorganizadas en los puntos de convergencia entre venas (Verna *et al.*, 2019). Esto sugiere que la señalización y el transporte polar de la auxina actúan de modo redundante en la formación del patrón de venación, ya que solo bloqueándolos a la vez se perturba la orientación de sus células.

Para explicar la formación de un patrón de venación en ausencia de los transportadores PIN, se ha propuesto que la auxina podría transportarse de forma polar mediante difusión facilitada por los plasmodesmos (Verna *et al.*, 2019; Ravichandran *et al.*, 2020), o que la síntesis local de la hormona desempeña un papel más relevante del que se le había atribuido (Kneuper *et al.*, 2021). Por otro lado, y dado que la señalización de la auxina es inherentemente no direccional, se desconoce cómo contribuye a la orientación de las células vasculares durante la formación de las venas (Ravichandran *et al.*, 2020).

IV.2.3.- Papel regulador de las regiones no traducidas (UTR) de los ARNm eucarióticos

IV.2.3.1.- Regulación mediada por las uORF de las 5' UTR

Algunos ARNm cuentan con pautas de lectura abierta (ORF, de open reading frame) en su 5' UTR, a las que se denomina uORF (de upstream ORF). Las uORF participan en la regulación postranscripcional de la expresión génica, ya que dificultan la traducción de la ORF principal (mORF, de main ORF). Tras la traducción de una uORF, la de la mORF adyacente requiere la así denominada reiniciación de la traducción: la terminación de la traducción de la uORF se interrumpe antes de que la subunidad 40S del ribosoma se separe del ARNm, y se unen al complejo de la traducción un nuevo metionil-ARNt y factores de iniciación; estos últimos hacen posible que la subunidad 40S reinicie la lectura del ARNm en busca del codón de iniciación de la mORF (von Arnim *et al.*, 2014).

Se ha estimado que un 35% de los genes de *Arabidopsis* contienen una o más uORF, algunas de las cuales codifican péptidos de secuencia conservada (Kim *et al.*, 2007; von Arnim *et al.*, 2014). La presencia o ausencia de las uORF en los ARNm parece estar relacionada con la naturaleza del producto de la mORF de estos últimos. Los ARNm cuyas mORF codifican proteínas implicadas en rutas de señalización suelen contener uORF, que no aparecen en la mayoría de los que codifican proteínas domésticas (Kim *et al.*, 2007; Hu *et al.*, 2016). Se han descrito en *Arabidopsis* dos mecanismos por los que una uORF puede regular

la traducción de la mORF adyacente: según la secuencia del péptido que codifica la uORF o su longitud. En el primer caso, el péptido nascente detiene el avance del ribosoma durante la fase de elongación de su traducción, al establecer interacciones con el túnel de salida del ribosoma (Ebina *et al.*, 2015; Hayashi *et al.*, 2017). El péptido nascente también puede interactuar con metabolitos como la sacarosa, el ascorbato o algunas poliaminas que impiden que el ribosoma finalice la traducción, regulando así su propio metabolismo (Laing *et al.*, 2015; Yamashita *et al.*, 2017; van der Horst *et al.*, 2020). En el segundo caso, se ha estimado que la traducción de las uORF de más de 48 nt evita la reiniciación de la traducción de la mORF situada aguas abajo, como consecuencia de la pérdida progresiva de factores de iniciación (David-Assael *et al.*, 2005; von Arnim *et al.*, 2014; Schepetilnikov y Ryabova, 2017).

El establecimiento del eje dorsoventral de las hojas y la formación de su patrón de venación acusan especialmente los efectos de la disfunción de la traducción en *Arabidopsis* (Tabla 1). Muchas mutaciones viables en genes que codifican proteínas ribosómicas reducen el tamaño de la roseta, cuyas dos primeras hojas se hacen apuntadas, y las restantes, indentadas (Byrne, 2009). También alteran el patrón de venación foliar, aparentemente como consecuencia de la perturbación de la homeostasis de la auxina. Las combinaciones de estas mutaciones con alelos de insuficiencia de función de los genes *AS1* y *AS2* rinden fenotipos

Tabla 1.- Genes que codifican proteínas relacionadas con la traducción, cuyas mutaciones alteran la regulación de la expresión génica mediada por las uORF y la formación del patrón de venación foliar

Gen (código AGI)	Transcritos con uORF cuya traducción se ve alterada	Referencias
<i>EIF3H*</i> (At1g10840)	<i>ARF2, ARF3, ARF4, ARF5, ARF6, ARF7, ARF11, CLV1</i>	1, 2, 3, 4
<i>RACK1</i> (At1g18080)	<i>SAC51</i>	5, 6
<i>RPL4A</i> (At3g09630)	<i>SAC51</i>	5, 6
<i>RPL10A</i> (At1g14320)	<i>SAC51</i>	5, 7
<i>RPL24B*</i> (At3g53020)	<i>ARF3</i>	2, 8, 9
<i>RPL4D*</i> (At5g02870)	<i>ARF3, ARF5, ARF7</i>	10, 11
<i>RPL5A*</i> (At3g25520)	<i>ARF3, ARF5, ARF7</i>	9, 10, 11, 12
<i>RPL5B*</i> (At5g39740)	-	9, 10, 13
<i>RPL7B*</i> (At2g01250)	-	10
<i>RPL28A*</i> (At2g19730)	-	9
<i>RPS6A*</i> (At4g31700)	-	10

*Sus alelos de insuficiencia de función rinden fenotipos sinérgicos en combinaciones dobles mutantes con los de *AS1* o *AS2*. ¹Kim *et al.* (2007); ²Zhou *et al.* (2010); ³Schepetilnikov *et al.* (2013); ⁴Zhou *et al.* (2014); ⁵Imai *et al.* (2006); ⁶Kakehi *et al.* (2015); ⁷Imai *et al.* (2008); ⁸Nishimura *et al.* (2005); ⁹Yao *et al.* (2008); ¹⁰Horiguchi *et al.* (2011); ¹¹Rosado *et al.* (2012); ¹²Pinon *et al.* (2008); y ¹³Van Minnebruggen *et al.* (2010).

sinérgicos: los dobles mutantes presentan diferentes grados de pérdida de la dorsoventralidad foliar, similares a los causados por los alelos hipomorfos y nulos de los genes de identidad dorsoventral (Figura 2F-H, en la página 11; Nishimura *et al.*, 2005; Pinon *et al.*, 2008; Yao *et al.*, 2008; Van Minnebruggen *et al.*, 2010; Horiguchi *et al.*, 2011; Rosado *et al.*, 2012).

Los mutantes *ribosomal protein 14d* (*rpl4d*) y *rpl5a* sirven de ejemplo de que la pérdida de función de algunas proteínas ribosómicas altera la regulación postranscripcional mediada por las uORF de los ARNm que codifican factores de transcripción de respuesta a la auxina. Se han obtenido construcciones en las que las uORF de los genes *ARF3*, *ARF5* o *ARF7* se han dispuesto aguas arriba de un gen testigo, cuya traducción dificultan, efecto que se potencia en los mutantes *rpl4d* y *rpl5a* (Rosado *et al.*, 2012). La mutación *rpl24b* también disminuye la eficacia de la reiniciación de la traducción de la mORF de *ARF3*. Además, la expresión de una variante truncada del ARNm de *ARF3*, que carece de su uORF, restablece parcialmente el fenotipo silvestre en el mutante *rpl24b* (Nishimura *et al.*, 2005).

Otro ejemplo de que la traducción de una uORF disminuye la eficacia de la maquinaria de la traducción lo proporcionan las mutaciones en el gen *EUKARYOTIC TRANSLATION INITIATION FACTOR 3H* (*EIF3H*) de *Arabidopsis*. La proteína eIF3h es necesaria para que la auxina promueva la traducción de moléculas de ARNm que contienen uORF. La auxina activa a la quinasa TARGET OF RAPAMYCIN (TOR), que a su vez fosforila a eIF3h. Esta fosforilación mantiene al complejo eIF3 unido al ribosoma durante la traducción de una uORF, propiciando así la reiniciación de la traducción en la mORF adyacente (Kim *et al.*, 2007; Schepetilnikov *et al.*, 2013). No obstante, la pérdida de función de eIF3h no solo altera la traducción de los ARNm que codifican ARF, ya que los dos alelos hipomorfos de *EIF3H* que se han descrito perturban severamente el desarrollo: un 75% de las plantas homocigóticas para dichos alelos no alcanza la etapa reproductiva, y las que lo consiguen presentan una fertilidad reducida (Kim *et al.*, 2004; Zhou *et al.*, 2014). La mitad de las plantas *eif3h* presentan hojas radializadas, como consecuencia del desarrollo aberrante del meristemo apical del tallo que a su vez se debe, al menos en parte, a una traducción insuficiente de la mORF del ARNm de *CLAVATA1* (*CLV1*), que contiene cuatro uORF; la proteína CLV1 regula la actividad del meristemo apical del tallo (Clark *et al.*, 1997; Zhou *et al.*, 2014).

La termoespermidina es una poliamina producida por la termoespermidina sintasa ACAULIS 5 (*ACL5*; Knott *et al.*, 2007) e inhibe la diferenciación del tejido vascular, al contrario que la auxina. Su implicación en la regulación de la diferenciación vascular se descubrió mediante una mutagénesis de segundos sitios, que se realizó con el objetivo de encontrar supresores extragénicos del fenotipo del mutante *acl5-1*, que presenta una proliferación excesiva del xilema, causada por la desrepresión de los cinco genes HD-ZIP III (Clay y Nelson,

2005; Imai *et al.*, 2006). Tras dicha mutagénesis se aislaron una mutación dominante, *suppressor of acaulis 51* (*sac51-d*), y tres semidominantes (*sac52-d*, *sac53-d* y *sac56-d*), en cuatro genes diferentes, todas las cuales rescatan parcialmente el fenotipo vascular de *acl5-1* y restablecen los niveles de expresión de los genes HD-ZIP III (Imai *et al.*, 2006).

El gen *SAC51* codifica un factor de transcripción de la superfamilia bHLH (basic helix-loop-helix; Imai *et al.*, 2006). La mutación *sac51-d* crea un codón de terminación prematuro en una de las cinco uORF del ARNm de *SAC51*. Las mutaciones *sac52-d*, *sac56-d* y *sac53-d* dañan genes que codifican dos proteínas ribosómicas (RPL10A y RPL4A) y un componente de la subunidad 40S (RECEPTOR FOR ACTIVATED C KINASE 1 A [RACK1]), respectivamente. Estas cuatro mutaciones facilitan la traducción de la mORF de *SAC51* en el mutante *acl5-1* (Imai *et al.*, 2008; Kakehi *et al.*, 2015), lo que indica que la termoespermidina producida por *ACL5* facilita la traducción de la mORF de *SAC51*, y que el efecto inhibitorio de las uORF de este último se ve contrarrestado por las perturbaciones de la maquinaria de la traducción. Dado que la termoespermidina sintetizada por *ACL5* promueve la traducción del factor de transcripción *SAC51*, se ha propuesto que este último es un intermediario de la represión de los genes HD-ZIP III por *ACL5* (Takahashi, 2018). *ATHB8*, a su vez, induce la expresión de *ACL5*, estableciendo un sistema que regula la diferenciación del tejido vascular (Figura 4; Baima *et al.*, 2014).

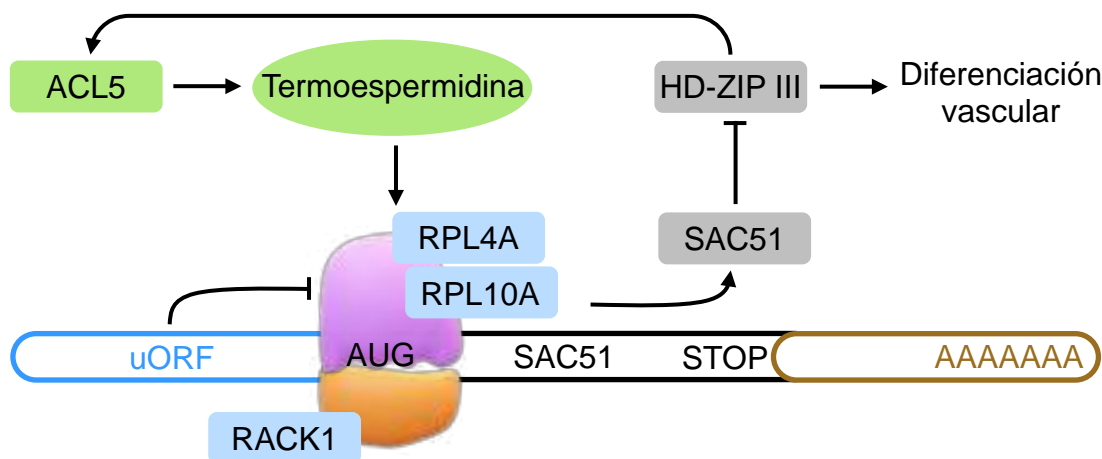


Figura 4.- Representación esquemática del mecanismo de acción de la termoespermidina sobre la regulación postranscripcional de *SAC51* y la diferenciación vascular. La termoespermidina (elipse verde) sintetizada por *ACL5* (rectángulo verde) promueve la traducción de la mORF de *SAC51* (región negra del ARNm), que es a su vez inhibida por la de una de las cinco uORF situadas aguas arriba (región en azul). El efecto inhibitorio de estas uORF depende del correcto funcionamiento del ribosoma, en concreto, de las proteínas RPL4A, RPL10A y RACK1 (rectángulos en azul). El factor de transcripción *SAC51* inhibe la expresión de los cinco genes HD-ZIP III, cuyos productos proteicos promueven la diferenciación vascular, así como la expresión de *ACL5*.

IV.2.3.2.- Regulación mediada por las 3' UTR

El único mecanismo molecular conocido que vincula las alteraciones de la maquinaria de la traducción con las aberraciones de la venación foliar en *Arabidopsis* es la regulación postranscripcional mediada por las uORF (Tabla 1, en la página 17). No obstante, las 3' UTR también participan en mecanismos de regulación postranscripcional que modulan la vida media de los ARNm y, en consecuencia, sus niveles y los de los productos de su traducción. Se ha descrito en *Arabidopsis* que la presencia de N⁶-metiladenosinas (m⁶A) en la 3' UTR de los ARNm incrementa su vida media, mientras que la unión de complejos de unión de exones (EJC, de exon-junction complex) la disminuye (Anderson *et al.*, 2018; Ohtani y Wachter, 2019; Wu *et al.*, 2020). Este segundo proceso ocurre mediante la degradación del ARNm mediada por mutaciones sin sentido (NMD, de nonsense-mediated decay), y está conservado en los eucariotas (Ohtani y Wachter, 2019). Un ejemplo de NMD se da en el ARNm del *EUKARYOTIC RELEASE FACTOR 1* (*eRF1*) de *Arabidopsis*, que codifica un factor de terminación de la traducción que regula su propia traducción. La presencia de un EJC en la 3' UTR del ARNm de *eRF1* reduce su vida media, y también su traducción. Cuando los niveles de la proteína eRF1 disminuyen en exceso, también lo hace la eficacia de la terminación de la traducción de su ARNm, por lo que el ribosoma tiende a no disociarse. Como consecuencia, el ribosoma se interna en la 3' UTR y desplaza al EJC, incrementando la vida media del ARNm de *eRF1* y a su vez el número de proteínas eRF1 (Nyikó *et al.*, 2017).

La proteína eRF1 está conservada en todos los eucariotas y las arqueas (aRF1), y requiere la actividad de una proteína ABCE para llevar a cabo la terminación de la traducción (Nürenberg y Tampé, 2013). De hecho, en *Saccharomyces cerevisiae* y en células humanas la insuficiencia de la función de ABCE1 conlleva la reiniciación de la traducción en la 3' UTR, y que el ribosoma desplace los factores reguladores que encuentra a su paso en esta región, alterando la regulación postranscripcional (Young *et al.*, 2015; Zhu *et al.*, 2020).

No se ha descrito relación alguna entre la regulación postranscripcional mediada por las 3' UTR y el desarrollo de la venación foliar. Sin embargo, el mutante *simple leaf3* (*sil3*) de la brassicácea *Cardamine hirsuta*, portador de una mutación en un gen que codifica una proteína ABCE, presenta alteraciones en la morfología y la venación de sus hojas, similares a las de los mutantes de *Arabidopsis* cuya maquinaria de la traducción está alterada. Aunque las hojas del tipo silvestre de *Cardamine hirsuta* son compuestas, las del mutante *sil3* son simples y presentan un menor número de venas de órdenes superiores y de venas de terminación libre. Se cree que la causa es la alteración de la homeostasis de la auxina, hormona que no solo promueve la diferenciación del tejido vascular, sino también la formación de los folíolos durante el desarrollo del primordio foliar (Kougioumoutzi *et al.*, 2013).

Dado el alto grado de conservación de los mecanismos de terminación de la traducción y de reciclaje de ribosomas entre los eucariotas y las arqueas, es verosímil que el fenotipo morfológico y fisiológico del mutante *si/3* se deba, al menos en parte, a una alteración de la regulación postranscripcional mediada por las 3' UTR, lo que indicaría que existe un mecanismo de regulación postranscripcional del desarrollo de la venación foliar adicional al mediado por las uORF.

IV.3.- Antecedentes y objetivos

IV.3.1.- Un abordaje mutacional al estudio del desarrollo foliar

La Organización de las Naciones Unidas declaró el 2020 como Año Internacional de la Sanidad Vegetal, a fin de concienciar a la población sobre la importancia de proteger la salud de las plantas. Entre otros, son dos los motivos principales por los que las plantas deberían recibir una gran atención: porque son la base de nuestra alimentación, y una herramienta imprescindible para reducir el paulatino incremento de la concentración de CO₂ en nuestra atmósfera como consecuencia del uso masivo de combustibles fósiles. En ambos aspectos las hojas desempeñan un papel clave ya que, mediante la fotosíntesis, fijan el CO₂ atmosférico y lo convierten en materia orgánica que la planta usará para su desarrollo y reproducción. De esta manera, el conocimiento generado por el estudio del desarrollo foliar sienta las bases para incrementar la capacidad fotosintética de las plantas y, en el caso de las especies de interés agronómico, su rendimiento (Micol, 2009).

Con el fin de realizar una disección genética del desarrollo foliar, se han llevado a cabo en el laboratorio de J.L. Micol varias búsquedas de mutantes de *Arabidopsis* que fueran viables y fértiles, y presentaran alteraciones en la morfología de sus hojas. Los mutantes identificados se agruparon en 19 clases fenotípicas en base a la forma, el tamaño y la pigmentación de sus hojas, y se asignaron a 116 grupos de complementación (Berná *et al.*, 1999; Robles Ramos, 1999; Serrano-Cartagena *et al.*, 1999). Desde entonces, se han identificado en el laboratorio de J.L. Micol las mutaciones causantes de los fenotipos de más de 60 de estos mutantes, que han resultado afectar a procesos tan diversos como el transporte o la señalización de la auxina (Pérez-Pérez *et al.*, 2010; Esteve-Bruna *et al.*, 2013; Karampelias *et al.*, 2016), la contribución del cloroplasto y la mitocondria al desarrollo foliar (Quesada *et al.*, 2011; Casanova-Sáez *et al.*, 2014b; Muñoz-Nortes *et al.*, 2017), la biogénesis del ribosoma y la traducción (Van Minnebruggen *et al.*, 2010; Horiguchi *et al.*, 2011; Casanova-Sáez *et al.*, 2014a), el transporte nucleocitoplásmico (Ferrández-Ayela *et al.*, 2013), o la regulación epigenética (Mateo-Bonmatí *et al.*, 2018).

IV.3.2.- Los mutantes *apiculata*

Los rasgos más característicos del fenotipo morfológico de los alelos mutantes de muchos de los genes que codifican componentes de la maquinaria de la traducción son las hojas de la roseta pequeñas, apuntadas e indentadas, a diferencia de las de los tipos silvestres de uso más común, que son más redondeadas y de margen total o casi totalmente liso. Comparten estos rasgos fenotípicos los mutantes aislados en el laboratorio de J.L. Micol que se incluyeron en las clases fenotípicas a las que se denominó Apiculata (Api) y Denticulata (Den; Figura 5). De hecho, 5 de los 6 genes *API* y *DEN* que fueron clonados posicionalmente con anterioridad a esta Tesis codifican proteínas ribosómicas (Horiguchi *et al.*, 2011; Casanova-Sáez *et al.*, 2014a) y, el sexto, un factor de biogénesis del ribosoma (Micol-Ponce *et al.*, 2020).

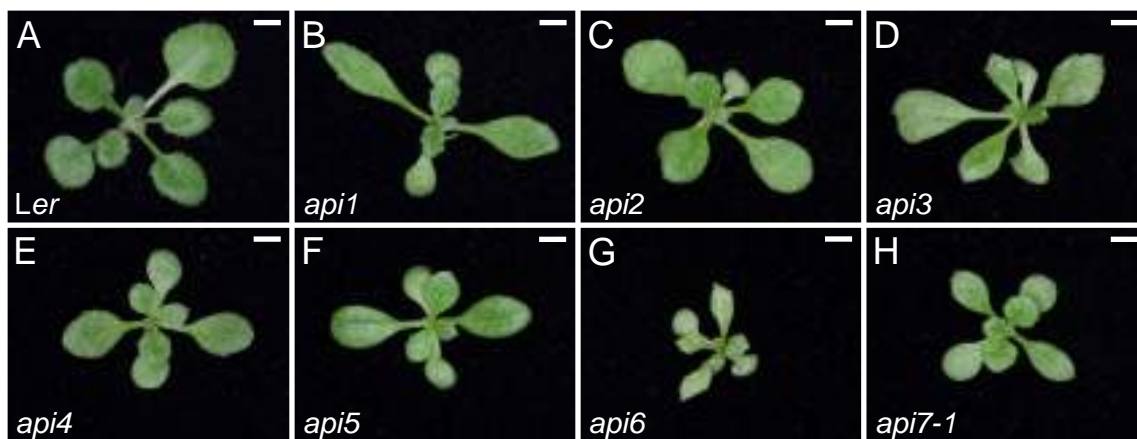


Figura 5.- Fenotipo foliar de los mutantes *apiculata*. Rosetas de (A) la estirpe silvestre *Ler*, y de los mutantes (B) *api1*, (C) *api2*, (D) *api3*, (E) *api4*, (F) *api5*, (G) *api6* y (H) *api7-1*. Las fotografías se tomaron 14 dde. Las barras de escala representan 2 mm. Adaptado de Casanova Sáez (2014).

La clase fenotípica Apiculata incluye a 8 mutantes que fueron aislados tras una mutagénesis con metanosulfonato de etilo (EMS) del acceso Landsberg *erecta* (*Ler*), que corresponden a 7 genes (*API1-API7*; Berná *et al.*, 1999). Aunque se conocen las posiciones de mapa de todos los genes *API*, solo se han clonado posicionalmente *API2* y *API7* (Robles y Micol, 2001; Casanova-Sáez *et al.*, 2014a). El gen *API2* (también denominado *RPL36a*) y su parólogo *RPL36aA* son funcionalmente redundantes: ambos codifican la proteína ribosómica RPL36a de la subunidad 60S del ribosoma citoplásmico, y la no complementación no alélica de los alelos hipomorfos *api2* y *rpl36aa* en plantas diheterocigóticas *API2/api2;RPL36aA/rpl36aa* rinde el mismo fenotipo que el de los mutantes simples homocigóticos (Figura 5C; Casanova-Sáez *et al.*, 2014a). El gen al que se denominó

inicialmente *API7* en el laboratorio de J.L. Micol es *ABCE2* y codifica una proteína que es esencial para el reciclaje del ribosoma citoplásmico en las arqueas y los eucariotas. El único alelo viable de *ABCE2* descrito es *api7-1*, cuyo fenotipo foliar es similar al de los alelos de insuficiencia de función de genes que codifican componentes de la maquinaria de la traducción (Figura 5H).

IV.3.3.- Objetivos de esta Tesis

Los dos objetivos generales definidos inicialmente para esta Tesis fueron completar la caracterización fenotípica del mutante *api7-1*, previamente iniciada en el laboratorio de J.L. Micol, y determinar, con el máximo grado de detalle posible, la función del gen *ABCE2* mediante abordajes genéticos y moleculares.

En concreto, nos propusimos: (1) revisar el estado del arte sobre la función de las proteínas ABCE en las especies en las que se hubiese estudiado; (2) confirmar que el gen *ABCE2* es el causante exclusivo del fenotipo del mutante *api7-1*, mediante la obtención de alelos adicionales de este gen y su análisis de complementación; (3) establecer la localización subcelular de la proteína *ABCE2*, mediante la construcción y visualización de la expresión de fusiones traduccionales del gen *ABCE2* y los de determinadas proteínas fluorescentes; (4) determinar el patrón de expresión espacial de *ABCE2* y *ABCE1*; (5) estudiar la eventual redundancia funcional de estos dos genes parálogos, mediante el intercambio de sus promotores; (6) llevar a cabo un análisis filogenético de *ABCE1* y *ABCE2*; (7) identificar proteínas interactoras de *ABCE2* que aportasen información sobre la participación de esta última en la traducción; (8) completar el estudio del fenotipo de *api7-1* a niveles morfológico, histoquímico y molecular, (9) prestando especial atención al patrón vascular de sus hojas; (10) estudiar una posible alteración de la homeostasis de la auxina en *api7-1*, visualizando la expresión de transgenes testigo de su transporte y percepción; (11) identificar otros procesos biológicos potencialmente alterados en *api7-1* mediante la secuenciación masiva de su transcriptoma; y (12) proponer un modelo que explicase la relación entre la función molecular de *ABCE2* y los efectos fenotípicos causados por la pérdida parcial de su función en el mutante *api7-1*.

V.- MATERIALES Y MÉTODOS

V.- MATERIALES Y MÉTODOS

Para la redacción de los apartados I a VII de esta memoria se han seguido las mismas pautas que en Tesis anteriores de los laboratorios de M.R. Ponce y J.L. Micol. En este apartado de Materiales y métodos se reproducen literalmente algunas frases procedentes de dichas Tesis. Se ha preferido usar los acrónimos castellanizados ADN y ARN —de uso común en los medios de comunicación españoles—, en lugar de los recomendados por la International Union of Pure and Applied Chemistry, DNA y RNA, para los ácidos desoxirribonucleico y ribonucleico, respectivamente. Esta elección no está basada en ningún argumento que se considere incontestable; ambas opciones son aceptadas por el *Diccionario de la Lengua Española* (vigésimotercera edición, 2014) de la Real Academia Española (RAE). Tal como recomienda la RAE en su *Ortografía de la lengua española* (2010), en esta memoria no se realiza el plural de las siglas añadiendo al final una s minúscula: se escribe “el ARN” y también “los ARN”.

La nomenclatura que se aplica en esta memoria a genes, mutaciones y fenotipos nuevos se atiene a las pautas propuestas para *Arabidopsis* por Meinke y Koornneef (1997). No hemos traducido al español muchos de los nombres de genes y proteínas que se mencionan en esta memoria; en estos casos solo hemos usado la cursiva para los genes. Los transgenes se denotan según lo establecido en las instrucciones a los autores de la revista *Plant Cell*. Los genotipos completos, como *api7-1/api7-2*, en los que los alelos de un gen en cromosomas homólogos se separan con una barra, se han utilizado únicamente cuando fue imprescindible. Salvo que se indique lo contrario, los individuos que se describen en este trabajo son homocigóticos para la mutación que se menciona en cada caso. Hemos utilizado en algunos casos un punto y coma como separador entre mutaciones no alélicas.

Las estirpes de *Arabidopsis*, su manipulación y las condiciones de cultivo usadas en esta Tesis se describen en la página 53. Hemos realizado análisis histológicos y morfométricos, histoquímicos y de microscopía confocal de los mutantes a estudio (en las páginas 54-56). Hemos aislado ARN para su retrotranscripción seguida de PCR cuantitativa y para su secuenciación masiva (en las páginas 56 y 57). Hemos generado construcciones de intercambio de promotores, y fusiones traduccionales con los genes de las proteínas fluorescentes verde y amarilla (en la página 54). También hemos realizado experimentos de coimmunoprecipitación de proteínas (en la página 58) y alineamientos de secuencias aminoacídicas, por parejas y múltiples, así como otros análisis bioinformáticos y búsquedas *in silico* (en la página 59).

VI.- RESULTADOS Y DISCUSIÓN

VI.- RESULTADOS Y DISCUSIÓN

En esta Tesis se ha realizado una disección genética y molecular de la función del gen *ABCE2* de *Arabidopsis*. Hemos confirmado mediante ensayos de complementación que *api7-1* es un alelo hipomorfo y viable, y *api7-2*, nulo y letal recesivo, de dicho gen (en la página 60). Hemos determinado los patrones de expresión de *ABCE2* y de su único parólogo, *ABCE1*, concluyendo que *ABCE2* es de expresión constitutiva y generalizada y que *ABCE1* se expresa muy poco (en la página 62). Mediante un ensayo de intercambio de promotores hemos comprobado que el transgén *ABCE2_{pro}:ABCE1*, pero no el *ABCE1_{pro}:ABCE2*, restablece parcialmente el fenotipo silvestre en las plantas *api7-1* (en la página 62).

Hemos estudiado el fenotipo de *api7-1* mediante la determinación de la longitud de su raíz principal, que es más corta que la silvestre; la cuantificación de los pigmentos fotosintéticos y los niveles de ploidía de las hojas de su roseta, que están reducidos e incrementados, respectivamente; el análisis de la filotaxia de la roseta, que es indistinguible de la silvestre; y la disección y observación de sus frutos, estableciendo que la fertilidad de *api7-1* es similar a la silvestre (en la página 60). Además, hemos analizado el patrón vascular de sus cotiledones, hojas del primer y tercer nudos de la roseta, hojas caulinares, sépalos y pétalos; las mayores diferencias con los órganos silvestres se apreciaron en las hojas del primer nudo de la roseta (en la página 65). En estas últimas se observó una venación más densa en torno al hidatodo apical y menos venas de órdenes superiores en el mutante *api7-1* que en su tipo silvestre. Hemos visualizado el transporte y la percepción de la auxina en plantas portadoras de transgenes testigo, concluyendo que en *api7-1* están disminuido e incrementada, respectivamente (en la página 66). También hemos secuenciado masivamente el transcriptoma de *api7-1*, constatando la desregulación de procesos biológicos relacionados con el metabolismo y la señalización de la auxina, las respuestas al déficit de iones de hierro y azufre, y el estrés oxidativo (en la página 67).

Hemos demostrado que *ABCE2* es una proteína citoplásmica, mediante la obtención de fusiones traduccionales *ABCE2:GFP* y *ABCE2:YFP* y la visualización de las proteínas híbridas correspondientes (en la página 63). Hemos realizado un ensayo de coimmunoprecipitación con la proteína de fusión *ABCE2:YFP*, identificado 20 presuntos interactores, la mayoría de los cuales están relacionados con la traducción (en la página 63), lo que sugiere que *ABCE2* participa en este proceso (Figura 6, en la página 26). La interacción de *ABCE2* con eIF3j que hemos observado en *Arabidopsis* también se ha constatado entre sus ortólogas en *Saccharomyces cerevisiae* y humanas; en estas especies se ha demostrado

que las ortólogas de ABCE2 disocian al ribosoma durante el reciclaje de los ribosomas (Young y Guydosh, 2019; Kratzat *et al.*, 2021).

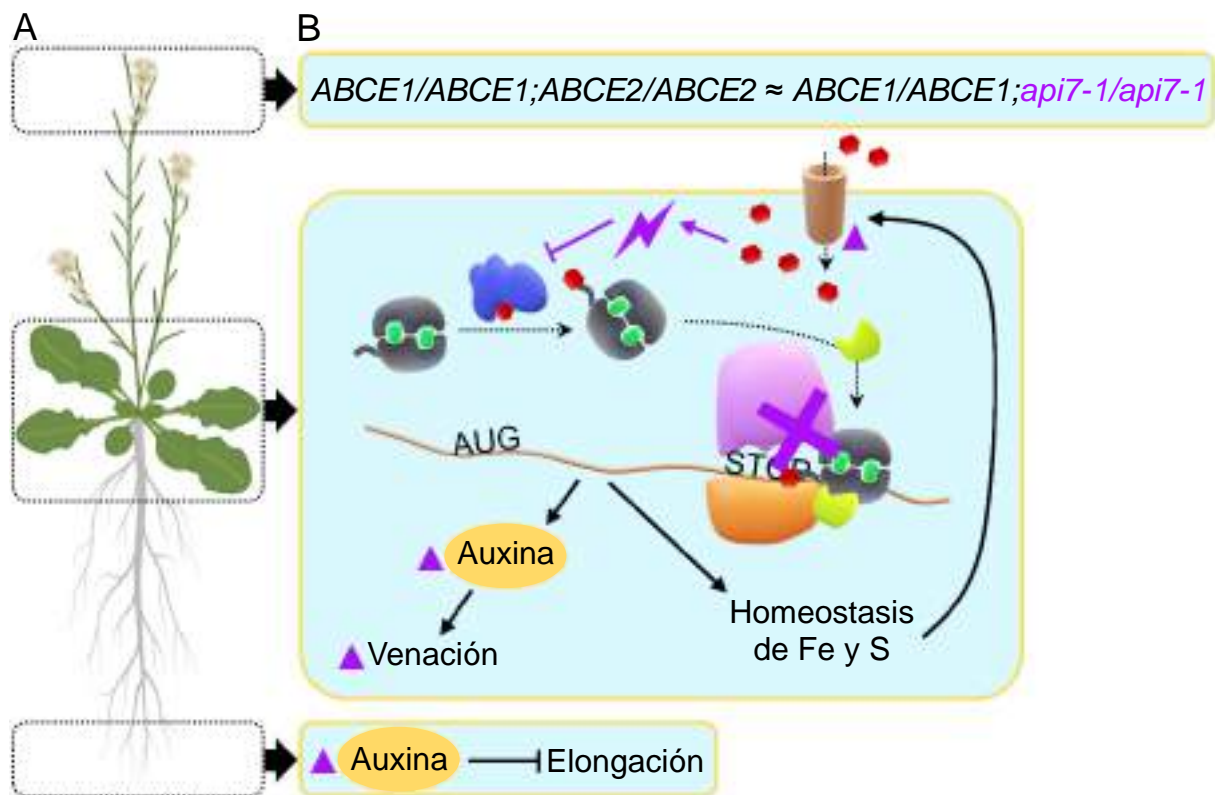


Figura 6.- Hipótesis sobre la función de la proteína ABCE2 y los efectos de la mutación *api7-1*. (A) Representación de la estructura de una planta adulta de *Arabidopsis*, con indicación, mediante rectángulos punteados, de los órganos del mutante *api7-1* estudiados en esta Tesis. Modificada a partir de Norris *et al.* (2021). (B) Modelo que proponemos para la función de ABCE2, representada como en la Figura 1, en la página 7. En una situación de insuficiencia de la función de ABCE2 como la que causa la mutación *api7-1*, ABCE1 podría mantener el fenotipo silvestre en las inflorescencias, pero no en las hojas o las raíces. La proteína codificada por At2g20830 (en azul) ensambla los grupos FeS en ABCE2. La subunidad eIF3j (en amarillo) contribuye con ABCE2 a la disociación del ribosoma. El ribosoma y el ARNm se representan como en la Figura 1; la auxina y las flechas, como en la Figura 2, en la página 11. Los elementos morados indican los efectos de la mutación *api7-1*: X: consecuencia directa; ▲: incremento; ⚡: especies reactivas del oxígeno.

Las proteínas ABCE tienen un dominio de unión a dos grupos FeS que las diferencia de las ABC solubles y es esencial para su función en la disociación de los ribosomas (Barthelme *et al.*, 2007). Nuestros resultados sugieren que ABCE2 también tiene un dominio de unión a FeS funcional. En efecto, ABCE2 interacciona con la proteína codificada por el gen At2g20830, que en otras especies es necesaria para el ensamblaje de grupos FeS (Zhai *et al.*, 2014; Paul *et al.*, 2015), y en el mutante *api7-1* está aparentemente activada la respuesta

al déficit de iones de hierro y azufre, quizás como consecuencia de la reducida actividad de la proteína ABCE2 mutante. Adicionalmente, un incremento intracelular de estos iones podría inducir la generación de especies reactivas del oxígeno (Briat *et al.*, 2010), tal como sugiere la activación de la respuesta al estrés oxidativo que hemos observado en *api7-1*. A su vez, el estrés oxidativo podría impedir el ensamblaje de grupos FeS en la proteína ABCE2 mutante, disminuyendo aún más su actividad (Alhebshi *et al.*, 2012; Sudmant *et al.*, 2018; Zhu *et al.*, 2020).

En el ápice de los primordios foliares se sintetiza la auxina de forma local, y su transporte polar basípeto induce la formación de los haces vasculares en todo el limbo (Linh *et al.*, 2018; Kneuper *et al.*, 2021). Un incremento en la síntesis de auxina en los primordios de *api7-1*, tal como sugieren los resultados de nuestro análisis transcriptómico, junto con una presunta disminución en su transporte polar, podrían ser las causas de la desigual diferenciación del tejido vascular observada a lo largo del eje proximodistal en las hojas de *api7-1*, y de su menor contenido en venas de órdenes superiores. Además, una producción excesiva de auxina en las raíces de *api7-1* podría inhibir su elongación (Fendrych *et al.*, 2018).

Por último, nuestros resultados sugieren que existe cierto grado de redundancia funcional entre *ABCE1* y *ABCE2*: *ABCE1* rescata parcialmente el fenotipo de *api7-1* cuando se expresa bajo el control del promotor de *ABCE2*. Que este rescate no sea completo puede deberse a que la secuencia de *ABCE1*, al igual que las de sus ortólogas en otras brassicáceas, está sujeta a una menor presión selectiva que sus parálogas *ABCE2*. No obstante, el órgano que muestra una mayor expresión de *ABCE1*, la flor, no presenta alteraciones evidentes en el mutante *api7-1*, que tampoco se aprecian en los patrones de venación de los sépalos y pétalos, lo que sugiere que *ABCE1* mantiene parte de su función ancestral.

VII.- CONCLUSIONES Y PERSPECTIVAS

VII.- CONCLUSIONES Y PERSPECTIVAS

VII.1.- Las proteínas ABCE de las plantas participan en la traducción

Las proteínas ABCE, presentes en los eucariotas y las arqueas, llevan a cabo el reciclaje de los ribosomas citoplásmicos, según se ha demostrado en algunas arqueas, levaduras y animales. En esta Tesis se han obtenido por primera vez indicios de la implicación de una proteína ABCE vegetal, la ABCE2 de *Arabidopsis*, en la traducción. Se requerirán ensayos adicionales para confirmar dicha implicación, como la secuenciación masiva de segmentos de ARNm unidos a ribosomas de *api7-1*. Este ensayo consiste en la digestión mediante una RNasa de un extracto de polisomas, y la posterior secuenciación masiva de los fragmentos de las moléculas de ARNm que no hayan sido digeridas como consecuencia de su unión a un ribosoma. Pueden identificarse así las posiciones en las que se encuentran los ribosomas en todas las moléculas de ARNm de una muestra. Se ha demostrado de este modo en células humanas y de *Saccharomyces cerevisiae* que la insuficiencia de la función de ABCE1 dificulta el reciclaje de los ribosomas, que tras la terminación de la traducción se internan en la 3' UTR, en la que desplazan los factores reguladores unidos al ARNm que encuentran a su paso.

Nuestros resultados también indican la existencia de redundancia funcional entre las proteínas ABCE2 y ABCE1, pero no entre los promotores de los genes que las codifican. La menor presión selectiva que parecen haber sufrido los genes *ABCE1* de las brasicáceas, así como el bajo nivel de expresión de *ABCE1* en *Arabidopsis*, sugieren que este último —y probablemente también sus ortólogos más próximos— ha sufrido un proceso de subfuncionalización o pseudogenización, mientras que ABCE2 mantiene la función ancestral. La obtención y el estudio de alelos mutantes de *ABCE1*, y de considerarse conveniente, la determinación de la localización subcelular de ABCE1 y la identificación de sus interactores, permitirían comprender su función, si es que la tiene.

VII.2.- La caracterización del mutante *api7-1* contribuye a la comprensión de la relación entre la traducción y el desarrollo

Una parte de esta Tesis es la revisión bibliográfica de los efectos sobre el desarrollo de la pérdida de la función de las proteínas ABCE, concluyéndose que estas proteínas son esenciales en todos los organismos estudiados, y que la mayoría de los alelos mutantes de los genes *ABCE* disponibles son nulos y letales recesivos, lo que dificulta el estudio de los efectos de la insuficiencia de función de estos genes durante el desarrollo. En esta memoria se describe un estudio de *api7-1*, un alelo hipomorfo del gen *ABCE2* de *Arabidopsis*, cuyo

fenotipo incluye algunos rasgos comunes a los asociados a la insuficiencia de función de genes que codifican componentes de la maquinaria de la traducción: una roseta pequeña con hojas apuntadas e indentadas y con una venación aberrante. Un fenotipo similar a este es el que causa *sil3*, un alelo hipomorfo del único gen *ABCE* identificado en *Cardamine hirsuta*, cuyas hojas son simples, mientras que las del tipo silvestre son compuestas, y presentan alteraciones en su venación. Autores anteriores han relacionado estos rasgos fenotípicos con la perturbación de la homeostasis de la auxina. La secuenciación masiva del transcriptoma de *api7-1* sugiere que sintetiza más auxina que el tipo silvestre. La cuantificación en *api7-1* del contenido en ácido indolacético —la auxina mayoritaria en las plantas— y sus metabolitos permitiría establecer si las alteraciones del transcriptoma que hemos constatado tienen consecuencias, tal como cabe esperar, en el metaboloma.

Además de las alteraciones relacionadas con la homeostasis de la auxina, nuestro análisis de enriquecimiento funcional del transcriptoma de *api7-1* identificó más de 200 procesos alterados en este mutante, entre los que destacan, por su relación con los grupos FeS de ABCE2, las respuestas a los déficits de hierro y azufre, y al estrés oxidativo. El gran número de procesos alterados en *api7-1* impide establecer cuáles son consecuencia directa de la pérdida de función de ABCE2. También en este aspecto la obtención de un perfil ribosómico de *api7-1* permitiría confirmar el papel de ABCE2 en la disociación de los ribosomas, así como identificar los ARNm más sensibles a la perturbación de este proceso.

**VIII.- BIBLIOGRAFÍA
DE LOS APARTADOS IV-VII**

VIII.- BIBLIOGRAFÍA DE LOS APARTADOS IV-VII

- Alhebshi, A., Sideri, T.C., Holland, S.L., y Avery, S.V. (2012). The essential iron-sulfur protein Rli1 is an important target accounting for inhibition of cell growth by reactive oxygen species. *Molecular Biology of the Cell* **23**, 3582-3590.
- Andersen, D.S., y Leever, S.J. (2007). The essential *Drosophila* ATP-binding cassette domain protein, Pixie, binds the 40 S ribosome in an ATP-dependent manner and is required for translation initiation. *Journal of Biological Chemistry* **282**, 14752-14760.
- Anderson, S.J., Kramer, M.C., Gosai, S.J., Yu, X., Vandivier, L.E., Nelson, A.D.L., Anderson, Z.D., Beilstein, M.A., Fray, R.G., Lyons, E., y Gregory, B.D. (2018). N⁶-Methyladenosine inhibits local ribonucleolytic cleavage to stabilize mRNAs in *Arabidopsis*. *Cell Reports* **25**, 1146-1157.
- Baima, S., Nobili, F., Sessa, G., Lucchetti, S., Ruberti, I., y Morelli, G. (1995). The expression of the *Athb-8* homeobox gene is restricted to provascular cells in *Arabidopsis thaliana*. *Development* **121**, 4171-4182.
- Baima, S., Forte, V., Possenti, M., Peñalosa, A., Leoni, G., Salvi, S., Felici, B., Ruberti, I., y Morelli, G. (2014). Negative feedback regulation of auxin signaling by ATHB8/ACL5–BUD2 transcription module. *Molecular Plant* **7**, 1006-1025.
- Barthelme, D., Scheele, U., Dinkelaker, S., Janoschka, A., MacMillan, F., Albers, S.V., Driessen, A.J., Stagni, M.S., Bill, E., Meyer-Klaucke, W., Schünemann, V., y Tampé, R. (2007). Structural organization of essential iron-sulfur clusters in the evolutionarily highly conserved ATP-binding cassette protein ABCE1. *Journal of Biological Chemistry* **282**, 14598-14607.
- Baum, S.F., Dubrovsky, J.G., y Rost, T.L. (2002). Apical organization and maturation of the cortex and vascular cylinder in *Arabidopsis thaliana* (Brassicaceae) roots. *American Journal of Botany* **89**, 908-920.
- Berleth, T., Mattsson, J., y Hardtke, C.S. (2000). Vascular continuity and auxin signals. *Trends in Plant Science* **5**, 387-393.
- Berná, G., Robles, P., y Micol, J.L. (1999). A mutational analysis of leaf morphogenesis in *Arabidopsis thaliana*. *Genetics* **152**, 729-742.
- Biedroń, M., y Banasiak, A. (2018). Auxin-mediated regulation of vascular patterning in *Arabidopsis thaliana* leaves. *Plant Cell Reports* **37**, 1215-1229.
- Bishopp, A., Help, H., El-Showk, S., Weijers, D., Scheres, B., Friml, J., Benková, E., Mähönen, A.P., y Helariutta, Y. (2011). A mutually inhibitory interaction between auxin and cytokinin specifies vascular pattern in roots. *Current Biology* **21**, 917-926.
- Boël, G., Smith, P.C., Ning, W., Englander, M.T., Chen, B., Hashem, Y., Testa, A.J., Fischer, J.J., Wieden, H.J., Frank, J., Gonzalez, R.L., Jr., y Hunt, J.F. (2014). The ABC-F protein EttA gates ribosome entry into the translation elongation cycle. *Nature Structural and Molecular Biology* **21**, 143-151.
- Briat, J.F., Duc, C., Ravet, K., y Gaymard, F. (2010). Ferritins and iron storage in plants. *Biochimica et Biophysica Acta* **1800**, 806-814.
- Bühler, J., Rishmawi, L., Pflugfelder, D., Huber, G., Scharr, H., Hülskamp, M., Koornneef, M., Schurr, U., y Jahnke, S. (2015). phenoVein—A tool for leaf vein segmentation and analysis. *Plant Physiology* **169**, 2359-2370.
- Byrne, M.E. (2009). A role for the ribosome in development. *Trends in Plant Science* **14**, 512-519.
- Caggiano, M.P., Yu, X., Bhatia, N., Larsson, A., Ram, H., Ohno, C.K., Sappl, P., Meyerowitz, E.M., Jönsson, H., y Heisler, M.G. (2017). Cell type boundaries organize plant development. *eLife* **6**, e27421.
- Campbell, L., y Turner, S. (2017). Regulation of vascular cell division. *Journal of Experimental Botany* **68**, 27-43.

- Candela, H., Martínez-Laborda, A., y Micol, J.L. (1999). Venation pattern formation in *Arabidopsis thaliana* vegetative leaves. *Developmental Biology* **205**, 205-216.
- Casanova-Sáez, R., Candela, H., y Micol, J.L. (2014a). Combined haploinsufficiency and purifying selection drive retention of *RPL36a* paralogs in Arabidopsis. *Scientific Reports* **4**, 4122.
- Casanova-Sáez, R., Mateo-Bonmatí, E., Kangasjärvi, S., Candela, H., y Micol, J.L. (2014b). *Arabidopsis* ANGULATA10 is required for thylakoid biogenesis and mesophyll development. *Journal of Experimental Botany* **65**, 2391-2404.
- Casanova Sáez, R. (2014). Contribución de los genes *ANGULATA10* y *APICULATA2* a la morfogénesis foliar en *Arabidopsis thaliana*. Tesis doctoral. Universidad Miguel Hernández.
- Clark, S.E., Williams, R.W., y Meyerowitz, E.M. (1997). The *CLAVATA1* gene encodes a putative receptor kinase that controls shoot and floral meristem size in Arabidopsis. *Cell* **89**, 575-585.
- Clay, N.K., y Nelson, T. (2005). Arabidopsis *thickvein* mutation affects vein thickness and organ vascularization, and resides in a provascular cell-specific spermine synthase involved in vein definition and in polar auxin transport. *Plant Physiology* **138**, 767-777.
- Chaffey, N., Cholewa, E., Regan, S., y Sundberg, B. (2002). Secondary xylem development in *Arabidopsis*: a model for wood formation. *Physiologia Plantarum* **114**, 594-600.
- Choi, C.C., y Ford, R.C. (2021). ATP binding cassette importers in eukaryotic organisms. *Biological Reviews of the Cambridge Philosophical Society*, doi: 10.1111/brv.12702
- David-Assael, O., Saul, H., Saul, V., Mizrachy-Dagri, T., Berezin, I., Brook, E., y Shaul, O. (2005). Expression of AtMHX, an *Arabidopsis* vacuolar metal transporter, is repressed by the 5' untranslated region of its gene. *Journal of Experimental Botany* **56**, 1039-1047.
- De Rybel, B., Adibi, M., Breda, A.S., Wendrich, J.R., Smit, M.E., Novák, O., Yamaguchi, N., Yoshida, S., Van Isterdael, G., Palovaara, J., Nijssse, B., Boekschoten, M.V., Hooiveld, G., Beeckman, T., Wagner, D., Ljung, K., Fleck, C., y Weijers, D. (2014). Integration of growth and patterning during vascular tissue formation in *Arabidopsis*. *Science* **345**, 1255215.
- Dean, M., y Allikmets, R. (2001). Complete characterization of the human ABC gene family. *Journal of Bioenergetics and Biomembranes* **33**, 475-479.
- Dean, M., y Annilo, T. (2005). Evolution of the ATP-binding cassette (ABC) transporter superfamily in vertebrates. *Annual Review of Genomics and Human Genetics* **6**, 123-142.
- Dhondt, S., Van Haerenborgh, D., Van Cauwenbergh, C., Merks, R.M., Philips, W., Beemster, G.T., e Inzé, D. (2012). Quantitative analysis of venation patterns of Arabidopsis leaves by supervised image analysis. *Plant Journal* **69**, 553-563.
- Donner, T.J., Sherr, I., y Scarpella, E. (2009). Regulation of preprocambial cell state acquisition by auxin signaling in *Arabidopsis* leaves. *Development* **136**, 3235-3246.
- Ebina, I., Takemoto-Tsutsumi, M., Watanabe, S., Koyama, H., Endo, Y., Kimata, K., Igarashi, T., Murakami, K., Kudo, R., Ohsumi, A., Noh, A.L., Takahashi, H., Naito, S., y Onouchi, H. (2015). Identification of novel *Arabidopsis thaliana* upstream open reading frames that control expression of the main coding sequences in a peptide sequence-dependent manner. *Nucleic Acids Research* **43**, 1562-1576.
- Esteve-Bruna, D., Pérez-Pérez, J.M., Ponce, M.R., y Micol, J.L. (2013). *incurvata13*, a novel allele of *AUXIN RESISTANT6*, reveals a specific role for auxin and the SCF complex in Arabidopsis embryogenesis, vascular specification, and leaf flatness. *Plant Physiology* **161**, 1303-1320.
- Fendrych, M., Akhmanova, M., Merrin, J., Glanc, M., Hagihara, S., Takahashi, K., Uchida, N., Torii, K.U., y Friml, J. (2018). Rapid and reversible root growth inhibition by TIR1 auxin signalling. *Nature Plants* **4**, 453-459.
- Ferrández-Ayela, A., Alonso-Peral, M.M., Sánchez-García, A.B., Micol-Ponce, R., Pérez-Pérez, J.M., Micol, J.L., y Ponce, M.R. (2013). Arabidopsis *TRANSCURVATA1* encodes NUP58, a component of the nucleopore central channel. *PLOS ONE* **8**, e67661.
- Fostier, C.R., Monlezun, L., Ousalem, F., Singh, S., Hunt, J.F., y Boël, G. (2021). ABC-F translation factors: from antibiotic resistance to immune response. *FEBS Letters* **595**, 675-706.

- Fu, Y., Xu, L., Xu, B., Yang, L., Ling, Q., Wang, H., y Huang, H. (2007). Genetic interactions between leaf polarity-controlling genes and *ASYMMETRIC LEAVES1* and *2* in *Arabidopsis* leaf patterning. *Plant and Cell Physiology* **48**, 724-735.
- García-Barrio, M., Dong, J., Ufano, S., y Hinnebusch, A.G. (2000). Association of GCN1–GCN20 regulatory complex with the N-terminus of eIF2 α kinase GCN2 is required for GCN2 activation. *EMBO Journal* **19**, 1887-1899.
- Govindaraju, P., Verna, C., Zhu, T., y Scarpella, E. (2020). Vein patterning by tissue-specific auxin transport. *Development* **147**, 1-7.
- Hayashi, N., Sasaki, S., Takahashi, H., Yamashita, Y., Naito, S., y Onouchi, H. (2017). Identification of *Arabidopsis thaliana* upstream open reading frames encoding peptide sequences that cause ribosomal arrest. *Nucleic Acids Research* **45**, 8844-8858.
- Heisler, M.G., Ohno, C., Das, P., Sieber, P., Reddy, G.V., Long, J.A., y Meyerowitz, E.M. (2005). Patterns of auxin transport and gene expression during primordium development revealed by live imaging of the *Arabidopsis* inflorescence meristem. *Current Biology* **15**, 1899-1911.
- Herud-Sikimić, O., Stiel, A.C., Kolb, M., Shanmugaratnam, S., Berendzen, K.W., Feldhaus, C., Höcker, B., y Jürgens, G. (2021). A biosensor for the direct visualization of auxin. *Nature* **592**, 768–772.
- Heuer, A., Gerovac, M., Schmidt, C., Trowitzsch, S., Preis, A., Kötter, P., Berninghausen, O., Becker, T., Beckmann, R., y Tampé, R. (2017). Structure of the 40S-ABCE1 post-splitting complex in ribosome recycling and translation initiation. *Nature Structural and Molecular Biology* **24**, 453-460.
- Higgins, C.F. (1992). ABC transporters: from microorganisms to man. *Annual Review of Cell Biology* **8**, 67-113.
- Holland, I.B., y Blight, M.A. (1999). ABC-ATPases, adaptable energy generators fuelling transmembrane movement of a variety of molecules in organisms from bacteria to humans. *Journal of Molecular Biology* **293**, 381-399.
- Hopfner, K.P. (2016). Architectures and mechanisms of ATP binding cassette proteins. *Biopolymers* **105**, 492-504.
- Horiguchi, G., Mollá-Morales, A., Pérez-Pérez, J.M., Kojima, K., Robles, P., Ponce, M.R., Micol, J.L., y Tsukaya, H. (2011). Differential contributions of ribosomal protein genes to *Arabidopsis thaliana* leaf development. *Plant Journal* **65**, 724-736.
- Hu, Q., Merchante, C., Stepanova, A.N., Alonso, J.M., y Heber, S. (2016). Genome-wide search for translated upstream open reading frames in *Arabidopsis thaliana*. *IEEE Transactions on NanoBioscience* **15**, 148-157.
- Imai, A., Hanzawa, Y., Komura, M., Yamamoto, K.T., Komeda, Y., y Takahashi, T. (2006). The dwarf phenotype of the *Arabidopsis acl5* mutant is suppressed by a mutation in an upstream ORF of a bHLH gene. *Development* **133**, 3575-3585.
- Imai, A., Komura, M., Kawano, E., Kuwashiro, Y., y Takahashi, T. (2008). A semi-dominant mutation in the ribosomal protein L10 gene suppresses the dwarf phenotype of the *acl5* mutant in *Arabidopsis thaliana*. *Plant Journal* **56**, 881-890.
- Inada, T. (2017). The ribosome as a platform for mRNA and nascent polypeptide quality control. *Trends in Biochemical Sciences* **42**, 5-15.
- Iwakawa, H., Iwasaki, M., Kojima, S., Ueno, Y., Soma, T., Tanaka, H., Semiarti, E., Machida, Y., y Machida, C. (2007). Expression of the *ASYMMETRIC LEAVES2* gene in the adaxial domain of *Arabidopsis* leaves represses cell proliferation in this domain and is critical for the development of properly expanded leaves. *Plant Journal* **51**, 173-184.
- Iwasaki, M., Takahashi, H., Iwakawa, H., Nakagawa, A., Ishikawa, T., Tanaka, H., Matsumura, Y., Pekker, I., Eshed, Y., Vial-Pradel, S., Ito, T., Watanabe, Y., Ueno, Y., Fukazawa, H., Kojima, S., Machida, Y., y Machida, C. (2013). Dual regulation of *ETTIN* (*ARF3*) gene expression by AS1-AS2, which maintains the DNA methylation level, is involved in stabilization of leaf adaxial-abaxial partitioning in *Arabidopsis*. *Development* **140**, 1958-1969.

- Izquierdo, Y., Kulasekaran, S., Benito, P., López, B., Marcos, R., Cascón, T., Hamberg, M., y Castresana, C. (2018). *Arabidopsis nonresponding to oxylipins* locus *NOXY7* encodes a yeast GCN1 homolog that mediates noncanonical translation regulation and stress adaptation. *Plant, Cell and Environment* **41**, 1438-1452.
- Kachroo, A.H., Laurent, J.M., Yellman, C.M., Meyer, A.G., Wilke, C.O., y Marcotte, E.M. (2015). Systematic humanization of yeast genes reveals conserved functions and genetic modularity. *Science* **348**, 921-925.
- Takehi, J., Kawano, E., Yoshimoto, K., Cai, Q., Imai, A., y Takahashi, T. (2015). Mutations in ribosomal proteins, RPL4 and RACK1, suppress the phenotype of a thermospermine-deficient mutant of *Arabidopsis thaliana*. *PLOS ONE* **10**, e0117309.
- Karampelias, M., Neyt, P., De Groeve, S., Aesaert, S., Coussens, G., Rolčík, J., Bruno, L., De Winne, N., Van Minnebruggen, A., Van Montagu, M., Ponce, M.R., Micol, J.L., Friml, J., De Jaeger, G., y Van Lijsebettens, M. (2016). ROTUNDA3 function in plant development by phosphatase 2A-mediated regulation of auxin transporter recycling. *Proceedings of the National Academy of Sciences USA* **113**, 2768-2773.
- Kärblane, K., Gerassimenko, J., Nigul, L., Piirsoo, A., Smialowska, A., Vinkel, K., Kylsten, P., Ekwall, K., Swoboda, P., Truve, E., y Sarmiento, C. (2015). ABCE1 is a highly conserved RNA silencing suppressor. *PLOS ONE* **10**, e0116702.
- Karcher, A., Schele, A., y Hopfner, K.P. (2008). X-ray structure of the complete ABC enzyme ABCE1 from *Pyrococcus abyssi*. *Journal of Biological Chemistry* **283**, 7962-7971.
- Kashima, I., Takahashi, M., Hashimoto, Y., Sakota, E., Nakamura, Y., e Inada, T. (2014). A functional involvement of ABCE1, eukaryotic ribosome recycling factor, in nonstop mRNA decay in *Drosophila melanogaster* cells. *Biochimie* **106**, 10-16.
- Kaundal, A., Ramu, V.S., Oh, S., Lee, S., Pant, B., Lee, H.K., Rojas, C.M., Senthil-Kumar, M., y Mysore, K.S. (2017). GENERAL CONTROL NONREPRESSIBLE4 degrades 14-3-3 and the RIN4 complex to regulate stomatal aperture with implications on nonhost disease resistance and drought tolerance. *Plant Cell* **29**, 2233-2248.
- Kelley, D.R., Arreola, A., Gallagher, T.L., y Gasser, C.S. (2012). ETTIN (ARF3) physically interacts with KANADI proteins to form a functional complex essential for integument development and polarity determination in *Arabidopsis*. *Development* **139**, 1105-1109.
- Kim, B.H., Cai, X., Vaughn, J.N., y von Arnim, A.G. (2007). On the functions of the h subunit of eukaryotic initiation factor 3 in late stages of translation initiation. *Genome Biology* **8**, R60.
- Kim, T.H., Kim, B.H., Yahalom, A., Chamovitz, D.A., y von Arnim, A.G. (2004). Translational regulation via 5' mRNA leader sequences revealed by mutational analysis of the Arabidopsis translation initiation factor subunit eIF3h. *Plant Cell* **16**, 3341-3356.
- Kneuper, I., Teale, W., Dawson, J.E., Tsugeki, R., Katifori, E., Palme, K., y Ditegou, F.A. (2021). Auxin biosynthesis and cellular efflux act together to regulate leaf vein patterning. *Journal of Experimental Botany* **72**, 1151-1165.
- Knott, J.M., Römer, P., y Sumper, M. (2007). Putative spermine synthases from *Thalassiosira pseudonana* and *Arabidopsis thaliana* synthesize thermospermine rather than spermine. *FEBS Letters* **581**, 3081-3086.
- Kougioumoutzi, E., Cartolano, M., Canales, C., Dupré, M., Bramsieve, J., Vlad, D., Rast, M., Ioio, R.D., Tattersall, A., Schnittger, A., Hay, A., y Tsiantis, M. (2013). *SIMPLE LEAF3* encodes a ribosome-associated protein required for leaflet development in *Cardamine hirsuta*. *Plant Journal* **73**, 533-545.
- Kratz, H., Mackens-Kiani, T., Ameismeier, M., Potocnjak, M., Cheng, J., Dacheux, E., Namane, A., Berninghausen, O., Herzog, F., Fromont-Racine, M., Becker, T., y Beckmann, R. (2021). A structural inventory of native ribosomal ABCE1-43S pre-initiation complexes. *EMBO Journal* **40**, e105179.

- Krogan, N.T., Marcos, D., Weiner, A.I., y Berleth, T. (2016). The auxin response factor MONOPTEROS controls meristem function and organogenesis in both the shoot and root through the direct regulation of *PIN* genes. *New Phytologist* **212**, 42-50.
- Laing, W.A., Martínez-Sánchez, M., Wright, M.A., Bulley, S.M., Brewster, D., Dare, A.P., Rassam, M., Wang, D., Storey, R., Macknight, R.C., y Hellens, R.P. (2015). An upstream open reading frame is essential for feedback regulation of ascorbate biosynthesis in *Arabidopsis*. *Plant Cell* **27**, 772-786.
- Liao, C.Y., Smet, W., Brunoud, G., Yoshida, S., Vernoux, T., y Weijers, D. (2015). Reporters for sensitive and quantitative measurement of auxin response. *Nature Methods* **12**, 207-210.
- Linh, N.M., Verna, C., y Scarpella, E. (2018). Coordination of cell polarity and the patterning of leaf vein networks. *Current Opinion in Plant Biology* **41**, 116-124.
- Liu, S., Li, Q., y Liu, Z. (2013). Genome-wide identification, characterization and phylogenetic analysis of 50 catfish ATP-binding cassette (ABC) transporter genes. *PLOS ONE* **8**, e63895.
- Locher, K.P. (2016). Mechanistic diversity in ATP-binding cassette (ABC) transporters. *Nature Structural and Molecular Biology* **23**, 487-493.
- Lu, H., Xu, Y., y Cui, F. (2016). Phylogenetic analysis of the ATP-binding cassette transporter family in three mosquito species. *Pesticide Biochemistry and Physiology* **132**, 118-124.
- Mähönen, A.P., Bonke, M., Kauppinen, L., Riikonen, M., Benfey, P.N., y Helariutta, Y. (2000). A novel two-component hybrid molecule regulates vascular morphogenesis of the *Arabidopsis* root. *Genes and Development* **14**, 2938-2943.
- Mähönen, A.P., Bishopp, A., Higuchi, M., Nieminen, K.M., Kinoshita, K., Törmäkangas, K., Ikeda, Y., Oka, A., Kakimoto, T., y Helariutta, Y. (2006). Cytokinin signaling and its inhibitor AHP6 regulate cell fate during vascular development. *Science* **311**, 94-98.
- Mancera-Martínez, E., Brito Querido, J., Valasek, L.S., Simonetti, A., y Hashem, Y. (2017). ABCE1: A special factor that orchestrates translation at the crossroad between recycling and initiation. *RNA Biology* **14**, 1279-1285.
- Marton, M.J., Vazquez de Aldana, C.R., Qiu, H., Chakraborty, K., y Hinnebusch, A.G. (1997). Evidence that GCN1 and GCN20, translational regulators of GCN4, function on elongating ribosomes in activation of eIF2 α kinase GCN2. *Molecular and Cellular Biology* **17**, 4474-4489.
- Mateo-Bonmatí, E., Esteve-Bruna, D., Juan-Vicente, L., Nadi, R., Candela, H., Lozano, F.M., Ponce, M.R., Pérez-Pérez, J.M., y Micol, J.L. (2018). *INCURVATA11* and *CUPULIFORMIS2* are redundant genes that encode epigenetic machinery components in *Arabidopsis*. *Plant Cell* **30**, 1596-1616.
- Mattsson, J., Ckurshumova, W., y Berleth, T. (2003). Auxin signaling in *Arabidopsis* leaf vascular development. *Plant Physiology* **131**, 1327-1339.
- Mazur, E., Kurczyńska, E.U., y Friml, J. (2014). Cellular events during interfascicular cambium ontogenesis in inflorescence stems of *Arabidopsis*. *Protoplasma* **251**, 1125-1139.
- McConnell, J.R., y Barton, M.K. (1995). Effect of mutations in the *PINHEAD* gene of *Arabidopsis* on the formation of shoot apical meristems. *Developmental Genetics* **16**, 358-366.
- Meinke, D., y Koornneef, M. (1997). Community standards for *Arabidopsis* genetics. *Plant Journal* **12**, 247-253.
- Micol-Ponce, R., Sarmiento-Mañús, R., Fontcuberta-Cervera, S., Cabezas-Fuster, A., de Bures, A., Sáez-Vásquez, J., y Ponce, M.R. (2020). SMALL ORGAN4 is a ribosome biogenesis factor involved in 5.8S ribosomal RNA maturation. *Plant Physiology* **184**, 2022-2039.
- Micol, J.L. (2009). Leaf development: time to turn over a new leaf? *Current Opinion in Plant Biology* **12**, 9-16.
- Möttus, J., Maiste, S., Eek, P., Truve, E., y Sarmiento, C. (2020). Mutational analysis of *Arabidopsis thaliana* ABCE2 identifies important motifs for its RNA silencing suppressor function. *Plant Biology* **23**, 21-31.
- Muñoz-Nortes, T., Pérez-Pérez, J.M., Ponce, M.R., Candela, H., y Micol, J.L. (2017). The *ANGULATA7* gene encodes a DnaJ-like zinc finger-domain protein involved in chloroplast function and leaf development in *Arabidopsis*. *Plant Journal* **89**, 870-884.

- Murina, V., Kasari, M., Takada, H., Hinno, M., Saha, C.K., Grimshaw, J.W., Seki, T., Reith, M., Putrinš, M., Tenson, T., Strahl, H., Hauryliuk, V., y Atkinson, G.C. (2019). ABCF ATPases involved in protein synthesis, ribosome assembly and antibiotic resistance: structural and functional diversification across the tree of life. *Journal of Molecular Biology* **431**, 3568-3590.
- Nelson, T., y Dengler, N. (1997). Leaf vascular pattern formation. *Plant Cell* **9**, 1121-1135.
- Nishimura, T., Wada, T., Yamamoto, K.T., y Okada, K. (2005). The *Arabidopsis* STV1 protein, responsible for translation reinitiation, is required for auxin-mediated gynoecium patterning. *Plant Cell* **17**, 2940-2953.
- Norris, K., Hopes, T., y Aspden, J.L. (2021). Ribosome heterogeneity and specialization in development. *Wiley Interdisciplinary Reviews: RNA* **12**, e1644.
- Nürenberg-Goloub, E., Heinemann, H., Gerovac, M., y Tampé, R. (2018). Ribosome recycling is coordinated by processive events in two asymmetric ATP sites of ABCE1. *Life Science Alliance* **1**, e201800095.
- Nürenberg, E., y Tampé, R. (2013). Tying up loose ends: ribosome recycling in eukaryotes and archaea. *Trends in Biochemical Sciences* **38**, 64-74.
- Nyikó, T., Auber, A., Szabadkai, L., Benkovics, A., Auth, M., Mérai, Z., Kerényi, Z., Dinnyés, A., Nagy, F., y Silhavy, D. (2017). Expression of the eRF1 translation termination factor is controlled by an autoregulatory circuit involving readthrough and nonsense-mediated decay in plants. *Nucleic Acids Research* **45**, 4174-4188.
- Ochando, I., Jover-Gil, S., Ripoll, J.J., Candela, H., Vera, A., Ponce, M.R., Martínez-Laborda, A., y Micol, J.L. (2006). Mutations in the microRNA complementarity site of the *INCURVATA4* gene perturb meristem function and adaxialize lateral organs in *Arabidopsis*. *Plant Physiology* **141**, 607-619.
- Ohashi-Ito, K., y Fukuda, H. (2003). HD-Zip III homeobox genes that include a novel member, *ZeHB-13* (*Zinnia*)/*ATHB-15* (*Arabidopsis*), are involved in procambium and xylem cell differentiation. *Plant and Cell Physiology* **44**, 1350-1358.
- Ohtani, M., y Wachter, A. (2019). NMD-based gene regulation—A strategy for fitness enhancement in plants? *Plant and Cell Physiology* **60**, 1953-1960.
- Pařízková, B., Žukauskaitė, A., Vain, T., Grones, P., Raggi, S., Kubeš, M.F., Kieffer, M., Doyle, S.M., Strnad, M., Kepinski, S., Napier, R., Doležal, K., Robert, S., y Novák, O. (2021). New fluorescent auxin probes visualise tissue-specific and subcellular distributions of auxin in *Arabidopsis*. *New Phytologist* **230**, 535-549.
- Paul, V.D., Mühlenhoff, U., Stümpfig, M., Seebacher, J., Kugler, K.G., Renicke, C., Taxis, C., Gavin, A.C., Pierik, A.J., y Lill, R. (2015). The deca-GX₃ proteins Yae1-Lto1 function as adaptors recruiting the ABC protein Rli1 for iron-sulfur cluster insertion. *eLife* **4**, e08231.
- Paytubi, S., Wang, X., Lam, Y.W., Izquierdo, L., Hunter, M.J., Jan, E., Hundal, H.S., y Proud, C.G. (2009). ABC50 promotes translation initiation in mammalian cells. *Journal of Biological Chemistry* **284**, 24061-24073.
- Pérez-Pérez, J.M., Candela, H., Robles, P., López-Torrejón, G., del Pozo, J.C., y Micol, J.L. (2010). A role for *AUXIN RESISTANT3* in the coordination of leaf growth. *Plant and Cell Physiology* **51**, 1661-1673.
- Pinon, V., Etchells, J.P., Rossignol, P., Collier, S.A., Arroyo, J.M., Martienssen, R.A., y Byrne, M.E. (2008). Three *PIGGYBACK* genes that specifically influence leaf patterning encode ribosomal proteins. *Development* **135**, 1315-1324.
- Popovic, M., Zaja, R., Loncar, J., y Smital, T. (2010). A novel ABC transporter: The first insight into zebrafish (*Danio rerio*) ABCH1. *Marine Environmental Research* **69**, S11-S13.
- Quazi, F., Lenevich, S., y Molday, R.S. (2012). ABCA4 is an N-retinylidene-phosphatidylethanolamine and phosphatidylethanolamine importer. *Nature Communications* **3**, 925.
- Quesada, V., Sarmiento-Mañús, R., González-Bayón, R., Hricová, A., Pérez-Marcos, R., Graciá-Martínez, E., Medina-Ruiz, L., Leyva-Díaz, E., Ponce, M.R., y Micol, J.L. (2011). *Arabidopsis*

- RUGOSA2* encodes an mTERF family member required for mitochondrion, chloroplast and leaf development. *Plant Journal* **68**, 738-753.
- Ramachandran, P., Carlsbecker, A., y Etchells, J.P. (2017). Class III HD-ZIPs govern vascular cell fate: an HD view on patterning and differentiation. *Journal of Experimental Botany* **68**, 55-69.
- Ravichandran, S.J., Linh, N.M., y Scarpella, E. (2020). The canalization hypothesis – challenges and alternatives. *New Phytologist* **227**, 1051-1059.
- Reinhart, B.J., Liu, T., Newell, N.R., Magnani, E., Huang, T., Kerstetter, R., Michaels, S., y Barton, M.K. (2013). Establishing a framework for the ad/abaxial regulatory network of *Arabidopsis*: ascertaining targets of class III HOMEODOMAIN LEUCINE ZIPPER and KANADI regulation. *Plant Cell* **25**, 3228-3249.
- Robles, P., y Micol, J.L. (2001). Genome-wide linkage analysis of *Arabidopsis* genes required for leaf development. *Molecular Genetics and Genomics* **266**, 12-19.
- Robles Ramos, P. (1999). Análisis genético de mutantes de *Arabidopsis thaliana* con alteraciones en la morfología de la hoja. Tesis doctoral. Universidad Miguel Hernández.
- Rosado, A., Li, R., van de Ven, W., Hsu, E., y Raikhel, N.V. (2012). *Arabidopsis* ribosomal proteins control developmental programs through translational regulation of auxin response factors. *Proceedings of the National Academy of Sciences USA* **109**, 19537-19544.
- Sachs, T. (1969). Polarity and the induction of organized vascular tissues. *Annals of Botany* **33**, 263-275.
- Sachs, T. (1981). The control of the patterned differentiation of vascular tissues. *Advances in Botanical Research* **9**, 151-262.
- Saha, J., Sengupta, A., Gupta, K., y Gupta, B. (2015). Molecular phylogenetic study and expression analysis of ATP-binding cassette transporter gene family in *Oryza sativa* in response to salt stress. *Computational Biology and Chemistry* **54**, 18-32.
- Sarmiento, C., Nigul, L., Kazantseva, J., Buschmann, M., y Truve, E. (2006). AtRLI2 is an endogenous suppressor of RNA silencing. *Plant Molecular Biology* **61**, 153-163.
- Scarpella, E., Francis, P., y Berleth, T. (2004). Stage-specific markers define early steps of procambium development in *Arabidopsis* leaves and correlate termination of vein formation with mesophyll differentiation. *Development* **131**, 3445-3455.
- Scarpella, E., Marcos, D., Friml, J., y Berleth, T. (2006). Control of leaf vascular patterning by polar auxin transport. *Genes and Development* **20**, 1015-1027.
- Scarpella, E., Barkoulas, M., y Tsiantis, M. (2010). Control of leaf and vein development by auxin. *Cold Spring Harbor Perspectives in Biology* **2**, a001511.
- Scarpella, E. (2017). The logic of plant vascular patterning. Polarity, continuity and plasticity in the formation of the veins and of their networks. *Current Opinion in Genetics and Development* **45**, 34-43.
- Schepetilnikov, M., Dimitrova, M., Mancera-Martínez, E., Geldreich, A., Keller, M., y Ryabova, L.A. (2013). TOR and S6K1 promote translation reinitiation of uORF-containing mRNAs via phosphorylation of eIF3h. *EMBO Journal* **32**, 1087-1102.
- Schepetilnikov, M., y Ryabova, L.A. (2017). Auxin signaling in regulation of plant translation reinitiation. *Frontiers in Plant Science* **8**, 1014.
- Serrano-Cartagena, J., Robles, P., Ponce, M.R., y Micol, J.L. (1999). Genetic analysis of leaf form mutants from the *Arabidopsis* Information Service collection. *Molecular and General Genetics* **261**, 725-739.
- Stewart, J.D., Cowan, J.L., Perry, L.S., Coldwell, M.J., y Proud, C.G. (2015). ABC50 mutants modify translation start codon selection. *Biochemical Journal* **467**, 217-229.
- Strunk, B.S., Novak, M.N., Young, C.L., y Karbstein, K. (2012). A translation-like cycle is a quality control checkpoint for maturing 40S ribosome subunits. *Cell* **150**, 111-121.
- Sturm, A., Cunningham, P., y Dean, M. (2009). The ABC transporter gene family of *Daphnia pulex*. *BMC Genomics* **10**, 170.

- Su, T., Izawa, T., Thoms, M., Yamashita, Y., Cheng, J., Berninghausen, O., Hartl, F.U., Inada, T., Neupert, W., y Beckmann, R. (2019). Structure and function of Vms1 and Arb1 in RQC and mitochondrial proteome homeostasis. *Nature* **570**, 538-542.
- Sudmant, P.H., Lee, H., Dominguez, D., Heiman, M., y Burge, C.B. (2018). Widespread accumulation of ribosome-associated isolated 3' UTRs in neuronal cell populations of the aging brain. *Cell Reports* **25**, 2447-2456.
- Takahashi, T. (2018). Thermospermine: an evolutionarily ancient but functionally new compound in plants. *Methods in Molecular Biology* **1694**, 51-59.
- ten Tusscher, K.H. (2021). What remains of the evidence for auxin feedback on PIN polarity patterns? *Plant Physiology* **186**, 804-807.
- ter Beek, J., Guskov, A., y Slotboom, D.J. (2014). Structural diversity of ABC transporters. *Journal of General Physiology* **143**, 419-435.
- Theodoulou, F.L., y Kerr, I.D. (2015). ABC transporter research: going strong 40 years on. *Biochemical Society Transactions* **43**, 1033-1040.
- Thomas, C., Aller, S.G., Beis, K., Carpenter, E.P., Chang, G., Chen, L., Dassa, E., Dean, M., Duong Van Hoa, F., Ekiert, D., Ford, R., Gaudet, R., Gong, X., Holland, I.B., Huang, Y., Kahne, D.K., Kato, H., Koronakis, V., Koth, C.M., Lee, Y., Lewinson, O., Lill, R., Martinoia, E., Murakami, S., Pinkett, H.W., Poolman, B., Rosenbaum, D., Sarkadi, B., Schmitt, L., Schneider, E., Shi, Y., Shyng, S.L., Slotboom, D.J., Tajkhorshid, E., Tieleman, D.P., Ueda, K., Váradi, A., Wen, P.C., Yan, N., Zhang, P., Zheng, H., Zimmer, J., y Tampé, R. (2020). Structural and functional diversity calls for a new classification of ABC transporters. *FEBS Letters* **594**, 3767-3775.
- van der Horst, S., Filipovska, T., Hanson, J., y Smeekens, S. (2020). Metabolite control of translation by conserved peptide uORFs: the ribosome as a metabolite multisensor. *Plant Physiology* **182**, 110-122.
- Van Minnebruggen, A., Neyt, P., De Groeve, S., Coussens, G., Ponce, M.R., Micol, J.L., y Van Lijsebettens, M. (2010). The *ang3* mutation identified the ribosomal protein gene *RPL5B* with a role in cell expansion during organ growth. *Physiologia Plantarum* **138**, 91-101.
- Verna, C., Ravichandran, S.J., Sawchuk, M.G., Linh, N.M., y Scarpella, E. (2019). Coordination of tissue cell polarity by auxin transport and signaling. *eLife* **8**, e51061.
- Verrier, P.J., Bird, D., Burla, B., Dassa, E., Forestier, C., Geisler, M., Klein, M., Kolukisaoglu, Ü., Lee, Y., Martinoia, E., Murphy, A., Rea, P.A., Samuels, L., Schulz, B., Spalding, E.J., Yazaki, K., y Theodoulou, F.L. (2008). Plant ABC proteins – a unified nomenclature and updated inventory. *Trends in Plant Science* **13**, 151-159.
- Voith von Voithenberg, L., Park, J., Stübe, R., Lux, C., Lee, Y., y Philippar, K. (2019). A novel prokaryote-type ECF/ABC transporter module in chloroplast metal homeostasis. *Frontiers in Plant Science* **10**, 1264.
- von Arnim, A.G., Jia, Q., y Vaughn, J.N. (2014). Regulation of plant translation by upstream open reading frames. *Plant Science* **214**, 1-12.
- Walker, J.E., Saraste, M., Runswick, M.J., y Gay, N.J. (1982). Distantly related sequences in the alpha- and beta-subunits of ATP synthase, myosin, kinases and other ATP-requiring enzymes and a common nucleotide binding fold. *EMBO Journal* **1**, 945-951.
- Wenzel, C.L., Schuetz, M., Yu, Q., y Mattsson, J. (2007). Dynamics of *MONOPTEROS* and *PINFORMED1* expression during leaf vein pattern formation in *Arabidopsis thaliana*. *Plant Journal* **49**, 387-398.
- Wu, G., Lin, W.C., Huang, T., Poethig, R.S., Springer, P.S., y Kerstetter, R.A. (2008). *KANADII* regulates adaxial-abaxial polarity in *Arabidopsis* by directly repressing the transcription of *ASYMMETRIC LEAVES2*. *Proceedings of the National Academy of Sciences USA* **105**, 16392-16397.
- Wu, J., Peled-Zehavi, H., y Galili, G. (2020). The m⁶A reader ECT2 post-transcriptionally regulates proteasome activity in *Arabidopsis*. *New Phytologist* **228**, 151-162.

- Xu, H., Blonder, B., Jodra, M., Malhi, Y., y Fricker, M. (2021). Automated and accurate segmentation of leaf venation networks via deep learning. *New Phytologist* **229**, 631-648.
- Yamashita, Y., Takamatsu, S., Glasbrenner, M., Becker, T., Naito, S., y Beckmann, R. (2017). Sucrose sensing through nascent peptide-mediated ribosome stalling at the stop codon of *Arabidopsis* *bZIP11* uORF2. *FEBS Letters* **591**, 1266-1277.
- Yao, Y., Ling, Q., Wang, H., y Huang, H. (2008). Ribosomal proteins promote leaf adaxial identity. *Development* **135**, 1325-1334.
- Yoshimoto, K., Takamura, H., Kadota, I., Motose, H., y Takahashi, T. (2016). Chemical control of xylem differentiation by thermospermine, xylemin, and auxin. *Scientific Reports* **6**, 21487.
- Young, D.J., Guydosh, N.R., Zhang, F., Hinnebusch, A.G., y Green, R. (2015). Rli1/ABCE1 recycles terminating ribosomes and controls translation reinitiation in 3'UTRs in vivo. *Cell* **162**, 872-884.
- Young, D.J., y Guydosh, N.R. (2019). Hcr1/eIF3j is a 60S ribosomal subunit recycling accessory factor in vivo. *Cell Reports* **28**, 39-50.
- Zeng, W., Brutus, A., Kremer, J.M., Withers, J.C., Gao, X., Jones, A.D., y He, S.Y. (2011). A genetic screen reveals *Arabidopsis* stomatal and/or apoplastic defenses against *Pseudomonas syringae* pv. *tomato* DC3000. *PLOS Pathogens* **7**, e1002291.
- Zhai, C., Li, Y., Mascarenhas, C., Lin, Q., Li, K., Vyrides, I., Grant, C.M., y Panaretou, B. (2014). The function of ORAOV1/LTO1, a gene that is overexpressed frequently in cancer: essential roles in the function and biogenesis of the ribosome. *Oncogene* **33**, 484-494.
- Zhang, Z., y Zhang, X. (2012). Argonautes compete for miR165/166 to regulate shoot apical meristem development. *Current Opinion in Plant Biology* **15**, 652-658.
- Zhou, F., Roy, B., y von Arnim, A.G. (2010). Translation reinitiation and development are compromised in similar ways by mutations in translation initiation factor eIF3h and the ribosomal protein RPL24. *BMC Plant Biology* **10**, 193.
- Zhou, F., Roy, B., Dunlap, J.R., Enganti, R., y von Arnim, A.G. (2014). Translational control of *Arabidopsis* meristem stability and organogenesis by the eukaryotic translation factor eIF3h. *PLOS ONE* **9**, e95396.
- Zhou, G.K., Kubo, M., Zhong, R., Demura, T., y Ye, Z.H. (2007). Overexpression of miR165 affects apical meristem formation, organ polarity establishment and vascular development in *Arabidopsis*. *Plant and Cell Physiology* **48**, 391-404.
- Zhu, X., Zhang, H., y Mendell, J.T. (2020). Ribosome recycling by ABCE1 links lysosomal function and iron homeostasis to 3' UTR-directed regulation and nonsense-mediated decay. *Cell Reports* **32**, 107895.

IX.- PUBLICACIONES



ABCE Proteins: From Molecules to Development

Carla Navarro-Quiles, Eduardo Mateo-Bonmatí and José L. Micol*

Instituto de Bioingeniería, Universidad Miguel Hernández, Elche, Spain

Most members of the large family of ATP-Binding Cassette (ABC) proteins function as membrane transporters. However, the most evolutionarily conserved group, the ABCE protein subfamily, comprises soluble proteins that were initially denoted RNase L inhibitor (RLI) proteins. ABCE proteins are present in all eukaryotes and archaea and are encoded by a single gene in most genomes, or by two genes in a few cases. Functional analysis of *ABCE* genes, primarily in *Saccharomyces cerevisiae*, has shown that ABCE proteins have essential functions as part of the translational apparatus. In this review, we summarize the current understanding of ABCE protein function in ribosome biogenesis and recycling, with a particular focus on their known and proposed developmental roles in different species. The ABCE proteins might represent another class of factors contributing to the role of the ribosome in gene expression regulation.

OPEN ACCESS

Edited by:

Elena M. Kramer,
Harvard University, United States

Reviewed by:

Uener Kolukisaoglu,
Universität Tübingen, Germany
Dora Szakonyi,
Instituto Gulbenkian de Ciência (IGC),
Portugal

*Correspondence:

José L. Micol
jlmicol@umh.es

Specialty section:

This article was submitted to
Plant Evolution and Development,
a section of the journal
Frontiers in Plant Science

Received: 29 March 2018

Accepted: 12 July 2018

Published: 03 August 2018

Citation:

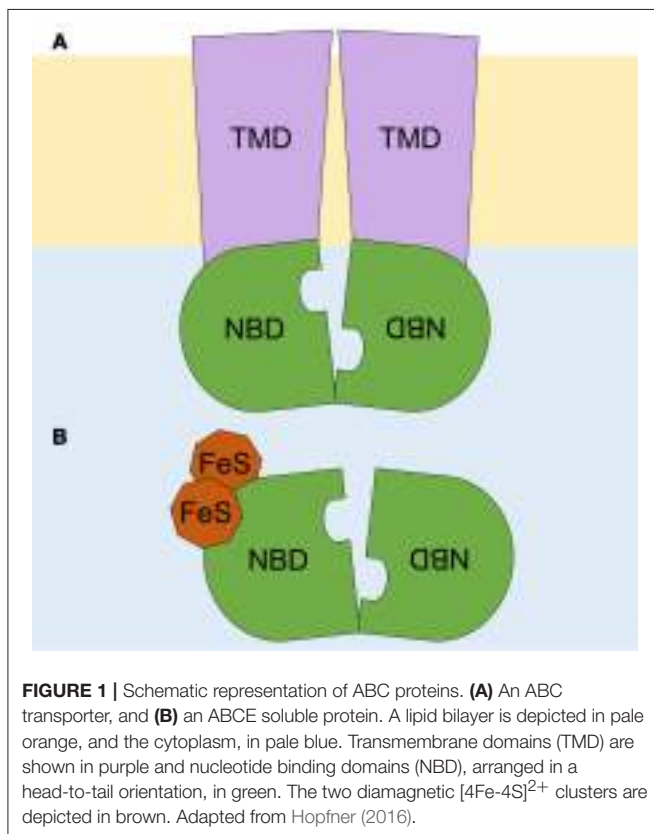
Navarro-Quiles C, Mateo-Bonmatí E
and Micol JL (2018) ABCE Proteins:
From Molecules to Development.
Front. Plant Sci. 9:1125.
doi: 10.3389/fpls.2018.01125

Keywords: ABCE, ribosome, translation, development, RLI

ABC PROTEIN STRUCTURE, FUNCTION, AND CLASSIFICATION

The ATP-Binding Cassette (ABC) proteins, which are present in all living organisms, constitute one of the largest known protein families. Actually, in prokaryotes, the ABC genes constitute 1–3% of the genome (Tomii and Kanehisa, 1998). The *Saccharomyces cerevisiae* and human genomes encode 30 and 48 ABC proteins, respectively (Dean et al., 2001; Paumi et al., 2009; Vasiliou et al., 2009). By contrast, in plants like *Arabidopsis thaliana*, there are more than 100 genes encoding ABC proteins (Verrier et al., 2008). Such multiplication and functional diversification of ABC proteins is consistent with the sessile nature of plants and their adaptation to changing terrestrial environments, as well as with the history of whole-genome duplications in plant evolution (Hwang et al., 2016).

Most ABC proteins transport solutes across cell membranes. These solutes, referred to as allocrites (Holland and Blight, 1999), range from small inorganic and organic molecules to large organic compounds. ABC transporters contain two transmembrane domains (TMDs) and two nucleotide-binding domains (NBDs), otherwise known as ATP-binding cassettes, which are hallmarks of the ABC family. TMDs and NBDs can be contained together in a unique full-sized protein, as commonly found in eukaryotes, or can be separated into individual peptides (subunits), as observed in prokaryotes. ABC proteins can also occur as homo- or heterodimers formed by half-sized proteins, which contain one TMD and one NBD or consist only of fused NBDs (Hyde et al., 1990). TMDs are responsible for allocrite specificity and have polyphyletic origins. TMDs belonging to a specific transporter subtype display similar membrane topologies among distant species. Each TMD typically comprises 6–10 α -helices that span the cell membrane, thus generating a pore that is accessible from the cytoplasm or from the extracellular space (Wang et al., 2009; Zheng et al., 2013).



In contrast to TMDs, NBDs are monophyletic with conserved sequences and structures (Higgins et al., 1986). The NBD regions that display the highest level of conservation are those that function specifically in ATP binding and hydrolysis, namely the Walker A and Walker B motifs; the LSGGQ signature or ABC motif; and the A-, D-, H-, and Q-loops, named after the conserved residues at their N- or C-termini (ter Beek et al., 2014). NBDs are arranged in a head-to-tail orientation, which allows them to bind two ATP molecules. These ATP molecules interact with motifs from both NBDs in a sandwich-like manner, bringing NBDs together in a closed conformation. ATP cleavage (hydrolysis) relaxes this conformation and drives the transport cycle by producing coupled conformational changes in the TMDs that recognize and translocate the allocrite across the membrane. Whether both NBDs stay in contact (continuous contact models) or totally separate (NBDs separation models) after ATP hydrolysis remains a matter of active debate. However, since there are several ABC transporter subtypes, it is reasonable to assume that more than one transport mechanism exists (Shi and Barna, 2015).

To facilitate ABC protein recognition and comparison among different species, a standardized nomenclature was proposed for all eukaryotes (Dean and Annilo, 2005; Verrier et al., 2008; Paumi et al., 2009; Xie et al., 2012; Dermauw and Van Leeuwen, 2014). Mammalian ABC proteins were divided into seven subfamilies (ABCA to ABCG) based on NBD sequence similarity (Dean et al., 2001). Two additional subfamilies were later proposed for

non-mammalian ABC proteins, specifically the ABCH subfamily, which is found in insects and osteichthyes (Dean and Annilo, 2005), and the ABCI subfamily, which is found exclusively in plants and contains prokaryotic-like ABC proteins, among others (Verrier et al., 2008). ABCA, ABCB, ABCC, ABCD, ABCG, and ABCH proteins function as transporters (Figure 1A; Hopfner, 2016).

By contrast, soluble ABC proteins belong to the ABCE and ABCF subfamilies, which lack TMDs but have the two NBDs in a single peptide chain (Figure 1B). ABCF proteins function in translation, as exemplified by eukaryotic elongation factor 3 (eEF3) (Andersen et al., 2006), or in chromosome segregation and DNA repair, as is the case for the Structural Maintenance of Chromosomes (SMC) proteins and the SMC-like protein Rad50 (Hirano, 2002). Here, we focus on the ABCE subfamily, which includes single-copy genes that, although initially thought to be specific to mammals (Bisbal et al., 1995), are found in both eukaryotes and archaea.

THE ABCE SUBFAMILY OF ABC PROTEINS

ABCE proteins display the highest level of conservation among the ABC subfamilies. For example, the yeast *ABCE1/Rli1* shares 68 and 43% sequence identity with its human and archaeal (*Sulfolobus solfataricus*) orthologs, respectively (Kispal et al., 2005; Barthelme et al., 2007). The ABCE subfamily is represented in most genomes by a single-copy, essential *ABCE1* gene (Kerr, 2004). However, two *ABCE* paralogs, specifically *ABCE1/RLI1* and *ABCE2/RLI2*, exist in plants such as *Arabidopsis thaliana* and *Oryza sativa* (Sarmiento et al., 2006; Verrier et al., 2008), and in animals such as catfish (Liu et al., 2013) and the mosquitoes *Anopheles gambiae*, *Aedes aegypti*, and *Culex pipiens quinquefasciatus* (Lu et al., 2016).

Loss-of-function of *ABCE1* genes, either via null alleles or RNAi suppression, is associated with a lethal phenotype in all studied species, and hypomorphic *ABCE1* alleles result in slow-growth phenotypes (Amsterdam et al., 2004; Dong et al., 2004; Estévez et al., 2004; Zhao et al., 2004; Coelho et al., 2005a; Kispal et al., 2005; Chen et al., 2006; Barthelme et al., 2007; Broehan et al., 2013; Kougioumoutzi et al., 2013; Table 1). Conversely, in *Saccharomyces cerevisiae*, *RLI1* overexpression leading to accumulation of either the wild-type protein or mutated versions disrupted in conserved residues or lacking entire conserved domains caused a dominant negative effect on growth (Dong et al., 2004; Khoshnevis et al., 2010).

Determination of the crystal structure of archaeal *ABCE1* (aABCE1) proteins (Karcher et al., 2005, 2008; Barthelme et al., 2011) showed that these proteins contain four conserved domains: (1–2) the two NBDs that are present in all ABC proteins; (3) a hinge region proposed to facilitate NBD orientation and function as a pivot point in the tweezer-like power stroke of NBDs following ATP binding (Karcher et al., 2005); and (4) an iron-sulfur (FeS) binding domain with eight cysteine residues that coordinate two diamagnetic $[4\text{Fe-4S}]^{2+}$ clusters present at the ABCE protein N-terminal region (Figure 1B; Barthelme et al., 2007; Karcher et al., 2008). The

TABLE 1 | Mutations affecting *ABCE* genes in different species.

Organism	Gene name	Loss of function caused by	Phenotype	References
<i>Drosophila melanogaster</i>	<i>pixie</i>	Strong hypomorphic alleles Weak hypomorphic alleles	Recessive lethal Slow growth; disproportionate organ sizes; slender bristles; eye roughening	Coelho et al., 2005a,b Coelho et al., 2005a,b
<i>Caenorhabditis elegans</i>	<i>abce-1</i>	RNAi	Slow growth; embryonic lethality	Kamath et al., 2003; Zhao et al., 2004
<i>Danio rerio</i>	<i>abce1</i>	Retroviral insertional allele	Small head and eyes; underdeveloped liver and gut; pericardial edema; lethal at 5 days post-fertilization	Amsterdam et al., 2004
<i>Xenopus laevis</i>	<i>abce1</i>	Antisense <i>ABCE1</i> morpholino oligonucleotides	Arrested growth at the gastrula stage	Chen et al., 2006
<i>Cardamine hirsuta</i>	<i>SIL3; ChRLI2</i>	Hypomorphic allele	Reduced growth; small and simple leaves; delayed leaf initiation; reduced auxin signaling; reduced cell proliferation; high rates of endoreplication	Kougoumoutzi et al., 2013
<i>Nicotiana benthamiana</i>	<i>RLIh</i>	Virus-induced gene silencing	Reduced growth; distorted leaves; whitened veins; reduced cell size and number	Petersen et al., 2004

latter domain plays an essential role in ABCE protein function (Kispal et al., 2005; Yarunin et al., 2005; Barthelme et al., 2007, 2011; Alhebshi et al., 2012). The high-level conservation among all ABCE amino acid sequences, in particular within their four conserved domains, allows to deduce the structure of eukaryotic ABCE orthologs based on that of aABCE1 (Karcher et al., 2005, 2008). Moreover, cryoelectron microscopy showed that *Pyrococcus furiosus* aABCE1 and yeast Rli1 associate similarly with ribosomes (Becker et al., 2012; Preis et al., 2014).

The function of the yeast ABCE1 protein Rli1 has been well characterized. Furthermore, based on the sequence conservation, ABCE1 protein function is likely to be well conserved among different organisms. Yeast Rli1 triggers the dissociation of ribosomes during different processes related to translation, as described in further detail below (Figure 2). Additional roles have been proposed for ABCE proteins in higher eukaryotes. For example, ABCE1 participates in the assembly of immature HIV-1 capsids in mammals (Zimmerman et al., 2002; Doohar and Lingappa, 2004), and ABCE proteins act as endogenous suppressors of RNA silencing in plants and humans (Sarmiento et al., 2006; Kärblane et al., 2015).

YEAST ABCE1/RLI1 FUNCTIONS IN RIBOSOME BIOGENESIS AND RECYCLING

The *Saccharomyces cerevisiae* genome encodes 30 ABC proteins, including one member of the ABCE subfamily, Rli1. *RLI1* encodes a canonical ABCE protein and contains two NBDs arranged in a head-to-tail manner (thus allowing the binding of two ATP molecules), and a FeS domain (Barthelme et al., 2007). The *Drosophila melanogaster* Rli1 ortholog, Pixie, localizes exclusively in the cytoplasm (Coelho et al., 2005a), whereas yeast Rli1 localizes in the cytoplasm and in the nucleus (Dong et al., 2004; Kispal et al., 2005; Yarunin et al., 2005).

Yeast Rli1 associates with eukaryotic translation initiation factors, 40S ribosomal subunits, 80S ribosomes, and polysomes. Suppression of *Rli1* strongly reduces polysome size and

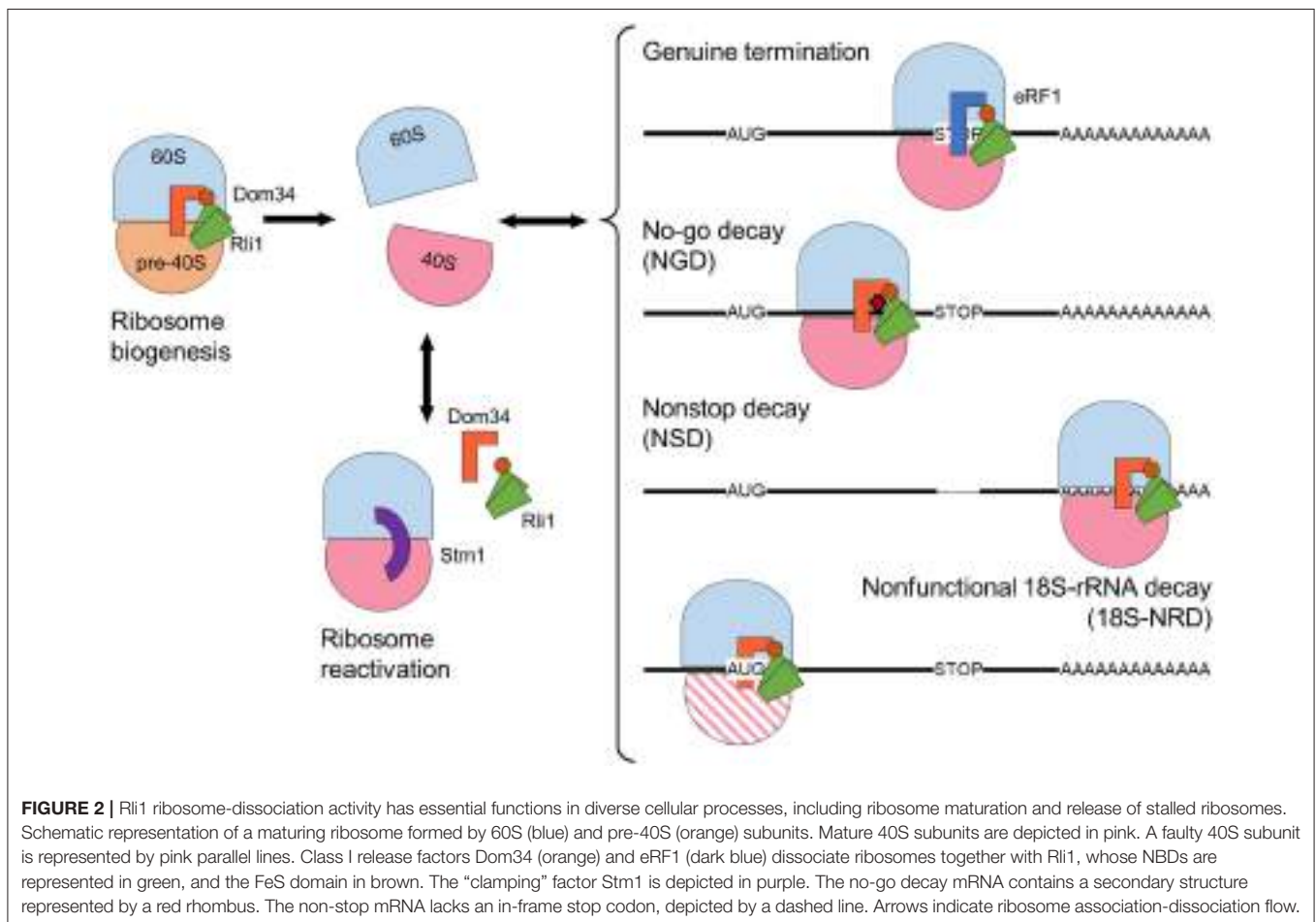
abundance, as well as translation rates (Dong et al., 2004; Kispal et al., 2005; Yarunin et al., 2005; Shoemaker and Green, 2011). These observations suggested that Rli1 participates in translation initiation by promoting assembly of the preinitiation complex. Equivalent observations were made for human ABCE1 (Chen et al., 2006) and *Drosophila* Pixie (Andersen and Leever, 2007). Additionally, ABCE proteins in *Trypanosoma brucei* (Estévez et al., 2004) and *Caenorhabditis elegans* (Zhao et al., 2004) were also implicated in translation. A role for yeast Rli1 and mammalian ABCE1 in translation initiation was confirmed following analysis of the 48S initiation and the post-splitting complexes (Heuer et al., 2017; Mancera-Martínez et al., 2017).

The role of Rli1 as a ribosome biogenesis factor is supported by the nuclear accumulation of 40S and 60S ribosome subunits when Rli1 function is compromised (Kispal et al., 2005; Yarunin et al., 2005). Nevertheless, the most well-known Rli1 function is that of ribosome disassembly (Figure 2). Indeed, Rli1 facilitates ribosomal subunit dissociation through its direct interaction with the class I release factor Suppressor 45 (Sup45), otherwise known as eukaryotic release factor 1 (eRF1) or its paralog Duplication of Multilocus region 34 (Dom34). Such interaction was confirmed by affinity pull-down, coimmunoprecipitation, and yeast two-hybrid analyses (Khoshnevis et al., 2010; Shoemaker and Green, 2011).

Yeast Rli1 Participates in Ribosome Recycling

Translation termination occurs when the stop codon of an mRNA enters the A site of the associated ribosome, after which the tRNA-mimicking eRF1 recognizes the stop codon via codon-anticodon recognition using its conserved NIKS (Asn-Ile-Lys-Ser) motif and occupies the A site of the ribosome (Song et al., 2000). Following this, the GTP bound to the eRF1-linked class II release factor Sup35/eRF3 is hydrolyzed, thus dissociating the post-termination complex.

During stop codon recognition, eRF3 has been proposed to facilitate the interaction between eRF1 and the ribosome.



This function is thought to resemble delivery of aminoacylated tRNA to the ribosome A site during peptide elongation, which is performed by the eRF3 paralog eEF1 α (Inagaki et al., 2003; Salas-Marco and Bedwell, 2004; des Georges et al., 2014). In an alternative scenario, DEAD-box protein 5 (Dbp5), an RNA helicase that participates in mRNA export, recruits eRF3-GTP to the ribosome following eRF1 stop codon recognition (Gross et al., 2007). Regardless of the exact protein-protein interactions, eRF3 must break down GTP and leave the ribosome to allow Rli1 binding (Shoemaker and Green, 2011; Preis et al., 2014).

The kinetic analysis of an *in vitro* reconstituted yeast translation system demonstrated that Rli1 induces eRF1 ribosome accommodation in an ATP-independent manner. Ribosome accommodation allows eRF1 to catalyze peptidyl-tRNA hydrolysis through its conserved GGQ (Gly-Gly-Gln) motif, which releases the newly synthesized peptide. ATP hydrolysis driven by Rli1 promotes ribosome subunit dissociation, demonstrating that eukaryotic translation termination and ribosome recycling are combined within the same release factor-mediated process. Such combination contrasts with the separation of the two processes observed in bacteria (Shoemaker and Green, 2011). In this manner, the 60S subunit is disassembled from the 40S subunit, which is

then released from the deacylated tRNA and mRNA molecules. During all this process of ribosome recycling, Rli1 remains bound to the 40S subunit and has been suggested to preclude 60S rejoining until a late-stage in the initiation complex (Heuer et al., 2017; Mancera-Martínez et al., 2017). In the case of archaea, it has been proposed that ribosome dissociation is caused by a conformational change following aABCE1-ribosome interaction, and that ATP hydrolysis is required to separate aABCE1 from the 30S subunit following ribosome dissociation (Barthelme et al., 2011; Kiosze-Becker et al., 2016).

Termination of translation can be inefficient. One of the known causes of inefficient translation termination is the continued association of ribosomes with defective mRNA molecules, which impairs translation and produces potentially deleterious peptides. To circumvent this, different mRNA surveillance pathways can degrade defective mRNA molecules and their translation products, and recycle the associated ribosomes. These mRNA surveillance pathways have been extensively reviewed (Franckenberg et al., 2012; Graille and Séraphin, 2012; Shoemaker and Green, 2012; Brandman and Hegde, 2016), so they are only briefly discussed here.

Each of the three primary mRNA surveillance mechanisms targets a different cause of ribosome stalling and Rli1 participates

in all three mechanisms. In no-go decay (NGD), a physical obstruction slows down or stops ribosome progression on the mRNA molecule. Physical obstructions can include an inhibitory secondary structure, chemical damage, or a polybasic sequence within the nascent protein (Doma and Parker, 2006; Kuroha et al., 2010). Non-stop decay (NSD) occurs when the mRNA lacks a genuine stop codon, possibly due to truncation or premature polyadenylation of the mRNA molecule. In NSD, the ribosome continues translation until it encounters an in-frame stop codon on the 3' UTR or comes to the poly(A) mRNA sequence (tail). Translation of the poly(A) tail generates a positively charged poly-lysine region that disturbs ribosome movement by interacting with its negatively charged translation tunnel (Frischmeyer et al., 2002; Ito-Harashima et al., 2007; Lu and Deutsch, 2008; Guydosh and Green, 2014). Lastly, non-functional 18S rRNA decay (18S-NRD) repairs errors in translation that are caused by dysfunctional ribosomes carrying an inactive or immature 40S subunit. 18S-NRD rapidly removes these faulty ribosomes that have initiated translation, but cannot produce an elongating peptide (LaRiviere et al., 2006; Soudet et al., 2010).

Each of these surveillance systems uses the same basic ribosome rescue machinery components. Ribosome rescue starts with recognition of the stalled ribosome by a ternary complex formed by Dom34 and Hsp70 subfamily B Suppressor 1 (Hbs1-GTP), which are paralogs of eRF1 and eRF3, respectively (Cole et al., 2009; Shoemaker et al., 2010; Tsuboi et al., 2012). Following this, Rli1 dissociates the ribosome into the 40S and 60S subunits via a similar mechanism as during the normal termination of translation. Dom34 lacks the conserved NIKS motif that is involved in stop codon recognition and the GGQ motif that catalyzes peptide release, which are characteristic features of eRF1 (Graille et al., 2008; Shoemaker et al., 2010).

The mRNA surveillance pathways appear to be conserved among all eukaryotes and archaea. For example, Pelota, the Dom34 paralog in *Drosophila melanogaster*, can restore NGD in Dom34-depleted yeast cells (Passos et al., 2009). Also, the human and fly Pelota-Hbs1 complex, together with ABCE1/Pixie, participates in NSD (Pisareva et al., 2011; Saito et al., 2013; Kashima et al., 2014). In archaea, the elongation factor aEF1 α , an ortholog of eRF3, interacts with aRF1 during the normal termination of translation and aPelota during mRNA surveillance, resulting in ribosome dissociation via aABCE1 action (Saito et al., 2010; Barthelme et al., 2011; Becker et al., 2012).

Rli1 Is Required for Ribosome Biogenesis and Reactivation

Yeast ribosome biogenesis begins in the nucleolus where the 35S and 5S rDNAs are transcribed. Following this, pre-35S and pre-5S rRNAs are cotranscriptionally assembled with ribosomal proteins, ribosome biogenesis factors (RBFs), and small nucleolar ribonucleoproteins (snoRNPs) to form the 90S or small subunit (SSU) processome, which is the earliest ribosome precursor. Cleavage of the 35S pre-rRNA creates the pre-60S and pre-40S particles, and the maturation of these continues in the

nucleoplasm and the cytoplasm (Gerhardy et al., 2014). Once in the cytoplasm, RBFs prevent premature translation initiation on immature pre-60S and pre-40S particles (Gartmann et al., 2010; Strunk et al., 2011; Greber et al., 2012).

Maturation of the pre-60S particle is complete when the pre-6S rRNA is processed to form 5.8S rRNA, all ribosomal proteins are assembled, and the last RBFs are released (Lo et al., 2010). The last step in 40S subunit maturation is performed in a translation-like cycle, whereby the initiation factor eIF5B links a pre-40S particle to a mature 60S subunit to form an empty 80S-like ribosome, which is necessary for 20S pre-rRNA cleavage into mature 18S rRNA. This process also serves as an additional checkpoint that, together with those performed during subunit maturation, ensures functionality of the ribosome (Strunk et al., 2012; Karbstein, 2013). Finally, Rli1, together with Dom34 and possibly Hbs1, dissociates the ribosomal subunits, which are then ready to enter the translation cycle (Shoemaker and Green, 2011; Strunk et al., 2012). Likewise, human Pelota and ABCE1 can dissociate empty ribosomes *in vitro* (Pisareva et al., 2011).

Protein synthesis is a cyclic process in which ribosomal subunits dissociate once they have processed an mRNA molecule and subsequently can reinitiate translation. However, in yeast cells subjected to stress conditions, some ribosomal subunits are complexed into inactive 80S ribosomes to reduce translation rates and increase the probability of surviving (Ashe et al., 2000; Uesono and Toh, 2002). In yeast, these inactive ribosomes are stabilized by the Suppressor of ToM1 (Stm1) factor (Balagopal and Parker, 2011; Ben-Shem et al., 2011; Van Dyke et al., 2013). Ribosomal inactivation is reversed once stress conditions are relieved and the ribosomal subunits can reenter the translation cycle. In glucose-starved yeast cells, dissociation of Stm1-bound ribosome requires the combined action of the Dom34-Hbs1 complex and Rli1. When yeast cells are grown in glucose-deficient media, translation rates rapidly decrease, associated with a decline in polysome levels and the accumulation of Stm1-inactivated 80S ribosomes. With the addition of glucose, translation rapidly resumes; however, Dom34 or Hbs1 loss-of-function prevents the recovery of translation, which causes a cessation in growth (Ashe et al., 2000; van den Elzen et al., 2014).

THE ROLE OF ABCE PROTEINS IN DEVELOPMENT

Yeast Rli1 is the best-characterized ABCE protein. In yeast and the unicellular protist *Trypanosoma brucei*, ABCE1 loss-of-function arrests growth (Dong et al., 2004; Estévez et al., 2004). Similar observations have been made in multicellular eukaryotes, showing that in some species, ABCE1 loss-of-function and overexpression both result in impaired growth (Table 1; Amsterdam et al., 2004; Estévez et al., 2004; Zhao et al., 2004; Coelho et al., 2005a; Chen et al., 2006; Kougioumoutzi et al., 2013). Consistent with the fundamental role of ABCE1 in ribosome biogenesis and recycling, ABCE1 expression is detected in most tissues and developmental stages in all studied organisms (Du et al., 2003; Zhao et al., 2004; Maeda et al., 2005; Sarmiento et al., 2006; Kougioumoutzi et al., 2013).

Many of the effects caused by *ABCE1* loss-of-function in eukaryotes have been revealed through genetic screens. For example, the *pixie* alleles were identified in a screen for ethyl methanesulfonate-induced dominant modifiers of a small-wing phenotype in *Drosophila melanogaster* (Coelho et al., 2005b). Null *pixie* alleles are recessive lethal, whereas hypomorphic alleles produce a severe delay in growth (Table 1). Nevertheless, the final body size of *pixie* mutants is comparable to that of the wild type. The *pixie* mutant phenotype resembles the *Minute* phenotype, which is associated with mutant alleles of genes encoding ribosomal proteins. Adult *pixie* flies display short thoracic bristles, occasional eye roughening, and an increased wing size relative to body size (Figures 3A,B). The increased wing size relative to body size is proposed to be due to extra cell divisions that act as a compensation mechanism triggered by high-level apoptosis observed in the wing imaginal discs during the development of *pixie* larvae (Coelho et al., 2005a).

ABCE proteins also function in vertebrate development. In a large screen for essential genes in embryo and early larval development in *Danio rerio*, mutations in *ABCE1* were found to cause lethality 5 days after fertilization. These *abce1* mutants exhibited underdeveloped liver/gut, pericardial edema, and small heads. Like the hypomorphic *pixie* alleles, the zebrafish *ABCE1* alleles also limit eye development (Table 1 and Figures 3C,D; Amsterdam et al., 2004). The *abce1* gene is also essential in *Caenorhabditis elegans* and *Xenopus laevis* as its suppression

by RNAi or antisense morpholino oligonucleotides, respectively, arrests growth (Table 1; Kamath et al., 2003; Zhao et al., 2004; Chen et al., 2006). The ability of the *ABCE1*-suppressed zebrafish and *Xenopus laevis* embryos to develop up to a certain point has been suggested to be due to the *ABCE1* maternal supply to the egg. The growth arrest would therefore occur after depletion of the maternal supply (Amsterdam et al., 2004; Chen et al., 2006).

ABCE1 genes also have essential functions in plants. In *Cardamine hirsuta*, *SIMPLE LEAF3* (*SIL3*, also named *ChRLI2*) plays a role in leaf complexity. While wild-type *Cardamine hirsuta* plants display compound leaves, which are divided into leaflets, homozygous plants carrying the putatively hypomorphic *sil3* allele show a substantial decrease in leaflet but not leaf number (Table 1 and Figures 3E,F; Kougioumoutzi et al., 2013). The *sil3* mutant has a reduced growth and its phenotype suggests alterations in auxin homeostasis at the whole-organism level. Further proof of perturbed auxin homeostasis was found by analyzing *sil3* leaves, which are small and exhibit aberrant venation patterns, as usually observed in mutants affected in auxin signaling. In addition, the lack of leaflets in *sil3* plants was explained by reduced cell proliferation on the regions where leaflets were expected to emerge. Nevertheless, leaf and leaflet initiation are controlled by the same general mechanisms that consist in the accumulation of auxin by its polarized flow through the PIN-FORMED1 (PIN1) transporters in the regions where leaf initiation occurs. Auxin accumulation

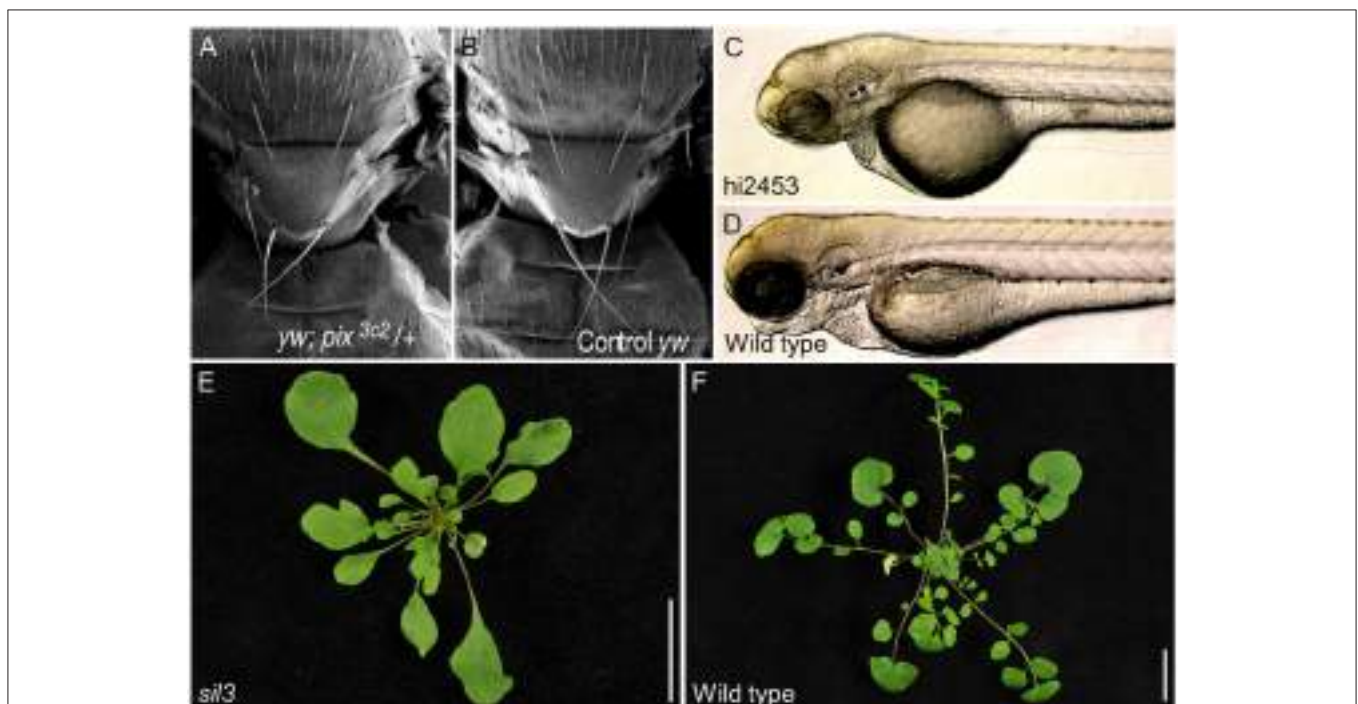


FIGURE 3 | Developmental effects of *ABCE* gene dysfunction in different species. **(A)** *Drosophila melanogaster* *pixie* mutants display thoracic bristles that are slenderer and shorter than those of **(B)** the wild type. **(C)** An insertional allele of *Danio rerio* *ABCE1* reduces head size compared with **(D)** wild type and produces pericardial edema and lethality at 5 days post-fertilization. **(E)** A hypomorphic allele of *Cardamine hirsuta* *SIL3* triggers loss of the leaflets that characterize **(F)** wild type leaves. Pictures of **(A,B)**, as well as **(C,D)**, were taken at the same scale. **(E,F)** Scale bars indicate 2 cm. Adapted with permission of authors and journals from **(A,B)** Coelho et al. (2005a), **(C,D)** Amsterdam et al. (2004) Copyright 2004 National Academy of Sciences, and **(E,F)** Kougioumoutzi et al. (2013).

then triggers leaf or leaflet initiation (Scarpella et al., 2010). Although the study of the *sil3* mutant is consistent with auxin homeostasis and signaling being sensitive to perturbation of ribosomal activity, the *sil3* mutant is interesting because leaflet number, but not leaf number, is reduced. To explain this observation, it has been suggested that the high energy demand from cells proliferating during leaflet development could not be satisfied in *sil3* plants due to suboptimal ribosome function (Kougioumoutzi et al., 2013). The two Arabidopsis *ABCE* genes have not been studied at a developmental level.

In addition, virus-induced gene silencing (VIGS) has been used to suppress expression of *RLIh* gene(s) in *Nicotiana benthamiana*, in which the number of *ABCE* paralogs remains to be established. For VIGS, 4-week-old plants were infected with potato virus X (PVX) or pea early browning virus (PEBV) vectors carrying partial *RLIh* cDNAs. *RLIh* silencing caused vein whitening, leaf distortion, and delayed growth, with silenced plants reaching only half of the height of controls, due to a reduction in cell size and number in shoot internodes (Table 1; Petersen et al., 2004). Again, these observations corroborate the important role of *ABCE* proteins in whole-organism development. Whether these developmental defects are due to the disruption of the *ABCE* function as a ribosome-dissociating factor (Franckenberg et al., 2012), an endogenous suppressor of RNA silencing (Sarmiento et al., 2006; Kärblane et al., 2015) or both, remains to be clarified.

CONCLUDING REMARKS

In this review, we have discussed the essential ribosome-dissociation activity of *ABCE* proteins, which is required for ribosome biogenesis and recycling. Furthermore, we have described the general growth defects associated with compromised *ABCE* protein function in all studied organisms. Most of these growth defects can be attributed to defective mRNA translation, which reduces protein levels and in turn prevents cells from generating the energy required for normal growth and/or proliferation. However, not all *abce* mutant phenotypes can be explained by a general depletion of cellular energy. As is the case for mutants affected in translation in several species, some phenotypes appear to be associated with compromised regulatory networks that remain uncharacterized. For instance, it is striking the fact that the *Cardamine hirsuta sil3* mutant shows a reduction in leaflet but not leaf number, given that both processes share common pathways. Future work is needed to clarify these and other questions and to determine whether there

are specific factors responsible for the differential requirements for *ABCE*s during development. Additional studies will also determine how *ABCE* dysfunction causes specific developmental aberrations in all studied organisms, as has been previously described for other proteins involved in ribosome biogenesis or function. In addition, the presence of more than one *ABCE* subfamily member in some genomes remains to be explained. Some plants and insects have two *ABCE* genes while other plants or *Drosophila melanogaster* have a single *ABCE* gene. The presence of two *ABCE* genes might be interpreted as an in-progress pseudogenization or a developing functional redundancy.

The ribosome has been proposed to represent a layer of post-transcriptional regulation of gene expression. Under the so-called filter hypothesis, the ribosome is viewed as a machine able to selectively influence or filter the translation of various mRNAs (Mauro and Edelman, 2002). There is increasing evidence of the existence of specialized ribosomes in different cell types, which are heterogeneous in either ribosomal protein composition, in their interactions with ribosome-associated factors, or both (Xue and Barna, 2012; Shi and Barna, 2015). These specialized ribosomes would differentially translate different mRNAs or mRNA groups. It follows from these assumptions that mutation of genes encoding discrete ribosomal proteins or ribosome-associated factors would render tissue- or organ-specific phenotypes. The *ABCE* proteins of *Drosophila melanogaster*, *Caenorhabditis elegans*, and *Cardamine hirsuta* might represent one such factors.

AUTHOR CONTRIBUTIONS

JLM designed the review. JLM, EM-B and CN-Q analyzed all literature data, prepared Figures 1–3, and Table 1 and wrote the manuscript. All authors have accepted the final version of the manuscript and agreed to be accountable for all aspects of the work.

ACKNOWLEDGMENTS

We thank Enrique Lopez-Juez for his useful comments on the manuscript. Research in the laboratory of JLM is supported by grants from the Ministerio de Economía y Competitividad of Spain (BIO2014-53063-P) and the Generalitat Valenciana (PROMETEOII/2014/006). CN-Q and EM-B hold predoctoral fellowships from the Universidad Miguel Hernández and Ministerio de Educación, Cultura y Deporte of Spain (FPU13/00371), respectively.

REFERENCES

- Alhebshi, A., Sideri, T. C., Holland, S. L., and Avery, S. V. (2012). The essential iron-sulfur protein Rli1 is an important target accounting for inhibition of cell growth by reactive oxygen species. *Mol. Biol. Cell* 23, 3582–3590. doi: 10.1091/mbc.e12-05-0413
- Amsterdam, A., Nissen, R. M., Sun, Z., Swindell, E. C., Farrington, S., and Hopkins, N. (2004). Identification of 315 genes essential for early zebrafish development. *Proc. Natl. Acad. Sci. U.S.A.* 101, 12792–11297. doi: 10.1073/pnas.0403929101
- Andersen, C. B., Becker, T., Blau, M., Anand, M., Halic, M., Balar, B., et al. (2006). Structure of eEF3 and the mechanism of transfer RNA release from the E-site. *Nature* 443, 663–668. doi: 10.1038/nature05126

- Andersen, D. S., and Leever, S. J. (2007). The essential *Drosophila* ATP-binding cassette domain protein, Pixie, binds the 40S ribosome in an ATP-dependent manner and is required for translation initiation. *J. Biol. Chem.* 282, 14752–14760. doi: 10.1074/jbc.M701361200
- Ashe, M. P., De Long, S. K., and Sachs, A. B. (2000). Glucose depletion rapidly inhibits translation initiation in yeast. *Mol. Biol. Cell* 11, 833–848. doi: 10.1091/mbc.11.3.833
- Balagopal, V., and Parker, R. (2011). Stm1 modulates translation after 80S formation in *Saccharomyces cerevisiae*. *RNA* 17, 835–842. doi: 10.1261/rna.2677311
- Barthelme, D., Dinkelaker, S., Albers, S. V., Londei, P., Ermler, U., and Tampé, R. (2011). Ribosome recycling depends on a mechanistic link between the FeS cluster domain and a conformational switch of the twin-ATPase ABCE1. *Proc. Natl. Acad. Sci. U.S.A.* 108, 3228–3233. doi: 10.1073/pnas.1015953108
- Barthelme, D., Scheele, U., Dinkelaker, S., Janoschka, A., Macmillan, F., Albers, S. V., et al. (2007). Structural organization of essential iron-sulfur clusters in the evolutionarily highly conserved ATP-binding cassette protein ABCE1. *J. Biol. Chem.* 282, 14598–14607. doi: 10.1074/jbc.M700825200
- Becker, T., Franckenberg, S., Wickles, S., Shoemaker, C. J., Anger, A. M., Armache, J. P., et al. (2012). Structural basis of highly conserved ribosome recycling in eukaryotes and archaea. *Nature* 482, 501–506. doi: 10.1038/nature10829
- Ben-Shem, A., Garreau De Loubresse, N., Melnikov, S., Jenner, L., Yusupova, G., and Yusupov, M. (2011). The structure of the eukaryotic ribosome at 3.0 Å resolution. *Science* 334, 1524–1529. doi: 10.1126/science.1212642
- Bisbal, C., Martinand, C., Silhol, M., Lebleu, B., and Salehzada, T. (1995). Cloning and characterization of a RNase L inhibitor. A new component of the interferon-regulated 2-5A pathway. *J. Biol. Chem.* 270, 13308–13317. doi: 10.1074/jbc.270.22.13308
- Brandman, O., and Hegde, R. S. (2016). Ribosome-associated protein quality control. *Nat. Struct. Mol. Biol.* 23, 7–15. doi: 10.1038/nsmb.3147
- Broehan, G., Kroeger, T., Lorenzen, M., and Merzendorfer, H. (2013). Functional analysis of the ATP-binding cassette (ABC) transporter gene family of *Tribolium castaneum*. *BMC Genomics* 14, 1–18. doi: 10.1186/1471-2164-14-6
- Chen, Z. Q., Dong, J., Ishimura, A., Daar, I., Hinnebusch, A. G., and Dean, M. (2006). The essential vertebrate ABCE1 protein interacts with eukaryotic initiation factors. *J. Biol. Chem.* 281, 7452–7457. doi: 10.1074/jbc.M510603200
- Coelho, C. M., Kolevski, B., Bunn, C., Walker, C., Dahanukar, A., and Leever, S. J. (2005a). Growth and cell survival are unevenly impaired in *pixie* mutant wing discs. *Development* 132, 5411–5424. doi: 10.1242/dev.02148
- Coelho, C. M., Kolevski, B., Walker, C. D., Lavagi, I., Shaw, T., Ebert, A., et al. (2005b). A genetic screen for dominant modifiers of a small-wing phenotype in *Drosophila melanogaster* identifies proteins involved in splicing and translation. *Genetics* 171, 597–614. doi: 10.1534/genetics.105.045021
- Cole, S. E., LaRivière, F. J., Merrick, C. N., and Moore, M. J. (2009). A convergence of rRNA and mRNA quality control pathways revealed by mechanistic analysis of nonfunctional rRNA decay. *Mol. Cell* 34, 440–450. doi: 10.1016/j.molcel.2009.04.017
- Dean, M., and Annilo, T. (2005). Evolution of the ATP-binding cassette (ABC) transporter superfamily in vertebrates. *Annu. Rev. Genom. Hum. Genet.* 6, 123–142. doi: 10.1146/annurev.genom.6.080604.162122
- Dean, M., Rzhetsky, A., and Allikmets, R. (2001). The human ATP-binding cassette (ABC) transporter superfamily. *Genome Res.* 11, 1156–1166. doi: 10.1101/gr.1649R
- Dermauw, W., and Van Leeuwen, T. (2014). The ABC gene family in arthropods: comparative genomics and role in insecticide transport and resistance. *Insect Biochem. Mol. Biol.* 45, 89–110. doi: 10.1016/j.ibmb.2013.11.001
- des Georges, A., Hashem, Y., Unbehaun, A., Grassucci, R. A., Taylor, D., Hellen, C. U., et al. (2014). Structure of the mammalian ribosomal pre-termination complex associated with eRF1-eRF3-GDPNP. *Nucleic Acids Res.* 42, 3409–3418. doi: 10.1093/nar/gkt1279
- Doma, M. K., and Parker, R. (2006). Endonucleolytic cleavage of eukaryotic mRNAs with stalls in translation elongation. *Nature* 440, 561–564. doi: 10.1038/nature04530
- Dong, J., Lai, R., Nielsen, K., Fekete, C. A., Qiu, H., and Hinnebusch, A. G. (2004). The essential ATP-binding cassette protein RL1 functions in translation by promoting preinitiation complex assembly. *J. Biol. Chem.* 279, 42157–42168. doi: 10.1074/jbc.M404502200
- Doohar, J. E., and Lingappa, J. R. (2004). Conservation of a stepwise, energy-sensitive pathway involving HP68 for assembly of primate lentivirus capsids in cells. *J. Virol.* 78, 1645–1656. doi: 10.1128/JVI.78.4.1645-1656.2004
- Du, X. L., Wang, D., Qian, X. Y., Jiang, L. Z., Chun, W., Li, K. G., et al. (2003). cDNA cloning and expression analysis of the rice (*Oryza sativa* L.) RNase L inhibitor. *DNA Seq.* 14, 295–301. doi: 10.1080/1085566031000141162
- Estévez, A. M., Haile, S., Steinbüchel, M., Quijada, L., and Clayton, C. (2004). Effects of depletion and overexpression of the *Trypanosoma brucei* ribonuclease L inhibitor homologue. *Mol. Biochem. Parasitol.* 133, 137–141. doi: 10.1016/j.molbiopara.2003.09.009
- Franckenberg, S., Becker, T., and Beckmann, R. (2012). Structural view on recycling of archaeal and eukaryotic ribosomes after canonical termination and ribosome rescue. *Curr. Opin. Struct. Biol.* 22, 786–796. doi: 10.1016/j.sbi.2012.08.002
- Frischmeyer, P. A., Van Hoof, A., O'donnell, K., Guerrero, A. L., Parker, R., and Dietz, H. C. (2002). An mRNA surveillance mechanism that eliminates transcripts lacking termination codons. *Science* 295, 2258–22561. doi: 10.1126/science.1067338
- Gartmann, M., Blau, M., Armache, J. P., Mielke, T., Topf, M., and Beckmann, R. (2010). Mechanism of eIF6-mediated inhibition of ribosomal subunit joining. *J. Biol. Chem.* 285, 14848–14851. doi: 10.1074/jbc.C109.096057
- Gerhardy, S., Menet, A. M., Peña, C., Petkowski, J. J., and Panse, V. G. (2014). Assembly and nuclear export of pre-ribosomal particles in budding yeast. *Chromosoma* 123, 327–344. doi: 10.1007/s00412-014-0463-z
- Graille, M., Chaillet, M., and Van Tilbeurgh, H. (2008). Structure of yeast Dom34: a protein related to translation termination factor eRF1 and involved in no-go decay. *J. Biol. Chem.* 283, 7145–7154. doi: 10.1074/jbc.M708224200
- Graille, M., and Séraphin, B. (2012). Surveillance pathways rescuing eukaryotic ribosomes lost in translation. *Nat. Rev. Mol. Cell Biol.* 13, 727–735. doi: 10.1038/nrm3457
- Greber, B. J., Boehringer, D., Montellese, C., and Ban, N. (2012). Cryo-EM structures of Arx1 and maturation factors Rei1 and Jjj1 bound to the 60S ribosomal subunit. *Nat. Struct. Mol. Biol.* 19, 1228–1233. doi: 10.1038/nsmb.2425
- Gross, T., Siepmann, A., Sturm, D., Windgassen, M., Scarcelli, J. J., Seedorf, M., et al. (2007). The DEAD-box RNA helicase Dbp5 functions in translation termination. *Science* 315, 646–649. doi: 10.1126/science.1134641
- Guydosh, N. R., and Green, R. (2014). Dom34 rescues ribosomes in 3' untranslated regions. *Cell* 156, 950–962. doi: 10.1016/j.cell.2014.02.006
- Heuer, A., Gerovac, M., Schmidt, C., Trowitzsch, S., Preis, A., Kötter, P., et al. (2017). Structure of the 40S-ABCE1 post-splitting complex in ribosome recycling and translation initiation. *Nat. Struct. Mol. Biol.* 24, 453–460. doi: 10.1038/nsmb.3396
- Higgins, C. F., Hiles, I. D., Salmond, G. P., Gill, D. R., Downie, J. A., Evans, I. J., et al. (1986). A family of related ATP-binding subunits coupled to many distinct biological processes in bacteria. *Nature* 323, 448–450. doi: 10.1038/323448a0
- Hirano, T. (2002). The ABCs of SMC proteins: two-armed ATPases for chromosome condensation, cohesion, and repair. *Genes Dev.* 16, 399–414. doi: 10.1101/gad.955102
- Holland, I. B., and Blight, M. A. (1999). ABC-ATPases, adaptable energy generators fuelling transmembrane movement of a variety of molecules in organisms from bacteria to humans. *J. Mol. Biol.* 293, 381–399. doi: 10.1006/jmbi.1999.2993
- Hopfner, K. P. (2016). Architectures and mechanisms of ATP binding cassette proteins. *Biopolymers* 105, 492–504. doi: 10.1002/bip.22843
- Hwang, J. U., Song, W. Y., Hong, D., Ko, D., Yamaoka, Y., Jang, S., et al. (2016). Plant ABC transporters enable many unique aspects of a terrestrial plant's lifestyle. *Mol. Plant* 9, 338–355. doi: 10.1016/j.molp.2016.02.003
- Hyde, S. C., Emsley, P., Hartshorn, M. J., Mimmack, M. M., Gileadi, U., Pearce, S. R., et al. (1990). Structural model of ATP-binding proteins associated with cystic fibrosis, multidrug resistance and bacterial transport. *Nature* 346, 362–365. doi: 10.1038/346362a0
- Inagaki, Y., Blouin, C., Susko, E., and Roger, A. J. (2003). Assessing functional divergence in EF-1 α and its paralogs in eukaryotes and archaeobacteria. *Nucleic Acids Res.* 31, 4227–4237. doi: 10.1093/nar/gkg440
- Ito-Harashima, S., Kuroha, K., Tatematsu, T., and Inada, T. (2007). Translation of the poly(A) tail plays crucial roles in nonstop mRNA surveillance via translation repression and protein destabilization by proteasome in yeast. *Genes Dev.* 21, 519–524. doi: 10.1101/gad.1490207

- Kamath, R. S., Fraser, A. G., Dong, Y., Poulin, G., Durbin, R., Gotta, M., et al. (2003). Systematic functional analysis of the *Caenorhabditis elegans* genome using RNAi. *Nature* 421, 231–237. doi: 10.1038/nature01278
- Kärblane, K., Gerassimenko, J., Nigul, L., Piirsoo, A., Smialowska, A., Vinkel, K., et al. (2015). ABCE1 is a highly conserved RNA silencing suppressor. *PLoS ONE* 10:e0116702. doi: 10.1371/journal.pone.0116702
- Karbstein, K. (2013). Quality control mechanisms during ribosome maturation. *Trends Cell Biol.* 23, 242–250. doi: 10.1016/j.tcb.2013.01.004
- Karcher, A., Büttner, K., Märtsens, B., Jansen, R. P., and Hopfner, K. P. (2005). X-ray structure of RLI, an essential twin cassette ABC ATPase involved in ribosome biogenesis and HIV capsid assembly. *Structure* 13, 649–659. doi: 10.1016/j.str.2005.02.008
- Karcher, A., Schele, A., and Hopfner, K. P. (2008). X-ray structure of the complete ABC enzyme ABCE1 from *Pyrococcus abyssi*. *J. Biol. Chem.* 283, 7962–7971. doi: 10.1074/jbc.M707347200
- Kashima, I., Takahashi, M., Hashimoto, Y., Sakota, E., Nakamura, Y., and Inada, T. (2014). A functional involvement of ABCE1, eukaryotic ribosome recycling factor, in nonstop mRNA decay in *Drosophila melanogaster* cells. *Biochimie* 106, 10–16. doi: 10.1016/j.biochi.2014.08.001
- Kerr, I. D. (2004). Sequence analysis of twin ATP binding cassette proteins involved in translational control, antibiotic resistance, and ribonuclease L inhibition. *Biochem. Biophys. Res. Commun.* 315, 166–173. doi: 10.1016/j.bbrc.2004.01.044
- Khoshevis, S., Gross, T., Rotte, C., Baierlein, C., Ficner, R., and Krebber, H. (2010). The iron-sulphur protein RNase L inhibitor functions in translation termination. *EMBO Rep.* 11, 214–219. doi: 10.1038/embor.2009.272
- Kiosze-Becker, K., Ori, A., Gerovac, M., Heuer, A., Nürenberg-Goloub, E., Rashid, U. J., et al. (2016). Structure of the ribosome post-recycling complex probed by chemical cross-linking and mass spectrometry. *Nat. Commun.* 7, 1–19. doi: 10.1038/ncomms13248
- Kispal, G., Sipos, K., Lange, H., Fekete, Z., Bedekovics, T., Janáky, T., et al. (2005). Biogenesis of cytosolic ribosomes requires the essential iron-sulphur protein Rli1p and mitochondria. *EMBO J.* 24, 589–598. doi: 10.1038/sj.emboj.7600541
- Kougioumoutzi, E., Cartolano, M., Canales, C., Dupré, M., Bramsiepe, J., Vlad, D., et al. (2013). *SIMPLE LEAF3* encodes a ribosome-associated protein required for leaflet development in *Cardamine hirsuta*. *Plant J.* 73, 533–545. doi: 10.1111/tpj.12072
- Kuroha, K., Akamatsu, M., Dimitrova, L., Ito, T., Kato, Y., Shirahige, K., et al. (2010). Receptor for activated C kinase 1 stimulates nascent polypeptide-dependent translation arrest. *EMBO Rep.* 11, 956–961. doi: 10.1038/embor.2010.169
- LaRivière, F. J., Cole, S. E., Ferullo, D. J., and Moore, M. J. (2006). A late-acting quality control process for mature eukaryotic rRNAs. *Mol. Cell* 24, 619–626. doi: 10.1016/j.molcel.2006.10.008
- Liu, S., Li, Q., and Liu, Z. (2013). Genome-wide identification, characterization and phylogenetic analysis of 50 catfish ATP-binding cassette (ABC) transporter genes. *PLoS ONE* 8:e63895. doi: 10.1371/journal.pone.0063895
- Lo, K. Y., Li, Z., Bussiere, C., Bresson, S., Marcotte, E. M., and Johnson, A. W. (2010). Defining the pathway of cytoplasmic maturation of the 60S ribosomal subunit. *Mol. Cell* 39, 196–208. doi: 10.1016/j.molcel.2010.06.018
- Lu, H., Xu, Y., and Cui, F. (2016). Phylogenetic analysis of the ATP-binding cassette transporter family in three mosquito species. *Pestic. Biochem. Physiol.* 132, 118–124. doi: 10.1016/j.pestbp.2015.11.006
- Lu, J., and Deutsch, C. (2008). Electrostatics in the ribosomal tunnel modulate chain elongation rates. *J. Mol. Biol.* 384, 73–86. doi: 10.1016/j.jmb.2008.08.089
- Maeda, T., Lee, J. M., Miyagawa, Y., Koga, K., Kawaguchi, Y., and Kusakabe, T. (2005). Cloning and characterization of a ribonuclease L inhibitor from the silkworm, *Bombyx mori*. *DNA Seq.* 16, 21–27. doi: 10.1080/10425170400028871
- Mancera-Martínez, E., Brito Querido, J., Valasek, L. S., Simonetti, A., and Hashem, Y. (2017). ABCE1: a special factor that orchestrates translation at the crossroad between recycling and initiation. *RNA Biol.* 14, 1279–1285. doi: 10.1080/15476286.2016.1269993
- Mauro, V. P., and Edelman, G. M. (2002). The ribosome filter hypothesis. *Proc. Natl. Acad. Sci. U.S.A.* 99, 12031–12036. doi: 10.1073/pnas.192442499
- Passos, D. O., Doma, M. K., Shoemaker, C. J., Muhrad, D., Green, R., Weissman, J., et al. (2009). Analysis of Dom34 and its function in no-go decay. *Mol. Biol. Cell* 20, 3025–3032. doi: 10.1091/mbc.e09-01-0028
- Paumi, C. M., Chuk, M., Snider, J., Stagljar, I., and Michaelis, S. (2009). ABC transporters in *Saccharomyces cerevisiae* and their interactors: new technology advances the biology of the ABC (MRP) subfamily. *Microbiol. Mol. Biol. Rev.* 73, 577–593. doi: 10.1128/MMBR.00020-09
- Petersen, B. O., Jørgensen, B., and Albrechtsen, M. (2004). Isolation and RNA silencing of homologues of the RNase L inhibitor in *Nicotiana* species. *Plant Sci.* 167, 1283–1289. doi: 10.1016/j.plantsci.2004.06.030
- Pisareva, V. P., Skabkin, M. A., Hellen, C. U., Pestova, T. V., and Pisarev, A. V. (2011). Dissociation by Pelota, Hbs1 and ABCE1 of mammalian vacant 80S ribosomes and stalled elongation complexes. *EMBO J.* 30, 1804–1817. doi: 10.1038/emboj.2011.93
- Preis, A., Heuer, A., Barrio-García, C., Hauser, A., Eyler, D. E., Berninghausen, O., et al. (2014). Cryoelectron microscopic structures of eukaryotic translation termination complexes containing eRF1-eRF3 or eRF1-ABCE1. *Cell Rep.* 8, 59–65. doi: 10.1016/j.celrep.2014.04.058
- Saito, K., Kobayashi, K., Wada, M., Kikuno, I., Takusagawa, A., Mochizuki, M., et al. (2010). Omnipotent role of archaeal elongation factor 1 alpha (EF1 α) in translational elongation and termination, and quality control of protein synthesis. *Proc. Natl. Acad. Sci. U.S.A.* 107, 19242–19247. doi: 10.1073/pnas.1009599107
- Saito, S., Hosoda, N., and Hoshino, S. (2013). The Hbs1-Dom34 protein complex functions in non-stop mRNA decay in mammalian cells. *J. Biol. Chem.* 288, 17832–17843. doi: 10.1074/jbc.M112.448977
- Salas-Marco, J., and Bedwell, D. M. (2004). GTP hydrolysis by eRF3 facilitates stop codon decoding during eukaryotic translation termination. *Mol. Cell Biol.* 24, 7769–7778. doi: 10.1128/MCB.24.17.7769-7778.2004
- Sarmiento, C., Nigul, L., Kazantseva, J., Buschmann, M., and Truve, E. (2006). ATRLI2 is an endogenous suppressor of RNA silencing. *Plant Mol. Biol.* 61, 153–163. doi: 10.1007/s11103-005-0001-8
- Scarpella, E., Barkoulas, M., and Tsiantis, M. (2010). Control of leaf and vein development by auxin. *Cold Spring Harb. Perspect. Biol.* 2:a001511. doi: 10.1101/cshperspect.a001511
- Shi, Z., and Barna, M. (2015). Translating the genome in time and space: specialized ribosomes, RNA regulons, and RNA-binding proteins. *Ann. Rev. Cell Dev. Biol.* 31, 31–54. doi: 10.1146/annurev-cellbio-100814-125346
- Shoemaker, C. J., Eyler, D. E., and Green, R. (2010). Dom34:Hbs1 promotes subunit dissociation and peptidyl-tRNA drop-off to initiate no-go decay. *Science* 330, 369–372. doi: 10.1126/science.1192430
- Shoemaker, C. J., and Green, R. (2011). Kinetic analysis reveals the ordered coupling of translation termination and ribosome recycling in yeast. *Proc. Natl. Acad. Sci. U.S.A.* 108, E1392–E1398. doi: 10.1073/pnas.1113956108
- Shoemaker, C. J., and Green, R. (2012). Translation drives mRNA quality control. *Nat. Struct. Mol. Biol.* 19, 594–601. doi: 10.1038/nsmb.2301
- Song, H., Mugnier, P., Das, A. K., Webb, H. M., Evans, D. R., Tuite, M. F., et al. (2000). The crystal structure of human eukaryotic release factor eRF1—mechanism of stop codon recognition and peptidyl-tRNA hydrolysis. *Cell* 100, 311–321. doi: 10.1016/S0092-8674(00)80667-4
- Soudet, J., Gélugne, J. P., Belhabich-Baumans, K., Caizergues-Ferrer, M., and Mougín, A. (2010). Immature small ribosomal subunits can engage in translation initiation in *Saccharomyces cerevisiae*. *EMBO J.* 29, 80–92. doi: 10.1038/emboj.2009.307
- Strunk, B. S., Loucks, C. R., Su, M., Vashisth, H., Cheng, S., Schilling, J., et al. and Skiniotis, G. (2011). Ribosome assembly factors prevent premature translation initiation by 40S assembly intermediates. *Science* 333, 1449–1453. doi: 10.1126/science.1208245
- Strunk, B. S., Novak, M. N., Young, C. L., and Karbstein, K. (2012). A translation-like cycle is a quality control checkpoint for maturing 40S ribosome subunits. *Cell* 150, 111–121. doi: 10.1016/j.cell.2012.04.044
- ter Beek, J., Guskov, A., and Slotboom, D. J. (2014). Structural diversity of ABC transporters. *J. Gen. Physiol.* 143, 419–435. doi: 10.1085/jgp.201411164
- Tomii, K., and Kanehisa, M. (1998). A comparative analysis of ABC transporters in complete microbial genomes. *Genome Res.* 8, 1048–1059. doi: 10.1101/gr.8.10.1048
- Tsuboi, T., Kuroha, K., Kudo, K., Makino, S., Inoue, E., Kashima, I., et al. (2012). Dom34:Hbs1 plays a general role in quality-control systems by dissociation of a stalled ribosome at the 3' end of aberrant mRNA. *Mol. Cell* 46, 518–529. doi: 10.1016/j.molcel.2012.03.013

- Uesono, Y., and Toh, E. A. (2002). Transient inhibition of translation initiation by osmotic stress. *J. Biol. Chem.* 277, 13848–13855. doi: 10.1074/jbc.M108848200
- van den Elzen, A. M., Schuller, A., Green, R., and Séraphin, B. (2014). Dom34-Hbs1 mediated dissociation of inactive 80S ribosomes promotes restart of translation after stress. *EMBO J.* 33, 265–276. doi: 10.1002/emboj.201386123
- Van Dyke, N., Chanchorn, E., and Van Dyke, M. W. (2013). The *Saccharomyces cerevisiae* protein Stm1p facilitates ribosome preservation during quiescence. *Biochem. Biophys. Res. Commun.* 430, 745–750. doi: 10.1016/j.bbrc.2012.11.078
- Vasiliou, V., Vasiliou, K., and Nebert, D. W. (2009). Human ATP-binding cassette (ABC) transporter family. *Hum. Genomics* 3, 281–290. doi: 10.1186/1479-7364-3-3-281
- Verrier, P. J., Bird, D., Burla, B., Dassa, E., Forestier, C., Geisler, M., et al. (2008). Plant ABC proteins – a unified nomenclature and updated inventory. *Trends Plant Sci.* 13, 151–159. doi: 10.1016/j.tplants.2008.02.001
- Wang, B., Dukarevich, M., Sun, E. I., Yen, M. R., and Saier, M. H. Jr. (2009). Membrane porters of ATP-binding cassette transport systems are polyphyletic. *J. Membr. Biol.* 231, 1–10. doi: 10.1007/s00232-009-9200-6
- Xie, X., Cheng, T., Wang, G., Duan, J., Niu, W., and Xia, Q. (2012). Genome-wide analysis of the ATP-binding cassette (ABC) transporter gene family in the silkworm, *Bombyx mori*. *Mol. Biol. Rep.* 39, 7281–7291. doi: 10.1007/s11033-012-1558-3
- Xue, S., and Barna, M. (2012). Specialized ribosomes: a new frontier in gene regulation and organismal biology. *Nat. Rev. Mol. Cell Biol.* 13, 355–369. doi: 10.1038/nrm3359
- Yarunin, A., Panse, V. G., Petfalski, E., Dez, C., Tollervey, D., and Hurt, E. C. (2005). Functional link between ribosome formation and biogenesis of iron-sulfur proteins. *EMBO J.* 24, 580–588. doi: 10.1038/sj.emboj.7600540
- Zhao, Z., Fang, L. L., Johnsen, R., and Baillie, D. L. (2004). ATP-binding cassette protein E is involved in gene transcription and translation in *Caenorhabditis elegans*. *Biochem. Biophys. Res. Commun.* 323, 104–111. doi: 10.1016/j.bbrc.2004.08.068
- Zheng, W. H., Västermark, A., Shlykov, M. A., Reddy, V., Sun, E. I., and Saier, M. H., et al. (2013). Evolutionary relationships of ATP-Binding Cassette (ABC) uptake porters. *BMC Microbiol.* 13, 1–20. doi: 10.1186/1471-2180-13-98
- Zimmerman, C., Klein, K. C., Kiser, P. K., Singh, A. R., Firestein, B. L., Riba, S. C., et al. (2002). Identification of a host protein essential for assembly of immature HIV-1 capsids. *Nature* 415, 88–92. doi: 10.1038/415088a

Conflict of Interest Statement: The authors declare that the research was conducted in the absence of any commercial or financial relationships that could be construed as a potential conflict of interest.

Copyright © 2018 Navarro-Quiles, Mateo-Bonmati and Micol. This is an open-access article distributed under the terms of the Creative Commons Attribution License (CC BY). The use, distribution or reproduction in other forums is permitted, provided the original author(s) and the copyright owner(s) are credited and that the original publication in this journal is cited, in accordance with accepted academic practice. No use, distribution or reproduction is permitted which does not comply with these terms.

The Arabidopsis ATP-Binding Cassette E protein ABCE2 is a conserved component of the translation machinery

Carla Navarro-Quiles, Eduardo Mateo-Bonmatí¹, Héctor Candela, Pedro Robles, Antonio
Martínez-Laborda², María Rosa Ponce, and José Luis Micol

Instituto de Bioingeniería, Universidad Miguel Hernández, Campus de Elche, 03202
Elche, Spain

Current address:

¹John Innes Centre, NR4 7UA, Norwich, United Kingdom

²Área de Genética, Universidad Miguel Hernández, Campus de Sant Joan, 03550 Sant
Joan d'Alacant, Spain

Corresponding author: J.L. Micol (telephone: 34 96 665 85 04; fax: 34 96 665 85 11; E-mail:
jlmicol@umh.es)

Keywords: Arabidopsis ABCE2, ribosome recycling, translation machinery, venation
pattern, auxin homeostasis

Word count (total): 14449.

Figures: 7

Tables: 0

Supplementary Figures: 14

Supplementary Tables: 6

ABSTRACT

ATP-Binding Cassette E (ABCE) proteins dissociate cytoplasmic ribosomes after translation terminates, thus linking termination to reinitiation of translation. This function has been demonstrated in animals, yeast, and archaea, but not in plants. In most species, ABCE is encoded by a single-copy gene; by contrast, *Arabidopsis thaliana* has two *ABCE* paralogs, of which *ABCE2* seems to conserve the ancestral function. Indeed, our co-immunoprecipitation experiments showed that *ABCE2* physically interacts with components of the translation machinery, including subunits of the EUKARYOTIC TRANSLATION INITIATION FACTOR 3 (eIF3) complex. We isolated *apiculata7-1* (*api7-1*), a viable, hypomorphic allele of *ABCE2*, which has a pleiotropic morphological phenotype reminiscent of mutations affecting ribosome biogenesis factors and ribosomal proteins. We also studied *api7-2*, a null, recessive lethal allele of *ABCE2*. To explore the biological processes affected by *ABCE2* depletion, we performed RNA-seq of the *api7-1* mutant, and observed increased responses to iron and sulfur starvation. We also found increased transcript levels of genes related to auxin signaling and metabolism. Our results indicate that the role of ABCEs in ribosome recycling is evolutionarily conserved in animal, fungal, plant, and archaeal lineages.

INTRODUCTION

The ATP-Binding Cassette (ABC) proteins are present in all living organisms and constitute one of the largest protein families known. Most ABC proteins consist of two transmembrane domains (TMDs), which transport solutes across cellular membranes, and two nucleotide binding domains (NBDs), which hydrolyze two ATP molecules to induce TMD movement and release of the cargo (1). In contrast to these typical ABC proteins, members of the ABCE and ABCF subfamilies of ABC proteins, as well as some members of the plant-specific ABCI subfamily, lack TMDs and are soluble (2). Human ABCE1 was first named RNASE L INHIBITOR (RLI) due to its ability to inhibit the activity of RNase L, an enzyme that is only present in mammals (3). Nevertheless, ABCE subfamily members are highly conserved among archaea and eukaryotes, and participate in ribosome recycling and translation reinitiation, as has been demonstrated for archaea, fungi, and animals, but not plants (4-10).

ABCE proteins contain an iron-sulfur cluster binding domain (FeSD), two NBDs (NBD1 and NBD2), and two hinge motifs (11-13). The first hinge motif is between the NBDs and allows NBD movement to bind and hydrolyze ATP. The second hinge motif, located at the C terminus, and a helix-loop-helix (HLH) motif within NBD1, allow the interaction of the ABCE protein with the ribosome. In this manner, occlusion of an ATP molecule favors ABCE binding to the translation termination complex. Next, the occlusion of another ATP molecule displaces the FeSD and promotes ribosome splitting. Finally, ATP hydrolysis allows ABCE detachment from the 30S/40S ribosome subunit (14-16). Alternatively, ABCE can retain the two ATP molecules and remain bound to the 30S/40S subunit in the post-splitting complex, where it is believed to prevent the premature recruitment of a 60S subunit until the late steps of translation initiation complex formation (5,6,10,15,17-20).

In most genomes, the ABCE subfamily is represented by a single-copy gene, usually named *ABCE1*, whose null alleles are lethal, while hypomorphic alleles result in developmental defects and slow-growth phenotypes in all studied organisms (21). *Arabidopsis thaliana* (hereafter referred to as *Arabidopsis*), however, has two *ABCE* paralogs named *ABCE1* and *ABCE2* (2,22). *Arabidopsis ABCE2* has been studied for its RNA silencing suppression activity (23,24). In contrast, *Cardamine hirsuta*, a close relative of *Arabidopsis* with compound leaves has only one *ABCE* gene, *SIMPLE LEAF3 (SIL3)*, which is required for leaflet formation and leaf development. The leaves of homozygotes for the hypomorphic *sil3* mutation are simple and have vascular defects, probably caused by an aberrant auxin homeostasis (25).

The upstream open reading frames (uORFs) of the 5' untranslated regions (5' UTRs) of some mRNAs serve as regulatory elements that reduce the efficiency of translation of the main ORF (mORF) of these mRNAs. In *Arabidopsis*, translation of a long uORF prevents

translation reinitiation on the adjacent mORF due to a progressive loss of initiation factors from the translating machinery (26,27). More than one third of Arabidopsis mRNAs contain uORFs, together with an mORF that usually encodes a transcription factor or other type of protein acting in a signaling pathway (27).

In fact, auxin signaling is known to be highly sensitive to perturbations in the translation machinery. Mutations in *RIBOSOMAL LARGE SUBUNIT 4 D (RPL4D)*, *RPL5A*, *RPL24B*, and *EUKARYOTIC TRANSLATION INITIATION FACTOR 3 SUBUNIT H (eIF3h)* reduce the ability of the translation machinery to reinitiate translation on mORFs, leading to low levels of several AUXIN RESPONSE FACTORS (ARFs) that are encoded by mRNAs containing uORFs (28-31). Among other developmental defects, these mutations cause aberrant leaf venation patterns, in agreement with a role for auxin in vascular patterning (32,33). In addition, auxin itself regulates translation by promoting reinitiation on the mORFs of the mRNAs of several *ARF* genes. Specifically, auxin induces the activation of TARGET OF RAPAMYCIN (TOR), a highly conserved growth regulator, which phosphorylates eIF3h, promoting translation reinitiation after the termination of the translation of a uORF (34).

Here, we describe a functional analysis of the Arabidopsis *ABCE1* and *ABCE2* genes. We studied two recessive alleles of *ABCE2*: the hypomorphic and viable *apiculata7-1 (api7-1)* allele, and the null and lethal *api7-2* allele. The *api7-1* mutant exhibits the typical morphological phenotype caused by mutation of genes encoding ribosome biogenesis factors and ribosomal proteins, which includes aberrant leaf venation patterns. We found by co-immunoprecipitation that *ABCE2* physically interacts with components of the translation machinery, and by RNA-seq that its partial loss of function triggers iron and sulfur deficiency responses related to FeS cluster biogenesis, as well as the upregulation of auxin biosynthesis genes. Our observations strongly support a conserved role for *ABCE* proteins in ribosome recycling in plants, as previously shown for the animal, fungal, and archaeal lineages.

MATERIALS AND METHODS

Plant materials, growth conditions, and crosses

The *Arabidopsis thaliana* (L.) Heynh. wild-type accessions Landsberg *erecta* (Ler) and Columbia-0 (Col-0), and the *asymmetric leaves1-1* (*as1-1*; N3374; in the Col-1 genetic background) and *as2-1* (N3117; in ER) mutants were initially obtained from the Nottingham Arabidopsis Stock Center (NASC; Nottingham, United Kingdom) and then propagated in our laboratory for further analysis. We introgressed the *as1-1* and *as2-1* mutations into the Col-0 background by crossing to Col-0 three times. The NASC also provided seeds of the *api7-2* (GABI_509C06; N448798) (35) and *PIN1_{pro}:PIN1:GFP DR5_{pro}:3XVENUS:N7* (N67931) (36) lines. The *ATHB8_{pro}:GUS* line (N296) was kindly provided by Simona Baima (37). The *api7-1* line was isolated in the Ler background after ethyl methanesulfonate (EMS) mutagenesis in our laboratory and then backcrossed twice to Ler (38). Unless otherwise stated, all the mutants mentioned in this work are homozygous for the mutations indicated.

Seed sterilization and sowing, plant culture, crosses, and allelism tests were performed as previously described (38-40). In brief, plants were grown under sterile conditions on half-strength Murashige and Skoog medium (Duchefa Biochemie) with 0.75% plant agar (Duchefa Biochemie) and 1% sucrose (Duchefa Biochemie), at 20°C ± 1°C, 60–70% relative humidity, and continuous illumination at ~75 μmol·m⁻²·s⁻¹.

Positional cloning and molecular characterization of *ABCE2* mutant alleles

Genomic DNA was extracted as previously described (41). The *ABCE2* gene was cloned as previously described (42). First, we mapped the *api7-1* mutation to a 123.5-kb candidate interval containing 30 genes using a mapping population of 273 F₂ plants derived from an *api7-1* × Col-0 cross, and the primers listed in Supplementary Table S1, as previously described (41,43). Then, the whole *api7-1* genome was sequenced by Fasteris (Geneva, Switzerland) using the Illumina HiSeq2000 platform. The bioinformatic analysis of the data was performed as previously described (42). The candidate mutation was verified by Sanger sequencing in an ABI Prism 3130xl Genetic Analyzer (Applied Biosystems).

Discrimination between the wild-type *ABCE2* and *api7-1* mutant alleles was done by PCR with the *api7-1_F* and *api7-1_R* primers (Supplementary Table S1), followed by restriction with *Eco57I* (Thermo Fisher Scientific), as the *api7-1* mutation (CTQCAG→CTICAG) creates an *Eco57I* restriction site. The presence and position of the *api7-2* T-DNA insertion in the GABI_509C06 line was confirmed by PCR amplification and Sanger sequencing, respectively, using gene-specific primers and the o8409 primer for the GABI-Kat T-DNA from the pAC161 vector (Supplementary Table S1).

Gene constructs and plant transformation

All inserts were PCR amplified from Col-0 genomic DNA using Phusion High Fidelity DNA Polymerase (Thermo Fisher Scientific) and primers that contained *attB* sites at their 5' ends (Supplementary Table S1). PCR products were purified using an Illustra GFX PCR DNA and Gel Band Purification Kit (Cytiva), and then cloned into the pGEM-T Easy221 vector, transferred to *Escherichia coli* DH5 α , and subcloned into the pEarleyGate 101, pMDC83, or pMDC107 destination vectors (44,45) as previously described (46).

To obtain the *ABCE2*_{pro}:*ABCE2* construct, a 4.54-kb segment of chromosome 4 was PCR amplified, including 1183 bp upstream of the start codon of *ABCE2*, and 489 bp downstream of the stop codon. For the *35S*_{pro}:*ABCE2*:*GFP* and *35S*_{pro}:*ABCE2*:*YFP* constructs, the 2.87-kb *ABCE2* transcription unit was amplified, excluding its stop codon. After purification, the PCR products were cloned into pGEM-T Easy221 and subcloned into pMDC83 and pEarleyGate 101, respectively.

For the promoter exchange assay, promoters and transcription units were separately PCR amplified and fused in a second amplification. For example, to obtain *ABCE1*_{pro}:*ABCE2*, a genomic region of 1485 bp upstream of *ABCE1* was amplified using the primers *ABCE1*_{pro}_F, which contained the *attB1* site, and *ABCE1*_{pro}_R, which included a 3' sequence complementary to the first 25 nucleotides of the *ABCE2* transcription unit. The 2.87-kb *ABCE2* transcription unit was obtained with *ABCE2*_{tu}_F, which is complementary to the *ABCE1*_{pro}_R sequence, and *ABCE2*_{tu}_R, which includes the stop codon and the *attB2* site. Then, the same amounts of purified PCR products were combined in a second PCR mix, and fused using the *ABCE1*_{pro}_F and *ABCE2*_{tu}_R primers to obtain *ABCE1*_{pro}:*ABCE2*. The *ABCE1*_{pro}:*ABCE2* and *ABCE2*_{pro}:*ABCE1* final PCR products were purified, cloned into pGEM-T Easy221, and subcloned into pMDC107.

All constructs were transferred to electrocompetent *Agrobacterium tumefaciens* GV3101 (C58C1 Rif^R) cells, which were used to transform *Ler*, *api7-1*, or *API7/api7-2* plants by the floral dip method (47). Putative transgenic plants were selected on plates supplemented with 15 $\mu\text{g}\cdot\text{ml}^{-1}$ hygromycin B (Thermo Fisher Scientific, Invitrogen).

Phenotypic analysis and morphometry

Photographs of Arabidopsis rosettes, inflorescences, flowers, and siliques were taken with a Nikon SMZ1500 stereomicroscope equipped with a Nikon DXM1200F digital camera. For larger specimens, four to five partial images from the same plant were taken and merged using the Photomerge tool of Adobe Photoshop CS3 software. Empty spaces resulting from the assembly were filled with black. To measure rosette size and root length, photographs of plants grown on Petri dishes, horizontally or vertically oriented, respectively, were taken with a Canon PowerShot S315 camera. For rosette size, rosette silhouettes were drawn on

the screen of a Cintiq 18SX Interactive Pen Display (Wacom) using Adobe Photoshop CS3, and their sizes were measured with the NIS Elements AR 3.1 image analysis package (Nikon). Root length was measured directly from photographs with the Freehand line tool from Fiji software (ImageJ; <https://imagej.net/ImageJ>) (48) on the screen of a Cintiq 18SX Interactive Pen Display. Rosette phyllotaxis was measured using the Fiji Angle tool on photographs taken from plants grown horizontally. The length of each root and the angles between consecutive leaves were measured per triplicate. Shoot length was measured *in vivo* with a millimeter ruler, from the soil to the apex of the main shoot.

Chlorophyll *a* and *b* and carotenoids were extracted as previously described (49), with some modifications. Each biological replicate contained 50–60 mg of fresh rosettes immediately frozen in liquid nitrogen after collection, to prevent pigment loss. After tissue homogenization with cold 80% (v/v) acetone, the cell debris was removed by centrifugation. Pigment content was spectrophotometrically determined as previously described (50), and normalized to the amount of collected tissue.

Sample preparation for flow-cytometry was performed as previously described (51). Nuclear DNA content was analyzed using a SH800S Cell Sorter (Sony Biotechnology) and the data were processed using the SH800 software (Sony Biotechnology). The endoreduplication index (EI) was calculated as previously described (52).

Differential interference contrast and bright-field microscopy, and GUS analyses

For differential interference contrast (DIC) and bright-field microscopy, all samples were cleared by immersion in a 2.67 g/ml chloral hydrate solution and mounted on glass slides with a solution of 2.67 g/ml chloral hydrate dissolved in 2:1 glycerol:water. DIC micrographs of epidermal and palisade mesophyll leaf layers were taken using a Leica DMRB microscope equipped with a Nikon DXM1200 digital camera. Micrographs of venation patterns from cotyledons, first- and third-node rosette leaves, cauline leaves, sepals and petals, and leaf primordia expressing *ATHB8_{pro}:GUS* were taken under bright field with a Nikon D-Eclipse C1 confocal microscope equipped with a Nikon DS-Ri1 camera, using the NIS-Elements AR 3.1 software (Nikon). When the organ did not fit into the objective field, the Scan Large Image tool from the NIS-Elements AR 3.1 software was used. Diagrams from leaf cells and venation patterns, and morphometric analysis of leaf cells were obtained as previously described (46,53). For venation pattern morphometry, the phenoVein (<http://www.plant-image-analysis.org>) (54) software was used. Leaf lamina circularity was calculated as $4 \cdot \pi \cdot \text{area} / \text{perimeter}^2$. Lamina area and perimeter were measured on diagrams from the leaf lamina with the Fiji Wand tool. GUS assays were performed as previously described (38).

Confocal microscopy and fluorescence quantification

Confocal laser scanning microscopy images were obtained using a Nikon D-Eclipse C1 confocal microscope equipped with a Nikon DS-Ri1 camera and processed with the operator software EZ-C1 (Nikon). Visualization of the fluorescent proteins and dyes was performed on primary roots mounted with deionized water on glass slides. GFP, YFP, and VENUS fluorescent proteins were excited at 488 nm with an argon ion laser, and their emissions were collected with a 515/30 nm barrier filter. Nuclei were stained by immersing complete seedlings in a $0.2 \mu\text{g}\cdot\text{ml}^{-1}$ 4',6-diamidino-2-phenylindole (DAPI) solution (Sony Biotechnology) for 12 min, and the seedlings were then transferred to deionized water. DAPI was excited at 408 nm with a diode laser, and detected with a 450/35 nm filter. Cell walls were stained by immersing the seedlings in $10 \mu\text{g}\cdot\text{ml}^{-1}$ propidium iodide (Sigma-Aldrich) for 8 min. Then, the seedlings were washed three times with deionized water before mounting their roots on glass slides. Propidium iodide was excited at 543 nm with a helium-neon laser, and detected with a 605/75 nm filter.

For fluorescence quantification of the *PIN1_{pro}:PIN1:GFP* and *DR5_{pro}:3XVENUS:N7* protein products, wild-type and *api7-1* seedlings homozygous for these transgenes were grown vertically on the same Petri dishes under identical conditions for 5 days. To further favor homogeneity between samples, wild-type and *api7-1* roots were mounted on the same slides in an alternating manner. Image acquisition was performed using a 40× objective with a 0.75 numerical aperture. The dwell time was set at 2.16 and 1.68 μs for PIN1:GFP and VENUS:N7, respectively. The fluorescent protein and propidium iodide images were consecutively acquired in different channels. Four images were acquired and averaged per optical section. Five optical sections encompassing 4 μm from the innermost root layers were photographed. Acquired images (.ids files) were used to generate flat images (.tiff files) with Fiji by stacking the optical sections from the fluorescent protein channel. Fluorescence quantification was performed using the Fiji Mean gray value measurement on the fluorescent regions from the flat images. The fluorescent regions were selected with a pre-established pixel intensity threshold.

RNA isolation, cDNA synthesis, and quantitative PCR

Samples for RNA extraction were collected on ice and immediately frozen for storage at -80°C until use. RNA was isolated using TRIzol reagent (Thermo Fisher Scientific, Invitrogen) and its concentration was estimated using a Pearl NanoPhotometer (Implen) spectrophotometer. Removal of contaminating DNA, cDNA synthesis, and quantitative PCR (qPCR) were performed as previously described (46). For removal of contaminating genomic DNA, approximately 8 μg of RNA were treated with a TURBO DNA-free Kit (Thermo Fisher, Invitrogen) following the instructions of the manufacturer.

First-strand cDNA was synthesized from 1.8 µg of total RNA using random hexamers and the Maxima Reverse Transcriptase system (Thermo Fisher Scientific) in a final volume of 20 µl, using a Bio-Rad T100 Thermal Cycler (10 min at 25°C, 1 h at 50°C, and 5 min at 85°C). Absence of contaminating genomic DNA on cDNA samples was confirmed by PCR amplifying a region of the *ORNITHINE TRANSCARBAMYLASE (OTC)* gene, which contains an intron, using the OTC3D and OTCR primers (55) (Supplementary Table S1), and a genomic DNA sample from Col-0 plants as a control. For qPCR, *ACTIN2 (ACT2)* was used as an internal control for relative expression analysis using the primers listed in Supplementary Table S1 (56). Three biological replicates, each with three technical replicates, were analyzed per genotype. PCR was performed using 7.5 µl of Maxima SYBR Green/ROX qPCR Master Mix (Thermo Fisher), 5 µl of the corresponding primer pair (1.5 µM each), 1 µl of cDNA, and water in a total volume of 20 µl, on a Step One Plus System (Applied Biosystems). The qPCR was performed as follows: 2 min at 50°C, 10 min at 95°C, followed by 41 cycles of 15 s at 95°C and 1 min at 60°C, and a final step of 15 s at 95°C. Relative quantification of gene expression data was performed using the comparative C_T method ($2^{-\Delta\Delta CT}$) (57).

RNA-seq analysis

Total RNA was isolated from 100 mg of *Ler* and *api7-1* rosettes collected 14 days after stratification (das) using TRIzol. Rosette samples were collected on ice and immediately frozen in liquid nitrogen. RNA concentration and quality were assessed using a 2100 Bioanalyzer (Agilent Genomics) with an RNA 600 Nano Kit (Agilent Technologies) as previously described (46). Three biological replicates per genotype, with more than 14 µg of total RNA per sample, and an RNA integrity number (RIN) higher than 7, were sent to Novogene (Cambridge, United Kingdom) for massive parallel sequencing. Sequencing libraries were generated using NEBNext Ultra RNA Library Prep Kit for Illumina (New England Biolabs) and fed into a NovaSeq 6000 Illumina platform with a S4 Flow Cell type, which produced paired-end reads of 150 bp. Read mapping to the Arabidopsis genome (TAIR10) using the 2.0.5 version of HISAT2 (58), with default parameters, and the identification of differentially expressed genes between *Ler* and *api7-1* with the 1.22.2 version of DESeq2 R package (59) were performed by Novogene. Genes with a *P*-value < 0.05 adjusted with the Benjamini and Hochberg's method, and with a fold change > 1.5 were considered differentially expressed. The gene ontology (GO) enrichment analysis of the differentially expressed genes was performed with the online tool DAVID (<https://david.ncifcrf.gov/home.jsp>) (60,61), using all the terms included in the GO Biological Process categorization (GOTERM_BP_ALL).

Co-immunoprecipitation assay

For protein extraction, 700 mg of whole *api7-1 35S_{pro}:ABCE2:YFP* seedlings were collected 10 das per biological replicate. The tissue was crosslinked with 1× phosphate-saline buffer containing 1% (v/v) formaldehyde as described in (62). For protein extraction, the tissue was ground to a fine powder with liquid nitrogen and then resuspended in a lysis buffer (50 mM Tris-HCl, pH 7.5; 0.1% [v/v] IGEPAL CA-630 [Sigma-Aldrich]; 2 mM phenylmethylsulfonyl fluoride [PMSF; Sigma-Aldrich]; 150 mM NaCl; and a cOmplete protease inhibitor cocktail tablet [Sigma-Aldrich]) using a vortexer. After incubation on ice for 10 min, the samples were centrifuged at 4°C and the supernatants were used as the protein extracts. Before co-immunoprecipitation, 20 µl from each extract were transferred to a new tube for use as inputs in a western blot.

Co-immunoprecipitation was performed with the µMACS GFP Isolation Kit (Milteny Biotec) following the instructions of the manufacturer, using proteins from three biological replicates. The immunoprecipitation of the ABCE2:YFP fusion protein was checked by western blotting using an anti-GFP-HRP antibody (Milteny Biotec), and the WesternSure chemiluminiscent substrate on a C-DiGit Blot Scanner (LI-COR).

The co-immunoprecipitates were analyzed by liquid chromatography electrospray ionization tandem mass spectrometry (LC-ESI-MS/MS) at the Centro Nacional de Biotecnología (CNB) Proteomics facility (Madrid, Spain). Tandem mass spectra were searched against Araport11 using the MASCOT search engine (Matrix Science, <http://www.matrixscience.com/>). Peptide sequences identified with a false discovery rate (FDR) < 1% were considered statistically valid (Supplementary Data Set 1). Proteins identified with at least 2 peptides without overlapping sequences in at least 2 biological replicates (namely, at least 4 peptides) were considered as identified with high confidence. To search for potential ABCE2:YFP interactors, proteins whose subcellular localization was not predicted to be cytoplasmic by SUBA4 (<https://suba.live/>) (63,64) were discarded, with the exception of At2g20830, which is predicted to localize to mitochondria (see Results). To further discard potential false positive interactions, all the proteins identified in three other co-immunoprecipitations of GFP-fused proteins performed in our laboratory under identical conditions to that of ABCE2:YFP, but functionally unrelated, were used to create a subtract list. Proteins identified in ABCE2:YFP samples with at least twice the number of peptides assigned to the same protein in the subtract list were considered enriched. The rest of the proteins, which contained a more similar number of peptides between the ABCE2:YFP list and the subtract list, were considered false positives and discarded. In addition, there were few proteins that were solely identified in ABCE2:YFP samples.

Additional bioinformatic and statistical analyses

The identity and similarity values between conserved proteins were obtained from global pairwise sequence alignments performed with EMBOSS Needle (https://www.ebi.ac.uk/Tools/psa/emboss_needle/) (65) with default parameters and pair output format. The multiple sequence alignment of ABCE orthologs was obtained with Clustal Omega (<https://www.ebi.ac.uk/Tools/msa/clustalo/>) (65) with default settings and ClustalW output format, and shaded with BOXSHADE (https://embnet.vital-it.ch/software/BOX_form.html).

A TBLASTN search was performed to identify *ABCE* genes within eudicots (taxid:71240) against the sequences contained in the Nucleotide collection database at the National Center for Biotechnology Information BLASTP server (NCBI; <https://blast.ncbi.nlm.nih.gov/Blast.cgi>) (66) using *Arabidopsis thaliana* ABCE2 protein as the query (NP_193656). Default parameters were used except for max target sequences, which was set at 1000, and word size, which was set at 2. Predicted *ABCE* coding sequences were downloaded from the NCBI Nucleotide database, except for *Eschscholzia californica* ABCE, which was downloaded from the Eschscholzia Genome DataBase (<http://eschscholzia.kazusa.or.jp/index.html>) (67) (Supplementary Table S2). The phylogenetic analysis was performed with MEGA X software (68): the multiple sequence alignment and the phylogenetic tree were obtained using codon recognition with Muscle (69,70), and the Neighbor-Joining method (71), respectively.

Hypothesis testing was performed as described in (46). The parametric Student's *t* test was used when the number of observations (*n*) was 10 or higher, under the assumption that most of the data followed a normal distribution. When the normality assumption could not be made (*n* < 10), the nonparametric Mann-Whitney *U* test for unpaired data was used. All *P*-values presented in this work are two-sided.

Accession numbers

Sequence data can be found at The Arabidopsis Information Resource (<https://www.arabidopsis.org/>) under the following accession numbers: *ABCE1* (At3g13640), *ABCE2* (At4g19210), *ACT2* (At3g18780), *ATHB8* (At4g32880), *OTC* (At1g75330), and *PIN1* (At1g73590).

RESULTS

The *api7-1* mutant exhibits a pleiotropic morphological phenotype

In a previous large-scale screen for EMS-induced mutations affecting leaf development, we identified 8 mutants with pointed rosette leaves and mild marginal indentations. The corresponding causal mutations were dubbed *apiculata* (*api*), and allelism tests demonstrated that they fell into 7 different complementation groups (*API1-API7*) (38). The phenotype of *api* plants is reminiscent of those of mutants carrying loss-of-function alleles of genes encoding ribosomal proteins or ribosome biogenesis factors (29,72-75). Indeed, *api2*, the only already characterized *api* mutant, carries a point mutation in the 5' UTR of the *RPL36aB* gene, which encodes a 60S ribosomal subunit protein (76).

The *api7-1* mutant, which we initially named *api7* (38), exhibits slow growth and leaves with reduced size (Figure 1). Its pleiotropic morphological phenotype includes rosette leaves that are pointed, indented, with pale green lamina and yellowish margins, and a reduced content of photosynthetic pigments, compared to its wild-type *Ler* (Figure 1A, B; Supplementary Figure S1A). DIC microscopy of *api7-1* and *Ler* first-node leaves cleared with chloral hydrate uncovered a marked reduction in cell size in the abaxial and adaxial epidermal layers, but not in the palisade mesophyll (Supplementary Figure S2). The ploidy levels of the *api7-1* leaves from the first to the fourth nodes, determined by flow cytometry, were slightly higher than in the wild type, suggesting an increased number of endoreduplication cycles (Supplementary Figure S3) (77).

The projected area of *api7-1* rosettes is significantly smaller than that of wild-type plants throughout the vegetative phase (Figure 1D), while rosette leaf phyllotaxis seemed unaffected (Supplementary Figure S1B). In addition, the primary root is shorter in *api7-1* than in *Ler* plants (Supplementary Figure S1C). Although the *api7-1* plants grow slower than the wild type, at the end of their life cycle the length of the main stem is similar to that of *Ler* plants (Figure 1E). The *api7-1* inflorescences and siliques are seemingly normal (Supplementary Figure 1D-I), although *api7-1* siliques carry a higher percentage of aborted or unfertilized ovules (7.91%; $n = 392$) than *Ler* siliques (4.22%; $n = 403$). Nevertheless, this reduced percentage of viable seeds per silique does not lead to a significant reduction in seed production: *api7-1* plants produced 479 ± 70 mg of seeds (mean \pm standard deviation; $n = 7$) with similar sizes to those of *Ler*, which produced 484 ± 66 mg ($n = 6$).

api7-1 is a viable mutant allele of the *ABCE2* gene

The *api7-1* mutation was previously mapped to chromosome 4 (78). To identify the mutated gene, we combined map-based cloning and next-generation sequencing, as previously described (42). First, we performed linkage analysis of an F_2 mapping population using the primers listed in Supplementary Table S1, as previously described (41,43), which allowed

us to delimit a candidate interval encompassing 30 annotated genes (Figure 2A). We then sequenced the whole *api7-1* genome, and, after discarding all the putative Ler/Col-0 polymorphisms, we identified 4 EMS-type nucleotide substitutions (3 G→A and 1 C→T) within the candidate interval (Supplementary Table S3; see Methods). Only one of these, a C→T transition in At4g19210, was predicted to be a missense mutation causing a Pro138→Ser substitution (Figure 2B).

The At4g19210 gene encodes ABCE2, a protein of 605 amino acids with a molecular mass of 68.39 kDa. The Pro138 residue, at the beginning of the HLH motif located within NBD1, is conserved across all eukaryotic ABCE proteins, except in *Caenorhabditis elegans*, in which it seems to have evolved more divergently (Supplementary Figure S4) (79). The conservation of this residue suggests that it is necessary for the proper function of ABCE proteins, specifically for the interactions with the ribosome and the post-splitting complex, which mainly occur through the HLH and hinge motifs (6,15,18).

To confirm that the mutation found in At4g19210 causes the phenotype of the *api7-1* mutant, we obtained the *ABCE2_{pro}:ABCE2* transgene, encompassing the whole At4g19210 transcriptional unit driven by its own promoter, which was transferred into *api7-1* plants. This transgene completely restored the wild-type rosette leaf shape and stem height (Figure 1C-E), as well as the photosynthetic pigment content (Supplementary Figure S1A), and percentage of aborted ovules (3.05%; $n = 426$). The *ABCE2_{pro}:ABCE2* transgene partially restored the root length, leaf epidermal cell sizes, and ploidy levels (Supplementary Figures S1C, S2, S3).

To provide further confirmation that *api7-1* is an allele of *ABCE2*, we performed an allelism test using GABI_509C06 plants, which were heterozygous for a T-DNA insertion in the 10th exon of At4g19210 (Figure 2B) (35). We named the insertional allele in GABI_509C06 *api7-2*. For the allelism test, we crossed *api7-1* to the *ABCE2/api7-2* heterozygous plants. In the F₂ population of this cross, no *api7-2/api7-2* plants were found, and *api7-1/api7-2* and *api7-1/api7-1* plants were phenotypically similar, confirming that these mutations are allelic and that loss of function of *ABCE2* is responsible for the phenotype of the *api7-1* mutant (Supplementary Figure S5A-C).

The absence of *api7-2/api7-2* plants derived from GABI_509C06 seeds and of ungerminated seeds in the F₁ progeny of selfed heterozygous *ABCE2/api7-2* plants, suggested an early lethality of this mutant allele. We dissected immature siliques from *ABCE2/api7-2* plants and found 21.95% aborted ovules ($n = 328$), which fits a 1:3 Mendelian segregation ratio ($\chi^2 = 1.63$; P -value = 0.202; degrees of freedom = 1). Col-0 siliques showed 1.37% aborted ovules ($n = 148$; Supplementary Figure S5F, G). The lethality caused by *api7-2* suggests that it is a null allele of *ABCE2*, while *api7-1* is hypomorphic. We also obtained *api7-2/api7-2 ABCE2_{pro}:ABCE2* plants, which were viable and phenotypically wild-

type (Supplementary Figure S5D, E).

The Arabidopsis genome contains two *ABCE* paralogs

Some animal (80,81) and plant (82,83) genomes, including that of Arabidopsis, encode two *ABCE* paralogs (2,22). To gather more information about the origin of Arabidopsis *ABCE* paralogs, we performed a phylogenetic analysis of *ABCE* coding sequences from some Rosidae species (rosids; Supplementary Figure S6). Among them, we found that other Brassicaceae genomes, namely *Arabidopsis lyrata*, *Capsella rubella*, *Eutrema salsugineum*, and *Brassica rapa*, also encode *ABCE1* and *ABCE2* proteins, but only *ABCE2* was identified in *Cardamine hirsuta*. Consistent with the whole-genome triplication in *Brassica rapa* (84), we found two and three *Brassica rapa* *ABCE1* and *ABCE2* sequences, respectively. All Brassicaceae *ABCE* genes clustered together in the phylogenetic tree that we obtained. Inside this clade and in all bootstrap replicates (1000 replicates), *ABCE1* genes grouped together and separately from their *ABCE2* paralogs, which formed other subclade. Additionally, rosids from other families contained only the *ABCE2* gene, suggesting that a duplication event of *ABCE* genes occurred before the divergence of Brassicaceae species. Although both *ABCE1* and *ABCE2* paralogs have been conserved, the phylogenetic tree shows that *ABCE1* orthologs have evolved more rapidly than their *ABCE2* paralogs, whose short evolutionary distances indicate that they are under strong evolutionary pressure, as expected for an essential gene.

As previously described (24,85), we observed that *ABCE2* is highly expressed throughout all Arabidopsis developmental stages. By contrast, the expression levels of its *ABCE1* paralog are very low in all studied organs, in which first-node leaves and flowers show the lowest and highest expression levels, respectively (Supplementary Figure S7A, B). The expression levels of *ABCE1* in *api7-1* plants were the same as in *Ler*, showing that *ABCE1* cannot compensate for the partial loss of *ABCE2* function (Supplementary Figure S7C). The low expression levels of *ABCE1* and its unresponsiveness to decreased *ABCE2* function may indicate that *ABCE1* is undergoing pseudogenization. However, *api7-1* flowers, where we observed the highest *ABCE1* expression levels, do not show apparent aberrations (Supplementary Figure S1E), suggesting that *ABCE1* might play a role during flower development.

ABCE1 and *ABCE2* proteins share 80.8% identity, suggesting that *ABCE1* and *ABCE2* might be functionally equivalent. To test this hypothesis, we performed a promoter swapping assay between the *ABCE1* and *ABCE2* genes (Figure 3). As expected from the lower expression levels driven by the *ABCE1* promoter, *api7-1* *ABCE1_{pro}:ABCE2* plants were indistinguishable from *api7-1* mutants, highlighting that correct protein levels are as important as the correct sequence for normal *ABCE2* function. In contrast, the

ABCE2_{pro}:ABCE1 transgene partially rescued the *api7-1* phenotype, showing that the ABCE1 and ABCE2 proteins are partially redundant.

ABCE2 is a cytoplasmic protein that physically associates with components of the translation machinery

ABCE proteins lack the TMDs found in most members of other ABC subfamilies and thus are expected to behave as soluble proteins (86). The single ABCE subfamily member in *Saccharomyces cerevisiae*, Rli1, is found at both the cytoplasm and the nucleoplasm (87-89), whereas its *Drosophila melanogaster* ortholog, Pixie, is exclusively cytoplasmic (90). To determine the subcellular localization of Arabidopsis ABCE2, we obtained an in-frame translational fusion of ABCE2 and GFP, driven by the constitutive *Cauliflower mosaic virus* 35S promoter: *35S_{pro}:ABCE2:GFP*. We then transferred this construct into *Ler* plants. We visualized the ABCE2:GFP fusion protein in root cells treated with propidium iodide, which mainly stains cell walls, and detected fluorescence only in the cytoplasm (Figure 4A, C, E). To further confirm the nuclear exclusion of ABCE2, we constructed and transferred a *35S_{pro}:ABCE2:YFP* transgene into *api7-1* plants, which restored the wild-type phenotype (Supplementary Figure S8A-C). We also observed the ABCE2:YFP fusion protein in roots stained with the nucleoplasm fluorescent dye DAPI and confirmed the nuclear exclusion of ABCE2 (Figure 4B, D, F).

To further investigate ABCE2 function, we performed a co-immunoprecipitation assay using the ABCE2:YFP protein from a homozygous *T₂ api7-1 35S_{pro}:ABCE2:YFP* line. We checked the purification of the fusion protein by western blotting using an anti-GFP antibody (Supplementary Figure S8D-F). Using LC-ESI-MS/MS, we identified 20 putative interactors of ABCE2, of which 13 participate in translation (6 subunits of the eIF3 complex, eIF5B, RPL3B, and ROTAMASE CYP 1 [ROC1]) or in the regulation of translation (At5g58410, EVOLUTIONARILY CONSERVED C-TERMINAL REGION 2 [ECT2], ILITYHIA [ILA], and REGULATORY-ASSOCIATED PROTEIN OF TOR 1 [RAPTOR1] or RAPTOR2), and two others had previously been shown to interact with ABCE orthologs (At2g20830, and EXPORTIN 1A [XPO1A] or XPO1B). The functions of the remaining 5 proteins that co-immunoprecipitated with ABCE2 are unclear and these proteins were therefore set aside for future characterization (Figure 5; Supplementary Figure S9; Supplementary Tables S4, S5; Supplementary Data Set 1).

XPO1 proteins are conserved nuclear transporters that translocate their cargoes from the nucleus to the cytoplasm through nuclear pore complexes. In *Saccharomyces cerevisiae*, *Xenopus laevis*, and humans, XPO1 modulates the nucleo-cytoplasmic partitioning of hundreds of cargoes, preventing their unwanted, and sometimes accidental, presence in the nucleus, as is the case of ABCE proteins (91). The interaction between

ABCE2 and Arabidopsis XPO1A or XPO1B (XPO1A/B) supports a conserved role of Arabidopsis XPO1A/B in excluding ABCE2 from the nucleus, which is also in agreement with its cytoplasmic localization.

At2g20830 encodes a folic acid binding/transferase that shares 30.2% and 26.7% identity with human ORAL CANCER OVEREXPRESSED 1 (ORAOV1) and *Saccharomyces cerevisiae* Lto1 (named after “required for biogenesis of the large ribosomal subunit and initiation of translation in oxygen”), respectively. ORAOV1 (Lto1), together with YAE1 (Yae1), constitute an essential complex for FeS cluster assembly on ABCE1 (Rli1) (92-94). Despite the observation that At2g20830 protein was predicted to localize to mitochondria, the high conservation level of this protein with its yeast and human orthologs prompted us to consider At2g20830 an ABCE2 interactor. Indeed, At2g20830 may be necessary for FeS cluster assembly on ABCE2, suggesting that ABCE2 has a functional FeSD, which supports its conserved role in ribosome dissociation.

The presence of RPL3B and several eIF3 complex subunits among the identified interactors further supports the functional conservation of ABCE2. In higher eukaryotes, including plants, there are 13 eIF3 complex subunits (eIF3a to eIF3m) of which eIF3j is a non-stoichiometric subunit (95). Our co-immunoprecipitation assay suggested that Arabidopsis ABCE2 interacts with 6 of these eIF3 subunits: eIF3a, c, d, e, k, and j. The ABCE orthologs Rli1 and Pixie also interact with the eIF3a, c, and j subunits (15,87-89,96,97). Those interactions have been related to the presence of the ABCE protein in the 40S subunit after ribosome dissociation, where it may be impeding premature joining of the 60S subunit until late steps of initiation of a new cycle of translation (5,15,18). Interestingly, the interaction between eIF3j (High-Copy suppressor of Rpg1 [Hcr1] in *Saccharomyces cerevisiae*) and ABCE1 (Rli1) also occurs in humans and *Saccharomyces cerevisiae*. In these species, eIF3j acts as an accessory factor for ABCE1-mediated ribosome dissociation (18,98), a function that seems to be conserved in Arabidopsis.

eIF5B was also found among the proteins that co-immunoprecipitated with ABCE2. In humans and *Saccharomyces cerevisiae*, this translation initiation factor and ABCE1 perform opposite roles, joining and dissociating the ribosomal subunits, respectively (7,99,100). In addition, they cannot coexist on the ribosome during translation initiation, since both bind to the 40S GTPase-binding site on the interface of the subunits (5,15). However, our identification of eIF5B among the proteins that co-immunoprecipitated with ABCE2 suggests that the mechanisms of pre-40S maturation and/or translation initiation might occur differently in plants, where eIF5B and ABCE2 can coexist in the same complex.

Some of the proteins identified in our assay might not be direct interactors of ABCE2, such as ROC1, a cyclophilin that catalyzes cis-trans isomerizations of prolyl bonds during protein folding (101,102); ECT2, a reader of methylated N⁶-adenosines (m⁶As) in 3' UTRs

of mRNA molecules (103-105); and ILA, a HEAT repeat protein that inhibits translation in response to different stresses (106-108). Instead, they seem to co-immunoprecipitate as part of the translational complexes in which ABCE2 participates. Another candidate to be part of an indirect interaction is At5g58410, which is annotated in UniProt as encoding the E3 ubiquitin-protein ligase listerin (LTN1; UniProt code: Q9FGI1) whose function in *Arabidopsis* remains unexplored. However, in *Saccharomyces cerevisiae*, *Drosophila melanogaster*, and humans, both ABCE1 and Ltn1 are necessary during nonstop mRNA decay (NSD) and ribosome quality control (RQC), two parallel pathways that act simultaneously to degrade stop codon-less mRNAs and their products, respectively (4,109-111). We also identified the RAPTOR1 or RAPTOR2 (RAPTOR1/2) proteins, which belong to the TORC1 complex, further composed of TOR and LETHAL WITH SEC THIRTEEN 8-1 (LST8-1). This complex is highly conserved in eukaryotes and regulates translation and ribosome biogenesis in response to internal and external stimuli (112). The ABCE2 interaction with the TORC1 complex is also supported by its interaction through LST8-1 (113), but further research is needed to ascertain its biological meaning.

ASYMMETRIC LEAVES 1 (AS1) and *AS2* encode transcription factors involved in leaf dorsoventral patterning and double mutant combinations of *as1* or *as2* with mutations in genes encoding ribosomal proteins or components of the translation machinery usually produce synergistic phenotypes. These phenotypes are easily distinguished by the presence of trumpet-like (peltate) or radial leaves originated by partial or complete loss of dorsoventrality, respectively (56,73,76,114). We obtained *api7-1 as1-1* and *api7-1 as2-1* double mutants, introgressed into the Col-0 background by a cross and two additional backcrosses to Col-0; these double mutants exhibited additive and synergistic phenotypes, respectively (Supplementary Figure S10). The presence of radial leaves in *api7-1 as2-1* plants (Supplementary Figure S10G) further supports a role for ABCE2 in translation.

Leaf and vascular defects in *api7-1* plants

Mutations that disrupt the translation machinery usually alter leaf vascular development (29,72-75). The *ATHB8 (ARABIDOPSIS THALIANA HOMEBOX GENE 8)* gene is expressed in pre-procambial cells that will differentiate into veins (37). To determine if *api7-1* leaf venation was altered, we crossed *api7-1* plants to an *ATHB8_{pro}:GUS* line, and studied the expression of the transgene in cleared first-node rosette leaf primordia of *api7-1 ATHB8_{pro}:GUS* F₃ plants. Consistent with the slow growth phenotype of *api7-1* plants, we observed that they exhibit delayed first-node leaf emergence (Supplementary Figure S11). At similar early developmental stages in wild-type (Supplementary Figure S11A-C) and *api7-1* (Supplementary Figure S11K-L) emerged primordia, the GUS signal was intense at the apical lamina region. Shortly after the formation of the first vascular elements in the

midvein of wild-type primordia (Supplementary Figure S11C), the GUS signal became uniformly distributed along the lamina (Supplementary Figure S11E-G). In contrast, *api7-1* primordia retained high GUS activity at their apical region even after the formation of the whole midvein (Supplementary Figure S11M), suggesting that vascular differentiation is more intense in that region (Supplementary Figure S11N). Additionally, the formation of higher-order veins in *api7-1* primordia seemed to be reduced.

To further assess these vascular defects, we cleared fully expanded *Ler* and *api7-1* first- and third-node leaves, which were examined under bright-field microscopy. We confirmed that *api7-1* first-node and, to a lesser extent, third-node leaves, contain fewer higher-order veins and more prominent indentations and vascularized hydathodes, in particular in the leaf apex, than *Ler* leaves (Figure 6; Supplementary Figure S12). In contrast, these phenotypic traits seemed to be unaffected on *api7-1* cotyledons, cauline leaves, sepals, and petals (Supplementary Figure S13).

To further characterize the defects in the venation pattern of *api7-1* flat organs, we performed a morphometric analysis of *api7-1* cotyledons, first- and third-node leaves, cauline leaves, sepals, and petals. The cotyledons have a higher vein density, accompanied by an increase in the number of branching points and free-ending veins. In contrast, but in accordance with the reduced number of higher-order veins, *api7-1* first- and third-node leaves have less than half the number of branching points and free-ending veins than in *Ler* plants. *api7-1* cauline leaves also show a slight decrease in branching points and free-ending veins. Regarding sepals and petals, we did not observe any remarkable differences between wild-type and *api7-1* plants (Supplementary Table S6). As expected from the rosette size measurements (Figure 1D), all *api7-1* organs, except sepals and petals, were smaller than those of *Ler*. In addition, *api7-1* first- and third-node leaves are more pointed, i.e., less circular, than those of *Ler*. In contrast, *api7-1* cauline leaves are more circular than in the wild type (Figure 6; Supplementary Figure S13; Supplementary Table S6).

Polar auxin transport and local auxin biosynthesis and signaling contribute to the establishment of leaf venation pattern (32,33). Therefore, the aberrant venation pattern observed in the *api7-1* mutant might be related to a potentially altered auxin homeostasis. The major player of auxin transport during venation patterning in leaf primordia is the PIN-FORMED1 (PIN1) exporter (115), while the main pathway for auxin biosynthesis is a two-step process that relies on the sequential action of TRYPTOPHAN AMINOTRANSFERASE OF ARABIDOPSIS 1 (TAA1) or TAA1-RELATED (TARs) and YUCCA (YUC) enzymes (116). Regarding auxin signaling, the synthetic auxin-responsive promoter *DR5* located upstream of the coding sequence of a reporter gene is widely used to assess auxin perception. To ascertain whether auxin transport or signaling are affected in the *api7-1* mutant, we crossed this mutant to plants carrying the *PIN1_{pro}:PIN1:GFP* and

DR5_{pro}:3XVENUS:N7 constructs (36). After several rounds of selfing and selection, we obtained wild-type and *api7-1* plants homozygous for either *PIN1_{pro}:PIN1:GFP* or *DR5_{pro}:3XVENUS:N7*. Then, we visualized and photographed the fluorescent signals of GFP and VENUS on primary roots stained with the cell wall dye propidium iodide, using confocal microscopy. Quantification of the fluorescence observed indicated that PIN1:GFP signal decreased, and that of VENUS:N7 increased, in *api7-1* roots, compared to the wild type (Figure 7). The high auxin perception found in *api7-1* roots is in agreement with a potential increase in local auxin biosynthesis triggered to compensate for the scarce amount of auxin imported from above-ground tissues due to reduced PIN1 expression, as similarly observed when auxin transport is inhibited in naphthylphthalamic acid (NPA)-treated plants, which overexpress auxin biosynthesis genes in their primary roots (117).

Genes related to auxin and iron homeostasis are deregulated in *api7-1* plants

To gain insight into the biological processes affected in the *api7-1* mutant, we performed an RNA-seq analysis of *Ler* and *api7-1* rosettes collected 14 das. We identified 3218 downregulated and 2135 upregulated genes in the *api7-1* mutant (Supplementary Data Set 2). A GO enrichment analysis performed separately for down- and upregulated genes showed that the downregulated genes were mainly related to responses to abiotic and biotic stresses and protein post-translational modifications. In contrast, upregulated genes grouped into more diverse Biological Process terms (Supplementary Data Set 3).

We found enriched terms referring to responses to several hormones among both the down- and the upregulated genes. Remarkably, the three terms related to auxin (response to auxin [GO:0009733], auxin-activated signaling pathway [GO:0009734], and auxin polar transport [GO:0009926]) were only enriched among the upregulated genes. In agreement with the increased response to auxin in the *api7-1* mutant, we observed that five out of seven genes that participate in the main auxin biosynthesis pathway in leaves were upregulated. They included the three genes encoding enzymes that convert tryptophan into indole-3-pyruvic acid (IPyA), *TAA1*, *TAR2*, and *TAR3*, and two *YUC* genes (*YUC2* and *YUC6*) encoding enzymes that turn IPyA into indole-3-acetic acid (IAA) (116). We also found that three genes involved in auxin inactivation, *IAA CARBOXYLMETHYLTRANSFERASE 1 (IAMT1)*, *GRETCHEN HAGEN 3.17 (GH3.17)*, and *DIOXYGENASE FOR AUXIN OXIDATION 2 (DAO2)*, were upregulated, and that three genes involved in auxin activation, *IAA-LEUCINE RESISTANT (ILR)-LIKE 2 (ILL2)*, *ILL3*, and *ILL4*, were downregulated, probably in response to high auxin levels (Supplementary Figure S14A).

In this manner, our results point to an increase in auxin biosynthesis in *api7-1* leaves, which might be partially compensated by inactivating auxin and preventing its reactivation. Nevertheless, the activation of these compensation mechanisms is insufficient to prevent a

phenotypic effect on *api7-1* plants. The potential high levels of active auxin during leaf primordia development in the *api7-1* mutant might be responsible for the dense vascularization observed in the apical region and hydathodes of *api7-1* leaves (Figure 6; Supplementary Figures S10; S11) (32,118). Accordingly, we observed that the genes encoding some members from the pathway that promotes provascular cell divisions, namely the transcription factors ARF5 and TARGET OF MONOPTEROS 5 (TMO5), and an enzyme involved in cytokinin biosynthesis (LONELY GUY 3 [LOG3]) (119-121), were upregulated in the *api7-1* mutant (Supplementary Figure S14A).

Interestingly, iron ion homeostasis and transport (GO:0055072 and GO:0006826), and response to iron and sulfur ion starvation (GO:0010106 and GO:0010438) terms were also enriched in the analysis of upregulated genes (Supplementary Data Set 3A). For instance, genes related to iron uptake, such as *IRON-REGULATED TRANSPORTER 1 (IRT1)* and *FERRIC CHELATE REDUCTASE DEFECTIVE 1 (FRD1)* (122,123), or to iron mobility, such as *NATURAL RESISTANCE-ASSOCIATED MACROPHAGE PROTEIN 3 (NRAMP3)* and *NRAMP6* (124,125), and several genes encoding transcription factors induced by iron and sulfur deficiencies were upregulated in the *api7-1* mutant. These pathways might be activated in *api7-1* plants to provide iron and sulfur for FeS cluster biogenesis, probably to compensate for the depletion in ABCE2 protein. Indeed, the gene that encodes the Arabidopsis NEET protein (termed after its conserved Asn-Glu-Glu-Thr sequence near its C-terminus) (126), which participates in FeS cluster transference during their biogenesis (127,128), was also upregulated (Supplementary Figure S14B).

Consequently, the iron content in *api7-1* cells might be higher than in the wild type, and might be inducing the formation of reactive oxygen species (ROS), as occurs in mutants affected in free iron storage (129). In agreement with this assumption, several terms related to oxidative stress responses were also enriched. Specifically, we found that *FERRITIN 2 (FER2)* and *FER3*, which encode iron storage proteins in response to high iron levels to avoid oxidative damage (129,130), were upregulated (Supplementary Figure S14B). In addition, previous studies have shown that ROS prevent FeS cluster assembly into ABCE proteins, which is necessary for their activity in ribosome recycling (94,131,132). In this manner, *api7-1* plants might experience a positive feedback loop where a response to iron starvation due to reduced activity of ABCE2 increases iron levels, inducing the production of ROS which, in turn, further disturbs ABCE2 activity. Nevertheless, further studies are needed to ascertain a potential relation among ABCE2 activity, iron homeostasis, and oxidative stress, which were beyond the scope of our research.

DISCUSSION

Plant ABCE proteins participate in translation in a cross-kingdom conserved manner

In this work, we studied Arabidopsis ABCE2, one of the most conserved proteins among archaea and eukaryotes (86). Although the ribosome-recycling activity of plant ABCE proteins still has not been assessed, the molecular function of these proteins has been widely investigated in the archaeon *Saccharolobus solfataricus*, the yeast *Saccharomyces cerevisiae*, the insect *Drosophila melanogaster*, and humans. In these species, ABCEs dissociate cytoplasmic ribosomes into their 30S/40S and 50S/60S subunits at different translation events, like pre-40S maturation, translation termination, and ribosome rescue during NSD (133). After ribosome dissociation, an ABCE escorts the 30S/40S subunit until the late steps of translation reinitiation, preventing premature joining of the 50S/60S subunit into the preinitiation complex (5,6,15,18).

Here, we found that Arabidopsis ABCE2 is exclusively located in the cytoplasm, like its *Drosophila melanogaster* ortholog, Pixie (90). *Saccharomyces cerevisiae* Rli1 has also been found in the nucleoplasm, where it overaccumulates in the *xpo1-1* mutant (87-89). In fact, as previously mentioned, XPO1 nuclear exporters prevent the presence of cytoplasmic proteins like ABCEs in the nucleus (91). Accordingly, we identified Arabidopsis XPO1A/B as interacting partners of ABCE2 in our co-immunoprecipitation assay, strongly suggesting a conserved role for XPO1 beyond fungi and animals.

In addition, we found that ABCE2 co-immunoprecipitates with several proteins related to translation reinitiation, especially with subunits of the eIF3 complex. Among these, the identification of the eIF3j subunit points to a conserved role for both ABCE2 and eIF3j in ribosome recycling. In humans and *Saccharomyces cerevisiae*, eIF3j (Hcr1) has been proposed as an accessory factor of ABCE1 during ribosome dissociation, as it boosts ABCE1 ribosome-dissociating activity (18,98). Interestingly, *Saccharomyces cerevisiae* *rli1*- and *hcr1*-depleted cells show an increase of translation reinitiation events on 3' UTRs, which in the latter case are restored to wild-type levels after *RLI1* overexpression. Indeed, *hcr1*-depleted cells overexpress *RLI1* and *LTO1*, which encodes a protein required for FeS cluster assembly on Rli1, together with genes required for FeS cluster biogenesis (92-94,98).

We observed similar trends in Arabidopsis. First, the responses to iron and sulphur starvation are activated in the hypomorphic *api7-1* mutant, suggesting that ribosome recycling and iron and sulphur homeostasis are also linked in Arabidopsis. Second, ABCE2 interacts with the At2g20830 protein, which is 26.7% and 30.2% identical to *Saccharomyces cerevisiae* Lto1 and its human ortholog, ORAOV1, respectively. Therefore, our observations suggest a novel function for the At2g20830 protein in FeS cluster assembly on cytoplasmic proteins like ABCE2. In turn, the presence of a functional FeSD in ABCE2 supports its role

in ribosome dissociation. Since iron is essential for photosynthesis and hence for crop yield, the relationship between the activity of ABCE proteins and iron homeostasis might lead to new ways to modulate plant growth in species with agronomic interest.

Although our co-immunoprecipitation assay did not allow us to discern direct from indirect ABCE2 interactors, the interactions with XPO1A/B, eIF3j, and At2g20830 are very likely to be direct, in agreement with previous studies (18,91-94,98). In contrast, the interactions observed with other eIF3 subunits, RPL3B, ROC1, ECT2, ILA, LTN1, and RAPTOR1/2, might occur indirectly as they are part of or interact with the translation machinery (4,101-108,111,134). However, the interaction between ABCE2 and eIF5B, which does not seem to occur in other species (5,15), will require further exploration.

Further supporting a role for ABCE2 in translation, we observed a synergistic interaction in the *api7-1 as2-1* double mutants, which show radial leaves, as previously described for double mutant combinations of loss-of-function alleles of *AS1* or *AS2* and other components of the translation machinery (56,73,76,114). In this manner, our results strongly suggest that Arabidopsis and, by extension, all plant ABCEs, participate in translation, probably by dissociating cytoplasmic ribosomes, as has been reported for species of other kingdoms (133). In addition, previous works also support a conserved role for the Arabidopsis ABCE2 and human ABCE1 proteins as suppressors of RNA silencing (23,24,85,135). However, we did not find any ABCE2 interactor potentially involved in this process, nor any enriched ontology term related to gene silencing in our RNA-seq assay. This might be due to the need for a cellular environment that triggers RNA silencing and exposes this novel function of ABCE proteins. Further research will help to assess a potential relationship between ribosome recycling and RNA silencing.

The developmental defects of the *api7-1* mutant link translation and auxin homeostasis

The essential function of ABCEs has been confirmed in several species, in addition to those mentioned above. Null alleles of *ABCE* genes in all studied organisms are lethal, while hypomorphic alleles cause severe growth aberrations (21). This is also the case for Arabidopsis. In this work, we describe the first hypomorphic and null alleles of Arabidopsis *ABCE2* gene, *api7-1* and *api7-2*, respectively (Figure 2). We showed that the *api7-2* mutation is lethal and that *api7-1* plants share developmental defects with other mutants affected in genes encoding ribosomal proteins or ribosome biogenesis factors. These phenotypic traits include a small rosette with pointed and dentate leaves, and a reduced growth rate. In addition, these mutants usually have small leaf epidermal cells and increased ploidy levels when compared to wild-type plants, as well as an aberrant leaf venation (73), as is the case for the *api7-1* mutant. Indeed, an allele of *SIMPLE LEAF3*, the

Cardamine hirsuta ABCE ortholog, also causes growth delay, increased leaf ploidy levels, and venation pattern defects related to an aberrant auxin homeostasis (25). Remarkably, both *sil3* and *api7-1* leaves contain a reduced number of branching points and free ending veins, and, consequently, fewer higher-order veins than their respective wild types (25).

In agreement with the involvement of local auxin biosynthesis, polar transport, and signalling in vascular development, we observed that auxin biosynthesis and auxin-induced genes were upregulated in the *api7-1* mutant (32,33,116). Among the auxin-induced genes, we found *ARF5* and its target, *TMO5*, which regulate vascular development. *TMO5* promotes the expression of *LOG3*, which is also upregulated in the *api7-1* mutant, and encodes an enzyme involved in cytokinin biosynthesis. Cytokinin is known to induce cell divisions in the embryo and root procambium (119-121,136). The overexpression of these genes, together with the altered *ATHB8* expression in *api7-1* leaves, might be the cause of their hypervascularized hydathodes. Regarding auxin biosynthesis, the upregulation of this pathway in *api7-1* leaves, and the increased auxin perception in *api7-1* roots reported by *DR5_{pro}:3XVENUS:N7*, strongly suggest that auxin is being overproduced in the whole mutant plant. In this sense, our previous hypothesis about a local overproduction of auxin in *api7-1* roots to compensate for its reduced arrival due to decreased PIN1 levels, seems less likely. The reduced PIN1:GFP levels that we observed in *api7-1* roots might be a consequence, rather than a cause, of a general auxin homeostasis deregulation.

In agreement with results obtained from human and *Saccharomyces cerevisiae* ABCE1-depleted cells (8,94), the *api7-1* mutation might impede proper ABCE2-dependent ribosome dissociation, allowing ribosomes to reinitiate translation in the 3' UTR. In turn, the passage of the ribosomes through the 3' UTR would displace the regulatory elements found within that region, increasing or decreasing the mRNA lifespan. The inability to dissociate ribosomes in *api7-1* plants might also affect uORF-mediated post-transcriptional regulation, disturbing, among other biological processes, auxin homeostasis in similar ways to those described for other mutations in the translation machinery in Arabidopsis (29,30,34).

The Arabidopsis ABCE1 and ABCE2 proteins are functionally redundant

Arabidopsis has two ABCE paralogs, *ABCE1* and *ABCE2* (2,22). In agreement with previous literature (24,85), we observed that *ABCE1* expression levels are low in all studied organs and throughout development, in contrast to the high expression of *ABCE2*, and that *ABCE2* disruption in the *api7-1* mutant does not trigger a compensation mechanism through *ABCE1* overexpression. These observations suggest that *ABCE1* is undergoing pseudogenization.

However, the wild-type phenotype of *api7-1* flowers, where we found the highest expression levels of *ABCE1*, and the ability of *ABCE2_{pro}:ABCE1* to complement the *api7-1*

mutant phenotype, indicate that *ABCE1* contributes to translation in the reproductive tissues. In addition, our phylogenetic analysis showed that the *ABCE* duplication event occurred early during the evolution of Brassicaceae, and that at least five species from this clade conserved an *ABCE1* gene that evolved more rapidly than its *ABCE2* paralog, suggesting that *ABCE2* conserved the ancestral function, whereas *ABCE1* underwent subfunctionalization.

To conclude, although ABCE proteins are encoded by a single gene in most species, they are essential for archaea and eukaryotes (21). Due to their importance, the molecular mechanisms by which they participate in ribosome recycling have been deeply studied, and remain a subject of intense research (5,6,15,16,18). Nevertheless, the biological consequences of ABCE disruption are poorly understood in all organisms. In this sense, future research linking the molecular function of ABCes with the phenotypic output of their disruption will contribute to determining the pathways through which translation modulates development, as we show here with the isolation and study of the hypomorphic and viable *api7-1* allele of the Arabidopsis *ABCE2* gene.

DATA AVAILABILITY

The raw data from genome resequencing and RNA-seq were deposited in the Sequence Read Archive (<https://www.ncbi.nlm.nih.gov/sra/>) database under accession numbers SRP065876 and PRJNA719000, respectively.

SUPPLEMENTARY DATA

Supplementary Data are available at NAR Online.

FUNDING

This work was supported by the Ministerio de Ciencia e Innovación of Spain [PGC2018-093445-B-I00 (MCI/AEI/FEDER, UE), to J.L.M.]; and the Generalitat Valenciana [PROMETEO/2019/117, to J.L.M.]. C.N.-Q. and E.M.B. held predoctoral fellowships from the Universidad Miguel Hernández [401PREDO] and the Ministerio de Educación, Cultura y Deporte of Spain [FPU13/00371], respectively. Funding for open access charge: Universidad Miguel Hernández.

Conflict of interest statement. None declared.

ACKNOWLEDGEMENTS

We thank B. Scheres for the pGEM-T Easy221 vector and S. Baima for the *ATBH8_{pro}:GUS* transgenic line. We also thank J. Castelló, J.M. Serrano, and M.J. Níguez for their excellent technical assistance, and M. Sendra-Ortolà and I.C. Pomares-Bri for helping in the phenotypic analysis of *api7-1* and some gene constructs.

AUTHOR CONTRIBUTIONS

J.L.M. conceived, designed, and supervised the research, provided resources, and obtained funding. Several experiments were codesigned by C.N.-Q., E.M.-B., and J.L.M. C.N.-Q. performed most of the experiments. E.M.-B. obtained the *ABCE2_{pro}:ABCE2* and *35S_{pro}:ABCE2:GFP* transgenes, and contributed to the phenotypic analysis of *api7-1*. E.M.-B. and H.C. obtained the *api7-1* as double mutants. C.N.-Q. and H.C. performed the phylogenetic analysis. H.C. and A.M.L. screened the Micol collection of leaf mutants for abnormal leaf venation patterns. P.R. performed preliminary morphometric analysis of cells and venation from *api7-1* leaves. M.R.P., H.C., and E.M.-B. performed the mapping and cloning of the *api7-1* mutation. C.N.-Q. and J.L.M. wrote the manuscript. All authors revised and approved the manuscript.

REFERENCES

1. Ford, R.C. and Beis, K. (2019) Learning the ABCs one at a time: structure and mechanism of ABC transporters. *Biochem. Soc. Trans.*, **47**, 23-36.
2. Verrier, P.J., Bird, D., Burla, B., Dassa, E., Forestier, C., Geisler, M., Klein, M., Kolukisaoglu, Ü., Lee, Y., Martinoia, E. *et al.* (2008) Plant ABC proteins – a unified nomenclature and updated inventory. *Trends Plant Sci.*, **13**, 151-159.
3. Bisbal, C., Martinand, C., Silhol, M., Lebleu, B. and Salehzada, T. (1995) Cloning and characterization of a RNase L inhibitor. A new component of the interferon-regulated 2-5A pathway. *J. Biol. Chem.*, **270**, 13308-13317.
4. Kashima, I., Takahashi, M., Hashimoto, Y., Sakota, E., Nakamura, Y. and Inada, T. (2014) A functional involvement of ABCE1, eukaryotic ribosome recycling factor, in nonstop mRNA decay in *Drosophila melanogaster* cells. *Biochimie*, **106**, 10-16.
5. Mancera-Martínez, E., Brito Querido, J., Valasek, L.S., Simonetti, A. and Hashem, Y. (2017) ABCE1: A special factor that orchestrates translation at the crossroad between recycling and initiation. *RNA Biol.*, **14**, 1279-1285.
6. Nürenberg-Goloub, E., Kratzat, H., Heinemann, H., Heuer, A., Kötter, P., Berninghausen, O., Becker, T., Tampé, R. and Beckmann, R. (2020) Molecular analysis of the ribosome recycling factor ABCE1 bound to the 30S post-splitting complex. *EMBO J.*, **39**, e103788.
7. Strunk, B.S., Novak, M.N., Young, C.L. and Karbstein, K. (2012) A translation-like cycle is a quality control checkpoint for maturing 40S ribosome subunits. *Cell*, **150**, 111-121.
8. Young, D.J., Guydosh, N.R., Zhang, F., Hinnebusch, A.G. and Green, R. (2015) Rli1/ABCE1 recycles terminating ribosomes and controls translation reinitiation in 3'UTRs in vivo. *Cell*, **162**, 872-884.
9. Hashimoto, Y., Takahashi, M., Sakota, E. and Nakamura, Y. (2017) Nonstop-mRNA decay machinery is involved in the clearance of mRNA 5'-fragments produced by RNAi and NMD in *Drosophila melanogaster* cells. *Biochem. Biophys. Res. Commun.*, **484**, 1-7.
10. Becker, T., Franckenberg, S., Wickles, S., Shoemaker, C.J., Anger, A.M., Armache, J.P., Sieber, H., Ungewickell, C., Berninghausen, O., Daberkow, I. *et al.* (2012) Structural basis of highly conserved ribosome recycling in eukaryotes and archaea. *Nature*, **482**, 501-506.
11. Barthelme, D., Scheele, U., Dinkelaker, S., Janoschka, A., MacMillan, F., Albers, S.V., Driessen, A.J., Stagni, M.S., Bill, E., Meyer-Klaucke, W. *et al.* (2007) Structural organization of essential iron-sulfur clusters in the evolutionarily highly conserved ATP-binding cassette protein ABCE1. *J. Biol. Chem.*, **282**, 14598-14607.

12. Karcher, A., Büttner, K., Märten, B., Jansen, R.P. and Hopfner, K.P. (2005) X-ray structure of RLI, an essential twin cassette ABC ATPase involved in ribosome biogenesis and HIV capsid assembly. *Structure*, **13**, 649-659.
13. Karcher, A., Schele, A. and Hopfner, K.P. (2008) X-ray structure of the complete ABC enzyme ABCE1 from *Pyrococcus abyssi*. *J. Biol. Chem.*, **283**, 7962-7971.
14. Barthelme, D., Dinkelaker, S., Albers, S.V., Londei, P., Ermler, U. and Tampé, R. (2011) Ribosome recycling depends on a mechanistic link between the FeS cluster domain and a conformational switch of the twin-ATPase ABCE1. *Proc. Natl. Acad. Sci. USA*, **108**, 3228-3233.
15. Heuer, A., Gerovac, M., Schmidt, C., Trowitzsch, S., Preis, A., Kötter, P., Berninghausen, O., Becker, T., Beckmann, R. and Tampé, R. (2017) Structure of the 40S-ABCE1 post-splitting complex in ribosome recycling and translation initiation. *Nat. Struct. Mol. Biol.*, **24**, 453-460.
16. Nürnberg-Goloub, E., Heinemann, H., Gerovac, M. and Tampé, R. (2018) Ribosome recycling is coordinated by processive events in two asymmetric ATP sites of ABCE1. *Life Sci. Alliance*, **1**, e201800095.
17. Gouridis, G., Hetzert, B., Kiosze-Becker, K., de Boer, M., Heinemann, H., Nürnberg-Goloub, E., Cordes, T. and Tampé, R. (2019) ABCE1 controls ribosome recycling by an asymmetric dynamic conformational equilibrium. *Cell Rep.*, **28**, 723-734.
18. Kratzat, H., Mackens-Kiani, T., Ameismeier, M., Potocnjak, M., Cheng, J., Dacheux, E., Namane, A., Berninghausen, O., Herzog, F., Fromont-Racine, M. *et al.* (2021) A structural inventory of native ribosomal ABCE1-43S pre-initiation complexes. *EMBO J.*, **40**, e105179.
19. Preis, A., Heuer, A., Barrio-Garcia, C., Hauser, A., Eyler, D.E., Berninghausen, O., Green, R., Becker, T. and Beckmann, R. (2014) Cryoelectron microscopic structures of eukaryotic translation termination complexes containing eRF1-eRF3 or eRF1-ABCE1. *Cell Rep.*, **8**, 59-65.
20. Simonetti, A., Guca, E., Bochler, A., Kuhn, L. and Hashem, Y. (2020) Structural insights into the mammalian late-stage initiation complexes. *Cell Rep.*, **31**, 107497.
21. Navarro-Quiles, C., Mateo-Bonmatí, E. and Micol, J.L. (2018) ABCE proteins: from molecules to development. *Front. Plant Sci.*, **9**, 1125.
22. Sánchez-Fernández, R., Davies, T.G., Coleman, J.O. and Rea, P.A. (2001) The *Arabidopsis thaliana* ABC protein superfamily, a complete inventory. *J. Biol. Chem.*, **276**, 30231-30244.
23. Möttus, J., Maiste, S., Eek, P., Truve, E. and Sarmiento, C. (2020) Mutational analysis of *Arabidopsis thaliana* ABCE2 identifies important motifs for its RNA silencing suppressor function. *Plant Biol.*, **23**, 21-31.

24. Sarmiento, C., Nigul, L., Kazantseva, J., Buschmann, M. and Truve, E. (2006) AtRLI2 is an endogenous suppressor of RNA silencing. *Plant Mol. Biol.*, **61**, 153-163.
25. Kougioumoutzi, E., Cartolano, M., Canales, C., Dupré, M., Bramsiepe, J., Vlad, D., Rast, M., Ioio, R.D., Tattersall, A., Schnittger, A. *et al.* (2013) *SIMPLE LEAF3* encodes a ribosome-associated protein required for leaflet development in *Cardamine hirsuta*. *Plant J.*, **73**, 533-545.
26. David-Assael, O., Saul, H., Saul, V., Mizrachy-Dagri, T., Berezin, I., Brook, E. and Shaul, O. (2005) Expression of AtMHX, an *Arabidopsis* vacuolar metal transporter, is repressed by the 5' untranslated region of its gene. *J. Exp. Bot.*, **56**, 1039-1047.
27. von Arnim, A.G., Jia, Q. and Vaughn, J.N. (2014) Regulation of plant translation by upstream open reading frames. *Plant Sci.*, **214**, 1-12.
28. Kim, B.H., Cai, X., Vaughn, J.N. and von Arnim, A.G. (2007) On the functions of the h subunit of eukaryotic initiation factor 3 in late stages of translation initiation. *Genome Biol.*, **8**, R60.
29. Rosado, A., Li, R., van de Ven, W., Hsu, E. and Raikhel, N.V. (2012) *Arabidopsis* ribosomal proteins control developmental programs through translational regulation of auxin response factors. *Proc. Natl. Acad. Sci. USA*, **109**, 19537-19544.
30. Zhou, F., Roy, B. and von Arnim, A.G. (2010) Translation reinitiation and development are compromised in similar ways by mutations in translation initiation factor eIF3h and the ribosomal protein RPL24. *BMC Plant Biol.*, **10**, 193.
31. Nishimura, T., Wada, T., Yamamoto, K.T. and Okada, K. (2005) The *Arabidopsis* STV1 protein, responsible for translation reinitiation, is required for auxin-mediated gynoecium patterning. *Plant Cell*, **17**, 2940-2953.
32. Kneuper, I., Teale, W., Dawson, J.E., Tsugeki, R., Katifori, E., Palme, K. and Ditegou, F.A. (2021) Auxin biosynthesis and cellular efflux act together to regulate leaf vein patterning. *J. Exp. Bot.*, **72**, 1151-1165.
33. Verna, C., Ravichandran, S.J., Sawchuk, M.G., Linh, N.M. and Scarpella, E. (2019) Coordination of tissue cell polarity by auxin transport and signaling. *eLife*, **8**, e51061.
34. Schepetilnikov, M., Dimitrova, M., Mancera-Martínez, E., Geldreich, A., Keller, M. and Ryabova, L.A. (2013) TOR and S6K1 promote translation reinitiation of uORF-containing mRNAs via phosphorylation of eIF3h. *EMBO J.*, **32**, 1087-1102.
35. Kleinboelting, N., Huep, G., Kloetgen, A., Viehoveer, P. and Weisshaar, B. (2012) GABI-Kat SimpleSearch: new features of the *Arabidopsis thaliana* T-DNA mutant database. *Nucleic Acids Res.*, **40**, D1211-1215.
36. Heisler, M.G., Ohno, C., Das, P., Sieber, P., Reddy, G.V., Long, J.A. and Meyerowitz, E.M. (2005) Patterns of auxin transport and gene expression during primordium

- development revealed by live imaging of the *Arabidopsis* inflorescence meristem. *Curr. Biol.*, **15**, 1899-1911.
37. Baima, S., Nobili, F., Sessa, G., Lucchetti, S., Ruberti, I. and Morelli, G. (1995) The expression of the *Athb-8* homeobox gene is restricted to provascular cells in *Arabidopsis thaliana*. *Development*, **121**, 4171-4182.
 38. Berná, G., Robles, P. and Micol, J.L. (1999) A mutational analysis of leaf morphogenesis in *Arabidopsis thaliana*. *Genetics*, **152**, 729-742.
 39. Ponce, M.R., Quesada, V. and Micol, J.L. (1998) Rapid discrimination of sequences flanking and within T-DNA insertions in the *Arabidopsis* genome. *Plant J.*, **14**, 497-501.
 40. Quesada, V., Ponce, M.R. and Micol, J.L. (2000) Genetic analysis of salt-tolerant mutants in *Arabidopsis thaliana*. *Genetics*, **154**, 421-436.
 41. Ponce, M.R., Robles, P., Lozano, F.M., Brotóns, M.A. and Micol, J.L. (2006) Low-resolution mapping of untagged mutations. *Methods Mol. Biol.*, **323**, 105-113.
 42. Mateo-Bonmatí, E., Casanova-Sáez, R., Candela, H. and Micol, J.L. (2014) Rapid identification of *angulata* leaf mutations using next-generation sequencing. *Planta*, **240**, 1113-1122.
 43. Ponce, M.R., Robles, P. and Micol, J.L. (1999) High-throughput genetic mapping in *Arabidopsis thaliana*. *Mol. Gen. Genet.*, **261**, 408-415.
 44. Curtis, M.D. and Grossniklaus, U. (2003) A Gateway cloning vector set for high-throughput functional analysis of genes in planta. *Plant Physiol.*, **133**, 462-469.
 45. Earley, K.W., Haag, J.R., Pontes, O., Opper, K., Juehne, T., Song, K. and Pikaard, C.S. (2006) Gateway-compatible vectors for plant functional genomics and proteomics. *Plant J.*, **45**, 616-629.
 46. Mateo-Bonmatí, E., Esteve-Bruna, D., Juan-Vicente, L., Nadi, R., Candela, H., Lozano, F.M., Ponce, M.R., Pérez-Pérez, J.M. and Micol, J.L. (2018) *INCURVATA11* and *CUPULIFORMIS2* are redundant genes that encode epigenetic machinery components in *Arabidopsis*. *Plant Cell*, **30**, 1596-1616.
 47. Clough, S.J. and Bent, A.F. (1998) Floral dip: a simplified method for *Agrobacterium*-mediated transformation of *Arabidopsis thaliana*. *Plant J.*, **16**, 735-743.
 48. Schindelin, J., Arganda-Carreras, I., Frise, E., Kaynig, V., Longair, M., Pietzsch, T., Preibisch, S., Rueden, C., Saalfeld, S., Schmid, B. et al. (2012) Fiji: an open-source platform for biological-image analysis. *Nat. Methods*, **9**, 676-682.
 49. Micol-Ponce, R., Sarmiento-Mañús, R., Fontcuberta-Cervera, S., Cabezas-Fuster, A., de Bures, A., Sáez-Vásquez, J. and Ponce, M.R. (2020) SMALL ORGAN4 is a ribosome biogenesis factor involved in 5.8S ribosomal RNA maturation. *Plant Physiol.*, **184**, 2022-2039.

50. Wellburn, A.R. (1994) The spectral determination of chlorophylls *a* and *b*, as well as total carotenoids, using various solvents with spectrophotometers of different resolution. *J. Plant Physiol.*, **144**, 307-313.
51. Rubio-Díaz, S., Pérez-Pérez, J.M., González-Bayón, R., Muñoz-Viana, R., Borrega, N., Mouille, G., Hernández-Romero, D., Robles, P., Höfte, H., Ponce, M.R. *et al.* (2012) Cell expansion-mediated organ growth is affected by mutations in three *EXIGUA* genes. *PLoS One*, **7**, e36500.
52. Sterken, R., Kiekens, R., Boruc, J., Zhang, F., Vercauteren, A., Vercauteren, I., De Smet, L., Dhondt, S., Inzé, D., De Veylder, L. *et al.* (2012) Combined linkage and association mapping reveals *CYCD5;1* as a quantitative trait gene for endoreduplication in *Arabidopsis*. *Proc. Natl. Acad. Sci. USA*, **109**, 4678-4683.
53. Pérez-Pérez, J.M., Rubio-Díaz, S., Dhondt, S., Hernández-Romero, D., Sánchez-Soriano, J., Beemster, G.T., Ponce, M.R. and Micol, J.L. (2011) Whole organ, venation and epidermal cell morphological variations are correlated in the leaves of *Arabidopsis* mutants. *Plant Cell Environ.*, **34**, 2200-2211.
54. Bühler, J., Rishmawi, L., Pflugfelder, D., Huber, G., Scharr, H., Hülskamp, M., Koornneef, M., Schurr, U. and Jahnke, S. (2015) phenoVein—A tool for leaf vein segmentation and analysis. *Plant Physiol.*, **169**, 2359-2370.
55. Quesada, V., Ponce, M.R. and Micol, J.L. (1999) *OTC* and *AUL1*, two convergent and overlapping genes in the nuclear genome of *Arabidopsis thaliana*. *FEBS Lett.*, **461**, 101-106.
56. Moschopoulos, A., Derbyshire, P. and Byrne, M.E. (2012) The *Arabidopsis* organelle-localized glycyl-tRNA synthetase encoded by *EMBRYO DEFECTIVE DEVELOPMENT1* is required for organ patterning. *J. Exp. Bot.*, **63**, 5233-5243.
57. Schmittgen, T.D. and Livak, K.J. (2008) Analyzing real-time PCR data by the comparative C_T method. *Nat. Protoc.*, **3**, 1101-1108.
58. Kim, D., Paggi, J.M., Park, C., Bennett, C. and Salzberg, S.L. (2019) Graph-based genome alignment and genotyping with HISAT2 and HISAT-genotype. *Nat. Biotechnol.*, **37**, 907-915.
59. Love, M.I., Huber, W. and Anders, S. (2014) Moderated estimation of fold change and dispersion for RNA-seq data with DESeq2. *Genome Biol.*, **15**, 550.
60. Huang, D.W., Sherman, B.T. and Lempicki, R.A. (2009) Bioinformatics enrichment tools: paths toward the comprehensive functional analysis of large gene lists. *Nucleic Acids Res.*, **37**, 1-13.
61. Huang, D.W., Sherman, B.T. and Lempicki, R.A. (2009) Systematic and integrative analysis of large gene lists using DAVID bioinformatics resources. *Nat. Protoc.*, **4**, 44-57.

62. Poza-Viejo, L., del Olmo, I. and Crevillén, P. (2019) Plant chromatin immunoprecipitation v.2. *protocols.io*, 25468.
63. Hooper, C.M., Castleden, I.R., Tanz, S.K., Aryamanesh, N. and Millar, A.H. (2017) SUBA4: the interactive data analysis centre for Arabidopsis subcellular protein locations. *Nucleic Acids Res.*, **45**, 1064-1074.
64. Hooper, C.M., Tanz, S.K., Castleden, I.R., Vacher, M.A., Small, I.D. and Millar, A.H. (2014) SUBAcon: a consensus algorithm for unifying the subcellular localization data of the *Arabidopsis* proteome. *Bioinformatics*, **30**, 3356-3364.
65. Madeira, F., Park, Y.M., Lee, J., Buso, N., Gur, T., Madhusoodanan, N., Basutkar, P., Tivey, A.R.N., Potter, S.C., Finn, R.D. *et al.* (2019) The EMBL-EBI search and sequence analysis tools APIs in 2019. *Nucleic Acids Res.*, **47**, 636-641.
66. Altschul, S.F., Madden, T.L., Schäffer, A.A., Zhang, J., Zhang, Z., Miller, W. and Lipman, D.J. (1997) Gapped BLAST and PSI-BLAST: a new generation of protein database search programs. *Nucleic Acids Res.*, **25**, 3389-3402.
67. Hori, K., Yamada, Y., Purwanto, R., Minakuchi, Y., Toyoda, A., Hirakawa, H. and Sato, F. (2018) Mining of the uncharacterized cytochrome P450 genes involved in alkaloid biosynthesis in california poppy using a draft genome sequence. *Plant Cell Physiol.*, **59**, 222-233.
68. Kumar, S., Stecher, G., Li, M., Knyaz, C. and Tamura, K. (2018) MEGA X: Molecular Evolutionary Genetics Analysis across computing platforms. *Mol. Biol. Evol.*, **35**, 1547-1549.
69. Edgar, R.C. (2004) MUSCLE: multiple sequence alignment with high accuracy and high throughput. *Nucleic Acids Res.*, **32**, 1792-1797.
70. Edgar, R.C. (2004) MUSCLE: a multiple sequence alignment method with reduced time and space complexity. *BMC Bioinformatics*, **5**, 113.
71. Saitou, N. and Nei, M. (1987) The neighbor-joining method: a new method for reconstructing phylogenetic trees. *Mol. Biol. Evol.*, **4**, 406-425.
72. Byrne, M.E. (2009) A role for the ribosome in development. *Trends Plant Sci.*, **14**, 512-519.
73. Horiguchi, G., Mollá-Morales, A., Pérez-Pérez, J.M., Kojima, K., Robles, P., Ponce, M.R., Micol, J.L. and Tsukaya, H. (2011) Differential contributions of ribosomal protein genes to *Arabidopsis thaliana* leaf development. *Plant J.*, **65**, 724-736.
74. Micol-Ponce, R., Sarmiento-Mañús, R., Ruiz-Bayón, A., Montacié, C., Sáez-Vasquez, J. and Ponce, M.R. (2018) Arabidopsis RIBOSOMAL RNA PROCESSING7 is required for 18S rRNA maturation. *Plant Cell*, **30**, 2855-2872.
75. Weis, B.L., Kovacevic, J., Missbach, S. and Schleiff, E. (2015) Plant-specific features of ribosome biogenesis. *Trends Plant Sci.*, **20**, 729-740.

76. Casanova-Sáez, R., Candela, H. and Micol, J.L. (2014) Combined haploinsufficiency and purifying selection drive retention of *RPL36a* paralogs in *Arabidopsis*. *Sci. Rep.*, **4**, 4122.
77. Katagiri, Y., Hasegawa, J., Fujikura, U., Hoshino, R., Matsunaga, S. and Tsukaya, H. (2016) The coordination of ploidy and cell size differs between cell layers in leaves. *Development*, **143**, 1120-1125.
78. Robles, P. and Micol, J.L. (2001) Genome-wide linkage analysis of *Arabidopsis* genes required for leaf development. *Mol. Genet. Genomics*, **266**, 12-19.
79. Chen, Z.Q., Dong, J., Ishimura, A., Daar, I., Hinnebusch, A.G. and Dean, M. (2006) The essential vertebrate ABCE1 protein interacts with eukaryotic initiation factors. *J. Biol. Chem.*, **281**, 7452-7457.
80. Liu, S., Li, Q. and Liu, Z. (2013) Genome-wide identification, characterization and phylogenetic analysis of 50 catfish ATP-binding cassette (ABC) transporter genes. *PLoS One*, **8**, e63895.
81. Lu, H., Xu, Y. and Cui, F. (2016) Phylogenetic analysis of the ATP-binding cassette transporter family in three mosquito species. *Pestic. Biochem. Physiol.*, **132**, 118-124.
82. Andolfo, G., Ruocco, M., Di Donato, A., Frusciante, L., Lorito, M., Scala, F. and Ercolano, M.R. (2015) Genetic variability and evolutionary diversification of membrane ABC transporters in plants. *BMC Plant Biol.*, **15**, 1-15.
83. Saha, J., Sengupta, A., Gupta, K. and Gupta, B. (2015) Molecular phylogenetic study and expression analysis of ATP-binding cassette transporter gene family in *Oryza sativa* in response to salt stress. *Comput. Biol. Chem.*, **54**, 18-32.
84. Zhang, L., Cai, X., Wu, J., Liu, M., Grob, S., Cheng, F., Liang, J., Cai, C., Liu, Z., Liu, B. et al. (2018) Improved *Brassica rapa* reference genome by single-molecule sequencing and chromosome conformation capture technologies. *Hortic. Res.*, **5**, 50.
85. Braz, A.S., Finnegan, J., Waterhouse, P. and Margis, R. (2004) A plant orthologue of RNase L inhibitor (RLI) is induced in plants showing RNA interference. *J. Mol. Evol.*, **59**, 20-30.
86. Hopfner, K.P. (2012) Rustless translation. *Biol. Chem.*, **393**, 1079-1088.
87. Dong, J., Lai, R., Nielsen, K., Fekete, C.A., Qiu, H. and Hinnebusch, A.G. (2004) The essential ATP-binding cassette protein RLI1 functions in translation by promoting preinitiation complex assembly. *J. Biol. Chem.*, **279**, 42157-42168.
88. Kispal, G., Sipos, K., Lange, H., Fekete, Z., Bedekovics, T., Janáky, T., Bassler, J., Aguilar Netz, D.J., Balk, J., Rotte, C. et al. (2005) Biogenesis of cytosolic ribosomes requires the essential iron-sulphur protein Rli1p and mitochondria. *EMBO J.*, **24**, 589-598.

89. Yarunin, A., Panse, V.G., Petfalski, E., Dez, C., Tollervey, D. and Hurt, E.C. (2005) Functional link between ribosome formation and biogenesis of iron-sulfur proteins. *EMBO J.*, **24**, 580-588.
90. Coelho, C.M., Kolevski, B., Bunn, C., Walker, C., Dahanukar, A. and Leever, S.J. (2005) Growth and cell survival are unevenly impaired in *pixie* mutant wing discs. *Development*, **132**, 5411-5424.
91. Kirli, K., Karaca, S., Dehne, H.J., Samwer, M., Pan, K.T., Lenz, C., Urlaub, H. and Görlich, D. (2015) A deep proteomics perspective on CRM1-mediated nuclear export and nucleocytoplasmic partitioning. *eLife*, **4**, e11466.
92. Zhai, C., Li, Y., Mascarenhas, C., Lin, Q., Li, K., Vyrides, I., Grant, C.M. and Panaretou, B. (2014) The function of ORAOV1/LTO1, a gene that is overexpressed frequently in cancer: essential roles in the function and biogenesis of the ribosome. *Oncogene*, **33**, 484-494.
93. Paul, V.D., Mühlhoff, U., Stümpfig, M., Seebacher, J., Kugler, K.G., Renicke, C., Taxis, C., Gavin, A.C., Pierik, A.J. and Lill, R. (2015) The deca-GX₃ proteins Yae1-Lto1 function as adaptors recruiting the ABC protein Rli1 for iron-sulfur cluster insertion. *eLife*, **4**, e08231.
94. Zhu, X., Zhang, H. and Mendell, J.T. (2020) Ribosome recycling by ABCE1 links lysosomal function and iron homeostasis to 3' UTR-directed regulation and nonsense-mediated decay. *Cell Rep.*, **32**, 107895.
95. Browning, K.S. and Bailey-Serres, J. (2015) Mechanism of cytoplasmic mRNA translation. *The Arabidopsis book*, **13**, e0176.
96. Andersen, D.S. and Leever, S.J. (2007) The essential *Drosophila* ATP-binding cassette domain protein, Pixie, binds the 40 S ribosome in an ATP-dependent manner and is required for translation initiation. *J. Biol. Chem.*, **282**, 14752-14760.
97. Khoshnevis, S., Gross, T., Rotte, C., Baierlein, C., Ficner, R. and Krebber, H. (2010) The iron-sulphur protein RNase L inhibitor functions in translation termination. *EMBO Rep.*, **11**, 214-219.
98. Young, D.J. and Guydosh, N.R. (2019) Hcr1/eIF3j is a 60S ribosomal subunit recycling accessory factor *in vivo*. *Cell Rep.*, **28**, 39-50.
99. Lebaron, S., Schneider, C., van Nues, R.W., Swiatkowska, A., Walsh, D., Böttcher, B., Granneman, S., Watkins, N.J. and Tollervey, D. (2012) Proofreading of pre-40S ribosome maturation by a translation initiation factor and 60S subunits. *Nat. Struct. Mol. Biol.*, **19**, 744-753.
100. Pestova, T.V., Lomakin, I.B., Lee, J.H., Choi, S.K., Dever, T.E. and Hellen, C.U. (2000) The joining of ribosomal subunits in eukaryotes requires eIF5B. *Nature*, **403**, 332-335.

101. Coaker, G., Falick, A. and Staskawicz, B. (2005) Activation of a phytopathogenic bacterial effector protein by a eukaryotic cyclophilin. *Science*, **308**, 548-550.
102. Coaker, G., Zhu, G., Ding, Z., Van Doren, S.R. and Staskawicz, B. (2006) Eukaryotic cyclophilin as a molecular switch for effector activation. *Mol. Microbiol.*, **61**, 1485-1496.
103. Arribas-Hernández, L., Bressendorff, S., Hansen, M.H., Poulsen, C., Erdmann, S. and Brodersen, P. (2018) An m⁶A-YTH module controls developmental timing and morphogenesis in Arabidopsis. *Plant Cell*, **30**, 952-967.
104. Scutenaire, J., Deragon, J.M., Jean, V., Benhamed, M., Raynaud, C., Favory, J.J., Merret, R. and Bousquet-Antonelli, C. (2018) The YTH domain protein ECT2 is an m⁶A reader required for normal trichome branching in Arabidopsis. *Plant Cell*, **30**, 986-1005.
105. Wei, L.H., Song, P., Wang, Y., Lu, Z., Tang, Q., Yu, Q., Xiao, Y., Zhang, X., Duan, H.C. and Jia, G. (2018) The m⁶A reader ECT2 controls trichome morphology by affecting mRNA stability in Arabidopsis. *Plant Cell*, **30**, 968-985.
106. Faus, I., Niñoles, R., Kesari, V., Llabata, P., Tam, E., Nebauer, S.G., Santiago, J., Hauser, M.T. and Gadea, J. (2018) Arabidopsis ILITHYIA protein is necessary for proper chloroplast biogenesis and root development independent of eIF2 α phosphorylation. *J. Plant Physiol.*, **224-225**, 173-182.
107. Izquierdo, Y., Kulasekaran, S., Benito, P., López, B., Marcos, R., Cascón, T., Hamberg, M. and Castresana, C. (2018) Arabidopsis *nonresponding to oxylipins* locus NOXY7 encodes a yeast GCN1 homolog that mediates noncanonical translation regulation and stress adaptation. *Plant Cell Environ.*, **41**, 1438-1452.
108. Wang, L., Li, H., Zhao, C., Li, S., Kong, L., Wu, W., Kong, W., Liu, Y., Wei, Y., Zhu, J.K. et al. (2017) The inhibition of protein translation mediated by AtGCN1 is essential for cold tolerance in *Arabidopsis thaliana*. *Plant Cell Environ.*, **40**, 56-68.
109. Bengtson, M.H. and Joazeiro, C.A. (2010) Role of a ribosome-associated E3 ubiquitin ligase in protein quality control. *Nature*, **467**, 470-473.
110. Doamekpor, S.K., Lee, J.W., Hepowit, N.L., Wu, C., Charenton, C., Leonard, M., Bengtson, M.H., Rajashankar, K.R., Sachs, M.S., Lima, C.D. et al. (2016) Structure and function of the yeast listerin (Ltn1) conserved N-terminal domain in binding to stalled 60S ribosomal subunits. *Proc. Natl. Acad. Sci. USA*, **113**, 4151-4160.
111. Shao, S., von der Malsburg, K. and Hegde, R.S. (2013) Listerin-dependent nascent protein ubiquitination relies on ribosome subunit dissociation. *Mol. Cell*, **50**, 637-648.
112. Takahara, T., Amemiya, Y., Sugiyama, R., Maki, M. and Shibata, H. (2020) Amino acid-dependent control of mTORC1 signaling: a variety of regulatory modes. *J. Biomed. Sci.*, **27**, 1-16.
113. Van Leene, J., Han, C., Gadeyne, A., Eeckhout, D., Matthijs, C., Cannoot, B., De Winne, N., Persiau, G., Van De Slijke, E., Van de Cotte, B. et al. (2019) Capturing the

- phosphorylation and protein interaction landscape of the plant TOR kinase. *Nat. Plants*, **5**, 316-327.
114. Pinon, V., Etchells, J.P., Rossignol, P., Collier, S.A., Arroyo, J.M., Martienssen, R.A. and Byrne, M.E. (2008) Three *PIGGYBACK* genes that specifically influence leaf patterning encode ribosomal proteins. *Development*, **135**, 1315-1324.
115. Govindaraju, P., Verna, C., Zhu, T. and Scarpella, E. (2020) Vein patterning by tissue-specific auxin transport. *Development*, **147**, 1-7.
116. Casanova-Sáez, R., Mateo-Bonmatí, E. and Ljung, K. (2021) Auxin metabolism in plants. *Cold Spring Harb. Perspect. Biol.*, **13**, a039867.
117. Brumos, J., Robles, L.M., Yun, J., Vu, T.C., Jackson, S., Alonso, J.M. and Stepanova, A.N. (2018) Local auxin biosynthesis is a key regulator of plant development. *Dev. Cell*, **47**, 306-318.
118. Wang, W., Xu, B., Wang, H., Li, J., Huang, H. and Xu, L. (2011) *YUCCA* genes are expressed in response to leaf adaxial-abaxial juxtaposition and are required for leaf margin development. *Plant Physiol.*, **157**, 1805-1819.
119. Schlereth, A., Möller, B., Liu, W., Kientz, M., Flipse, J., Rademacher, E.H., Schmid, M., Jürgens, G. and Weijers, D. (2010) MONOPTEROS controls embryonic root initiation by regulating a mobile transcription factor. *Nature*, **464**, 913-916.
120. De Rybel, B., Möller, B., Yoshida, S., Grabowicz, I., Barbier de Reuille, P., Boeren, S., Smith, R.S., Borst, J.W. and Weijers, D. (2013) A bHLH complex controls embryonic vascular tissue establishment and indeterminate growth in *Arabidopsis*. *Dev. Cell*, **24**, 426-437.
121. Vera-Sirera, F., De Rybel, B., Úrbez, C., Kouklas, E., Pesquera, M., Álvarez-Mahecha, J.C., Minguet, E.G., Tuominen, H., Carbonell, J., Borst, J.W. *et al.* (2015) A bHLH-based feedback loop restricts vascular cell proliferation in plants. *Dev. Cell*, **35**, 432-443.
122. Eide, D., Broderius, M., Fett, J. and Guerinot, M.L. (1996) A novel iron-regulated metal transporter from plants identified by functional expression in yeast. *Proc. Natl. Acad. Sci. USA*, **93**, 5624-5628.
123. Robinson, N.J., Procter, C.M., Connolly, E.L. and Guerinot, M.L. (1999) A ferric-chelate reductase for iron uptake from soils. *Nature*, **397**, 694-697.
124. Lanquar, V., Lelièvre, F., Bolte, S., Hamès, C., Alcon, C., Neumann, D., Vansuyt, G., Curie, C., Schröder, A., Krämer, U. *et al.* (2005) Mobilization of vacuolar iron by AtNRAMP3 and AtNRAMP4 is essential for seed germination on low iron. *EMBO J.*, **24**, 4041-4051.
125. Li, J., Wang, Y., Zheng, L., Li, Y., Zhou, X., Li, J., Gu, D., Xu, E., Lu, Y., Chen, X. *et al.* (2019) The intracellular transporter AtNRAMP6 is involved in Fe homeostasis in *Arabidopsis*. *Front. Plant Sci.*, **10**, 1124.

126. Colca, J.R., McDonald, W.G., Waldon, D.J., Leone, J.W., Lull, J.M., Bannow, C.A., Lund, E.T. and Mathews, W.R. (2004) Identification of a novel mitochondrial protein ("mitoNEET") cross-linked specifically by a thiazolidinedione photoprobe. *Am. J. Physiol. Endocrinol. Metabol.*, **286**, 252-260.
127. Nechushtai, R., Conlan, A.R., Harir, Y., Song, L., Yogev, O., Eisenberg-Domovich, Y., Livnah, O., Michaeli, D., Rosen, R., Ma, V. *et al.* (2012) Characterization of *Arabidopsis* NEET reveals an ancient role for NEET proteins in iron metabolism. *Plant Cell*, **24**, 2139-2154.
128. Zandalinas, S.I., Song, L., Sengupta, S., McInturf, S.A., Grant, D.G., Marjault, H.B., Castro-Guerrero, N.A., Burks, D., Azad, R.K., Mendoza-Cozatl, D.G. *et al.* (2020) Expression of a dominant-negative AtNEET-H89C protein disrupts iron-sulfur metabolism and iron homeostasis in *Arabidopsis*. *Plant J.*, **101**, 1152-1169.
129. Briat, J.F., Duc, C., Ravet, K. and Gaymard, F. (2010) Ferritins and iron storage in plants. *Biochim. Biophys. Acta*, **1800**, 806-814.
130. Reyt, G., Boudouf, S., Boucherez, J., Gaymard, F. and Briat, J.F. (2015) Iron- and ferritin-dependent reactive oxygen species distribution: impact on *Arabidopsis* root system architecture. *Mol. Plant*, **8**, 439-453.
131. Alhebshi, A., Sideri, T.C., Holland, S.L. and Avery, S.V. (2012) The essential iron-sulfur protein Rli1 is an important target accounting for inhibition of cell growth by reactive oxygen species. *Mol. Biol. Cell*, **23**, 3582-3590.
132. Sudmant, P.H., Lee, H., Dominguez, D., Heiman, M. and Burge, C.B. (2018) Widespread accumulation of ribosome-associated isolated 3' UTRs in neuronal cell populations of the aging brain. *Cell Rep.*, **25**, 2447-2456.
133. Nürenberg-Goloub, E. and Tampé, R. (2019) Ribosome recycling in mRNA translation, quality control, and homeostasis. *Biol. Chem.*, **401**, 47-61.
134. Sesma, A., Castresana, C. and Castellano, M.M. (2017) Regulation of translation by TOR, eIF4E and eIF2 α in plants: current knowledge, challenges and future perspectives. *Front. Plant Sci.*, **8**, 644.
135. Kärblane, K., Gerassimenko, J., Nigul, L., Piirsoo, A., Smialowska, A., Vinkel, K., Kylsten, P., Ekwall, K., Swoboda, P., Truve, E. *et al.* (2015) ABCE1 is a highly conserved RNA silencing suppressor. *PLoS One*, **10**, e0116702.
136. Mähönen, A.P., Bishopp, A., Higuchi, M., Nieminen, K.M., Kinoshita, K., Törmäkangas, K., Ikeda, Y., Oka, A., Kakimoto, T. and Helariutta, Y. (2006) Cytokinin signaling and its inhibitor AHP6 regulate cell fate during vascular development. *Science*, **311**, 94-98.

FIGURE LEGENDS

Figure 1. Morphological phenotype of the *api7-1* mutant. (A–C) Rosettes from (A) the wild-type *Ler*, (B) the *api7-1* mutant, and (C) an *api7-1 ABCE2_{pro}:ABCE2* mutant and transgenic plant. Pictures were taken 16 days after stratification (das). Scale bars indicate 2 mm. (D, E) Growth progression of (D) rosette area and (E) main stem length. Bars indicate (D) mean and (E) median values. Error bars represent (D) standard deviation and (E) median absolute deviation. Asterisks indicate a significant difference with *Ler* in a (D) Student's *t* test ($10 < n < 17$) or (E) Mann-Whitney *U* test ($n = 8$) (* $P < 0.05$, ** $P < 0.001$).

Figure 2. Fine mapping by linkage analysis of the *api7-1* mutation. (A) A mapping population of 273 F_2 plants derived from an *api7-1* × *Col-0* cross allowed us to delimit a candidate region of 123.5 kb in chromosome 4, flanked by the T18B16 and g3883 markers. The names and physical map positions of the molecular markers used for linkage analysis are shown. All values outside parentheses indicate Mb. The number of recombinant chromosomes found (from a total of 546 chromosomes analyzed) is indicated in parentheses. (B) Structure of the At4g19210 (*ABCE2*) gene, located within the candidate region, with indication of the nature and position of the *api7* mutations studied in this work. Boxes and lines indicate exons and introns, respectively. White boxes represent UTRs. The arrow indicates the *api7-1* point mutation. The triangle indicates the *api7-2* T-DNA insertion (GABI_509C06).

Figure 3. Effects of the *ABCE2_{pro}:ABCE1* and *ABCE1_{pro}:ABCE2* transgenes on the morphological phenotype of the *api7-1* mutant. Rosettes from (A) *Ler*, (B) *api7-1*, (C) *api7-1 ABCE2_{pro}:ABCE1*, and (D) *api7-1 ABCE1_{pro}:ABCE2* plants. Pictures were taken 14 das. Scale bars indicate 2 mm.

Figure 4. Subcellular localization of the *ABCE2* protein in cells from the root elongation zone. Confocal laser scanning micrographs of (A, C, E) *Ler 35S_{pro}:ABCE2:GFP* and (B, D, F) *api7-1 35S_{pro}:ABCE2:YFP* transgenic plants. Fluorescent signals correspond to (A) GFP, (B) YFP, (C) propidium iodide, and (D) DAPI staining, and (E, F) the overlay of (E) GFP and propidium iodide, and (F) YFP and DAPI. Pictures were taken (A, C, E) 14 and (B, D, F) 5 das. Scale bars indicate 20 μ m.

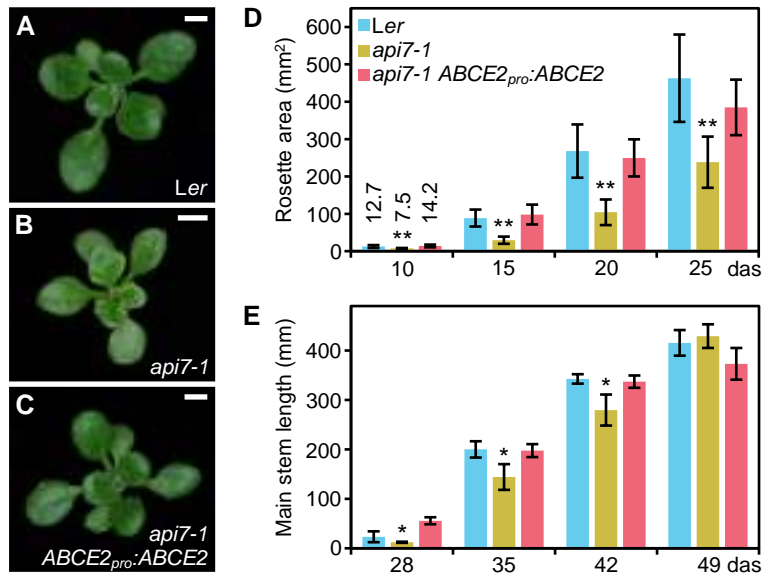
Figure 5. Proteins identified in an *ABCE2:YFP* co-immunoprecipitation assay. Proteins were grouped within dashed boxes according to their annotated functions for Arabidopsis (names in black letters) or orthologous (names in blue letters) proteins. Green and blue boxes represent complexes that have been described in Arabidopsis and other species,

respectively. Proteins in striped boxes were not identified in our assay but have been included in this figure because they are known to belong to a given complex. Continuous and dashed lines connecting boxes indicate physical and genetic interactions described elsewhere for *Arabidopsis* (black) or other species (blue), respectively. For references, see Supplementary Table S5. Names in bold and plain letters indicate proteins unique to or enriched in ABCE2:YFP samples, respectively.

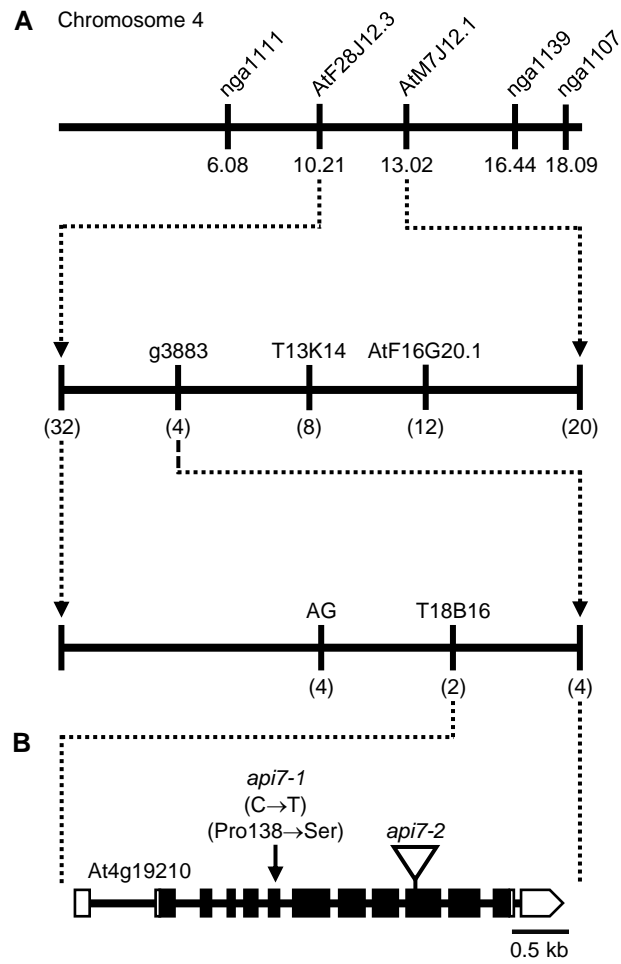
Figure 6. Venation pattern of *api7-1* first- and third-node leaves. Representative diagrams of mature (A, B) first- and (C, D) third-node leaves from (A, C) *Ler* and (B, D) *api7-1* plants. Margins were drawn in black, primary veins in green, secondary veins in blue, higher-order connected veins in yellow, and higher-order disconnected veins in pink. Organs were collected 21 das. Scale bars indicate 1 mm.

Figure 7. Auxin transport and perception in *api7-1* roots. Visualization of the expression of reporter transgenes for auxin (A, B) transport and (C, D) perception, in (A, C) wild-type and (B, D) *api7-1* roots. Cell walls were stained with propidium iodide. Values indicate average fluorescence intensities \pm standard deviation from (A, B) GFP and (C, D) VENUS, which are significantly different from the wild type in a Student's *t* test [(A, B) $P < 0.001$, $n = 25$; (C, D) $P < 0.05$, $n = 27$]. Pictures were taken 5 das. Scale bars indicate 50 μm .

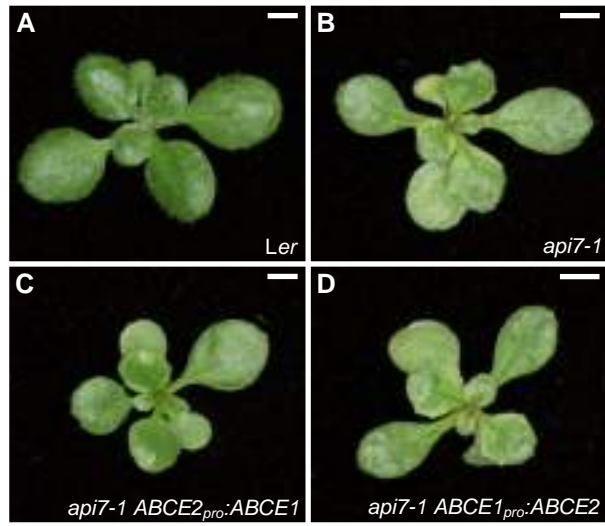
Navarro-Quiles *et al.*, Figure 1



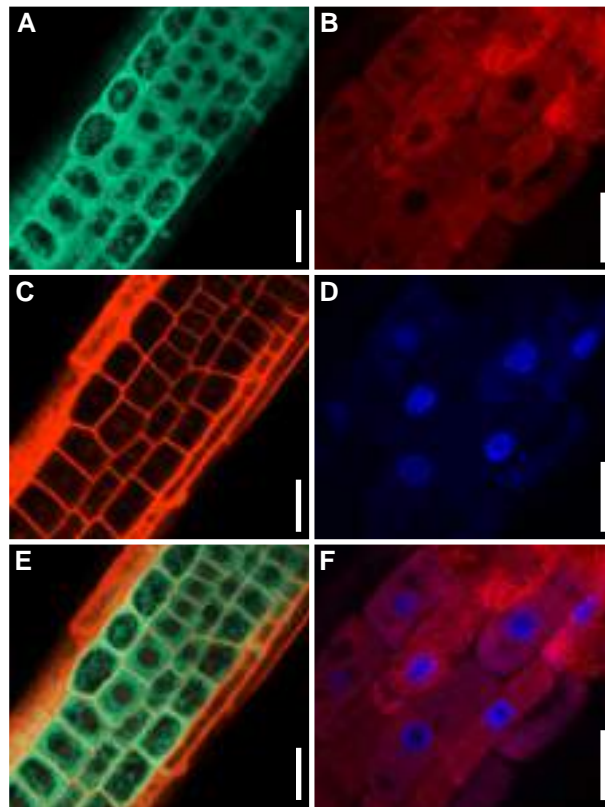
Navarro-Quiles *et al.*, Figure 2



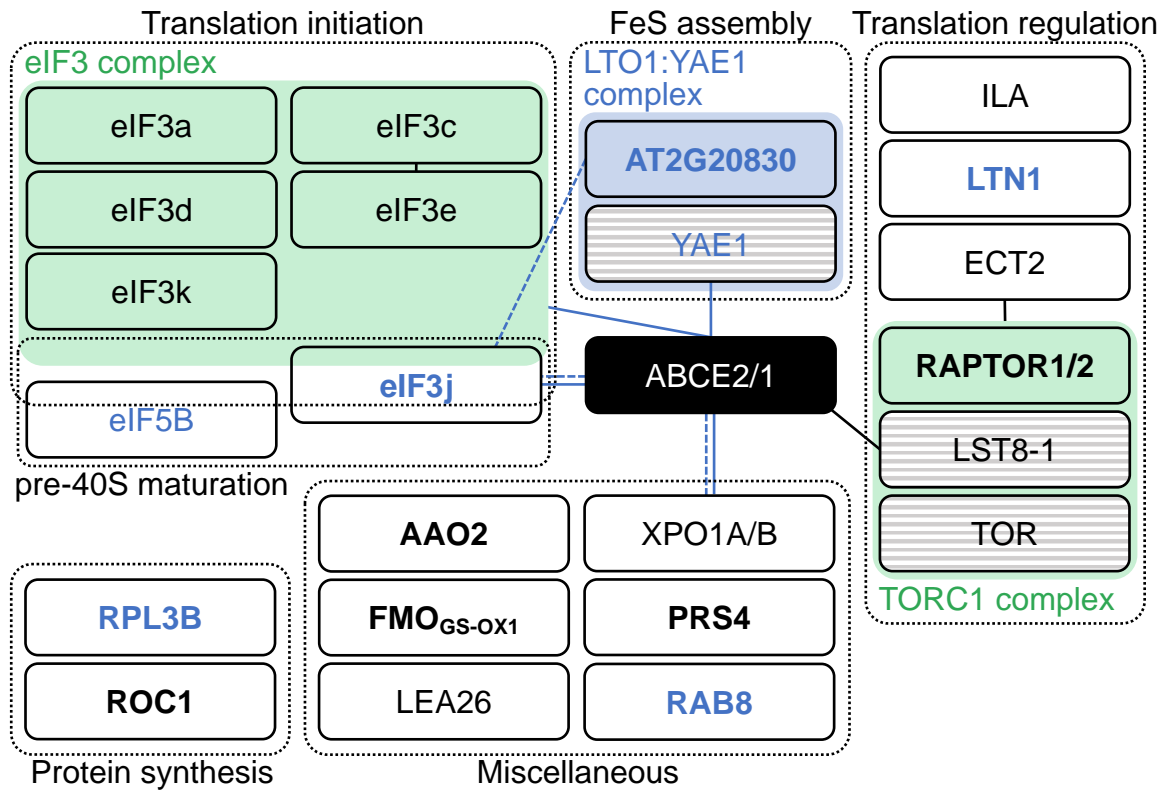
Navarro-Quiles et al., Figure 3



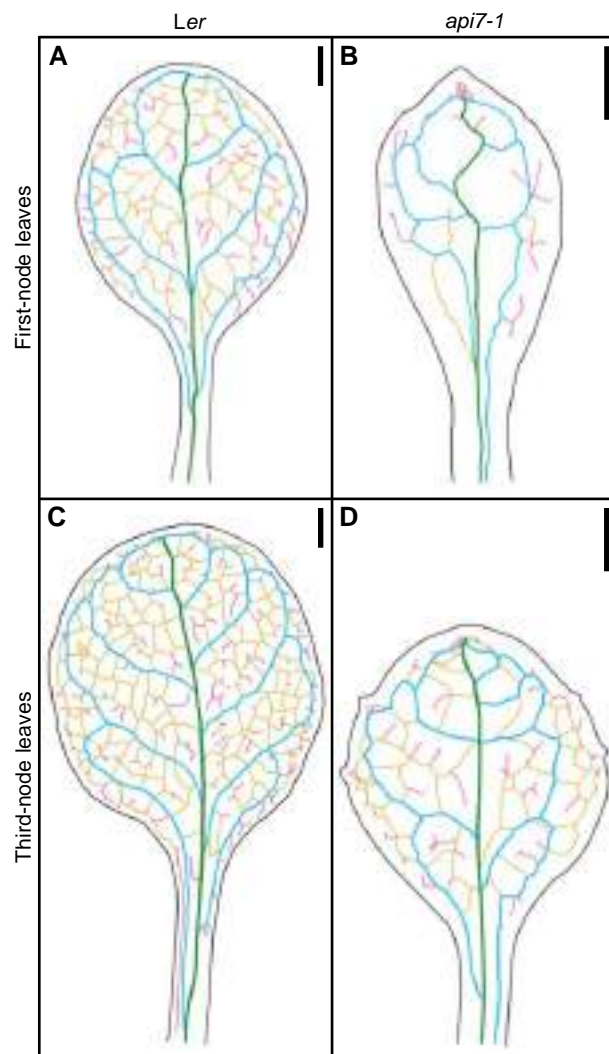
Navarro-Quiles *et al.*, Figure 4



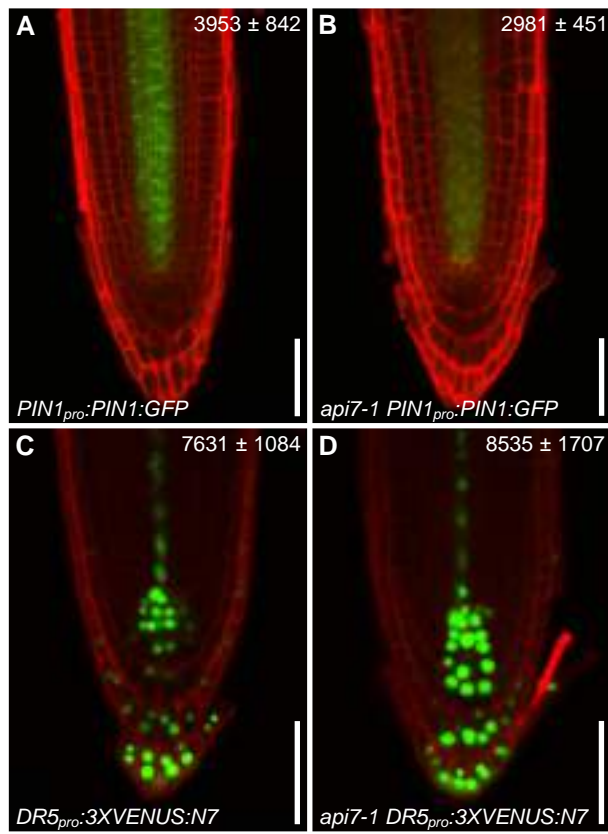
Navarro-Quiles *et al.*, Figure 5



Navarro-Quiles *et al.*, Figure 6



Navarro-Quiles et al., Figure 7



Arabidopsis ATP-Binding Cassette E2 is a conserved component of the translation machinery

Carla Navarro-Quiles, Eduardo Mateo-Bonmatí, Héctor Candela,
Pedro Robles, Antonio Martínez-Laborda, María Rosa Ponce,
and José Luis Micol

Instituto de Bioingeniería, Universidad Miguel Hernández, Campus de Elche,
03202 Elche, Spain

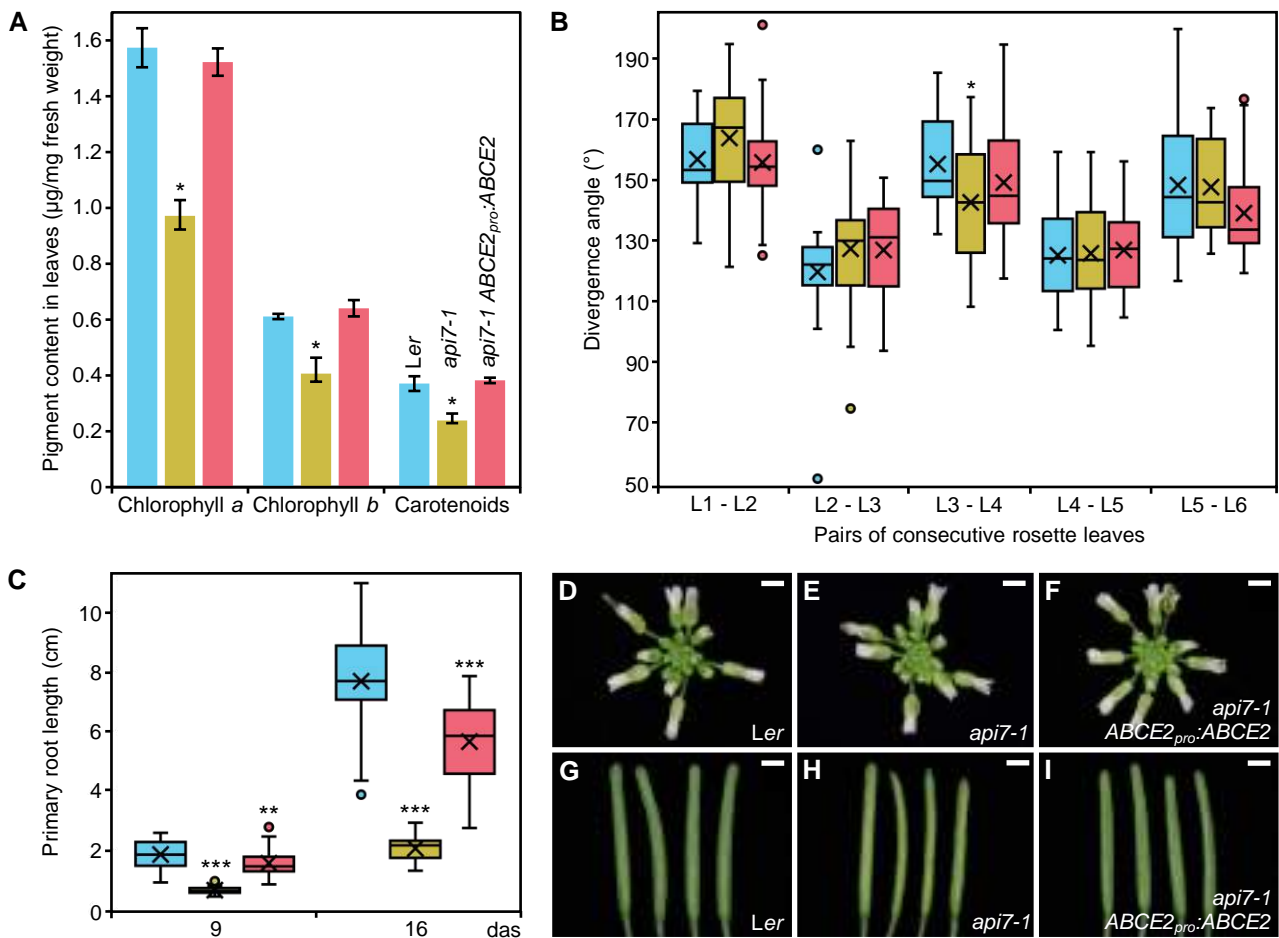
Supplementary Figures and Tables

Supplementary Data Sets not included in this file

Navarro-Quiles et al_Data Set 1.xlsx

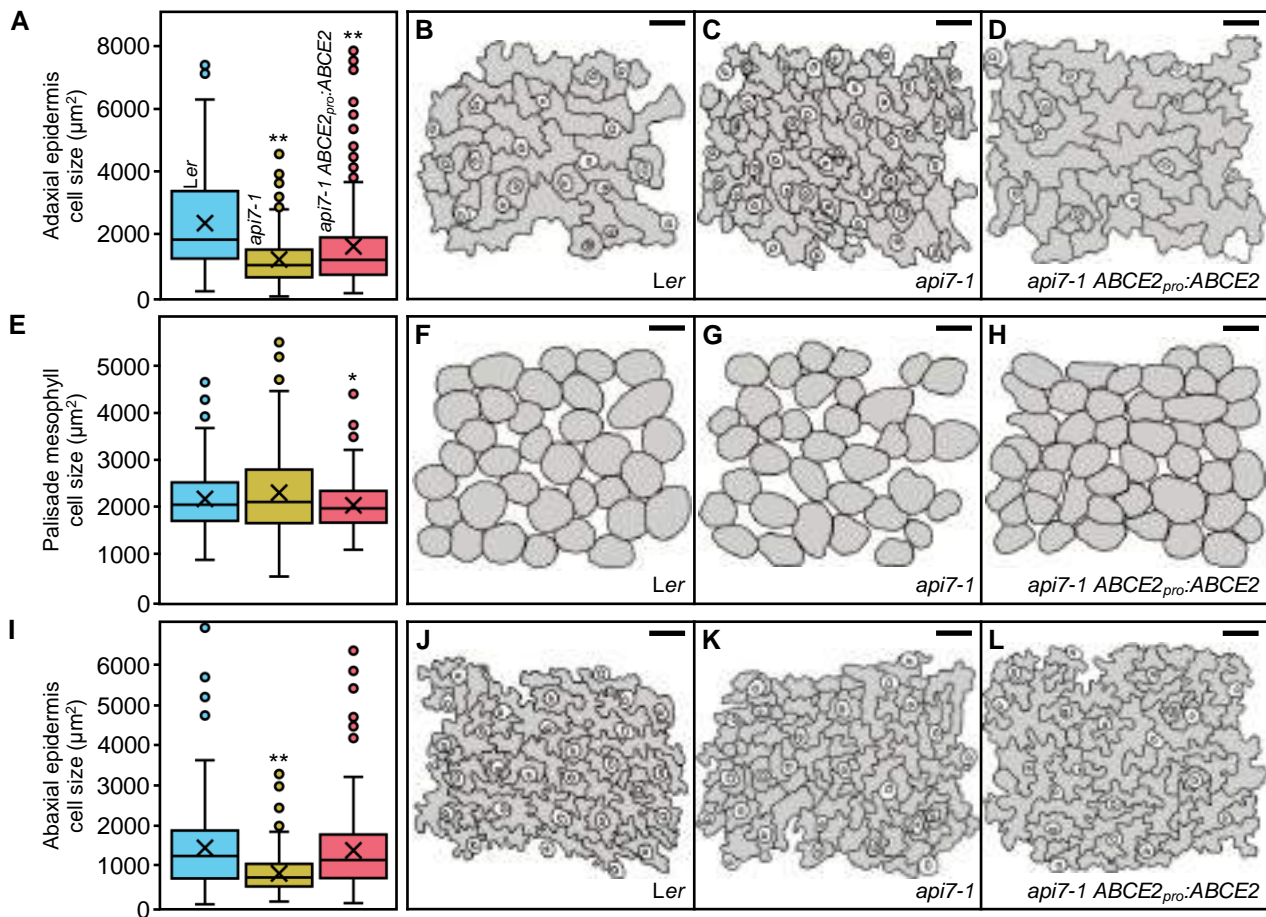
Navarro-Quiles et al_Data Set 2.xlsx

Navarro-Quiles et al_Data Set 2.xlsx



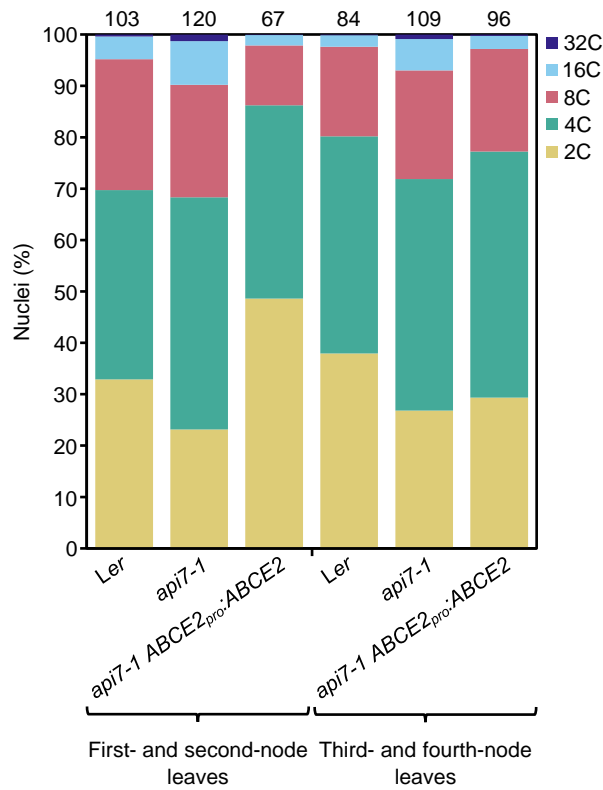
Supplementary Figure S1. Pigment content in leaves, rosette phyllotaxis, primary root length, and inflorescence and silique morphological phenotypes of *Ler*, *api7-1*, and *api7-1 ABCE2_{pro}:ABCE2* plants.

(A) Chlorophyll *a* and *b*, and carotenoid content in wild-type *Ler*, *api7-1* mutant, and *api7-1 ABCE2_{pro}:ABCE2* mutant and transgenic rosettes collected 16 das. Median values are shown. Error bars represent median absolute deviation. (B) Rosette leaf phyllotaxis in plants of the genotypes mentioned in (A). The divergence angles between consecutive leaves are shown: L1 - L2, first- and second-node leaves; L2 - L3, second- and third-node leaves; L3 - L4, third- and fourth-node leaves; L4 - L5, fourth- and fifth-node leaves; L5 - L6, fifth- and sixth-node leaves. (C) Primary root growth progression between 9 and 16 das in plants of the genotypes mentioned in (A). Boxes in (B) and (C) are delimited by the first (Q1, lower hinge) and third (Q3, upper hinge) quartiles. Whiskers represent the values within the distribution that are immediately higher than $Q1 - 1.5 \cdot IQ$ (lower) and lower than $Q3 + 1.5 \cdot IQ$ (upper), where $IQ = Q3 - Q1$. x: Mean. —: Median. o: Outlier. Measurements were made (A) 16, (B) 18, and (C) 9 and 16 das. Asterisks indicate a significant difference with *Ler* in a (A) Mann-Whitney *U* ($n = 5$) or (B, C) Student's *t* test (B, $n = 23$; C, $28 < n < 35$) ($*P < 0.05$, $**P < 0.01$, $***P < 0.001$). (D–F) Inflorescences and (G–I) siliques of (D, G) *Ler*, (E, H) *api7-1*, and (F, I) *api7-1 ABCE2_{pro}:ABCE2* plants. Pictures were taken 40 das. Scale bars indicate 2 mm.



Supplementary Figure S2. Leaf cell phenotypes of *Ler*, *api7-1*, and *api7-1 ABCE2_{pro}:ABCE2* plants.

(A, E, I) Boxplot distributions of cell area in the (A) adaxial epidermis, (E) subepidermal layer of palisade mesophyll, and (I) abaxial epidermis, from first-node leaves collected 21 das. Other details as described in the legend of Supplementary Figure S1 for its (B) and (C) sections. Between 144 and 351 cells were analyzed from at least 4 different samples. Asterisks indicate a significant difference with the *Ler* wild-type in a Student's *t* test (* $P < 0.05$, ** $P < 0.001$). (B–D, F–H, J–L) Representative diagrams of the (B–D) adaxial epidermis, (F–H) subepidermal layer of palisade mesophyll, and (J–L) abaxial epidermis, from (B, F, J) *Ler*, (C, G, K) *api7-1*, and (D, H, L) *api7-1 ABCE2_{pro}:ABCE2* plants.



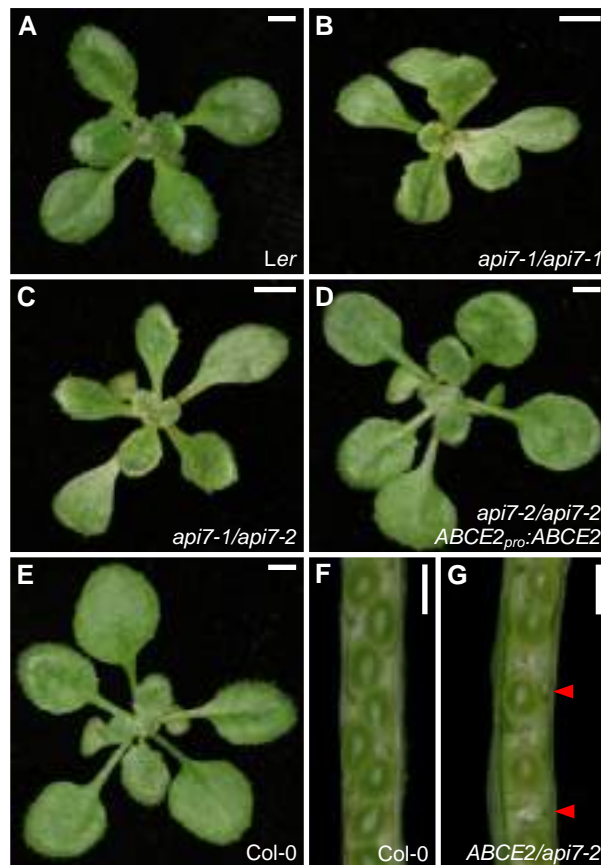
Supplementary Figure S3. Nuclear ploidy levels in *Ler*, *api7-1*, and *api7-1 ABCE2_{pro}:ABCE2* rosette leaves.

DNA content was measured in nuclei from whole first- and second-node leaves, as well as third- and fourth-node leaves. The value at the top of each column indicates the mean endoreduplication index (EI) from three biological replicates. Each biological replicate was composed of either 6 first- and 6 second-node leaves or 6 third- and 6 fourth-node leaves. At least 20,000 events were analyzed in each biological replicate. Measurements were made 18 das.

<i>S. solfataricus</i>	453	LESNVNDLSGGELQKIYIAATLAKKADLYVLDEPSSSYLDVEERYIVAKAIKRVTREKAV
<i>P. furiosus</i>	447	YDREVNELSGGELQRVAAATLLRDADLYLIDEPSAYLDVEQRIAVSRATIRHLEKNEKT
<i>C. elegans</i>	465	IDRNVKELSGGELQRVALLALCLGKTPASLYLIDEPSAYLDSEQRIHAAKVIKRFIMHAKKT
<i>S. cerevisiae</i>	461	IDQEVQHLSGGELQRVAVLALGIPADLYLIDEPSAYLDSEQRIICSKVIRRFILHNKKT
<i>O. sativa</i>	460	MDQEVINLSGGELQRVATLCLGKPADLYLIDEPSAYLDSEQRIVASKVIKRFILHAKKT
<i>S. lycopersicum</i>	461	MDQEVVNLSSGGELQRVALLALCLGKPADLYLIDEPSAYLDSEQRIVASKVIKRFILHAKKT
<i>A. thaliana</i>	461	MDQEVVNLSSGGELQRVATLCLGKPADLYLIDEPSAYLDSEQRIVASKVIKRFILHAKKT
<i>C. hirsuta</i>	461	MDQEVINLSGGELQRVALLALCLGKPADLYLIDEPSAYLDSEQRIVASKVIKRFILHAKKT
<i>D. melanogaster</i>	463	MDQEVQNLSSGGELQRVAVLCLGKPADVYLIDEPSAYLDSEQRLVAAKVIKRYILHAKKT
<i>H. sapiens</i>	455	IDQEVQTLSSGGELQRVALLALCLGKPADVYLIDEPSAYLDSEQRLMAARVVKRFILHAKKT
<i>O. cuniculus</i>	455	IDQEVQTLSSGGELQRVALLALCLGKPADVYLIDEPSAYLDSEQRLMAARVVKRFILHAKKT
<i>D. rerio</i>	455	IDQDVQNLSSGGELQRVALLALCLGKPADVYLIDEPSAYLDSEQRLMAARVIKRFILHAKKT
consensus	481* *****.....*.....*.....*.....*.....*.....*.....*
<i>S. solfataricus</i>	513	TFIIDHDLSDHDYIADRIIVEKGEPEKAGLATSPTVTLKTMNEFLRELEVTFRRDAETGR
<i>P. furiosus</i>	507	ALVVEHDVLMIDYVSDRLMVEEGEPGKYGRALPPMGMRGMRNFLASIGITFRRDPDTGR
<i>C. elegans</i>	525	AFVVEHDFIMATYLADRVVVEEGQPSVKCTACKPQSLLEGMNRFLLKMLDITFRRDQETGR
<i>S. cerevisiae</i>	521	AFVVEHDFIMATYLADRVVVEEGIPSKNAHARAPESLLTGCNRFLLKMLNVTFRRDPNSFR
<i>O. sativa</i>	520	AFVVEHDFIMATYLADRVVVEGRPSIDCTANAPQSLVSGMKNFLSHLDITFRRDPINFR
<i>S. lycopersicum</i>	521	AFVVEHDFIMATYLADRVVVEEGTIPSIDCVANAPQSLLTGMNLFSLHLDITFRRDPINFR
<i>A. thaliana</i>	521	AFVVEHDFIMATYLADRVVVEEGQPSIDCTANCPQSLLSGMNLFSLHLDITFRRDPINFR
<i>C. hirsuta</i>	521	AFVVEHDFIMATYLADRVVVEEGQPSIDCTANCPQSLLSGMNLFSLHLDITFRRDPINFR
<i>D. melanogaster</i>	523	GFVVEHDFIMATYLADRVVVEEGQPSVKTTAFSPQSLLNGMNRFLELIGITFRRDPNFR
<i>H. sapiens</i>	515	AFVVEHDFIMATYLADRVVVEEGVPSKNTVANSPTQLLAGMKNFLSLEITFRRDPNFR
<i>O. cuniculus</i>	515	AFVVEHDFIMATYLADRVVVEEGVPSKNTVANSPTQLLAGMKNFLSLEITFRRDPNFR
<i>D. rerio</i>	515	AFVVEHDFIMATYLADRVVVEEGVPSRTTNANAPQTLLAGMKNFLAOLEITFRRDPNFR
consensus	541**.....*.....*.....*.....*.....*.....*.....*.....*.....*
<i>S. solfataricus</i>	573	PRVNKIGSYLDRVQKERGDYYSMVLSTQ-
<i>P. furiosus</i>	567	PRANKEGSKDREQEKCEYYYIA-----
<i>C. elegans</i>	585	PRINKLDSVKDVEQKSGOFFFLDDN----
<i>S. cerevisiae</i>	581	PRINKLDSOMKQKSSGNYFFLDNTGI-
<i>O. sativa</i>	580	PRINKLDSVKDREQKSAGSYYYLDD----
<i>S. lycopersicum</i>	581	PRINKLESTKDREQKSAGSYYYLDD----
<i>A. thaliana</i>	581	PRINKLESTKDREQKSAGSYYYLDD----
<i>C. hirsuta</i>	581	PRINKLESTKDREQKSAGSYYYLDD----
<i>D. melanogaster</i>	583	PRINKNNSVKDTEQKRSQOFFFLEDEACN
<i>H. sapiens</i>	575	PRINKLNSIKDVEQKSGNYFFLDD----
<i>O. cuniculus</i>	575	PRINKLNSIKDVEQKSGNYFFLDD----
<i>D. rerio</i>	575	PRINKLNSIKDVEQKSGNYFFLDD----
consensus	601	**...*...*...*...*...*...*.....*

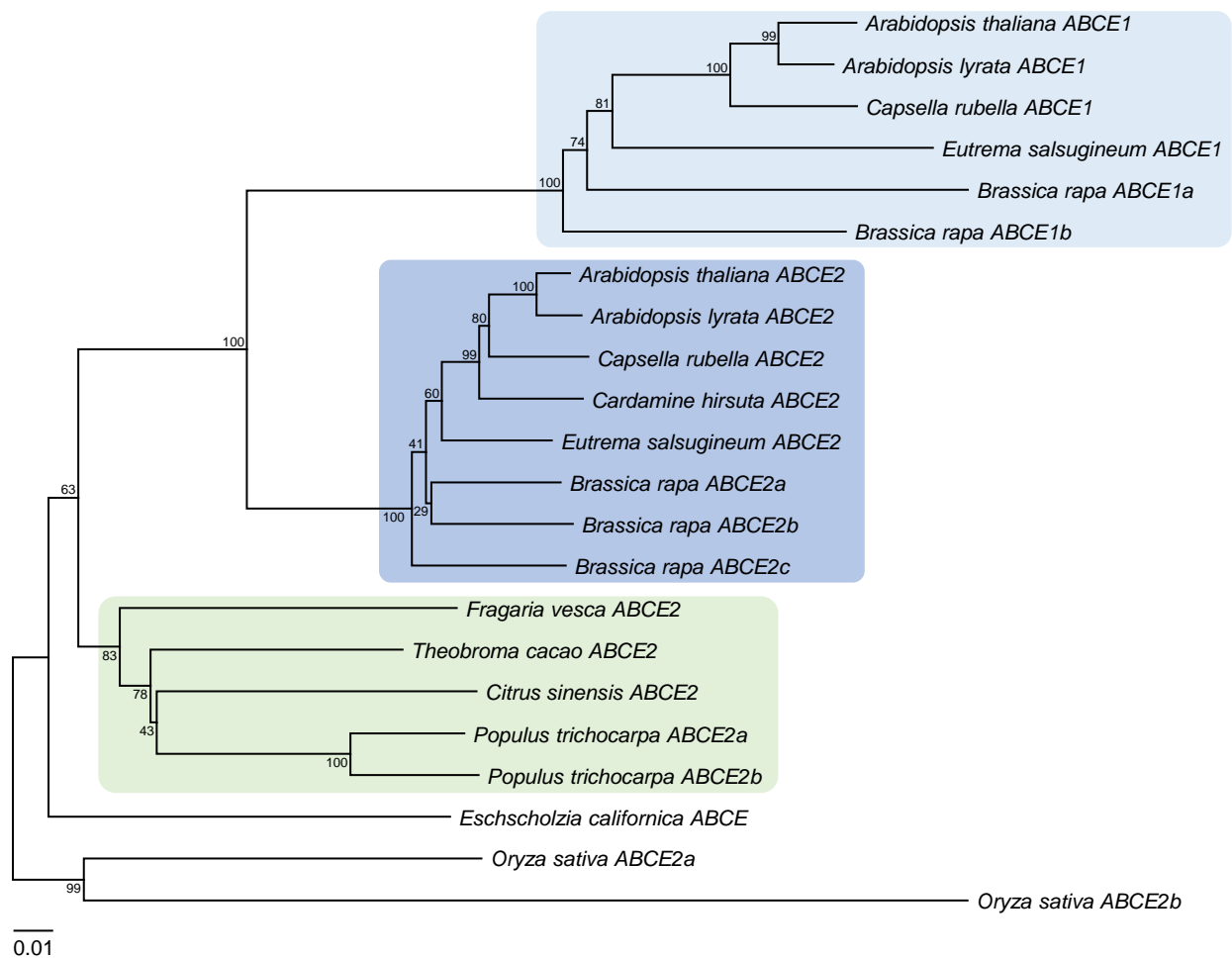
Supplementary Figure S4. Sequence conservation among ABCE orthologs.

Multiple sequence alignment of full-length ABCE proteins from the archaea *Saccharolobus solfataricus* (Q980K5) and *Pyrococcus furiosus* (I6V0C7), and the eukaryotes *Caenorhabditis elegans* (Q9U2K8), *Saccharomyces cerevisiae* (Q03195), *Oryza sativa* (A0A0P0Y344), *Solanum lycopersicum* (A0A3Q7H7H5), *Arabidopsis thaliana* (At4g19210), *Cardamine hirsuta* (L7VNS9), *Drosophila melanogaster* (Q9VSS1), *Homo sapiens* (P61221), *Oryctolagus cuniculus* (G1SG72), and *Danio rerio* (Q6TNW3). Full-length protein sequences were obtained from UniProt (<https://www.uniprot.org/>), except that of *Arabidopsis thaliana*, which was obtained from The Arabidopsis Information Resource (TAIR; <https://www.arabidopsis.org/>). The alignment was obtained with Clustal Omega 1.2.4 with default settings, and shaded with BOXSHADE with output format RTF_new. Identical and similar residues across at least eight out of the twelve sequences are shaded in black and gray, respectively. Asterisks and periods indicate identical and conserved residues, respectively. Numbers indicate residue positions. The conserved Pro138 residue, which is replaced by Ser in the *api7-1* mutant, is highlighted in red.



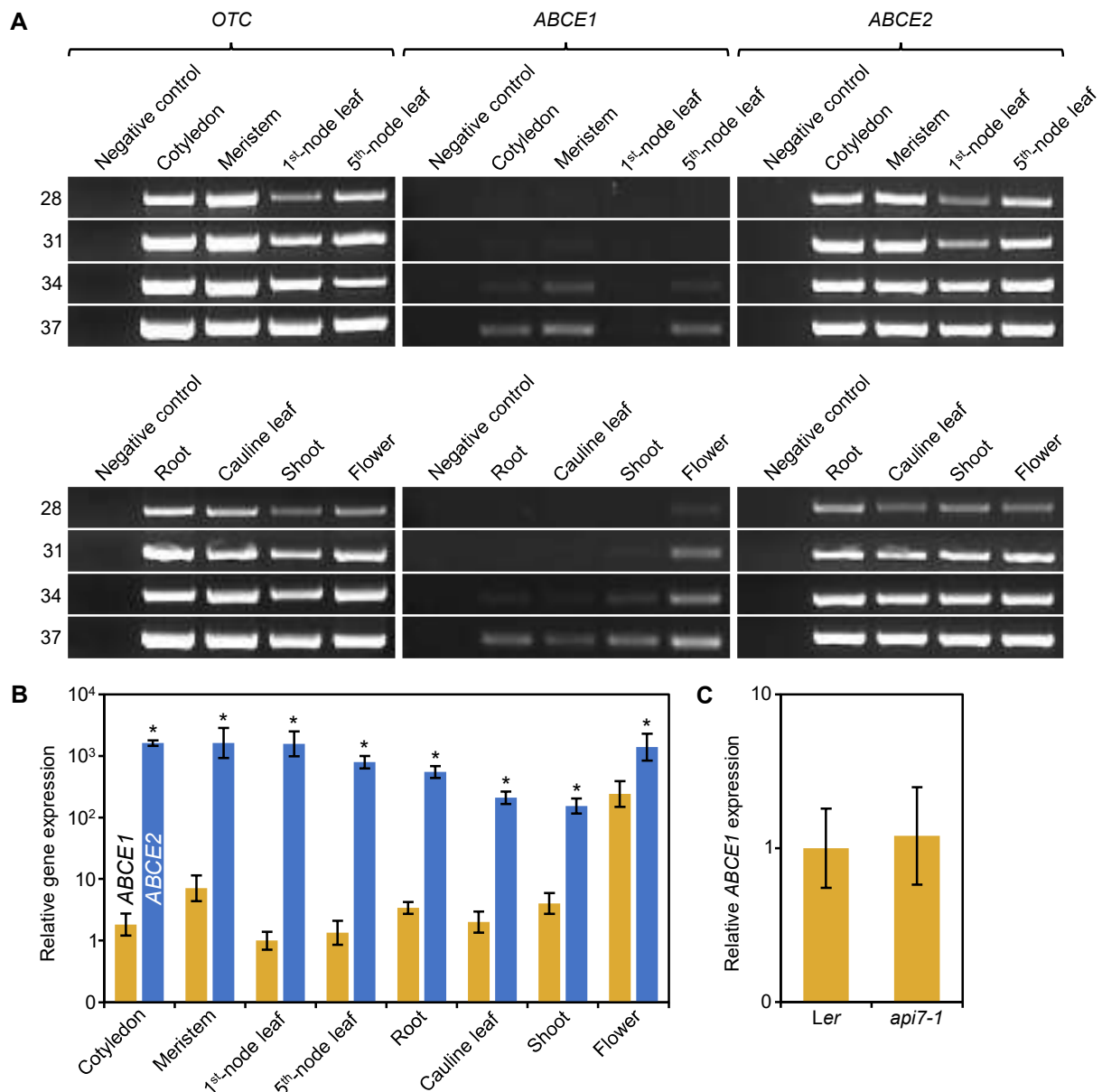
Supplementary Figure S5. *api7-2* is a lethal allele of *ABCE2*.

(A–E) Rosettes from (A) Ler, (B) *api7-1/api7-1*, (C) *api7-1/api7-2*, (D) *api7-2/api7-2* *ABCE2_{pro}:ABCE2*, and (E) Col-0 plants. (F, G) Dissected immature siliques from (F) Col-0 and (G) *ABCE2/api7-2* plants. Red arrowheads indicate aborted or unfertilized ovules. Pictures were taken (A–E) 16 and (F, G) 57 das. Scale bars indicate (A–E) 2 mm and (F, G) 500 μ m.



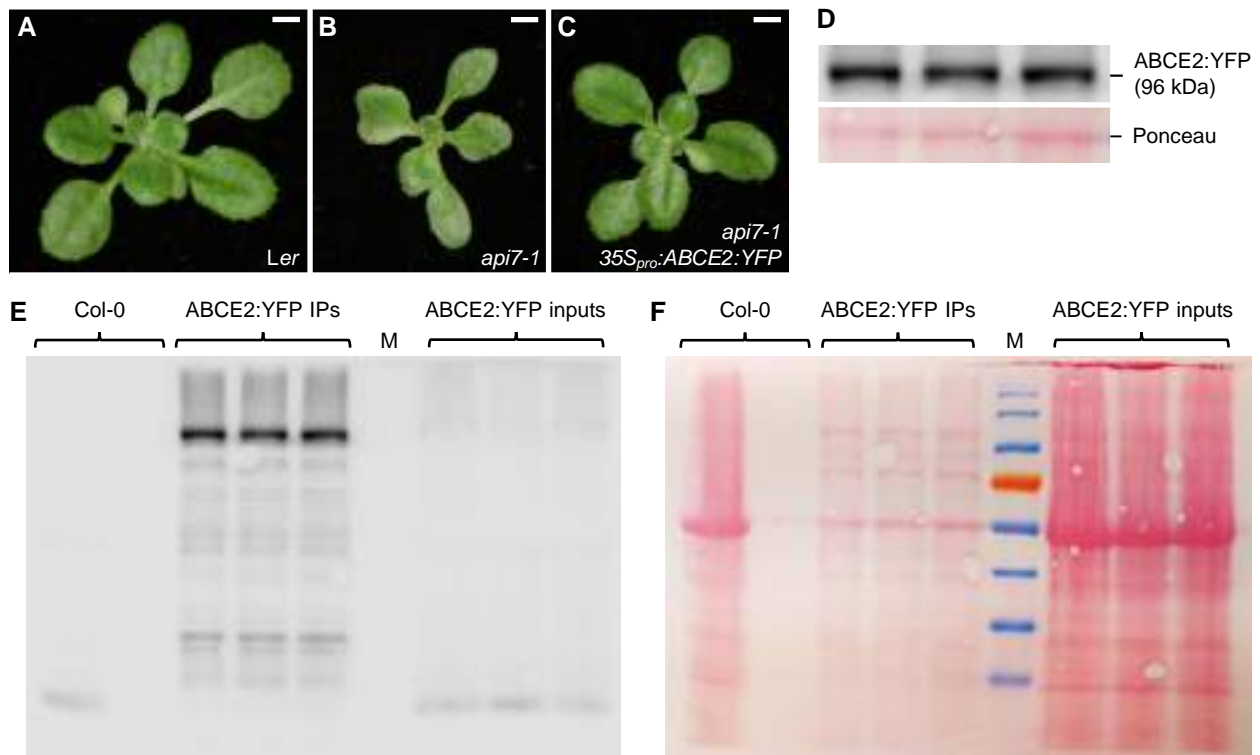
Supplementary Figure S6. Phylogenetic analysis of some plant ABCE genes.

Phylogenetic analysis of some Rosidae ABCE genes. Rectangles indicate Brassicaceae ABCE1 (clear blue), ABCE2 (dark blue), and other rosids ABCE2 (green) genes. *Eschscholzia californica* and *Oryza sativa* ABCE sequences were used as outgroups. Multiple ABCE1 or ABCE2 genes from *Brassica rapa*, *Populus trichocarpa*, and *Oryza sativa* are distinguished with arbitrarily given a, b, and c designations. Refer to Supplementary Table S2 to see the NCBI Nucleotide codes of the sequences used during the multiple sequence alignment. The phylogenetic tree was obtained using the Neighbor-Joining method. All positions containing gaps and missing data were eliminated (complete deletion option). The percentage of replicate trees in which the associated taxa clustered together in the bootstrap test (1000 replicates) are shown next to the branches. The tree was rooted on the midpoint. The scalebar indicates the evolutionary distance as the number of base substitutions per site, and was computed using the Tamura 3-parameter method.



Supplementary Figure S7. *ABCE1* and *ABCE2* expression analyses.

(A) Semiquantitative and (B) quantitative PCR analyses of *ABCE1* and *ABCE2* expression in Col-0 plants. (A) The domestic *OTC* gene was used as a control. Negative control samples had no template. The PCR products were visualized after 28, 31, 34, and 37 amplification cycles. (A, B) Samples were collected 7 (cotyledons), 14 (meristems, first- and fifth-node leaves, and roots), or 28 (cauline leaves, shoots, and flowers) das. (C) *ABCE1* expression in wild-type *Ler* and mutant *api7-1* first-node leaves. Samples were collected 14 das. (B, C) *ABCE1* expression levels in (B) first-node leaves and (C) *Ler* were used as the reference value. Error bars indicate the interval delimited by $2^{-(\Delta\Delta C_T \pm SD)}$, where SD is the standard deviation of the $\Delta\Delta C_T$ values. Note that the relative gene expression levels are in a logarithmic scale. (B) Asterisks indicate values significantly different between *ABCE1* and *ABCE2* in a Mann-Whitney *U* test ($*P < 0.001$). (B, C) Three different biological replicates were analyzed in triplicate.



Supplementary Figure S8. The $35S_{pro}:ABCE2:YFP$ transgene fully restores the wild-type phenotype in *api7-1* plants.

(A–C) Rosettes from (A) *Ler*, (B) *api7-1*, and (C) *api7-1 35S_{pro}:ABCE2:YFP* plants. Pictures were taken 16 das. Scale bars indicate 2 mm. (D) The ABCE2:YFP fusion protein was detected from three independent immunoprecipitates in a western blot probed against GFP. Immunoprecipitates were obtained by immunoprecipitation with anti-GFP magnetic beads of whole-protein extracts from *api7-1 35S_{pro}:ABCE2:YFP* plants collected 10 das. A band from the Ponceau staining of the membrane is shown as a loading control. (E, F) Full pictures of (E) the detection of ABCE2:YFP and (F) the membrane stained with Ponceau, from the whole-protein extracts previous to immunoprecipitation (inputs) and the immunoprecipitated samples (IPs). A protein extract from wild-type Col-0 seedlings was used as a control: input and immunoprecipitation were loaded in the left and right lanes, respectively. M: we used the EZ-Run Prestained Rec Protein Ladder (Thermo Fisher Scientific, Fisher BioReagents) molecular weight marker.

At4g19210 (ABCE2; 62%)

MADRLTRIAIVSSDRCKPKKCRQECKKSCPVVKTGKLCIEVTVGSKLAFISEELCIGCGICVKKCPFEAIQIINLPRDL
 EKDTTHRYGANTFKLHRLPVP RPQV LGLVGTNGIGKSTALKILAGKLPNLGRFTSPDPWQEILTHFRGSELQNYFTR
 ILEDNLKAIKPKQYVDHIPRAVKGNGVGEVLDQKDERDKKAEKADLELNQVIDRDVENLSGGELQRFIAIVVAIQNAEI
 YMFDEPSSYLDVKQRLKAAQVVRSLLRPNYSYIVVEHDLVLDYLSDFICCLYGRPGAYGVVTLPFVREGINIFLAGF
 VPTENLRFDESILTFKVAETPQESAEIISYARYKYPTMTKTQGNFRLRVSEGEFTDSQIIVMLGENGTGKTTFFIRMLA
 GLLKPPDDTEGPDREIPEFNVSYKPKQISPKFQNSVRHLLHQKIRDSYMHPQFMSDVMKPLQIEQLMDQEVVNLSSGGELQ
 RVALTLCLGKPADIYLIDEP SAYLDSEQRIVASKVIKRFILHAKKTAFVVEHDFIMATYLADRIVIVYEGQPSIDCTANC
 PQSLLSGMNLFLSHLNI TFRDPTNFRPRINKLES TKDREQKSAGSYYLDD

At3g13640 (ABCE1; 11%)

MSDRLTRIAIVSEDRCKPKKCRQECKKSCPVVKTGKLCIEVGSTSKSAFISEELCIGCGICVKKCPFEAIQIINLPKDL
 AKDTTHRYGANGFKLHRLPIPRPGQV LGLVGTNGIGKSTALKILAGKLPNLGRFNTPPDWEEILTHFRGSELQSYFIR
 VVEENLKTAIKPQHVDYIKEVVRGNLGMLEKLDERGLMEEICADMELNQLEREARQVSGGELQRFIAIAAVFVKKADI
 YMFDEPSSYLDVQRKAAQVIRSLLRHDSYIVVEHDLVLDYLSDFVCCLYGRPGAYGVVTLPFVREGINIFLAGF
 IPTENLRFDESILTFRVSETTQENDGEVKSARYKYPNMTKQLGDFKLEVMEGEFTDSQIIVMLGENGTGKTTFFIRMLA
 GAFPREEGVQSEIPEFNVSYKPKQNDKREKTRVQLLHDKIRDACAHQFMSDVIRPLQIEQLMDQVVKTLSSGGELQRF
 AITLCLGKPADIYLIDEP SAHL DSEQRITASKVIKRFILHAKKTAFIVEHDFIMATYLADRIVIVYEGQPAVKCIAHSPQ
 SLLSGMNLFLSHLNI TFRDPTNFRPRINKLES IKDKEQKTAGSYYLDD

At4g11420 (eIF3a; 32%)

MANFAKPENALKRADELINVQKQDALQALHDLITTSKRYRAWQKPLEKIMFKYLDLCVDLKRGRFAKDGLIQYRIVCQQ
 VNVSSLEEVIKHFLHLATDKAEQARSQADALEEALDVEDLEADRKPEDLQLSIVSGEKGDORSRELVTWFKFLWETY
 RTVLEILRNNKLEALYAMTAHKAQFQCKYKRTTEFRRLCEIRNHLANLNKYRDQRDRPDL SAPESLQLYLDRTRFDQ
 LKVATELGLWQEAFRSVEDIYGLMCMVKKTPKSSLLMVYYSKLTETEFWISSSHLYHAYAWFKLFLSQKNFNKNLSQKDL
 QLIASSVLAALSIPFDRAQSASHMELENEKERNLRMANLIGFNLEPKFEGKMLSR SALLSELVSKGVLSCASQEVK
 DLFHVLEHEFHPLDLGSKIQPLLEKISKSGGKLS SAPSLPEVQLSQYVPSLEK LATLRLLOQVSKIYQTIRESLSQLV
 PFFQFSEVEKISVDAVKNNFVAMKVDHMKGVVIFGNLGIESDGLRDHLAVFAESLSKVRAMLVPVPSKASKLAGVIPNL
 ADTVEKEHKRLLARKSII EK RKEDQERQQLEMEREEEQKRLKQLKLT EAEQKRLAELAEERKQRILREIEEKELEEA
 QALLEETEKRMMKGGKPPLLDGEKVTQSVKERALTEQLKERQEMEKKLQKLAKTMDYLERAKREEAAPLIEAAYQRRL
 VEEREFEYEREQQREVELSKERHESDLKEKNRSLRMLGNKEIFQAQVISRRQAEFDRIRTEREERISKIIREKKQERDIK
 RKQIYYLKIIEERIRKLQEEEEARKQEEAERLKKVEAERKANLDKAFKQRQREIELEEKSRREREELLRGTNAPPARL
 AEPVTPVGTTPAAAAAAGAPAAPYPVKWRQTTEVSGPSAPTSSETDRRSNRGPPPGDDHWGSNRGAAQNTDRWTS
 NRERSGPPAEGGDRWGS GPRGSDRRRSTFGSSRPRPTQR

At3g56150 (eIF3c; 14%)

MTSRFFTQVGSESEDES DYEVNEVQNDVNNRYLQSGSEDDDDTDTKRVVVKPAKDKRFEEMTYTVDQMKNAMKINDW
 VSLQENFDKVNKQLEKVMRITTEAVKPPPLYIKTLVMLEDFLNEALANKEAKKMSSTNSKALNSMKQKLNKNNLYEDD
 INKYREAPEVEEEKQPEDDDDDDDDEVEDDDSSIDGPTVDPGSDVDEPTDNLTWEKMLSKDKLLEKLMNKDPKEI
 TWDVWNKKFKEI VAARGKKG TARFELVDQLTHLTKIAKTPAQKLEILFSVISAQFDVNPGLSGHMPINWKKCVLNLMT
 IILDILVKYSNIVDDTVEPDENETSKPTDYDGKIRVWGNLVAFLERVDTEFFKSLQCIDPH TREYVERLRDEPMLALA
 QNIQDYFERMGDFKAAAKVALRRVEAIYKPKQEVYDAMRKLAE LVEEEEEETEEAKEESGPPTS FIVVPEVVPKPTFPE
 SSRAMMDILVSLIYRNGDERTKARAMLCDINH HALMDNFVTARDLLLSHLQDNIQHMDISTQILFNRITMAQLGLCAFR
 AGMITESHSCLS ELYSGQRVRELLAQVQSRYHEKTPEQERMERRRQMPYHMLNLELLEAVHLICAMLLEVPNMAAN
 SHDAKRRI VSKNFRLLLEISERQAFTAPPENVRDHVMAATRALT KGDFQKAFEV LNSLEVWRLLKNRDSILDMVKDRIK
 EEALRTYLFYSSSYESLSLDQLAKMFDVSEPQVHSIVSKMINEELHASWDQPTRCIVFHVEVQHSRLQSLAFQLTEKIL
 SILAESNERAMESRTGGGGLDLSSRRRDNNQDYAGAASGGGGYWDKANYGQGRQGNRSYGGGRRSSGQNGQWSGQNRG
 GGYAGR VSGNRGMQMDGSSRMVSLNRGVRT

At3g57290 (eIF3e; 40%)

MEESKQNYDLTPLIAPNDRHLVFPIFEFLQERQLYPDEQILKSKIQLLNQTNMVDYAMDIHKSLYHTEDAPQEMVERR
 TEVVARLKSLLEAAAPLVSFLLNPNVQELRADKQYNLQMLKERYQIGPDQIEALYQYAKFQFECGNYSGAADYLYQYR
 T LCSNLERSL SALWGK LASEILMQNWDIALEELNRLKEIIDSKSFSSPLNQVQNR IWL MHWGLYIFFNHDNGR TQIIDL
 FNQDKYLNAIQTSAPHLRLRYLATAFIVNKRRRPQLKEFIKVIQQEHYSYKDP IIEFLACVFVNYDFDGAQKMKKECEEV
 IVNDPFLGKRVEDGNFSTVPLRDEFELENARLFVFETYCKIHQRIDMGVLAEKLNLNVEEAERWIVNLI RTSKLD AKIDS
 ESGTVIMEPTQPNVHEQLINHTKGLSGRTYKLVNQLEHTQAQATR

At1g64790 (ILA; 4%)

MSYSMVNASSAVSSPETAKNSDEPPPISSEAVNVLFPSVDPNSKLFNRNSLNITISREAPPLTTSRIDFLSLFIFCKLTH
 WLSLNPSSHRDEEEEEASPFYFFTIVLTYQPGPGQSPWKEMASPLESLLSISGSVSTSSSTLIRLRIFRHDIP EILQNSD
 MTSDIAPVIVDMIFQTLAIYDDRASRKAVDDLIVKGLGNVTFMKTFAAMLVQVMEKQLKFCFDTVCYRLLIWSCLLLEK
 SQFATVSKNAFVRVASTQASLLRIMESSFRMRACKRFMFHLSQSQAISLYMDEVKGSRIPIYKDSPELLGLLLEFS
 CSSPALFEQSKAIFVDIYVKDVLNSREKQKPNLSNCFKPLLQRLSHEEFQTVILPAAVKMLKRNPEIVLESVGFLLANV
 NIDL SKYAL ELLPVL PQA RHTDEDRRLGALSVMVCLSEKSSNPDTI EAMFASVKAIIGGSEGRLOSPHQRI GMLNAVQ
 ELASAP EGYIGSLSR TICSF LIACYKDEGNEDVKLSILSAVASWASRSSVAIQPNLVSFIAAGLKEKEALRRGHLCV
 RIIICRNPD TISQISD LLSPLIQLVK TGF TKAVQR LDGIYALLIVSKIAACDIKAEDTMVKEKLTWLTISQNEPSLVQITL
 ASKLSDDCVVCVDLLEVLVVEHSSRVLEAFSLKSLSQLLLFLLCHPSWNVKRKTAYNSVTKIFLATSQLATTLLEDFSD
 FLSITGDQIVSSRTSDADNPADHQAPFVPSVEVLVKALIVISSAAVAGPPSSWIVRAIFCSHPSIVGTGKRDAVWKRL
 QKCLKTCGFDVATFLSTNGESVCKSLLGPMGLTSAKTP EQQA AVYSLSTMMSLAPEDTFTVFKMHLQDLPDRLSHDMLS
 ETDIKIFHTPEGMLLSEQGVYAQTIGAKYTKQEPSSNHS LKGLASRETANSGRRD TAKLTKKADKGKTAKEEARELM
 LKEEASTRENVHRIQKSLSLVLHALGEMGLANPVFCHSQLPFLATFLDPLLRSPIVSAAAFENLVKLARCTVQPLCNWA
 LEISTALRLIAIDEVDTSFDFRPSVDKAGKTYEGLFERIVNGLSISCKSGPLPVDTFIFPVLYHVLGVVPAYQASVG
 PALNELCGLQADDVANALYGVYSKDVHVRACLNAVKCI PAVSKCSLPQNVKIATNIWIALHDPEK SVAESADDLWAR
 YGHDLGTDYSGIFKALSHINLNVRLAAAALADALHESPSSIQLSLSLTFSLYIRDATSGEDVFDAGWIGRQGI ALALQ
 SAADVLTTKDLPAVMTFLISRALADPN TDVR GKMINAGIMI IDKHGKENVSLFP IFENYLNKEASDEEEYDLVREGVV
 IFTGALAKHLARDDPKVHNVVEKLEVLNTPSES VQRAVSTCLSPLVLSK QEEAPALFLRLLDKLMKSDKYGERRGA AF
 GLAGVVMGFGISSLKKYGLIVTLQEALIDRNSAKRREGALLAFECLCEKLGKLFEPYVIKMLPLLLVSFSDQVGAVREA
 AECAARAMMSQLSAYGVKLVLP SLLK GLEDKAWRTKQSSVQLLGAMAFCAPQQLSQCLPRVVPKLTVEFKTIQVLT DTH
 PKVQSAGQALAQVGSVIKNPEISSLVPTLLLAL TDPNEYTRHALDTLLQTT FVNSVDAPSLALLVPIVHRGLRERSSE
 TKKKASQIVGNMCSLVTEPKDMIPYIGLLLPEVKVLDVPIPEVRSVAAR AVGSLIRGMGEDNFPDLVPWLFETLKS DT
 SNVERYGAAQGLSEVIAALGTDYFENILPDLIRHCSHQKASVRDGYLTLFKFLPRSLGAQFQKYLQVLVPAILDGLADE
 NESVRDAALGAGHVLVEHHATTSLPLLLPAVEDGIFNDNWRIRQSSVELLGDLLFKVAGTSGKALLEGGS DDEGASTE A
 QGRAIIDILGMDKRNEVLAALYMVRTDVSLSVRQAALH VWKTIIVANTPK TLKEIMPILMSTLISSLASPSSERRQVAGR
 SLGELVRKLGGERVLP LIPILSK GLKDPDVKRQGVCI GLNEVMASAGRSQLLS FMDQLIPTIRTALCDSALEVRESAG
 LAFSTLYKSAGLQAMDEIIP TLLEALEDDEMSTTALDGLKQIISVRTAAVLP HILPKLVHLP LSALNAHALGALAEVAG
 AGFNTHLGTILPALLS AMGGENKEVQELAQEAAERVVLVIDEEGVETLLSELKGVSDSQASIRRSSAYLIGYFFKSSK
 LYLIDEAPNMISTLIVMLS DSDSTTVAVSWEALARVIGSVPEKVLPSYIKLVRDAVSTARDKERRKRKGGYVVIPGLCL
 PKSLKPLLPVFLQGLISGSAELREQA AIGL GELIEVTSEQALKEFVIPITGPLIRIIGDRFPWQVKSAILATLIILIQR
 GGMALKPFLPQLQTT FVKCLQDSTR TIRSSAAVALGKLSALSTRIDPLVGDLMTSFQAADSGVREAILSAMRGVIKHAG
 KSIGPAVRVRIFDLLKDLMHEDDQVRI SATSMLGVL SQYLEAAQLSVLLQEVNDLSASQNWGARHGSVLCISSLLKHN
 PSTIMTSSLSFSSMLNSLKS SLKDEKFP LRESSTKALGRLLKQLATDP SNTKVVIDVLS SIVSALHDDSSEVRRRALSS
 LKAFADNP SATMANISVIGPPLAECLKDGNTPVRLAAERCALHVFQLTKGAENVQAAQKYITGLDARRLSKFPEQSDD
 SESDDDNVSG

At2g44060 (LEA26; 23%)

MSTSEDKPEIISR VVHQEGDVEIVDRSQKDKDEEKEEGKGGFLDKVKDFIHDIGEKELEGTIGFGKPTADVSAIHIPKIN
 LERADIVVDVLVKNPNPVP IPLIDVNYLVESDGRKLV SGLIPDAGTLKAHGEETVKIPLTLIYDDIKSTYNDINPGMII
 PYRIKVDLIVDVPVLGR LTLPLEKCGEIPPKKPDVDIEKIKFQKFSLEETVAILHVR LQNMNDFDLGLNLDLDCVWLC
 DVSIGKAEIADSIKLDKNGSGLINVPMTFRPKDFGSALWDMIRGKGTGYTIKGNIDVDT PFGAMKLP IIEGGETRLKK
 EDDDDDEE

At4g20980 (eIF3d; 13%)

MVTEAFEFVAVPFNSDVGWPPDASDVSSSASPTSVAAANLLPNVPFASFSSRSDKLGRVADWTRNLSNPSARPNTGSKSD
 PSAVFDFAFAIDEGFGLASSGGNPDEDAAFRLVDGKPPPRPKFGPKWRFNPHHNRNQLPQRRDEEVEAKKRDAEKERA
 RRDRLYNNRNNIHHQRREAAAFKSSVDIQPEWNMLEQIPFSTFSKLSYTVQEPEDLLLCCGGLEYNRLFDRITPKNER
 RLERFKNRNFFKVTTSDDPVIRRLAKEDKATVFATDAILAALMCAPRSVYSWDIVIQRVGNKLFDFDKRDGSQLDLLSVH
 ETSQEPLPEKDDINSAHSLGVEAAAYINQNFSSQVLRDGGKETFDEANPFANEGEREIASVAYRYRRWKLDDNMHLVAR
 CELQSVADLNNQRSEFLTLNALNEFDPKYSGVDWRQKLETQRGAVLATELKNNGNKLAKWTAQALLANADMMKIGFVSRV
 HPRDHFHNVILSVLGYKPKDFAGQINLNTSNMWGIVKSIVDLCMKLSEGRVVLVKDPSKPQVRIYEVPPDAFENDYVEE
 PLPEDEQVQPTTEENTEGAEASVAATKETEKKADDAQA

At5g44320 (eIF3d; 9%)

MVFEAFEVGTVPFNSDVGWPPDASDTSSTSVAAANLLPNVPFASFSSRSEKLRVADWTRALSNSARPHTGSKSDPSAI
 FDFSAFAVDEGFGLTNSGGNADEDAAFRLVDGKPPPRPKFGPKWRFNQYHNRNQLPQRRDEEVEAKKREAEKDRARRDR
 LYNNRNNIHHQRREAAAFKSSVDIQPEWNMLEQIPFSTFSKLSFTVSEPEDLLLCCGGLESYDRSFDRIITPKADRRLER
 FKNRSFKVTTSDDLVIRRLAKEDKATVFATDAILAALMCAPRSVYSWDLVIQRVGNKLFDFDKRDGSQLDLLSVHETSQE
 PLPEGKDDINSAHSLGLEAAAYINQNFQAQVVLKNGKRETFDEPIPNEGEENASIA YRYRRWKLDDSMYLVARCELQS
 TVDLNNQRSEFLTLNALNEFDPKYSGVDWRQKLETQRGAVLANELKNNGNKLAKWTAQALLANADMMKIGFVSRVHPRDH
 FNVILSVLGYKPKDFAGQINLNTSNMWGIVKSIVDLCMKLSEGRVVLVKDPSKPQVRIYEVPPDAFNDYVEEPLPED
 EQVQPPEENTDAGAETNGVSSSTNVAVEDKKSEVEA

At5g17020 (XPO1A; 6%)

MAAEKLRDLSQPIDVGVLDATVAFAFFVTGSKEERAAADQILRDLQANPDMWLQVVHILQNTNSLDTKFFALQVLEGVIK
 YRWNALPVEQRDGMKNYISEVIVQLSSNEASFRSERLYVNKLNVILVQIVKHDWPAKWTSFIPDLVAAAKTSETICENC
 MAILKLLSEEVDFDFSRGEMTQQKIKELKQSLNSEFKLIHELCLYVLSASQRQDLIRATLSALHAYLSWIPLGYIFESTL
 LETLLKFFFPAYRNLTIQCLTEVAALNFGDFYNVQYVKMYTIFIGQLRIILPPSTKIPEAYSSSGSGEEQAFIQNLALF
 FTSFFKLFHIRVLESTPEVVSLLLAGLEYLINISYVDDTEVFKVCLDYWNSLVLELFDHNSNDNPAVSASLMGLQPFPLP
 GMVDGLGSQVMQRRQLYSHPMKLRGLMINRMAKPEEVLIVEDENGNIVRETMKDNDVLVQYKIMRETLIYLSHLHDHDD
 TEKQMLRKLKQLSGEEWAWNNLNTLCWAIGSISGSMADQENRFLVMVIRDLLNLCEITKGKDNKAVIASNIMYVVGQ
 YPRFLRAHWKFLKTVVNLKLFEFMHETHPGVQDMACDTFLKIVQKCKRKFVIVQVGENEPFVSELLTGLATTVDLEPHQ
 IHSFYESVGNMIIQAESDPQKRDEYLQRLMALPNQKWAEIIGQARHSVEFLKQVVRTVLNLTNTSAATSLGTYFLS
 QISLIFLDMLNVYRMYSELVSTNITEGGPYASKTSFVKLLRSVKRETLKLIETFLDKAEDQPHIGKQFVPPMMESVLGD
 YARNVPDARESEVLSLFATLINKYKATMLDDVPHIFEAVFQCTLEMITKNFEDYPEHRLKFFSLLRAIATFCFPALIKL
 SSPQLKLVMSI IWAFRHTERNIAETGLNLLLEMLKNFQQSEFCNQFYRSYFMQIEQEIFAVLTDTFHKPGFKLHVVLV
 QQLFCLPESGALTEPLWDATTVPYPYDPNVAFVREYTIKLLSSSFPNMTAAEVTQFVNGLYESRNDPSGFKNNIRDFLV
 QSKEFSAQDNKDLYAEAAAAQRERERQRMLSIPGLIAPNEIQDEMVD

At3g03110 (XPO1B; 2%)

MAAEKLRDLSQPIDVLLDATVEAFYSTGSKEERASADNLRDLKANPDTWLQVVHILQNTSSHTTKFFALQVLEGVIK
 YRWNALPVEQRDGMKNYISDVIVQLSRDEASFRTERLYVNKLNIILVQIVKQEWPAKWKSFIPDLVIAAKTSETICENC
 MAILKLLSEEVDFDFSKGEMTQQKIKELKQSLNSEFQLIHELCLYVLSASQRQELIRATLSALHAYLSWIPLGYIFESPL
 LEILLKFFFPAYRNLTQCLSEVASLNFGDFYDMQYVKMYSIFMNQLQAAILPLNLIPEAYSTGSSEEQAFIQNLALF
 FTSFFKLFHIKILESAPENISLLLAGLGYLISISYVDDTEVFKVCLDYWNSLVLELFGTRHHACHPALTPSLFGLQMAFL
 PSTVDGVKSEVTERQKLYSDPMSKLRGLMISRTAKPEEVLIVEDENGNIVRETMKDNDVLVQYKIMRETLIYLSHLHDE
 DTEKQMLSKLSKQLSGEEWAWNNLNTLCWAIGSISGSMVVEQENRFLVMVIRDLLSLCEVVKGKDNKAVIASNIMYVVG
 QYSRFLRAHWKFLKTVVHKLFEFMHETHPGVQDMACDTFLKIVQKCKRKFVIVQVGESEPFVSELLSGLATIVDGLQPH
 QIHTFYESVGSMIQAESDPQKRGEYLQRLMALPNQKWAEIIGQARQSADILKEPDVIRTVLNLTNTNTRVATSLGTFFL
 SQISLIFLDMLNVYRMYSELVSSSIANGGPYASRTSLVKLLRSVKREILKLIETFLDKAENQPHIGKQFVPPMMDQVLG
 DYARNVPDARESEVLSLFATLINKYKVMRDEVPLIFEAVFQCTLEMITKNFEDYPEHRLKFFSLLRAIATFCFRALIQ
 LSSEQLKLVMSI IWAFRHTERNIAETGLNLLLEMLKNFQKSDFCNKFYQTYFLQIEQEVFAVLTDTFHKPGFKLHVVLV
 LQHLFSLVESGSLAEPLWDAATVPHYPYNNVAVFLEYTTKLLSSSFPNMTTTEVTQFVNGLYESRNDVGRFKDNIRDFL
 IQSKEFSAQDNKDLYAEAAAAQMERERQRMLSIPGLIAPSEIQDDMADS

At1g61580 (RPL3B; 12%)

MSHRKFHPRHGSGLGFLPRKASRHRGKVKAFPKDDPTKPCRLTSFLGYKAGMTHIVRDVEKPGSKLHKKETCEAVTII
ETPPMVVVGVVGYVKTTPRGLRSLCTVWAQHLSEELRRRFYKNWAKSKKAFTRYSKKHETEKGKDIQSQLEKMKKYCS
VIRVLAHTQIRKMKGLKQKKAHLNEIQINGGDIKVDYACSLFEKQVPVDAIFQKDEMIDIIGVTKGKGYEGVVTRWG
VTRLPRKTHRGLRKKVACIGAWHPARVSYTVARAGQNGYHHRTEMNKKVYRVGKVGQETHSAMTEYDRTEKDITPMGGFP
HYGIVKEDYLMIKGCCVGPKKRVVTLRQTLKQTSRLAMEEIKLKFIDAASNGGHGRFQTSQEKAKFYGRITKA

At4g38740 (ROC1; 38%)

MAFPKVYFDMTIDGQPAGRIVMELYTDKTPRTAENFRALCTGEKGVGGTGKPLHFKGSKFHRVIPNFMCGGDFTAGNG
TGGESIYSGKFEDEFERKHTGPGILSMANAGANTNGSQFFICTVKTWDLDGKHVVFGQVVEGLDVVKAIEKVGSSSGK
PTKPVVADCGQLS

At3g13460 (ECT2; 11%)

MATVAPPADQATDLLQKLSLSDSPAKASEIPEPNKKTAVYQYGGVDVHGQVPSYDRSLTPMLPSDAADPSVCYVPNPYNP
YQYYNVYVSGQEWTDYPAYTNPEGVDMNSGIYGENGTVVYPQGYGYAAYPSPATSPAPQLGGEGQLYGAQQYQYPNYF
PNSGPYASSVATPTQPDLSANKPAGVKTLPADSNVVASAAGITKGSNGSAPVKPTNQATLNTSSNLYGMGAPGGGLAAG
YQDPRYAYEGYYAPVPHDGSKYSDVQRVPSGSGVASSYSKSSVTPSSRNQYRSNSHYTSVHQPSVVTGYGTAQGYN
RMYQNKLYGQYGSTGRSALGYGSSCYDSRTNNGRWAATDNKYRSWGRGNSYYYGNENNVDGLNELNRGPRAKGTKNQK
NLDDSLVKEEQTGESNVTEVGEADNTCVVPDREQYNKEDFPVDYANAMFFIIKSYSEDDVHKS IKYNVWASTPNGNKKL
AAAYQEAQQKAGGCPIFLFFSVNASGQFVGLAEMTGPVDFNTNVEYWQDKWTGFSFPLKWHIVKDVPSNLLKHITLLENN
ENKPVNTSRDTQEVKLEQGLKIVKIFKEHSSKTCILDDFSFYEVQRKTI LEKKAKQTQKQVSEKVTDEKESATAESA
SKESPAAVQTSDDVKVAENGSVAKPVTGDVVANGC

At4g33250 (eIF3k; 23%)

MGVEIQSPQEQQSSYTVQLVALNPFNPEILPDLENYVNVTSQYTSLEVNLCLLRLYQFEPERMNTHIVARILVKALMAM
PTPDFSLCLFLIPERVQMEEQFKSLIVLSHYLETGRFQQFWDEAAKNRHILEAVPGFEQAIQAYASHLLSLSYQKVPRS
VLAEAVNMDGASLDKFI EQQVTNSGWIVEKEGGSI VLPQNEFNHPELKKNTGENVPLEHIARIFPILG

At1g76810 (eIF5B; 4%)

MGRKKPSARGGDAEQPPASSLVGATSKKKKGAQIDDDDEYSIGTELSEESKVEEEKVVVITGKKKGGKGNKKGTTQDDDD
DDFSDKVSAAAGVKDDVPEIAFVGKKKSKGKGGGVSFALLDDEDEKEDNESDGDKDDEPVISFTGKKHASKKGGKGN
SFAASAFDALGSDDDDDTEEVHEDEEEESPITFSGKKKSSKSSKNTNSFTADLLDEEETDASNSRDDENTIEDEESP
EVTFSGKKKSSKGGGSLASVGDSDVADETKTSDTKNVEVVETGKSKKKKNNKSGRTVQEEEDLDKLLAALGETPAA
ERPASSTPVEEKAAQPEPVAPVENAGEKEGEEETAAKSKKKKKEKEKKAATASSVEVKEEKQESVTEPLQP
KKKDAKGKAAEKIPKHVREMQEALARRQEAERKKKEEEEKLRKEEEERRRQEELEAQAEAKRKRKEKEKLLRKK
LEGKLLTAKQKTEAQKREAFKNQLLAAGGLPVADNDGATSSKRPYANKKSSRQKIDTQVGEDEVEPKENQADE
QDTLGEVGLTDTGKVDLIELVNTDENS GPADVAQENGVEEDEDEWDASWGTVDLNLKGFDFDEEEEAQPVVKELK
DAISKAHDSEPEAEKPTAKPAGTGKPLIAAVKATPEVEDATRTKRATRAKDASKKGLAPSESIEGEENLRSPICCIM
GHVDTGKTKLLDCIRGTNVQEGEAGGITQQIGATYFPAENIRERTKELKADAKLKVGLLVIDTPGHESFTNLRSGSS
LCDLAILVVDIMHGLEPQTIESLNLRLMRNTEFIVALNKVDRLYGWTCKNAPIVKAMKQONKDVINEFNLRKNIINE
FQEQLNTELYYKNKDMGDTFSIVPTSAISGEGVPDLLLLWLQWAQKTMVEKLYVDEVQCTVLEVKVI EGHGTTIDVV
LVNGELHEGDQIVVCGLQGPVTTIRALLTPHPMKELRVKGYLHYKEIKAAQGIKITAQGLEHAIAGTALHVGPDDD
IEAIKESAMEDMESVLSRIDKSGEGVYVQASTLGSLEALLEYLKSPAVKIPVSGIGIGPVHKKDVMKAGVMLERKKEYA
TILAFDVKVTTEARELADEMGVKIFCADIYHFLDFLKAYIENIKEKKKESADEAVFPCVLQILPNCVFNKCDPIVLG
VDVIEGILKIGTPICVPGREFIDIGRIASIENNHKPVYAKKGNKVAIKIVGSNAEEQKMFGRHFDEDELVSHISRRS
IDILKSNYRDELSLEEWKLVVKKLKNIFKIQ

At3g53610 (RAB8; 18%)

MAAPPARARADYDYLIKLLLLIGDSGVGKSCLLLRFSGDSFTTSFITIGIDFKIRTIELDGKRIKLIQIWDTAGQERFRT
ITTAYYRGAMGILLVYDVTDSSFNIRNWIRNIEQHASDSVNIKLVGNKADMDESKRAVPKSKGQALADEYGMKFFET
SAKTNLNVEEVFFSIAKDIKQRLADTDARAEPQTIKINQSDQGAGTSQATQKSACCGT

At5g37475 (eIF3j; 16%)

MDDWEAEDFQPLPSKVELKSNWDDDEDVDENDIKDSWEEEDVSAPPPIVKPASEKAPKKPAVKAVEKKVKTVEAPKGTSR
 EEPLDPIAEKLRMORLVEEADYQSTAEELFGVKTEEKSVDMILPKSESDFLDYAELISQRLVPFEKSFHYIGLLKAVMRL
 SVANMKAADVKKDVASSITATAANEKLLKAEKEAAAAGKKKSGKKKQLHVDKPDDDLVSQPYDAMDDDDDFM

At3g43600 (AAO2; 3%)

MSLVFAINGQRFELELSSVDPSTTLLEFLRYQTSFKSVKLSCEGEGCGACVVLLSKFDPVLQKVEDFTVSSCLTLLCSV
 NHCNITTSEGLGNSRDGFHP IHKRLSGFHASQCGFCTPGMSVSLFSALLDADKSQYSDLTVVEAEKAVSGNLCRCCTGYR
 PIVDACKSFASDVIDIEDLGLNSFCRKGDKDSSSLTRFDSEKRICTFPEFLKDEIKSVDSGMYRWCS PASVEELSSLEA
 CKANSNTVSMKLVAGNTSMGYKDEREQNYDKYIDITRIPHLKEIRENQNGVEIGSVVTISKVIAALKEIRVSPGVEKI
 FGKLATHMEMIAARFIRNFGSIGGNLVAQRKQFPSPDMATILLAAGAFVNIMSSSRGLEKLTLEEFFLERSPLEAHDVLV
 SIEIPFWHSETNSELFFETYRAAPRPHGSALAYLNAFLAEVKDTMVVNCRLAFGAYGTKHAIRCKEIEEFLSGKVIDT
 KVLVEAITLLGNVVVPEDGTSNPAYRSSLAPGFLFKFLHTLMTHTTDPKPSNGYHLDPPKPLPMLSSQNVPINNEYNP
 VGQPVTKVGASLQASGEAVYVDDIPSPTNCLYGAFIYSKPPFARIKGIHFKDDLVP TGVVAVISRKDVPKGGKNIGMKI
 GLGSDQLFAEDFTTSVGECIAFVVADTQRHADA AVNLA VVEYETEDLEPPILSVEDAVKKSSLFDIIPFLYPOQVGDTS
 KGM AEADHQILSSEIRLGSQYVFYMETQTALAVGDEDCIVVYSSTQTPQYVQSSVAACLGIPENNIRVITRRVGGGFG
 GKS VKSMPVATACALAAKKLQRPVRTYVNRKTD MIMTGGRHPMKITYSVGFKSTGKITALELEILIDAGASYGFSMFIP
 SNLIGSLKKNW GALSFDIKLCKTNLLSRAIMRSPGDVQGT YIAEAIENIASSLSLEVD TIRKINLH THE SLALFYKD
 GAGEPHEYTLSSMWDKVGVS SKFEERSVSVREFNESNMWRKRGISRVPIIYEVLLLFATPGRVSVLSDGTIVVEIGGIEL
 GQGLWTKVKQMTSYALGMLQCDGTEELLEKIRVIQSDLSMVQGNFTGGSTTSEGSCAAVRLCCE TLVERL KPLMERSD
 GPITWNELISQAYAQSVNLSASDLYTPKDTMPQYLYNGTAVSEVEVDLVTGQTTVLQTDILYDCGKSLNPAVDLGQIEG
 SFVQGLGFFMLEEYIEDPEGLLLTDSTWYKIP TVDTIPKQFNVEILNGGCHEKRVLSSKASGEP LLLAASVHCATRO
 AVKEARKQLCMWKGENGSSGS AFQLPVPATMPVVKELCGLDIIESYLEWKLHDNSNL

At1g65860 (FMO GS-OX1; 4%)

MAPTQNTICSKHVAVIGAGAAGLVTARELRREGHTVVVFDREKQVGLWNYSSKADSDPLSLDTTRTIVHTSIYESLRT
 NLPRECMGFTDFPFVPRIHDIRDSRRYP SHREVLAYLQDFAREFKIEEMVRFETEVVCVEPVNGKWSVRSKNSVGF AA
 HEIFDAVVVCSGHFTEPNVAHIPGIKSWPGKQI HSHNYRVPGPFNNEVVVIGNYASGADISRDIAKVAKEVHIASRAS
 ESDTYQKLPVPQNNLWVHSEIDFAHQDGSILFKNGKVYADTIVHCTGYKYFFP FLETNGYININENRVEPLYKHVFLP
 ALAPSLSF IGLPGMAIQFVMFEIQSKWVA AVL SGRVILPSQDKMEDIIEWYATLDVLGIPKRHTHKLGKISCEYLNWI
 AEECHCSPVENWRIQEVERGFQRMVSHPEIYRDEWDDDDLMEEA YKDFARKKLIS SHPSYFLES

At2g20830 (Folic acid binding / transferase; 8%)

MSSGLNEDFLDCIVRLLEETHVQQGFDEGYEEGLVSGREDARHLGLKLGFTGELIGFYRGCSALWNSALRIDPTRFSPQ
 LHKHLNDFHVLLDKIPLLDPEDEAKDG IKDDL RVKFSI ICASLGF SKKQFEWSEEMLEMLGCKVYISEARNKTALEA
 IERALKPFP PAAIVNKFEDAAYGRVGYTVVSSLANGSSSLKNAVFAMVK TALDTINLELHCGSHPR LGVVDHICFHPL
 SQT SIEQVSSVANSLAMDIGSILRVPTYLYGAAEKEQCTLDSIRKLG YFKANREGHEWAGGF DLEMVPLKPDAGPQEV
 SKAKGVVAVGACGWVSNYNVPVMSNDL KAVRRIARKT SERGGGLASVQTMALVHGEGVIEVACNLLNPSQVGGDEVQGL
 IERLGREEGLLVGKGYTDTYTPDQIVERYMDLLNS

At5g58410 (HEAT/U-box domain-containing protein; 1%)

MGKPKGDAARSKARPSSSSLAASLLPSGSAAA VFGG YVGS SRFQTSLSNEDSASFLLDLDSEVAQHLQRLSRKDPTTKI
 KALASLSELVKQKQKELLPIIPQWTFEYKKLILDYSRDVRRATHDVMNTNVVTGAGRDIAPHLKSI MGPPWFSQFDLAS
 EVSQAAKSS FQVGS SFGNSVFLVEAAFP AQEKRLHALNLCSAEIFAYLEENLKLTPQNLSDKSLASDELEEMYQQMISS
 SLVGLATLLDILLREPDNTGSANINSESKLASKARAVATSSAEKMFSSHKCFNLFLKSESPSIRSATYLLSSFIKNVP
 EVFGEQDVR**SLAPALLGVFR**ENNP TCHSSMWEAVLLFSKFKFPQSWVYLVNHKSVLNHLWQFLRNGCYGSPQVSYPALIL
 FLEVMPAQSVESDKFFVNFNFKNLLAGRSMCESSSTDQLSLLRATTECFWGLRNASRYCDVPNSI HDLQVDLIDKVLVK
 ILWADFTELSKGISPPNQRKSAENLGMNSVSYLQELGRCILEILSGINLLEQNLLSFFCKAVQESFLNMLQQGDLEIV
 AGSMRKMIDFLLLLERYSVLEGESWPLHQFMGPLLKSAFPWIRSEL LDGVKLLSVSVSVFGPRKVVPVLIDDIETSTL
 LSVEKEKNMSPEKLIKVFQEIFIPWCMGDYDSS TAARQDLLFSLLDDECF TQQWSDVISYVFNQQHQGFNNLAAMK**MLL**
EKARDEITKRSSGQELNQRIGSRPEHWHHTLIESTAISLVHSSATTTSAVQFLCSVLGGSTQDSSISFVSRSSVLIIY
 RGILEKLLSFIKQSPLCSVNDTCSSSLIVEAIAFDSSSSVDVIVAKFAAEVIDGSFFSLKSLSQDATLLTTVLSSIFII
 DLENRMTSLVDNTLSESKEKRKDRNFVCDYVHAVCSKMDNQFWKSIN YDVRKSSASTLAQFLRSVVLLEDDLQPFELTL
 LCASRMTEVLEYLSLDQSD EENICGLLLLLESDAWPIWVSPSSASIDTHGMPVQLCELKRSKRSQRYVSFIDSLIMKLG I
 HRFIVGHKDHGFASQAWLSVEILCTWEWPGGKQVTSFLPNLVSFCKDEPSSGGLLNSIFDILLNGALVHVKDEEEGLGN
 MWVDFNNNIVDVVEPFLRALVSFLHILFKEDLWGEEMAAFKMITDKLFIGEETSKNCLRIIPYIMSIISPLR TKVK
 SGGSGKDTLLPLEVLLRNWLESLSFPLVLWQSGEDIQDFQLVISCYVSDKAEAEKELQRHLSTEERTLLLDLFRK
 QKQDPGASTVVTQLPAVQILLARLIMIAVSYCGNDFNEDDWFVFNKRLIQSAVVMEETSENVNDFISGVSSMEKE
 KENDTLEGLGHIVFISDPSINSAQNALSAFSLLNALVNHSVEGEDNLKSLADETWDPVKDRILEGLVRLFFCTGLTEA
 IAASYSPEAASIVASFRVDHLQFWELVAHLVVDSSPRARDRAVRAVEFWGLSRGSISSLYAIMFSSNPISLQLAAYTV
 LSTEPISRLAIVADLNAPLNDES LNDQDSSNAGLPSEDKLLLREDEVSCMVEKLDHELDDTLTAPERVQTF LAWSLLS
 NVNSLPSLTQGRERLVQYIEKTANPLILDLSLFQHIPLELYMGQSLKKKGDIPSELSVVASAATRAIITGSSSLSTVESL
 WPIETGKMASLAGAIYGLMLRVLPAVREWFSEMRDRSASSLIEAFTRTWCSPLIKNELSQIKKADFNDESFSVSIK
 AANEVVATYTKDETGM DLVIRLPVSYPLKPV DNVCAKSIGISEAKQRKWLMSMQMFVRHQNGALAEAIRIWKRN SDKEF
 EGVEDCPICVSIIHGNHSLPRRACVTCKYKFHKACLDKWFYTSNKKLCLCQSPC

At2g42910 (PRS4; 8%)

MSENAANNIMETKICTDAIVSELQKKKVHLFYCLECEELARNIAAESDHITLQ SINWRSFADGFPNLFINNAHDIRGQH
 VAFLASFSSPAVIFEQISVIYLLPRLFVASFTLVLPFFPTG SFERMEEEGDVATAFTMAR**IVSNIPISRGGPTSVVIYD**
THALQERFYFADQVLP LFETGIPLLTKRLQQLPETEKVIVAFPDGAWKRFHKLLDHYPTV VCTKVRREGDKRIVRLKEG
 NPAGCHVVIVDDL VQSGGTLIECQKVLA AHGAVKVSAYVTHGVFPKSSWERFTHKKNGLEEAFAYFWITDSCPQTVKAI
 GNKAPFEVLSLAGSIADALQI

At3g08850 (RAPTOR1; 1%)

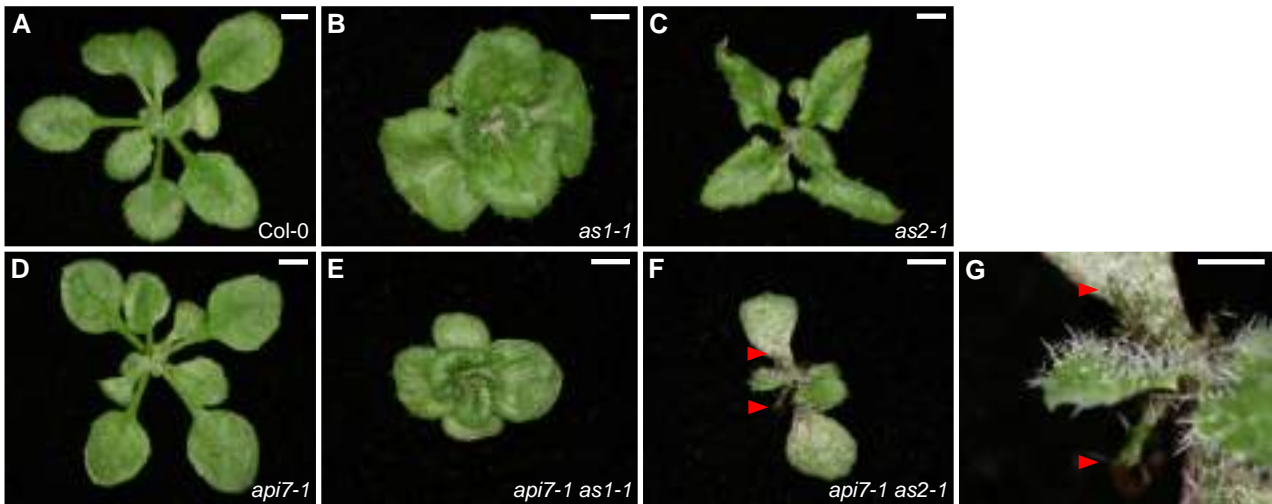
MALGDLMSRFSQSSVSLVSNHRYDEDCVSSHDDGDSRRKDSEAKSSSSSYGNGTTEGAATATSMAYLPQTIVLCEL RHD
 ASEASAPLGTSEIVLVPKWR LKERMKTGCVALVLC LNI TVDPPDVIKISPCARIEAWIDPF SMAPPKALETIGKNLSTQ
 YERWQPRARYKVQLDPTVDEVRKLC LTRCRYAKTERVLFHYNGHGVKPTANGEIWFNKS YTYIPLPISELDSWLKT
 PSIIYVFDCSAARMILNAFAELHDWGSSGSSSRDCILL AACDVHETLPQSV EFPADVFTSCLTTP IKMALKWFCRRSL
 LKEI IDESLIDRIPGRQNDRKTLLGELNWI FTAVTDTIAWNVL PHEL FQRLFR**QDLLVASLFR**NFLLAERIMRSANCNP
 ISHPMLPPTHQHMMWDAWMAAEICLSQLPQLVLDPSTEFQSPFFTEQLTAFEVWLDHGSEHKKPEQLPIVLQVLLS
 QCHRFRAL**VLLGR**FLDMGSAVVDLALSVGIFPYVLKLLQTTNELRQILVFIWTKILALDKSCQIDL VKDGGHTYFIRF
 LDSSGAFPEQRAMA AFVLAVIDGHRRGQEACLEANLIGVCLGHLEASRP SDPQPEPLFLQWLCLCLGKLWEDFMEAQI
 MGREANAFEKLAPLLSEPQPEVRAAAVFALGTL LDIGFDSNKS VVEDEFDDDEKIRAEDAIKSLLDVSDGSPLVRAE
 VAVALARFAFGHKQHLKLA AASYWK PQSSSLTSLPSIAKFHDPGSATIVSLHMSPLTRASTDSQPVARESRISSPLG
 SSGLMQGSPLSDDSSLSHSDSGMMHDSVSN GAVHQPRLLDNAVYSQCVRAMFALAKDPSPRIASLGRRVLSIIGIEQVVA
 KPSKPTGRPGEAATTSH TPLAGLARSSSWFDMHAGNLP LPSFRTPPVSPPR TNYLSGLRRVCSLEFRPHLLGSPDSGLAD
 PLLGASGSESRLLPLSTIYGWSCGHFSKPLLGGADASQEIAAKREEKEKFALEHIAKQHSSISKLNPNIANWDTRFE
 TGTKTALLHPFSPIVVAADENERIRVWNYEATLLNGFDNHDFPDKGISKLCLINELDDSLLVASCDG SVRIWKNYAT
 KGKQKLVTFGSSIQGHKPGARDLNAVVDWQQQSGYLYASGETSTVTLWDLEKEQLVRSVPSESECGVTALSASQVHGGQ
 LAAGFADGSLRLYDVR SPEPLVCATRPHQKVERV VGLSFQPLGDPKVV SASQAGDIQFLDLRTRTDTYLTIDAHRGSL
 TALAVHRHAPIIASGSAKQLIKVFSLQGEQLGIIRYYP SFMAQKIGSVSCLTFHPYQVLLAAGAADS FVSIYTHDNSQA
 R

At5g01770 (RAPTOR2; 1%)

MALGDLMVSRLSQSSVTVVVTHLYDDDDNCASSAHDDSRVSI IASPRVASSSYENLSAATSMAYLPQTLVLCDLRHDDA
 SDIVQPPRWRLKERMKTGCVALVMCLHITVDPPDVIKISPCARLECWIDPF SMFP RRRALEAIGQNLSIQYERWLLARAR
 YKVELDPTKDDVRKLCCLSCRKYAKTERVLFHYNGHGVPKPTPNGEI WVYNKNFTQYIPLPVSELD SWLKTPTIYVFDCS
 AARVILNAFAEGESSGPPKDCILLAACDVHETLPQSVEFPADVFTSCLTTPINIALKWFCCRSLLEKFIDESLIDRIPG
 RQNRKTLGELNWI FTAVTDTI AAWNVLPRELFRQRLFRQDILLVASLFRNFFLLAERIMRSGNCTPISHPMLPPTHQHMMW
 DAWDMAAEICLSQLPQFFLDPNTEFQPS SFFTEQLTAFEVWLDHGSEHKKPPEQLPIV LQVLLSQCHRYR **ALVLLGRFL**
 DMGPWAVDLALSVGIYPCVVKLLQTTTIELRQILVFIWTKILALDKSCQVDLVKDRGHIYFIRFLDSSDAFPEQRAMAA
 FILAVIVDGYKRGQESCLEANLI AVCLGHLEATQLCDPPPEPLFLQWLCLCLGKLWEDYLEAQIMGREANASENLIAGH
 TNLLQVRAAAVFALGTL LDVGFDSGKGVCD EEFDDDENIVEDII IKSLLDVVSDGSP LVRTEVAVALARFAFGHKQHLK
 SVADSYWKPQNSLR TSLPSMAK FHD SGT SIVASSDMGSLTRASPDSQP VAREGRISSSLQEPFSGLMQGSPLADSS LH
 SDVGI IHDGVSNGVVHQP RPLDNAIYSQSVLAMFTLAKDPSPRIASLGRRVLSVIGIEQIVAKPSKSNRGPGEAASASH
 TPLAGLVRSSSWFDMHTGHLPLTFRTPPVSP PQTSYLTGLRRVCSLELRPHLLGSPDGLADPILGVSGSERSLLPQST
 IYNWSCGHFSKPLLGGADANEEIAAQREKKKFSLEHIAKCQHSSISGLSNIPIANWDTKFETGTKTALLHPFSPIVVA
 ADENERIRVWNYEEATLLNGFDNNDFFPKGISNLCLVNELD D SLLLVASCNVPTLSRASFAIRIWKDYATKGRQKLV TG
 FSSIQQQKPGASGLNAVVDWQQQSGYLYVSGESLSIMVWLDLKEQLVKSM PFESGCSVTALSASQVHGSQLAAGFADGS
 VRLYDVRTPDFLVCATRPHQRVEKVVGLSFQPLDPAKIVSASQAGDIQFLDLRRPKETYLTIDAHRGSLTALGVHRHA
 PIIASGSAKQLIKVFSLKGEQLGI IKYHTSFMGQQIGPVSCLA FHPYQMLLAAGAAGSFVSLYTHHNTQLPR

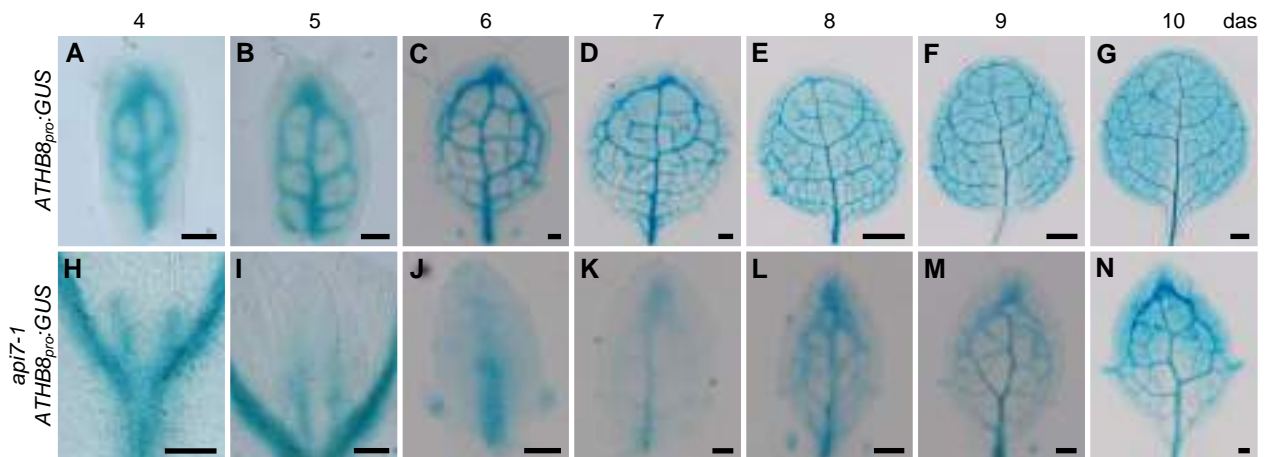
Supplementary Figure S9. Amino acid sequences of proteins identified by LC-ESI-MS/MS in co-immunoprecipitated ABCE2:YFP protein.

The Arabidopsis Genome Initiative (AGI) gene identifier (AtNgNNNNN) is shown, together with the TAIR10 annotation or protein name and peptide coverage (in percentage) for each protein. Full-length protein sequences were obtained from TAIR. The unique peptides identified by LC-ESI-MS/MS are shaded in black; some unique peptide sequences overlap. Peptide coverage was calculated by dividing the total number of residues of each protein by that of those covered by the peptides.



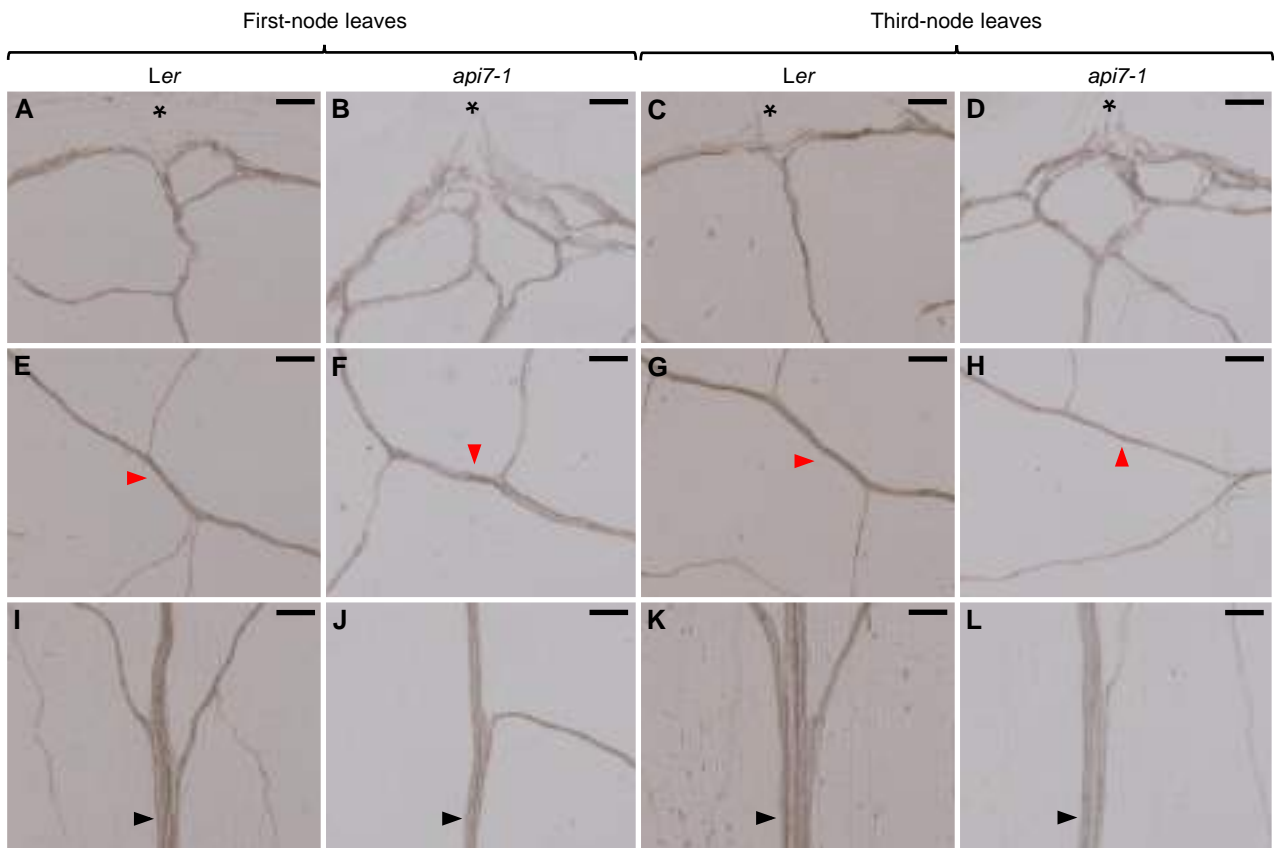
Supplementary Figure S10. Genetic interactions of *api7-1* with *as1-1* and *as2-1*.

(A–F) Rosettes from (A) the wild-type Ler, the (B) *as1-1*, (C) *as2-1*, and (D) *api7-1* single mutants, and the (E) *api7-1 as1-1* and (F) *api7-1 as2-1* double mutants. (G) Close up of (F). Red arrowheads indicate radial leaves. Pictures were taken 16 das. Scale bars indicate (A–F) 2 mm and (G) 1 mm.



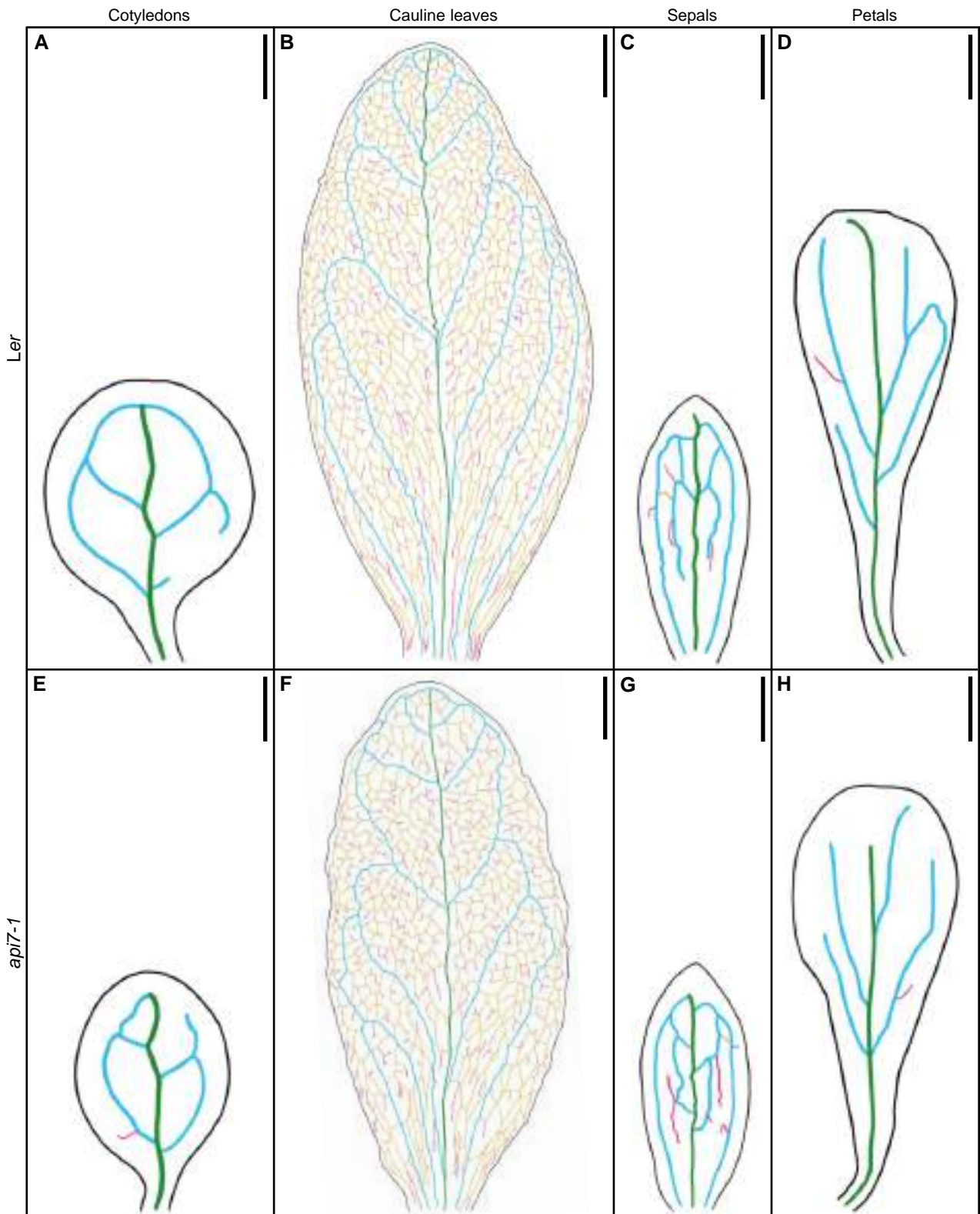
Supplementary Figure S11. Vascularization in *api7-1* leaf primordia.

Vascular fate specification is shown as *ATHB8_{pro}::GUS* activity at expanding first-node leaf primordia in (A–G) *Ler* and (H–N) *api7-1* backgrounds. Pictures were taken (A, H) 4, (B, I) 5, (C, J) 6, (D, K) 7, (E, L) 8, (F, M) 9, and (G, N) 10 das. Scale bars indicate (A–C, H–J) 50, (D, K–N) 100, and (E–G) 500 μm .



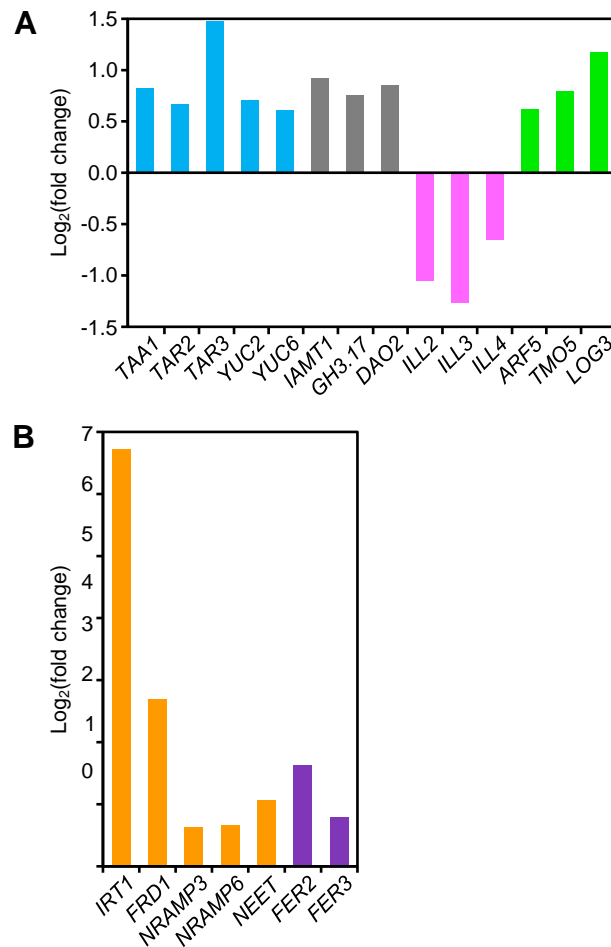
Supplementary Figure S12. Some details of the vascular phenotype of first- and third-node leaves from *Ler* and *api7-1* plants.

Veins from (A, C, E, G, I, K) *Ler* and (B, D, F, H, J, L) *api7-1* (A, B, E, F, I, J) first- and (C, D, G, H, K, L) third-node leaves. (A–D) Venation on the apical region (an asterisk indicates the most apical region) of the lamina, (E–H) a secondary vein (red arrowheads) bifurcating to render tertiary veins, and (I–L) the primary vein (black arrowheads), close to the base of the lamina. We observed 6 first- and third-node leaves from *Ler* and 18 from *api7-1* with similar vascular phenotypes to the ones shown. Pictures were taken 21 das. Scale bars indicate 100 μm .



Supplementary Figure S13. Venation pattern of *api7-1* cotyledons, cauline leaves, sepals, and petals.

Representative diagrams of (A, E) cotyledons, (B, F) cauline leaves, (C, G) sepals, and (D, H) petals from (A–D) *Ler* and (E–H) *api7-1* plants. Margins and veins were drawn as described in Figure 6. Organs were collected (A, E) 6 and (B–D, F–H) 35 das. Scale bars indicate (A, C–E, G, H) 0.5 and (B, F) 2.5 mm.



Supplementary Figure S14. Expression levels of some genes deregulated in *api7-1* plants. Expression levels of genes related to (A) auxin metabolism (biosynthesis, blue; inactivation, grey; activation, pink) and provascular cell division (green), and (B) iron homeostasis and FeS cluster biogenesis (orange), and response to oxidative stress (purple). Values are shown as the binary logarithm of the foldchange between *api7-1* and *Ler* mean reads. Mean reads were calculated from three biological replicates.

Supplementary Table S1. Primer sets used in this work

Purpose	Name	Forward primer (F; 5' → 3')	Reverse primer (R; 5' → 3')
Linkage analysis	nga1111_F/R	GGTTTCGGTTACAATCGTGT	AGTTCCAGATTGAGCTTTGAGC
	AtF28J12.3_F/R	GCTCCGCCGTTGGATTCTG	GTTCCGGGTTTAATTCTCGGGT
	AtM7J12.1_F/R	AGCAACTTGTGTTCTCATTT	TTATAGGGTACGACAACCAT
	nga1139_F/R	CTAGGCTCGGGTGAGTCAC	TTTTTCCTTGTGTTGCATTCC
	nga1107_F/R	GCGAAAAACAAAAAATCCA	CGACGAATCGACAGAATTAGG
	g3883_F/R	CATCCATCAAACAACTCC	TGTTTCAGAGTAGCCAATTC
	T13K14_F/R	CTGAAACATATAAGAGAATCATCC	ACTCGTAGTTTGGTGTGAGAC
	AtF16G20.1_F/R	TCAGTGTTACTATGTACCAAGTA	TAGGACGTAATATCCTTAGTTAC
	AG_F/R	CAACAGGTTTCTTCTTCTC	CAAACACCATTTAATCTTGACA
T18B16_F/R	TAACTTCTGCAGCCTCTGAAG	TTCTATTGGGATGCTGCCCTC	
Sequencing of ABCE1 and ABCE2	ABCE1_F1/R1	GGTTAGCTAGTCCCTTTCAAAG	GAAGTATGCTAATGTGGCCC
	ABCE1_F2/R2	ACTACCTCTTGCGCAGACTC	GGCATCAGACTCACTTCATGA
	ABCE1_F3/R3	GGAAGTGAAGTCCTATGCAAGA	CTTGAAATCTCCAAGTTGCTTAGT
	ABCE1_R4		CTGCCAAGATTTGGTTTGAG
	ABCE2_F1/R1	TCGGTTCACCATTTTTATCTGAAG	CACCACAAGATGCTAACAATGAT
	ABCE2_F2/R2	AGCCTGCGGATATATACCTGAT	GGTCGTATCTTTCTCCAAGTCT
	ABCE2_F3/R3	GTTACACCGTATGGGCAAGAG	GGAGACTTACAGATAAGAAGAGA
	ABCE2_F4/R4	CTTAGAACAATCGGCACACG	AGAGAAATCGAGATTAGTACCTGAG
	ABCE2_F5/R5	GTTCTGATACCCTGTGCATG	ATCTCTTCAGCACTTTCTTGTG
Genotyping	api7-1_F/R	TGCCTCTAGAAATGGCACCT	GTATGGCAACAACAGCGATT
	GABI_509C06_LP/RP	TTCTTGGTCTGAAATTGGTGG	TGGCTGGATTTGTTCTACAG
	o8409 (GABI-Kat lines) ¹	ATATTGACCATCATACTCATTGC	
	M13_F/R	TGTAACACGACGGCCAGT	GGAAACAGCTATGACCATGATT
	GFP_R		CACGTATCCCTCAGGCATGG
	YFP_R		GACTTGAAGAAGTCGTGCTGC

Supplementary Table S1 (continued). Primer sets used in this work

Purpose	Name	Forward primer (F; 5' → 3')	Reverse primer (R; 5' → 3')
qRT-PCR	qABCE1_F/R	CCTAAATCTTCGGAAAGTGAAC	GGCCATGAACCAACTTACGC
	qABCE2_F/R	GACAACTACCAAGAGAATATAGG	CAACTCAGGAAGTACAAAGCC
	qACTIN2_F/R ²	GCACCCTGTTCTTCTTACCG	AACCCTCGTAGATTGGCACA
	OTC3D/OTCR ³	TCCTTGCCAAATCATGGCCG	GCATGCATGCGATTCTCCGC
Gateway cloning	ABCE2pro:ABCE2_F/R	GGGACAAGTTTGTACAAAAAAGCAGGCT TTTCTATCTTGTTATTCTTCGTTTT	GGGACCACCTTTGTACAAGAAAGCTGGGT AGTTTTCTATATCAGTGAGTTAG
	35Spro:ABCE2:GFP-YFP_F/R	GGGACAAGTTTGTACAAAAAAGCAGGCT GGATGGCAGATCGATTGACACGTA	GGGACCACCTTTGTACAAGAAAGCTGGGT CATCATCCAAGTAGTAGTATGAGC
	ABCE1pro_F/R	GGGACAAGTTTGTACAAAAAAGCAGGCT TACTTTTCTCTCGGCCGTACT	CAATACGTGTCAATCGATCTGCCATCTCTC TTGAGAATATTACATACAAG
	ABCE2tu_F/R	CTTGTATGTAATATTCTCAAGAGAGATGGC AGATCGATTGACACGTATTG	GGGACCACCTTTGTACAAGAAAGCTGGGT CTAATCATCCAAGTAGTAGTA
	ABCE2pro_F/R	GGGACAAGTTTGTACAAAAAAGCAGGCT TTTCTATCTTGTTATTCTTCGTTTT	AATCCGCGTCAATCGATCTGACATCTCTCA ACAGACCTACAAAATACATG
	ABCE1tu_F/R	CATGTATTTTGTAGGTCTGTTGAGAGATGT CAGATCGATTGACGCGGATT	GGGACCACCTTTGTACAAGAAAGCTGGGT TCAATCGTCTAAGTAGTAGTA

Sequences were taken from ¹(S1), ²(S2), and ³(S3).

Supplementary Table S2. NCBI accession numbers of the sequences used for phylogenetic analysis

Species	ABCE1 gene	ABCE2 gene
<i>Arabidopsis thaliana</i>	NM_112210.3	ABCE2 NM_118041.5
<i>Arabidopsis lyrata</i> subsp. <i>lyrata</i>	XM_021033623.1	XM_021033596.1
<i>Capsella rubella</i>	XM_006299733.2	XM_006285967.2
<i>Cardamine hirsuta</i>	-	JX097073.1
<i>Eutrema salsugineum</i>	XM_006418662.2	XM_006413929.2
<i>Brassica rapa</i> (a)	XM_033286408.1	XM_033276765.1
<i>Brassica rapa</i> (b)	XM_009119375.3	XM_009138752.3
<i>Brassica rapa</i> (c)	-	XM_018655198.2
<i>Fragaria vesca</i> subsp. <i>vesca</i>	-	XM_004291176.2
<i>Theobroma cacao</i>	-	XM_018117748.1
<i>Citrus sinensis</i>	-	XM_015531558.2
<i>Populus trichocarpa</i> (a)	-	XM_024599960.1
<i>Populus trichocarpa</i> (b)	-	XM_024597900.1
<i>Eschscholzia californica</i>	-	Eca_sc194497.1_g0120.1*
<i>Oryza sativa</i> (a)	-	XM_015762126.2
<i>Oryza sativa</i> (b)	-	XM_026023394.1

Multiple *ABCE1* or *ABCE2* genes from *Brassica rapa*, *Populus trichocarpa*, and *Oryza sativa* are distinguished with arbitrarily given *a*, *b*, and *c* designations. *Obtained from Eschscholzia Genome DataBase (<http://eschscholzia.kazusa.or.jp/cgi-bin/list.cgi>).

Supplementary Table S3. Mutations identified in the *api7-1* candidate interval

Mutation	Region affected	Predicted effect
G→A	At4g19185, 1 st intron	-
G→A	At4g19185, 1 st exon	Cys55→Cys (Synonymous)
C→T	At4g19210, 6 th exon	Pro138→Ser
G→A	At4g19390, 2 nd exon	Ile128→Ile (Synonymous)

Supplementary Table S4. ABCE2 interactors identified in a co-immunoprecipitation assay

AGI gene code	Protein		Peptides		Peptide coverage (%)
	Abbreviation	Full name	Total ¹	Unique ²	
At4g19210	ABCE2	ATP-BINDING CASSETTE E2	153 (20)	26 (5)	62
At3g13640	ABCE1	ATP-BINDING CASSETTE E1			
-	YFP	Yellow fluorescent protein	59	10	-
At4g11420	eIF3a ³	EUKARYOTIC TRANSLATION INITIATION FACTOR 3 SUBUNIT A	48	24	32
At3g56150	eIF3c ³	EUKARYOTIC TRANSLATION INITIATION FACTOR 3 SUBUNIT C	29	11	14
At3g57290	eIF3e ³	EUKARYOTIC TRANSLATION INITIATION FACTOR 3 SUBUNIT E	25	15	40
At1g64790	ILA ³	ILITYHIA	17	11	4
At2g44060	LEA26 ³	LATE EMBRYOGENESIS ABUNDANT 26	15	6	23
At4g20980	eIF3d ³	EUKARYOTIC TRANSLATION INITIATION FACTOR 3 SUBUNIT D	13 (8)	6 (4)	13
At5g44320	eIF3d ³	EUKARYOTIC TRANSLATION INITIATION FACTOR 3 SUBUNIT D			
At5g17020	XPO1A ³	EXPORTIN 1A	12 (4)	5 (2)	6
At3g03110	XPO1B ³	EXPORTIN 1B			
At1g61580	RPL3B	RIBOSOMAL PROTEIN L3 B	12	4	12
At4g38740	ROC1	ROTAMASE CYP 1	11	5	38
At3g13460	ECT2 ³	EVOLUTIONARILY CONSERVED C-TERMINAL REGION 2	8	6	11
At4g33250	eIF3k ³	EUKARYOTIC TRANSLATION INITIATION FACTOR 3 SUBUNIT K	8	4	23
At1g76810	eIF5B ³	EUKARYOTIC TRANSLATION INITIATION FACTOR 5B	6	4	4
At3g53610	RAB8	RAB GTPASE HOMOLOG 8	6	3	18
At5g37475	eIF3j	EUKARYOTIC TRANSLATION INITIATION FACTOR 3 SUBUNIT J	5	3	16
At3g43600	AAO2	ALDEHYDE OXIDASE 2	4	3	3
At1g65860	FMO GS-OX1	FLAVIN-MONOOXYGENASE GLUCOSINOLATE S-OXYGENASE 1	4	3	4
At2g20830	- ⁴	FOLIC ACID BINDING / TRANSFERASE	4	2	8
At5g58410	LTN1	E3 UBIQUITIN-PROTEIN LIGASE LISTERIN	4	2	1

Supplementary Table S4 (continued). ABCE2 interactors identified in a co-immunoprecipitation assay

AGI gene code	Protein		Peptides		Peptide coverage (%)
	Abbreviation	Full name	Total ¹	Unique ²	
At2g42910	PRS4	PHOSPHORIBOSYL DIPHOSPHATE SYNTHASE 4	4	2	8
At3g08850	RAPTOR1	REGULATORY-ASSOCIATED PROTEIN OF TOR 1	4 (3)	2 (2)	1
At5g01770	RAPTOR2	REGULATORY-ASSOCIATED PROTEIN OF TOR 2			

Three biological replicates were assayed and we identified 20 candidate interactors. Translation initiation factors were named according to (S4). ¹Sum of the number of peptides identified in the three biological replicates. ²Number of associated peptides with significantly different sequences from each other. Values within parentheses refer to the second protein of the paralogous group, whose peptides were also associated with the first protein in all cases. ³Enriched proteins (identified with at least twice the number of peptides associated with the same protein in the control co-immunoprecipitations). The rest of the proteins were unique to ABCE2:YFP samples. ⁴This protein was included after being first discarded due to its predicted mitochondrial localization.

Supplementary Table S5. Conservation level and described functions of putative ABCE2 interactors

AGI gene code	Protein	Conservation between orthologs (%) ¹			Described molecular function(s) and available evidence of its interaction with ABCE proteins ²
		Arabidopsis and <i>S. cerevisiae</i>	Arabidopsis and <i>H. sapiens</i>	<i>S. cerevisiae</i> and <i>H. sapiens</i>	
At4g19210	ABCE2	68.9 (82.6)	75.4 (86.0)	68.3 (82.9)	In Arabidopsis: suppression of RNA silencing (S5,S6). In yeast (Rli1): ribosome dissociation (S7). In humans (ABCE1): inhibition of RNase L, suppression of RNA silencing, and ribosome dissociation (S8,S9,S10).
At4g11420	eIF3a	26.3 (43.4)	25.7 (41.6)	18.3 (32.0)	In Arabidopsis, yeast (Rpg1), and humans (EIF3A): translation initiation (S11).
At3g56150	eIF3c	24.3 (41.7)	34.5 (49.9)	23.4 (39.2)	In Arabidopsis, yeast (Nip1), and humans (EIF3C): translation initiation (S11).
At4g20980	eIF3d	NC	39.0 (54.4)	NC	In Arabidopsis and humans (EIF3D): translation initiation (S11).
At3g57290	eIF3e	NC	50.1 (69.0)	NC	In Arabidopsis and humans (EIF3E): translation initiation (S11).
At5g37475	eIF3j	22.5 (37.0)	29.7 (45.1)	26.2 (40.9)	In yeast (Hcr1): translation initiation and, as a non-stoichiometric subunit of the eIF3 complex, participates in pre-40S maturation, and as an accessory factor for Rli1-mediated ribosome dissociation (S12,S13). In humans (EIF3J): start codon selection and eIF3 complex formation during translation initiation (S14,S15). It is also present in the 40S post-splitting complex with ABCE1 (S16).
At4g33250	eIF3k	NC	31.4 (50.7)	NC	In Arabidopsis and humans (EIF3K): translation initiation (S11) .
At1g76810	eIF5B	36.3 (50.1)	39.7 (55.6)	36.5 (54.1)	In yeast (Fun12): 40S and 60S joining during pre-40S maturation and translation initiation (S17,S18,S19,S20).
At1g61580	RPL3B	65.3 (79.6)	64.9 (80.4)	65.3 (80.0)	In Arabidopsis, yeast (Rpl3), and humans (RPL3): ribosomal protein. Translation (S21,S22).

Supplementary Table S5 (continued). Conservation level and described functions of putative ABCE2 interactors

AGI code	Protein	Conservation between orthologs (%) ¹			Described molecular function(s) and available evidence of its interaction with ABCE proteins ²
		Arabidopsis and <i>S. cerevisiae</i>	Arabidopsis and <i>H. sapiens</i>	<i>S. cerevisiae</i> and <i>H. sapiens</i>	
At1g64790	ILA	27.6 (45.1)	32.4 (50.2)	27.7 (47.1)	In Arabidopsis: translation regulation through two pathways, one involving GCN2 and eIF2 α , and the other involving GCN20 (S23,S24). In yeast (Gcn1): translation downregulation by binding to translating ribosomes with Gcn2 and Gcn20 (S25,S26).
At3g13460	ECT2	12.5 (19.6)	25.5 (35.9)	15.5 (24.6)	In Arabidopsis: m ⁶ A reader that regulates 3'UTR processing in the nucleus and mRNA stability in the cytoplasm (S27,S28,S29). In yeast (Pho92) and humans (YTHDF2): m ⁶ A reader that decreases mRNA stability (S30,S31).
At5g58410	LTN1	19.2 (36.1)	22.5 (37.9)	20.8 (36.8)	In yeast, <i>Drosophila melanogaster</i> , and humans: ubiquitination of nascent non-stop proteins for their degradation during ribosome quality control (S32,S33,S34).
At4g38740	ROC1	64.0 (74.4)	67.4 (80.2)	64.2 (74.5)	In Arabidopsis, yeast (Cpr1), and humans (PPIA): it is a cyclophilin that belongs to the peptidyl-prolyl cis-trans isomerase family and participates in protein folding (S35,S36,S37).
At3g08850	RAPTOR1	27.3 (42.1)	40.4 (54.7)	31.8 (45.3)	In Arabidopsis, yeast (Kog1), and humans (RAPTOR): it is part of the TORC1 complex, composed of TOR, RAPTOR, and LST8-1 proteins. It controls cellular growth in response to different signals through regulation of translation, as it promotes translation reinitiation and ribosome biogenesis (S38,S39). In Arabidopsis: ABCE2 has been shown to interact with LST8-1 (S40).
At2g20830	-	26.7 (47.2)	30.2 (43.4)	27.8 (50.9)	In Arabidopsis: not studied. A BLASTp search suggested homology to <i>Saccharomyces cerevisiae</i> Lto1 and human ORAOV1. In yeast and humans: FeS cluster assembly on Rli1 and ABCE1, respectively (S41,S42).

Supplementary Table S5 (continued). Conservation level and described functions of putative ABCE2 interactors

AGI code	Protein	Conservation between orthologs (%) ¹			Described molecular function(s) and available evidence of its interaction with ABCE proteins ²
		Arabidopsis and <i>S. cerevisiae</i>	Arabidopsis and <i>H. sapiens</i>	<i>S. cerevisiae</i> and <i>H. sapiens</i>	
At5g17020	XPO1A	40.7 (61.7)	48.5 (67.6)	46.2 (65.8)	In Arabidopsis, yeast (Crm1), and humans (XPO1): nuclear export receptor (S43,S44). In yeast, humans, and <i>Xenopus laevis</i> : ABCE might be an XPO1 cargo (S45). In yeast: <i>xpo1-1</i> mutants accumulate Rli1 in nucleus (S46,S47).
At2g42910	PRS4	20.7 (38.2)	19.2 (40.0)	60.3 (76.6)	In yeast (Prs4) and humans (PRPS1): synthesis of phosphoribosylpyrophosphate (PRPP), which is required for nucleotide biosynthesis (S48).
At1g65860	FMO GS-OX1	NC	NC	NC	In Arabidopsis: synthesis of aliphatic glucosinolates (S49).
At3g53610	RAB8	51.1 (70.0)	58.7 (73.1)	48.9 (67.0)	In Arabidopsis: it might be involved in post-Golgi transport to the plasma membrane (S50,S51). In yeast (Sec4): involved in membrane trafficking during cytokinesis and autophagy (S52,S53).
At3g43600	AAO2	NC	29.6 (48.1)	NC	In Arabidopsis: it might be involved in ABA biosynthesis (S54,S55). In humans (AOX1): it is an oxidase with broad substrate specificity (S56).
At2g44060	LEA26	NC	NC	NC	In Arabidopsis: unknown.

¹Identity and similarity (between parentheses) percentages were obtained by global pairwise sequence alignments between pairs of protein sequences using the Needle EMBOSS tool. Protein sequences were obtained from TAIR for Arabidopsis, *Saccharomyces* Genome Database (SGD; <https://www.yeastgenome.org/>) for *Saccharomyces cerevisiae*, and UniProt for *Homo sapiens* proteins. NC: not conserved. ²The abbreviated names for *Saccharomyces cerevisiae* and *Homo sapiens* orthologs are indicated in parentheses. The full names of Arabidopsis proteins are provided in Supplementary Table S3.

Supplementary Table S6. Morphometry of the leaf venation pattern of the *api7-1* mutant

Organ	Genotype	Area (mm ²)	Circularity	Vein density	Vein branching points	Free-ending veins
Cotyledons	<i>Ler</i>	2.9 ± 0.5	0.84 ± 0.03	2.7 ± 0.2	6.5 ± 0.5	2.1 ± 1.7
	<i>api7-1</i>	1.9 ± 0.5	0.85 ± 0.01	3.1 ± 0.3	8.2 ± 2.4	4.4 ± 2.2
First-node leaves	<i>Ler</i>	33.9 ± 8.3	0.86 ± 0.02	3.1 ± 0.2	178.6 ± 35.6	77.8 ± 17.1
	<i>api7-1</i>	11.2 ± 4.8	0.76 ± 0.05	3.0 ± 0.3	72.4 ± 24.6	35.9 ± 10.8
Third-node leaves	<i>Ler</i>	51.3 ± 11.2	0.85 ± 0.01	3.8 ± 0.3	361.7 ± 56.9	126.9 ± 24.4
	<i>api7-1</i>	18.8 ± 4.0	0.84 ± 0.02	3.5 ± 0.4	145.2 ± 25.1	52.7 ± 10.6
Cauline leaves	<i>Ler</i>	200.6 ± 32.8	0.56 ± 0.23	3.9 ± 0.3	1307.6 ± 213.8	439.9 ± 66.1
	<i>api7-1</i>	136.6 ± 50.5	0.69 ± 0.04	4.2 ± 0.5	1023.0 ± 201.1	373.3 ± 73.4
Sepals	<i>Ler</i>	1.4 ± 0.2	0.66 ± 0.05	6.6 ± 0.7	13.4 ± 4.2	9.5 ± 2.3
	<i>api7-1</i>	1.3 ± 0.1	0.65 ± 0.04	7.0 ± 1.0	14.7 ± 4.1	10.8 ± 4.8
Petals	<i>Ler</i>	2.4 ± 0.4	0.70 ± 0.03	4.2 ± 0.6	6.4 ± 0.8	6.5 ± 1.8
	<i>api7-1</i>	2.2 ± 0.2	0.70 ± 0.03	4.0 ± 0.4	5.9 ± 1.1	7.7 ± 2.1

All values are means ± standard deviation from 12 measurements. Organs were collected 6 (cotyledons), 21 (first- and third-node leaves), and 35 (cauline leaves, petals, and sepals) days. Values in italics, bold, or bold and italics are significantly different from those of *Ler* in a Student's *t* test, with $P < 0.05$, $P < 0.01$, or $P < 0.001$, respectively.

SUPPLEMENTARY REFERENCES

- S1. Kleinboelting, N., Huet, G., Kloetgen, A., Viehoveer, P. and Weisshaar, B. (2012) GABI-Kat SimpleSearch: new features of the *Arabidopsis thaliana* T-DNA mutant database. *Nucleic Acids Res.*, **40**, D1211-1215.
- S2. Moschopoulos, A., Derbyshire, P. and Byrne, M.E. (2012) The *Arabidopsis* organelle-localized glycyl-tRNA synthetase encoded by *EMBRYO DEFECTIVE DEVELOPMENT1* is required for organ patterning. *J. Exp. Bot.*, **63**, 5233-5243.
- S3. Quesada, V., Ponce, M.R. and Micol, J.L. (1999) *OTC* and *AUL1*, two convergent and overlapping genes in the nuclear genome of *Arabidopsis thaliana*. *FEBS Lett.*, **461**, 101-106.
- S4. Browning, K.S. and Bailey-Serres, J. (2015) Mechanism of cytoplasmic mRNA translation. *The Arabidopsis book*, **13**, e0176.
- S5. Möttus, J., Maiste, S., Eek, P., Truve, E. and Sarmiento, C. (2020) Mutational analysis of *Arabidopsis thaliana* ABCE2 identifies important motifs for its RNA silencing suppressor function. *Plant Biol.*, **23**, 21-31.
- S6. Sarmiento, C., Nigul, L., Kazantseva, J., Buschmann, M. and Truve, E. (2006) AtRLI2 is an endogenous suppressor of RNA silencing. *Plant Mol. Biol.*, **61**, 153-163.
- S7. Shoemaker, C.J. and Green, R. (2011) Kinetic analysis reveals the ordered coupling of translation termination and ribosome recycling in yeast. *Proc. Natl. Acad. Sci. USA*, **108**, E1392-E1398.
- S8. Kärblane, K., Gerassimenko, J., Nigul, L., Piirsoo, A., Smialowska, A., Vinkel, K., Kylsten, P., Ekwall, K., Swoboda, P., Truve, E. *et al.* (2015) ABCE1 is a highly conserved RNA silencing suppressor. *PLOS ONE*, **10**, e0116702.
- S9. Pisarev, A.V., Skabkin, M.A., Pisareva, V.P., Skabkina, O.V., Rakotondrafara, A.M., Hentze, M.W., Hellen, C.U. and Pestova, T.V. (2010) The role of ABCE1 in eukaryotic posttermination ribosomal recycling. *Mol. Cell*, **37**, 196-210.
- S10. Bisbal, C., Martinand, C., Silhol, M., Lebleu, B. and Salehzada, T. (1995) Cloning and characterization of a RNase L inhibitor. A new component of the interferon-regulated 2-5A pathway. *J. Biol. Chem.*, **270**, 13308-13317.
- S11. Burks, E.A., Bezerra, P.P., Le, H., Gallie, D.R. and Browning, K.S. (2001) Plant initiation factor 3 subunit composition resembles mammalian initiation factor 3 and has a novel subunit. *J. Biol. Chem.*, **276**, 2122-2131.
- S12. Valášek, L., Hašek, J., Nielsen, K.H. and Hinnebusch, A.G. (2001) Dual function of eIF3j/Hcr1p in processing 20 S pre-rRNA and translation initiation. *J. Biol. Chem.*, **276**, 43351-43360.
- S13. Young, D.J. and Guydosh, N.R. (2019) Hcr1/eIF3j is a 60S ribosomal subunit recycling accessory factor *in vivo*. *Cell Rep.*, **28**, 39-50.

- S14. Borgo, C., Franchin, C., Salizzato, V., Cesaro, L., Arrigoni, G., Matricardi, L., Pinna, L.A. and Donella-Deana, A. (2015) Protein kinase CK2 potentiates translation efficiency by phosphorylating eIF3j at Ser127. *Biochim. Biophys. Acta*, **1853**, 1693-1701.
- S15. ElAntak, L., Wagner, S., Herrmannová, A., Karásková, M., Rutkai, E., Lukavsky, P.J. and Valášek, L. (2010) The indispensable N-terminal half of eIF3j/HCR1 cooperates with its structurally conserved binding partner eIF3b/PRT1-RRM and with eIF1A in stringent AUG selection. *J. Mol. Biol.*, **396**, 1097-1116.
- S16. Kratzat, H., Mackens-Kiani, T., Ameismeier, M., Potocnjak, M., Cheng, J., Dacheux, E., Namane, A., Berninghausen, O., Herzog, F., Fromont-Racine, M. *et al.* (2021) A structural inventory of native ribosomal ABCE1-43S pre-initiation complexes. *EMBO J.*, **40**, e105179.
- S17. Fringer, J.M., Acker, M.G., Fekete, C.A., Lorsch, J.R. and Dever, T.E. (2007) Coupled release of eukaryotic translation initiation factors 5B and 1A from 80S ribosomes following subunit joining. *Mol. Cell. Biol.*, **27**, 2384-2397.
- S18. Lebaron, S., Schneider, C., van Nues, R.W., Swiatkowska, A., Walsh, D., Böttcher, B., Granneman, S., Watkins, N.J. and Tollervey, D. (2012) Proofreading of pre-40S ribosome maturation by a translation initiation factor and 60S subunits. *Nat. Struct. Mol. Biol.*, **19**, 744-753.
- S19. Strunk, B.S., Novak, M.N., Young, C.L. and Karbstein, K. (2012) A translation-like cycle is a quality control checkpoint for maturing 40S ribosome subunits. *Cell*, **150**, 111-121.
- S20. Wang, J., Johnson, A.G., Lapointe, C.P., Choi, J., Prabhakar, A., Chen, D.H., Petrov, A.N. and Puglisi, J.D. (2019) eIF5B gates the transition from translation initiation to elongation. *Nature*, **573**, 605-608.
- S21. García-Gómez, J.J., Fernández-Pevida, A., Lebaron, S., Rosado, I.V., Tollervey, D., Kressler, D. and de la Cruz, J. (2014) Final pre-40S maturation depends on the functional integrity of the 60S subunit ribosomal protein L3. *PLOS Genet.*, **10**, e1004205.
- S22. Meskauskas, A. and Dinman, J.D. (2007) Ribosomal protein L3: gatekeeper to the A-site. *Mol. Cell*, **25**, 877-888.
- S23. Faus, I., Niñoles, R., Kesari, V., Llabata, P., Tam, E., Nebauer, S.G., Santiago, J., Hauser, M.T. and Gadea, J. (2018) Arabidopsis ILITHYIA protein is necessary for proper chloroplast biogenesis and root development independent of eIF2 α phosphorylation. *J. Plant Physiol.*, **224-225**, 173-182.
- S24. Izquierdo, Y., Kulasekaran, S., Benito, P., López, B., Marcos, R., Cascón, T., Hamberg, M. and Castresana, C. (2018) Arabidopsis *nonresponding to oxylipins* locus NOXY7 encodes a yeast GCN1 homolog that mediates noncanonical translation regulation and stress adaptation. *Plant Cell Environ.*, **41**, 1438-1452.

- S25. Lee, S.J., Swanson, M.J. and Sattlegger, E. (2015) Gcn1 contacts the small ribosomal protein Rps10, which is required for full activation of the protein kinase Gcn2. *Biochem. J.*, **466**, 547-559.
- S26. Sattlegger, E. and Hinnebusch, A.G. (2005) Polyribosome binding by GCN1 is required for full activation of eukaryotic translation initiation factor 2 α kinase GCN2 during amino acid starvation. *J. Biol. Chem.*, **280**, 16514-16521.
- S27. Arribas-Hernández, L., Bressendorff, S., Hansen, M.H., Poulsen, C., Erdmann, S. and Brodersen, P. (2018) An m⁶A-YTH module controls developmental timing and morphogenesis in Arabidopsis. *Plant Cell*, **30**, 952-967.
- S28. Scutenaire, J., Deragon, J.M., Jean, V., Benhamed, M., Raynaud, C., Favory, J.J., Merret, R. and Bousquet-Antonelli, C. (2018) The YTH domain protein ECT2 is an m⁶A reader required for normal trichome branching in Arabidopsis. *Plant Cell*, **30**, 986-1005.
- S29. Wei, L.H., Song, P., Wang, Y., Lu, Z., Tang, Q., Yu, Q., Xiao, Y., Zhang, X., Duan, H.C. and Jia, G. (2018) The m⁶A reader ECT2 controls trichome morphology by affecting mRNA stability in Arabidopsis. *Plant Cell*, **30**, 968-985.
- S30. Kang, H.J., Jeong, S.J., Kim, K.N., Baek, I.J., Chang, M., Kang, C.M., Park, Y.S. and Yun, C.W. (2014) A novel protein, Pho92, has a conserved YTH domain and regulates phosphate metabolism by decreasing the mRNA stability of *PHO4* in *Saccharomyces cerevisiae*. *Biochem. J.*, **457**, 391-400.
- S31. Wang, X., Lu, Z., Gomez, A., Hon, G.C., Yue, Y., Han, D., Fu, Y., Parisien, M., Dai, Q., Jia, G. *et al.* (2014) N⁶-methyladenosine-dependent regulation of messenger RNA stability. *Nature*, **505**, 117-120.
- S32. Bengtson, M.H. and Joazeiro, C.A. (2010) Role of a ribosome-associated E3 ubiquitin ligase in protein quality control. *Nature*, **467**, 470-473.
- S33. Kashima, I., Takahashi, M., Hashimoto, Y., Sakota, E., Nakamura, Y. and Inada, T. (2014) A functional involvement of ABCE1, eukaryotic ribosome recycling factor, in nonstop mRNA decay in *Drosophila melanogaster* cells. *Biochimie*, **106**, 10-16.
- S34. Shao, S., von der Malsburg, K. and Hegde, R.S. (2013) Listerin-dependent nascent protein ubiquitination relies on ribosome subunit dissociation. *Mol. Cell*, **50**, 637-648.
- S35. Coaker, G., Zhu, G., Ding, Z., Van Doren, S.R. and Staskawicz, B. (2006) Eukaryotic cyclophilin as a molecular switch for effector activation. *Mol. Microbiol.*, **61**, 1485-1496.
- S36. Davis, T.L., Walker, J.R., Campagna-Slater, V., Finerty, P.J., Paramanathan, R., Bernstein, G., MacKenzie, F., Tempel, W., Ouyang, H., Lee, W.H. *et al.* (2010) Structural and biochemical characterization of the human cyclophilin family of peptidyl-prolyl isomerases. *PLOS Biol.*, **8**, e1000439.

- S37. Haendler, B., Keller, R., Hiestand, P.C., Kocher, H.P., Wegmann, G. and Movva, N.R. (1989) Yeast cyclophilin: isolation and characterization of the protein, cDNA and gene. *Gene*, **83**, 39-46.
- S38. Kim, D.H. and Sabatini, D.M. (2004) Raptor and mTOR: subunits of a nutrient-sensitive complex. *Curr. Top. Microbiol. Immunol.*, **279**, 259-270.
- S39. Schepetilnikov, M., Dimitrova, M., Mancera-Martínez, E., Geldreich, A., Keller, M. and Ryabova, L.A. (2013) TOR and S6K1 promote translation reinitiation of uORF-containing mRNAs via phosphorylation of eIF3h. *EMBO J.*, **32**, 1087-1102.
- S40. Van Leene, J., Han, C., Gadeyne, A., Eeckhout, D., Matthijs, C., Cannoot, B., De Winne, N., Persiau, G., Van De Slijke, E., Van de Cotte, B. *et al.* (2019) Capturing the phosphorylation and protein interaction landscape of the plant TOR kinase. *Nat. Plants*, **5**, 316-327.
- S41. Paul, V.D., Mühlenhoff, U., Stümpfig, M., Seebacher, J., Kugler, K.G., Renicke, C., Taxis, C., Gavin, A.C., Pierik, A.J. and Lill, R. (2015) The deca-GX₃ proteins Yae1-Lto1 function as adaptors recruiting the ABC protein Rli1 for iron-sulfur cluster insertion. *eLife*, **4**, e08231.
- S42. Zhai, C., Li, Y., Mascarenhas, C., Lin, Q., Li, K., Vyrides, I., Grant, C.M. and Panaretou, B. (2014) The function of ORAOV1/LTO1, a gene that is overexpressed frequently in cancer: essential roles in the function and biogenesis of the ribosome. *Oncogene*, **33**, 484-494.
- S43. Xu, X., Wan, W., Jiang, G., Xi, Y., Huang, H., Cai, J., Chang, Y., Duan, C.G., Mangrauthia, S.K., Peng, X. *et al.* (2019) Nucleocytoplasmic trafficking of the *Arabidopsis* WD40 repeat protein XIW1 regulates ABI5 stability and abscisic acid responses. *Mol. Plant*, **12**, 1598-1611.
- S44. Zhu, G., Chang, Y., Xu, X., Tang, K., Chen, C., Lei, M., Zhu, J.K. and Duan, C.G. (2019) EXPORTIN 1A prevents transgene silencing in *Arabidopsis* by modulating nucleocytoplasmic partitioning of HDA6. *J. Integra. Plant Biol.*, **61**, 1243-1254.
- S45. Kirli, K., Karaca, S., Dehne, H.J., Samwer, M., Pan, K.T., Lenz, C., Urlaub, H. and Görlich, D. (2015) A deep proteomics perspective on CRM1-mediated nuclear export and nucleocytoplasmic partitioning. *eLife*, **4**, e11466.
- S46. Kispal, G., Sipos, K., Lange, H., Fekete, Z., Bedekovics, T., Janáky, T., Bassler, J., Aguilar Netz, D.J., Balk, J., Rotte, C. *et al.* (2005) Biogenesis of cytosolic ribosomes requires the essential iron-sulphur protein Rli1p and mitochondria. *EMBO J.*, **24**, 589-598.
- S47. Yarunin, A., Panse, V.G., Petfalski, E., Dez, C., Tollervey, D. and Hurt, E.C. (2005) Functional link between ribosome formation and biogenesis of iron-sulfur proteins. *EMBO J.*, **24**, 580-588.
- S48. Hernando, Y., Carter, A.T., Parr, A., Hove-Jensen, B. and Schweizer, M. (1999) Genetic analysis and enzyme activity suggest the existence of more than one minimal functional

- unit capable of synthesizing phosphoribosyl pyrophosphate in *Saccharomyces cerevisiae*. *J. Biol. Chem.*, **274**, 12480-12487.
- S49. Hansen, B.G., Kliebenstein, D.J. and Halkier, B.A. (2007) Identification of a flavin-monooxygenase as the S-oxygenating enzyme in aliphatic glucosinolate biosynthesis in *Arabidopsis*. *Plant J.*, **50**, 902-910.
- S50. Rutherford, S. and Moore, I. (2002) The *Arabidopsis* Rab GTPase family: another enigma variation. *Curr. Opin. Plant Biol.*, **5**, 518-528.
- S51. Speth, E.B., Imboden, L., Hauck, P. and He, S.Y. (2009) Subcellular localization and functional analysis of the *Arabidopsis* GTPase RabE. *Plant Physiol.*, **149**, 1824-1837.
- S52. Geng, J., Nair, U., Yasumura-Yorimitsu, K. and Klionsky, D.J. (2010) Post-Golgi Sec proteins are required for autophagy in *Saccharomyces cerevisiae*. *Mol. Biol. Cell*, **21**, 2257-2269.
- S53. Lepore, D., Spassibojko, O., Pinto, G. and Collins, R.N. (2016) Cell cycle-dependent phosphorylation of Sec4p controls membrane deposition during cytokinesis. *J. Cell Biol.*, **214**, 691-703.
- S54. Khan, M., Imran, Q.M., Shahid, M., Mun, B.G., Lee, S.U., Khan, M.A., Hussain, A., Lee, I.J. and Yun, B.W. (2019) Nitric oxide- induced *AtAO3* differentially regulates plant defense and drought tolerance in *Arabidopsis thaliana*. *BMC Plant Biol.*, **19**, 602.
- S55. Seo, M., Aoki, H., Koiwai, H., Kamiya, Y., Nambara, E. and Koshiba, T. (2004) Comparative studies on the *Arabidopsis* aldehyde oxidase (AAO) gene family revealed a major role of *AAO3* in ABA biosynthesis in seeds. *Plant Cell Physiol.*, **45**, 1694-1703.
- S56. Cheshmazar, N., Dastmalchi, S., Terao, M., Garattini, E. and Hamzeh-Mivehroud, M. (2019) Aldehyde oxidase at the crossroad of metabolism and preclinical screening. *Drug Metab. Rev.*, **51**, 428-452.

X.- AGRADECIMIENTOS

X.- AGRADECIMIENTOS

La realización de esta Tesis ha sido posible gracias a la financiación del trabajo que se realiza en el laboratorio de José Luis Micol por la Generalitat Valenciana (GJIDI/2018/A/214, PROMETEO/2019/117, IDIFEDER/2020/019 e IDIFEDER/2021/033) y el Ministerio de Ciencia e Innovación (EQC2018-005181-P, EQC2019-006592-P, BIO2014-53063-P y PGC2018-093445-B-I00). Durante mi periodo predoctoral he sido beneficiaria de un contrato predoctoral de la Universidad Miguel Hernández (401PREDO).

Gracias en primer lugar a mi director de Tesis, José Luis Micol, por depositar su confianza en mí y permitirme realizar esta Tesis en su laboratorio; y por plantearme retos que en su momento me parecieron imposibles, pero que me enseñaron que con paciencia y dedicación se convertían en posibles.

A María Rosa, por su inestimable apoyo y por abrirme las puertas, no solo de su laboratorio, sino también de la investigación.

A todos los profesores del Área de Genética, por su interés en mis progresos. En especial a José Manuel, por brindarme la oportunidad de aprender en su laboratorio. A Héctor, por su paciencia y su disposición a ayudarme en todo lo que necesitara. A Víctor y Pedro, cuyos consejos siempre me resultaron útiles. Y a Sara y Raquel, las profes de prácticas que me enseñaron a manejar en una clase llena de estudiantes.

A Juan, nuestro técnico de laboratorio, cuya curiosidad ha superado no pocas veces la mía. A María José, de quien aprendí que para poder hacer mil cosas a la vez solo necesitas un poco de orden y una sonrisa en la cara.

A los que ya no están en el laboratorio: David Wilson, Tamara Muñoz y José Manuel Serrano, que me enseñaron que el dedicarse a la investigación y disfrutar de la vida no eran mutuamente excluyentes. Edu, qué te voy a decir: tú me guiaste y me ayudaste en todo momento, y lo sigues haciendo. Has sido fundamental en esta etapa de mi vida, aunque suene cursi, y me salvaste algunas neuronas aquel día en que doné sangre.

A mis compañeros presentes, y mis amigos: Alejandro, Sergio, Samuel, Rosa, Sara, Adrián, Uri, Lucía, y Riad. Hemos sido una piña, y entre todos hemos mantenido ese excelente ambiente de trabajo y compañerismo que heredamos de nuestros predecesores. Àngela, no me he olvidado de ti, vas en el párrafo siguiente. A Joan, Sergio Ibáñez, Aurora, María Salud, Ricardo, Eva y Jimmy, con quienes también he compartido almuerzos, comidas, meriendas, penas, y alegrías.

A mis estudiantes: quizás he aprendido yo más de vosotros de lo que yo os he llegado a enseñar. A Irene, por sus interesantes preguntas y su sinceridad. Y a Àngela, antes mi estudiante y ahora mi compañera, por su incansable disposición a ayudarme.

A Maggie y Alejandra, siempre he podido contar con vosotras. A Riad y Karima, por su amistad sincera que durará toda la vida. A toda mi familia, de Aspe y de Novelda. Especialmente a mis tías Merce y Enri, y a mi prima Alba. A mis suegros, Daniel y Loly. A mis padres, Pedro y Reme, mi hermana Alejandra, y a David, por soportarme, apoyarme y motivarme durante todo este viaje.